

NASA Reference Publication 1010

(NASA-RP-1010) CHLOROFLUOROMETHANES AND THE
STRATOSPHERE (NASA) HC A12/MF A01

CSCCL 04A

Chlorofluoromethanes and the Stratosphere

N77-31694

THRU

N77-31699

Unclas

H1/46 47596

August 1977

REPRODUCED BY
NATIONAL TECHNICAL
INFORMATION SERVICE
U. S. DEPARTMENT OF COMMERCE
SPRINGFIELD, VA. 22161

NASA

1. Report No. RP-1010	2. Government Accession No.	3. Recipient's Catalog No.
4. Title and Subtitle Chlorofluoromethanes in the Stratosphere	5. Report Date September 1, 1977	6. Performing Organization Code 624
	7. Author(s) R. D. Hudson, et al.	8. Performing Organization Report No. G-7725
9. Performing Organization Name and Address Goddard Space Flight Center Greenbelt, Maryland 20771	10. Work Unit No. 198-20-01	11. Contract or Grant No.
	12. Sponsoring Agency Name and Address National Aeronautics and Space Administration Washington, D.C. 20546	13. Type of Report and Period Covered Reference Publication
14. Sponsoring Agency Code A-12	15. Supplementary Notes	
16. Abstract This document reports the conclusions of a workshop held by the National Aeronautics and Space Administration to assess the current knowledge of the impact of chlorofluoromethane release in the troposphere on stratospheric ozone concentrations. The document is divided into five sections: Laboratory Measurements, Ozone Measurements and Trends, Minor Species and Aerosol Measurements, One-Dimensional Modeling, and Multidimensional Modeling.		
17. Key Words (Selected by Author(s)) Halocarbons, Stratosphere, Ozone, Chlorofluoromethanes	18. Distribution Statement Unclassified - Unlimited STAR 23 Chemistry and Materials	
19. Security Classif. (of this report) Unclassified	20. Security Classif. (of this report) Unclassified	

* For sale by the National Technical Information Service, Springfield,

NASA Reference Publication 1010

Chlorofluoromethanes and the Stratosphere

Robert D. Hudson, *Editor*

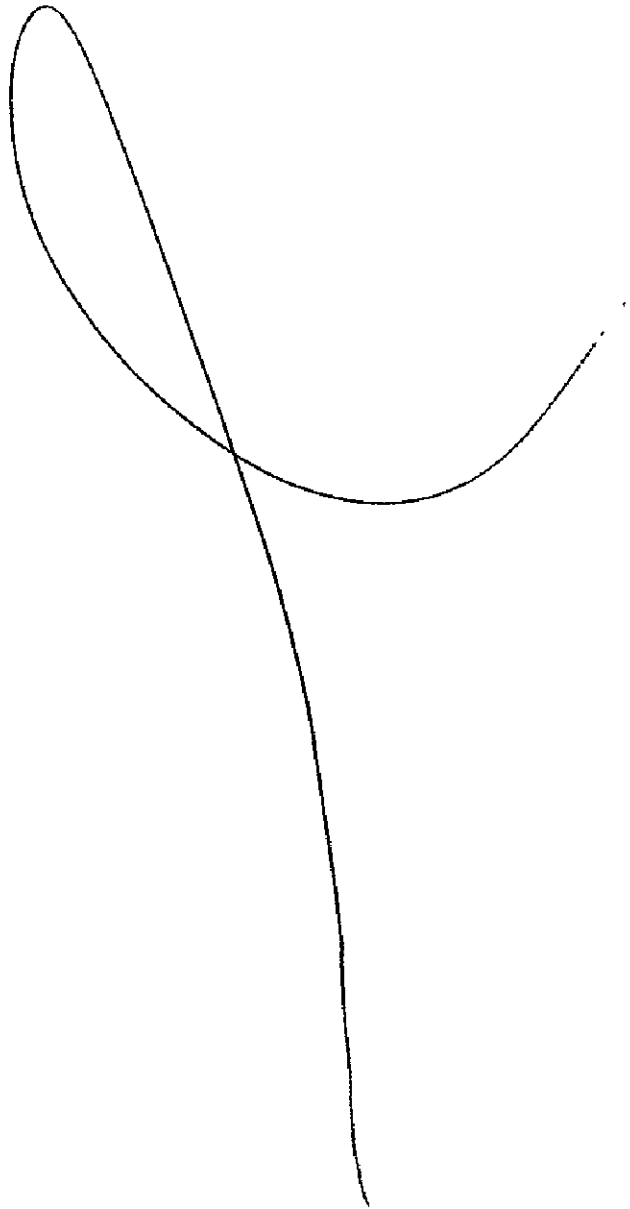
Goddard Space Flight Center
Greenbelt, Maryland

NASA

National Aeronautics
and Space Administration

Scientific and Technical
Information Office

1977



PREFACE

In 1976, the National Aeronautics and Space Administration (NASA) made a commitment to provide, by September 1977, an assessment of the effect on the stratospheric ozone of the release of chlorofluoromethanes into the troposphere. It was recognized at that time that the NASA report would closely follow a report prepared by the National Academy of Sciences, "Halocarbons: Effects on Stratospheric Ozone," dated September 1976. Therefore, the NAS report was used as the starting point in the preparation of the NASA report.

To gather the latest information for such a technical update, the Goddard Space Flight Center organized a workshop at the Airlie House, Warrenton, Virginia, during the week of January 10, 1977. The workshop was centered around five working groups: a Laboratory Measurements working group chaired by Dr. W. B. DeMore of the Jet Propulsion Laboratory; an Ozone Measurements and Trends working group chaired by Prof. J. London of the University of Colorado; a Minor Species and Aerosol Measurements working group chaired by Prof. R. Megill of Utah State University; a One-Dimensional Modeling working group chaired by Dr. R. S. Stolarski of the Goddard Space Flight Center; and a Multi-dimensional Modeling working group chaired by Prof. M. Geller of the University of Illinois. The overall chairman for the workshop and for the production of the workshop report was Dr. R. D. Hudson of the Goddard Space Flight Center.

Each working group was further subdivided, and prominent scientists who are active and expert in stratospheric studies were asked to prepare position papers to cover selected topics of research. In addition to preparing position papers, in October 1976, modeling groups were approached to "run" their models using a standard set of input data supplied by the Goddard Space Flight Center. Specific output data, as well as the predicted ozone changes, were requested so that realistic model intercomparisons could be made.

In all, over sixty scientists attended the workshop, representing most of the institutions engaged in stratospheric research in the United States, Canada, and Europe. A complete list of the position-paper authors and participants, with working group assignments, is given in the Appendix.

Each working group prepared a summary document, and these have been assembled into this report. The report has been updated since January 1977 by soliciting written comments from the participants and as a result of further meetings of the Laboratory Measurements and the One-Dimensional Modeling working groups in June and July 1977. Thus, the report should represent current knowledge as of June 1977.

Goddard Space Flight Center and the National Aeronautics and Space Administration express their thanks to the Working Group Chairmen, the position-paper authors, and the participants for the time and efforts that they contributed to the preparation of this report.

CONTENTS

	Page
PREFACE	iii
CHAPTER 1 – LABORATORY MEASUREMENTS	1
INTRODUCTION	1
Nitrogen Oxides	1
Hydrogen Oxides	2
Chlorine Oxides	3
Bromine Reactions	4
Fluorine Reactions	5
Photochemical Processes	5
DEFINITIONS	6
Units	6
Reliability Estimates	6
Rate Parameters	7
SUMMARY OF RATE-CONSTANT RECOMMENDATIONS	7
Notes to Table 1	14
CROSS SECTIONS AND QUANTUM YIELDS	25
Introduction	25
Discussion of Photodissociation Reactions	26
HETEROGENEOUS CHEMISTRY	45
Removal of Chlorofluoromethanes (CFM's)	46
Removal of Cl _x	47
Catalytic Processes	48
CHAPTER 2 – MEASUREMENTS AND ANALYSIS OF OZONE VARIATIONS	51
INTRODUCTION	51
MEASUREMENTS	52
Total Ozone	52
Ozone Vertical Distribution	57

CONTENTS (Continued)

	Page
ANALYSIS OF OZONE VARIATIONS	67
Data Availability	67
Long-Term Variations	71
Some Inferences on Photochemical Models Derived from Ozone-Variation Observations	80
COMMENTS ON THE ANALYSIS OF OZONE DATA	82
Distinguishing Between Natural and Anthropogenic Trends	82
Statistical Analysis Applied to Present Data Sets	84
Threshold of Detectability	84
SUMMARY AND CONCLUSIONS	86
CHAPTER 3 – MINOR SPECIES AND AEROSOLS	89
INTRODUCTION	89
SUMMARY OF ATMOSPHERIC MEASUREMENTS	92
SOURCE SPECIES	92
SINK TERMS	95
RADICAL SPECIES	103
SOLAR FLUX AND O/O ₃ RATIO	115
TRANSPORT MEASUREMENTS	121
Winds and Dynamics	122
Aerosol Measurements	125
RECOMMENDATIONS	128
Measurements	128
Hydrogen Species	129
Nitrogen Species	130
Halogen Species	131
CHAPTER 4 – ONE-DIMENSIONAL MODELS	133
INTRODUCTION	133
PARAMETRIC SIMULATION OF NET VERTICAL TRANSPORT IN 1-D MODELS	134

CONTENTS (Continued)

	Page
Conceptual Basis for the Introduction of K_z	135
Chemical Tracers	136
Radionuclide Tracers	138
GCM Tracer Experiments	139
DIURNAL AVERAGING EFFECTS	139
MULTIPLE-SCATTERING EFFECTS	144
Photodissociation Coefficients	144
Species Concentration Profiles	148
Model Sensitivity	152
Summary	152
COMPARISON OF THEORY AND MEASUREMENT: HO_x	152
COMPARISON OF THEORY AND MEASUREMENT: NO_x	157
COMPARISON OF THEORY AND MEASUREMENT: ClO_x	168
Introduction	168
Sources of Stratospheric Odd Chlorine	169
Measurements and Theoretical Predictions for ClX Species	172
TROPOSPHERIC AND STRATOSPHERIC SINKS FOR CHLOROFLUOROMETHANES	178
Introduction	178
Removal by Oceans	180
Photodissociation in the Troposphere	181
Reaction with OH Radicals in Troposphere	181
Removal by Pyrolysis	182
Ion-Molecule Reactions	183
Active Removal in Stratosphere	184
Conclusion	184
EFFECT OF TEMPERATURE FEEDBACK MECHANISM	185
UNCERTAINTIES IN THE PREDICTIONS OF 1-D STRATOSPHERIC MODELS	186
Introduction	186
Reaction Rates	186

CONTENTS (Continued)

	Page
CONCLUSIONS	189
CHAPTER 5 – MULTIDIMENSIONAL CFM-O ₃ MODELING . . .	197
INTRODUCTION	197
RADIATIVE-DYNAMICAL/PHOTOCHEMICAL FEEDBACK MECHANISMS	199
Background	199
Feedback Mechanisms	200
Concluding Remarks	205
TWO-DIMENSIONAL MODELING	205
Types of Models	206
Chemical Model	207
Atmospheric Transport Prescriptions for 2-D Models	208
Chemistry and Transport	210
Boundary Conditions	210
Applications	211
Summary	213
THREE-DIMENSIONAL MODELING	214
TRANSPORT PARAMETERIZATIONS IN 3-D MODELING OF THE STRATOSPHERE	218
Subgrid-Scale Mixing	219
Vertical Transport Across the Tropopause	220
OBSERVATIONAL NEEDS OF MULTIDIMENSIONAL MODELS OF THE STRATOSPHERE	221
CONCLUSIONS	226
Assessment Uncertainty Due to Transport	226
Contributions of Multidimensional Models	227
Observational Needs	228
REFERENCES	231
APPENDIX – CHLOROFLUOROMETHANE WORKSHOP ATTENDEES	261

CHAPTER 1

LABORATORY MEASUREMENTS

INTRODUCTION

This section presents a compilation of chemical and photochemical data that is relevant to stratospheric modeling. There are three broad categories of data: (1) rate constants for chemical reactions, including (when possible) temperature and pressure dependencies along with product distributions; (2) absorption cross sections, photodissociation quantum yield, and photolysis products; and (3) heterogeneous chemical processes.

The complexity of stratospheric chemistry, combined with the need for accurate model predictions, has resulted in stringent demands for reliable laboratory data in the categories noted above. In many instances, adequate measurements are still not available, partly because measurement programs are not complete and partly because satisfactory measurement techniques are either unavailable or have become available only very recently. Moreover, agreement among measurements by different techniques has occasionally been unsatisfactory, as the detailed discussion in subsequent subsections will show.

The recommendations are based entirely on laboratory measurements, with occasional extrapolations using theory. An example of the latter is the pressure falloff in the rate constant for ClNO_3 formation at pressures relevant to the stratosphere. (This question is discussed in detail in subsequent subsections.) No "tuning" of rate data to fit stratospheric measurements was employed. All laboratory data judged to be reliable were considered, including measurements of absolute rate constants and ratios of rate constants.

NITROGEN OXIDES

The reactions forming and destroying NO , NO_2 , NO_3 , and HNO_3 have been part of modern atmospheric modeling since the beginning of the consideration of the environmental effects of supersonic transport aircraft. As a result, considerable attention has been paid to the measurement of the rate constants of these reactions. For many of them, the reliabilities are near the limit of the measurement art (perhaps 25 to 40 percent agreement between laboratories). Also, for many of them, these reliabilities appear to be sufficient for modeling purposes as judged from sensitivity calculations.

However, there are reactions for which the data base is weak and for which difficult, and occasionally arbitrary, decisions have necessarily been made. These reactions, which become candidates for further study, are listed below; the problems are discussed in the notes that accompany table 1.

- $\text{OH} + \text{NO}_2 + (\text{N}_2 \text{ and } \text{O}_2) \rightarrow \text{HNO}_3 + (\text{N}_2 \text{ and } \text{O}_2)$ at low temperatures and high pressures—One set of such measurements exists. It is difficult to correlate with theory. Verification is needed.
- $\text{HO}_2 + \text{NO}_2 (+\text{M}) \rightarrow \text{HO}_2\text{NO}_2 (+\text{M})$ under all stratospheric conditions—Peroxyntic acid is a molecule that has not yet been used in atmospheric models but must be considered.
- Photochemistry of HO_2NO_2 and its reactions with O, OH, and other free radicals—The chemistry of HO_2NO_2 must be known before this species can be introduced in the models.
- $\text{N} + \text{NO}_2 \rightarrow \text{N}_2\text{O} + \text{O}$ and $\text{N} + \text{O}_3 \rightarrow \text{NO} + \text{O}_2$ to determine the temperature dependences that have been estimated in the absence of data.

The reaction-rate data for $\text{O}(^1\text{D})$ are reasonably reliable but have some unresolved problems. Measurements using two different analytical techniques (in two laboratories) differ systematically by more than the known uncertainty of either. It has been decided to base the recommendations on one of these sets. Experiments to resolve this incompatibility would improve the reliability of the recommendations. In addition, the reactions of $\text{O}(^1\text{D})$ with chlorocarbons and halogenated derivatives of formaldehyde require more study. The products of the chemical reactions have not been determined, and it is not known whether the observed rate constants contain an appreciable contribution from physical quenching.

HYDROGEN OXIDES

There are only two HO_x reactions that may be known well enough to require no additional study:

- $\text{H} + \text{O}_2 + \text{M} \rightarrow \text{HO}_2 + \text{M}$
- $\text{OH} + \text{CH}_4 \rightarrow \text{CH}_3 + \text{H}_2\text{O}$

The characteristic situation for the remaining reactions (especially atom/radical and radical/radical) are a reasonably well-known room temperature rate constant, but there is no temperature dependence data. These require further study, preferably by direct techniques. In view of the sensitivity study carried out in conjunction with this assessment, top priority should be focused on the following reactions:

- $\text{OH} + \text{HO}_2 \rightarrow \text{H}_2\text{O} + \text{O}_2$
- $\text{HO}_2 + \text{HO}_2 \rightarrow \text{H}_2\text{O}_2 + \text{O}_2$
- $\text{HO}_2 + \text{NO} \rightarrow \text{NO}_2 + \text{OH}$
- $\text{HO}_2 + \text{O}_3 \rightarrow \text{OH} + 2\text{O}_2$
- $\text{OH} + \text{O}_3 \rightarrow \text{HO}_2 + \text{O}_2$
- $\text{HO}_2 + \text{O} \rightarrow \text{OH} + \text{O}_2$

Existing data for the first three reactions are mutually inconsistent, and, thus, further work is required on all three. The rate constants recommended here are an adjusted set, as discussed in note B1 to table 1. The remaining three reactions contribute significantly to the total uncertainty of the stratospheric models.

CHLORINE OXIDES

Although many ClO_x reactions are listed in table 1, Summary of Recommended Rate Constants, they are not of equal importance. Accurate models require precise kinetic data for reactions 44 through 50 because the catalytic efficiency is strongly dependent on the absolute magnitude of these reaction-rate constants. Although it is essential to include reactions 51 through 77 in any complete photochemical model calculation, these reactions are of less importance, and, thus, a lower precision can be tolerated in the kinetic-rate data for these processes. Whether reaction 49 plays an important role in stratospheric chemistry is highly dependent on the $[\text{HO}_2]$ profile that is governed by HO_x reactions. Therefore, whereas an uncertainty of 20 percent in knowledge of the values of k_{44} through k_{50} may be significant, an uncertainty by a factor of 2 or more in the values of k_{51} through k_{77} may not be particularly important for calculating the magnitude of the ozone depletion. However, accurate rate-constant data may be required for a larger set of reactions if an understanding is required of

the concentration of some minor chlorine containing species in the atmosphere (e.g., HOCl).

One reaction that had not been previously studied at all ($\text{ClO} + \text{NO}_2 + \text{M} \rightarrow \text{ClONO}_2 + \text{M}$) has now been the subject of extensive investigations at low pressures (equal to or less than 6 torr), but none at the relevant stratospheric pressures (approximately 50 torr). The recommended rate constant for ClONO_2 formation is based on the evaluation of Zahniser et al. (1977). Data for that evaluation were obtained from three low-pressure, discharge-flow, temperature-dependent studies (Leu et al., 1977; Zahniser and Kaufman, 1977*; and Birks, 1977). In the absence of experimental data for pressure falloff behavior, Zahniser et al. (1977) fitted the pressure dependence to a theoretical Rice-Ramsperger-Kassel-Marcus (RRKM) model, as described by Smith and Golden (1977).

To date, there have been no quantitative determinations of the products of the $\text{ClO} + \text{NO}_2 + \text{M}$ reaction, and, at present, it is not possible to rule out the existence of two primary reaction channels. Consequently, because this reaction is of importance, it must be studied experimentally within the relevant pressure regime with a quantitative determination of the reaction products. Additional studies of the $\text{NO} + \text{ClO}$ reaction and, to a lesser extent, the $\text{O} + \text{ClO}$ reaction are required.

Reactions 78 through 88 have been included in this compilation for the sake of completeness so that tropospheric lifetimes can be calculated for these compounds.

BROMINE REACTIONS

Compared to current knowledge of ClO_x reaction-rate data, there is a dearth of precise kinetic information for BrO_x reactions. However, there is probably sufficient information to perform a meaningful sensitivity calculation. The basic set of key reactions in the BrO_x system is similar to that in the ClO_x system, with the following exceptions: (1) the $\text{Br} + \text{H}_2$ and $\text{Br} + \text{CH}_4$ reactions are highly endothermic and are too slow to be significant, and (2) the radical/radical reactions (reactions 91 and 92) play an important role. The reactions that require the most immediate attention, if the BrO_x system is to be modeled with any real accuracy, are 95, 90, and 93. Although there is no evidence for reaction 93, if it had a significant

*M. S. Zahniser and F. Kaufman, University of Pittsburgh, manuscript in preparation, 1977.

rate constant ($\geq 10^{-17} \text{ cm}^3 \text{ s}^{-1}$), it would play a major role in the destruction of odd oxygen. The BrO_x system can be generalized by stating that the reactivity of atomic bromine is less than that of atomic chlorine, whereas the reactivity of BrO is similar to, or greater than, that of ClO . All BrO_x reactions require additional study.

FLUORINE REACTIONS

Although both atomic fluorine and the FO radical are extremely reactive species, the catalytic efficiency of FO_x for the destruction of odd oxygen is very low due to the unreactive nature of the HF molecule. Atomic fluorine is highly reactive toward any hydrogen containing molecule and abstracts a hydrogen atom to form HF . HF does not react with the OH radical or the $\text{O} (^3\text{P})$ atom and does not photolyse in the stratosphere. Therefore, as FO_x quickly forms HF , the catalytic chain length is very short. However, this simple approach neglects the role of FO_2 radicals that are produced in the $\text{F} + \text{O}_2 + \text{M}$ reaction.

PHOTOCHEMICAL PROCESSES

Among the photolytic reactions mentioned later in table 3, the following are singled out as requiring further study:

- $\text{O}_3 + h\nu \rightarrow \text{O} (^1\text{D}) + \text{O}_2$ —The quantum yield values have been measured relative to the value below 300 nanometers, which is found to be nearly constant and assumed to be unity. There are, however, indications that the quantum yield is less than unity below 300 nanometers.
- $\text{ClONO}_2 + h\nu \rightarrow \text{Products}$ —The temperature dependence of the cross sections above 300 nanometers should be measured, and the identity of the photolytic fragments needs to be established.
- $\text{N}_2\text{O}_5 + h\nu \rightarrow \text{Products}$ —The quantum yield for photodissociation and the identity of the products have not been determined yet.
- The mechanism of photo-oxidation of the chlorofluoromethanes is not clearly understood, and the chemistry of the intermediate peroxy radicals should be studied further. In addition, the quantum yields for the photolysis of CF_2O and CFCIO should be measured.

DEFINITIONS

UNITS

Definitions are provided in the subsections that follow for use with table 1. The rate constants are given in terms consistent with concentrations in molecules per cubic centimeter and time in seconds. Thus, for first-, second-, and third-order reactions, the units of k are s^{-1} , $cm^3 \text{ molecule}^{-1} s^{-1}$, and $cm^6 \text{ molecule}^{-2} s^{-1}$, respectively.

RELIABILITY ESTIMATES

Reliability estimates are listed in table 1 under the column headed " $\pm \log k$ (230 K)" and apply at 230 K. They allow for any extrapolation of data from higher temperatures. The reliability stated in table 1 is a factor to be used to find the limits within which k probably lies. It is used in either of the following equivalent forms:

$$\log_{10} k_L = \log_{10} k_o - \log_{10} \alpha \quad \log_{10} k_U = \log_{10} k_o + \log_{10} \alpha$$

$$k_L = k_o / \alpha \quad k_U = k_o \times \alpha$$

where k_o is the central value reported for the rate constant, and $\log \alpha$ is the entry in the $\pm \log k$ (230 K) column.

These reliabilities are estimates of overall accuracy. They include consideration of precision of measurement, performance of the methods on other reactions, agreement of measurements made in different laboratories, interrelationships among values of k for several reactions, and reasonableness in terms of theory. The recorded reliability, $\log_{10} \alpha$, has been scaled to be roughly analogous to one standard deviation, σ , because it is used as a measure of precision. This means that, for these reliabilities, the odds are 5 to 3 that k will lie within the calculated upper and lower limits.

Twice the value of $\log_{10} \sigma$ may be used to calculate limits analogous to the 95-percent confidence interval (i.e., odds of 19 to 1 that k will lie between the limits). These definitions are to be taken as descriptions of ranges and not as implying a normal distribution of errors of measurement. There are usually two few sets of measurements to permit the distribution to be studied. When there are many measurements from several laboratories, there is no clear evidence that the distribution is normal.

RATE PARAMETERS

The rate constants given in table 1 are expressed, almost without exception, in the form $k = A \exp(-B/T)$. This is the simple Arrhenius form, with A being the "pre-exponential factor" and B the "activation temperature." Here, $B = E^*/R$, where E^* is the apparent activation energy, and R is the gas constant.

The values of A and B reported here have been developed to reproduce the experimental rate data that have been accepted as reliable. Both A and B should be considered to be empirical fitting parameters, suitable for deriving a value of k for the limited temperature range 200 to 300 K.

On the basis of theoretical models and experience, kineticists expect values of A for particular classes of reactions to lie within fairly well-defined ranges. These ranges correlate with the expected structures of the transition states. Many of the values of A reported here meet these general criteria. However, some do not, and these are usually lower than expected. This is a warning that either the transition state or mechanism is not understood or that there are systematic errors in the trend of k with temperature. When faced with an unexplainable discrepancy between observed and expected parameters, an empirical fit to the data has usually been favored and a more generous uncertainty assigned than would be indicated by the experiments alone.

SUMMARY OF RATE-CONSTANT RECOMMENDATIONS

A summary list of recommended rate constants is given in table 1. Recommendations with explanatory notes designated "A," followed by a numeral, are derived from the position paper prepared for this assessment by D. Garvin and R. Hampson of the National Bureau of Standards (NBS). Similarly, reactions with notes designated by "B" and "C" are from position papers prepared by J. Margitan of the University of Michigan and R. Watson of the Jet Propulsion Laboratory, respectively. Reactions with notes designated by "D" represent recommendations made by the working group. Table 2 is an analytical expression for the rate constant of the reaction $\text{OH} + \text{NO}_2 + \text{M} \rightarrow \text{HONO}_2 + \text{M}$, which is not suitable for representation in the Arrhenius form.

Table 1
Summary of Recommended Rate Constants

Reaction	k	$\pm \log k$ (230 K)	Note*
1. $O_3 + NO \rightarrow NO_2 + O_2$	$2.1 \times 10^{-12} \exp(-1450/T)$	0.08	A1
2. $O + NO_2 \rightarrow NO + O_2$	9.1×10^{-12}	0.03	A2
3. $N + O_2 \rightarrow NO + O$	$5.5 \times 10^{-12} \exp(-3220/T)$	0.1	A3
4. $N + NO \rightarrow N_2 + O$	$8.2 \times 10^{-11} \exp(-410/T)$	0.1	A4
5. $OH + NO_2 (+M) \rightarrow HNO_3 (+M)$	See table 2	0.1	A5
6. $OH + HNO_3 \rightarrow H_2O + NO_3$	8×10^{-14}	0.05	A6
7. $N + NO_2 \rightarrow N_2O + O$	$2 \times 10^{-11} \exp(-800/T)$	0.15	A7
8. $NO + O + M \rightarrow NO_2 + M$	$1.55 \times 10^{-32} \exp(+584/T)$	0.05	A8
9. $NO_2 + HO_2 + N_2 \rightarrow HO_2 NO_2 + N_2$	See note	-	A11
10. $N + O_3 \rightarrow NO + O_2$	$2 \times 10^{-11} \exp(-1070/T)$	0.15	A9
11. $NO_2 + O_3 \rightarrow NO_3 + O_2$	$1.2 \times 10^{-13} \exp(-2450/T)$	0.04	A10
12. $O(^1D) + N_2O \rightarrow N_2 + O_2$	5.5×10^{-11}	0.1	A12
13. $O(^1D) + N_2O \rightarrow NO + NO$	5.5×10^{-11}	0.1	A12
14. $O(^1D) + H_2O \rightarrow OH + OH$	2.3×10^{-10}	0.1	A12
15. $O(^1D) + CH_4 \rightarrow OH + CH_3$	1.3×10^{-10}	0.05	A12
16. $O(^1D) + CH_4 \rightarrow H_2 + CH_2O$	1.4×10^{-11}	0.1	A12
17. $O(^1D) + N_2 + M \rightarrow N_2O + M$	3.5×10^{-37}	0.5	A12
18. $O(^1D) + H_2 \rightarrow OH + H$	9.9×10^{-11}	0.05	A12
19. $O(^1D) + N_2 \rightarrow O + N_2$	$2.0 \times 10^{-11} \exp(+107/T)$	0.05	A12
20. $O(^1D) + O_2 \rightarrow O + O_2$	$2.9 \times 10^{-11} \exp(+67/T)$	0.1	A12

*Notes appear in the text.

Table 1 (Continued)

Reaction	k	log k (230 K)	Note*
21. $O(^1D) + O_3 \rightarrow O_2 + O_2$	1.2×10^{-10}	0.1	A12
22. $O(^1D) + O_3 \rightarrow O_2 + O + O$	1.2×10^{-10}	0.1	A12
23. $O(^1D) + HCl \rightarrow OH + Cl$	1.4×10^{-10}	0.05	A12
24. $O(^1D) + CFCI_3 \rightarrow \text{products}$	2.3×10^{-10}	0.1	A12
25. $O(^1D) + CF_2Cl_2 \rightarrow \text{products}$	2.0×10^{-10}	0.1	A12
26. $O(^1D) + CCl_2O \rightarrow \text{products}$	1.7×10^{-10}	0.1	A12
27. $O(^1D) + CFCIO \rightarrow \text{products}$	1.0×10^{-10}	0.1	A12
28. $O(^1D) + CF_2O \rightarrow \text{products}$	4.5×10^{-11}	0.1	A12
29. $OH + HO_2 \rightarrow H_2O + O_2$	3×10^{-11}	0.25	B1
30. $HO_2 + HO_2 \rightarrow H_2O_2 + O_2$	2.5×10^{-12}	0.3	B1
31. $NO + HO_2 \rightarrow NO_2 + OH$	8×10^{-12}	{ +0.15 -0.45	B1
32. $HO_2 + O_3 \rightarrow OH + 2O_2$	$7.3 \times 10^{-14} \exp(-1275/T)$	0.3	B2
33. $OH + O_3 \rightarrow HO_2 + O_2$	$1.5 \times 10^{-12} \exp(-1000/T)$	0.15	B3
34. $O + OH \rightarrow O_2 + H$	4.2×10^{-11}	0.15	B4
35. $O + HO_2 \rightarrow OH + O_2$	3.5×10^{-11}	0.15	B4
36. $O + H_2O_2 \rightarrow OH + HO_2$	$2.75 \times 10^{-12} \exp(-2125/T)$	0.15	B5
37. $H + O_2 + M \rightarrow HO_2 + M$	$2.1 \times 10^{-32} \exp(+290/T)$	0.1	B6
38. $H + O_3 \rightarrow OH + O_2$	$1.2 \times 10^{-10} \exp(-560/T)$	0.15	B7
39. $OH + OH \rightarrow H_2O + O$	$1 \times 10^{-11} \exp(-550/T)$	0.2	B8

*Notes appear in the text.

Table 1 (Continued)

Reaction	k	$\pm \log k$ (230 K)	Note*
40. $\text{OH} + \text{OH} + \text{M} \rightarrow \text{H}_2\text{O}_2 + \text{M}$	$1.25 \times 10^{-32} \exp(+900/T)$	0.15	B9
41. $\text{OH} + \text{H}_2\text{O}_2 \rightarrow \text{H}_2\text{O} + \text{HO}_2$	$1 \times 10^{-11} \exp(-750/T)$	0.15	B10
42. $\text{OH} + \text{CO} \rightarrow \text{CO}_2 + \text{H}$	1.4×10^{-13}	0.1	B11
43. $\text{OH} + \text{CH}_4 \rightarrow \text{H}_2\text{O} + \text{CH}_3$	$2.35 \times 10^{-12} \exp(-1710/T)$	0.1	B6
44. $\text{Cl} + \text{O}_3 \rightarrow \text{ClO} + \text{O}_2$	$2.7 \times 10^{-11} \exp(-257/T)$	0.06	C1, 2
45. $\text{O} + \text{ClO} \rightarrow \text{Cl} + \text{O}_2$	$7.7 \times 10^{-11} \exp(-130/T)$	0.1	C1, 3
46. $\text{NO} + \text{ClO} \rightarrow \text{Cl} + \text{NO}_2$	$1.0 \times 10^{-11} \exp(+200/T)$	0.15	C4
47. $\text{OH} + \text{HCl} \rightarrow \text{Cl} + \text{H}_2\text{O}$	$3.0 \times 10^{-12} \exp(-425/T)$	0.05	C1, 5
48. $\text{Cl} + \text{CH}_4 \rightarrow \text{HCl} + \text{CH}_3$	$7.3 \times 10^{-12} \exp(-1260/T)$	{ +0.06 -0.18	C1, 6
49. $\text{Cl} + \text{HO}_2 \rightarrow \text{HCl} + \text{O}_2$	3×10^{-11}	0.3	C1, 7
50. $\text{ClO} + \text{NO}_2 + \text{N}_2 \rightarrow \text{ClONO}_2 + \text{N}_2$	$3.3 \times 10^{-23} T^{-3.34}$	{ +0.15 -0.06	C8
51. $\text{O} + \text{ClONO}_2 \rightarrow \text{products}$	$1 + 8.7 \times 10^{-9} T^{-0.6} M^{0.5}$		
52. $\text{OH} + \text{ClONO}_2 \rightarrow \text{products}$	$3.0 \times 10^{-12} \exp(-808/T)$	0.15	C1, 9
53. $\text{Cl} + \text{ClONO}_2 \rightarrow \text{products}$	$1.2 \times 10^{-12} \exp(-333/T)$	0.18	C1, 10
54. $\text{O} + \text{HCl} \rightarrow \text{Cl} + \text{OH}$	$1.68 \times 10^{-12} \exp(-607/T)$	0.3	C11
55. $\text{O} + \text{HCl} \rightarrow \text{Cl} + \text{OH}$	$1.14 \times 10^{-11} \exp(-3370/T)$	0.13	C1, 12
56. $\text{Cl} + \text{OH} \rightarrow \text{O} + \text{HCl}$	$1.0 \times 10^{-11} \exp(-2970/T)$	0.13	C13
57. $\text{Cl} + \text{H}_2 \rightarrow \text{HCl} + \text{H}$	$3.5 \times 10^{-11} \exp(-2290/T)$	0.06	C1, 14
57. $\text{Cl} + \text{H}_2\text{O}_2 \rightarrow \text{HCl} + \text{HO}_2 \rightarrow \text{HOCl} + \text{OH} (?)$	$1.7 \times 10^{-12} \exp(-384/T)$	0.18	C1, 15

*Notes appear in the text.

Table 1 (Continued)

Reaction	k	log k (230 K)	Note*
58. $\text{Cl} + \text{HNO}_3 \rightarrow \text{HCl} + \text{NO}_3$	$1.0 \times 10^{-11} \exp(-2170/T)$	0.3	C1, 16
59. $\text{Cl} + \text{NO}_2 + \text{M} \rightarrow \text{ClNO}_2 + \text{M}$	7.2×10^{-31}	0.3	C1
60. $\text{Cl} + \text{NO} + \text{N}_2 \rightarrow \text{ClNO} + \text{N}_2$	$1.7 \times 10^{-32} \exp(+530/T)$	0.3	C1
61. $\text{Cl} + \text{ClNO} \rightarrow \text{NO} + \text{Cl}_2$	3.0×10^{-11}	0.1	C1
62. $\text{Cl} + \text{O}_2 + \text{M} \rightarrow \text{ClOO} + \text{M}$	1.7×10^{-33}	{ +1.0 -0.5	C1, 17
63. $\text{ClOO} + \text{M} \rightarrow \text{Cl} + \text{O}_2 + \text{M}$	$5.8 \times 10^{-9} \exp(-3580/T)$	{ +1.0 -0.5	C1, 17
$K_{\text{eq}} = k_{62}/k_{63}$	$2.95 \times 10^{-25} \exp(+3580/T)$	1.0	C1, 17
64a. $\text{Cl} + \text{ClOO} \rightarrow \text{Cl}_2 + \text{O}_2$	1.6×10^{-10}	{ +0.3 -1.0	C1, 18
64b. $\text{Cl} + \text{ClOO} \rightarrow \text{ClO} + \text{ClO}$	1.1×10^{-11}	{ +0.5 -1.0	C1, 18
65. $\text{ClOO} + \text{HO}_2 \rightarrow \text{HCl} + 2\text{O}_2$	No recommendation		C19
66. $\text{ClO} + \text{HO}_2 \rightarrow \text{HOCl} + \text{O}_2$	2×10^{-13}	1.0	C20
67. $\text{ClO} + \text{CH}_4 \rightarrow \text{products}$	$\leq 1 \times 10^{-12} \exp(-3700/T)$	2.0	C1, 21
68. $\text{ClO} + \text{H}_2 \rightarrow \text{products}$	$\leq 1 \times 10^{-12} \exp(-4800/T)$	2.0	C1, 21
69. $\text{ClO} + \text{CO} \rightarrow \text{products}$	$\leq 1 \times 10^{-12} \exp(-3700/T)$	2.0	C1, 21
70. $\text{ClO} + \text{N}_2\text{O} \rightarrow \text{products}$	$\leq 1 \times 10^{-12} \exp(-4260/T)$	2.0	C1, 21

*Notes appear in the text

Table 1 (Continued)

Reaction	k	$\pm \log k$ (230 K)	Note*
71a. $\text{ClO} + \text{BrO} \rightarrow \text{Br} + \text{OCIO}$	6.7×10^{-12}	0.18	C1
71b. $\text{ClO} + \text{BrO} \rightarrow \text{Br} + \text{ClOO}$	6.7×10^{-12}	0.18	C1
72a. $\text{ClO} + \text{ClO} \rightarrow \text{Cl} + \text{ClOO}$	$1 \times 10^{-12} \exp(-1238/T)$	0.1	C1, 22
72b. $\text{ClO} + \text{ClO} \rightarrow \text{Cl}_2 + \text{O}_2$	$5 \times 10^{-13} \exp(-1238/T)$	0.1	C1, 22
72c. $\text{ClO} + \text{ClO} \rightarrow \text{OCIO} + \text{Cl}$	$2.1 \times 10^{-12} \exp(-2200/T)$	0.55	C1, 22
73. $\text{ClO} + \text{ClO} + \text{M} \rightarrow \text{Cl}_2 + \text{O}_2 + \text{M}$	No recommendation	-	C1, 23
74a. $\text{ClO} + \text{O}_3 \rightarrow \text{ClOO} + \text{O}_2$	$1 \times 10^{-12} \exp(-4000/T)$	{ +0.3 -1.0	C1, 24
74b. $\text{ClO} + \text{O}_3 \rightarrow \text{OCIO} + \text{O}_2$	$1 \times 10^{-12} \exp(-4000/T)$	{ +0.3 -1.0	C1, 24
75. $\text{Cl} + \text{OCIO} \rightarrow \text{ClO} + \text{ClO}$	5.9×10^{-11}	0.1	C1
76. $\text{NO} + \text{OCIO} \rightarrow \text{NO}_2 + \text{ClO}$	$2.5 \times 10^{-12} \exp(-600/T)$	0.3	C1, 25
77. $\text{O} + \text{OCIO} \rightarrow \text{ClO} + \text{O}_2$	$2 \times 10^{-11} \exp(-1100/T)$	0.3	C1, 25
78. $\text{OH} + \text{CH}_3\text{Cl} \rightarrow \text{CH}_2\text{Cl} + \text{H}_2\text{O}$	$2.2 \times 10^{-12} \exp(-1142/T)$	0.1	C1, 26
79. $\text{OH} + \text{CH}_2\text{Cl}_2 \rightarrow \text{CHCl}_2 + \text{H}_2\text{O}$	$5.2 \times 10^{-12} \exp(-1094/T)$	0.1	C1, 26
80. $\text{OH} + \text{CHCl}_3 \rightarrow \text{CCl}_3 + \text{H}_2\text{O}$	$4.7 \times 10^{-12} \exp(-1134/T)$	0.1	C1, 26
81. $\text{OH} + \text{CHFCl}_2 \rightarrow \text{CFCl}_2 + \text{H}_2\text{O}$	$1.3 \times 10^{-12} \exp(-1127/T)$	0.1	C1, 26
82. $\text{OH} + \text{CHF}_2\text{Cl} \rightarrow \text{CF}_2\text{Cl} + \text{H}_2\text{O}$	$1.2 \times 10^{-12} \exp(-1660/T)$	0.04	C1, 26
83. $\text{OH} + \text{CH}_2\text{ClF} \rightarrow \text{CHClF} + \text{H}_2\text{O}$	$2.8 \times 10^{-12} \exp(-1259/T)$	0.1	C1, 26
84. $\text{OH} + \text{CH}_3\text{CCl}_3 \rightarrow \text{H}_2\text{O} + \text{CH}_2\text{CCl}_3$	$3.5 \times 10^{-12} \exp(-1562/T)$	0.18	C1, 26

*Notes appear in the text.

Table 1 (Continued)

Reaction	k	log k (230 K)	Note*
85. $\text{OH} + \text{C}_2\text{Cl}_4 \rightarrow \text{C}_2\text{Cl}_4\text{OH}$	$9.4 \times 10^{-12} \exp(-1199/T)$	0.18	C1, 27
86. $\text{OH} + \text{C}_2\text{HCl}_3 \rightarrow \text{C}_2\text{Cl}_3\text{OH}$	2.3×10^{-12}	0.18	C1, 28
87. $\text{OH} + \text{CFCl}_3 \rightarrow \text{products}$	$< 1 \times 10^{-12} \exp(-3650/T)$	-	C1, 29
88. $\text{OH} + \text{CF}_2\text{Cl}_2 \rightarrow \text{products}$	$< 1 \times 10^{-12} \exp(-3560/T)$	-	C1, 29
89. $\text{Br} + \text{O}_3 \rightarrow \text{BrO} + \text{O}_2$	$3.0 \times 10^{-11} \exp(-937/T)$	0.1	C30
90. $\text{O} + \text{BrO} \rightarrow \text{Br} + \text{O}_2$	3×10^{-11}	0.4	C31
91. $\text{NO} + \text{BrO} \rightarrow \text{Br} + \text{NO}_2$	2.1×10^{-11}	0.18	C32
92. $\text{BrO} + \text{BrO} \rightarrow 2\text{Br} + \text{O}_2$	$2.9 \times 10^{-11} \exp(-450/T)$	0.18	C33
93. $\text{BrO} + \text{O}_3 \rightarrow \text{Br} + 2\text{O}_2$	$< 10^{-14}$	-	C34
94. $\text{Br} + \text{H}_2\text{O}_2 \rightarrow \text{HBr} + \text{HO}_2$	$5 \times 10^{-12} \exp(-1570/T)$	0.3	C35
95. $\text{Br} + \text{HO}_2 \rightarrow \text{HBr} + \text{O}_2$	5×10^{-12}	0.7	C36
96. $\text{OH} + \text{HBr} \rightarrow \text{H}_2\text{O} + \text{Br}$	5.1×10^{-12}	0.18	C37
97. $\text{O} + \text{HBr} \rightarrow \text{OH} + \text{Br}$	$7.6 \times 10^{-12} \exp(-1571/T)$	0.4	C38
98. $\text{OH} + \text{CH}_3\text{Br} \rightarrow \text{CH}_2\text{Br} + \text{H}_2\text{O}$	$7.93 \times 10^{-13} \exp(-889/T)$	0.1	C39
99. $\text{CH}_3 + \text{O}_2 + \text{M} \rightarrow \text{CH}_3\text{O}_2 + \text{M}$			D1
100. $\text{CH}_3\text{O}_2 + \text{NO} \rightarrow \text{CH}_3\text{O} + \text{NO}_2$	$3.3 \times 10^{-12} \exp(-500/T)$	1.0	D2
101. $\text{CH}_3\text{O} + \text{O}_2 \rightarrow \text{CH}_2\text{O} + \text{HO}_2$	$1.6 \times 10^{-13} \exp(-3300/T)$	1.0	D2
102. $\text{CH}_2\text{O} + \text{OH} \rightarrow \text{HCO} + \text{H}_2\text{O}$	$3 \times 10^{-11} \exp(-250/T)$	0.2	D3
103. $\text{CH}_2\text{O} + \text{O} \rightarrow \text{OH} + \text{HCO}$	$2 \times 10^{-11} \exp(-1450/T)$	0.2	D3
104. $\text{HCO} + \text{O}_2 \rightarrow \text{CO} + \text{HO}_2$	6×10^{-12}	0.2	D2

*Notes appear in the text.

Table 2
Parameters for an Analytical Expression for the
Second-Order Rate Constant of the Reaction
 $\text{HO} + \text{NO}_2(+\text{N}_2) \rightarrow \text{HONO}_2(+\text{N}_2)$

$$\log_{10}(k) = -A/T(B+T) - 0.5 \log_{10}(T/280)$$

$$A = A_1 + A_2Z + A_3Z^2 + A_4Z^3$$

$$B = B_1 + B_2Z + B_3Z^2$$

$$A_1 = 31.62273$$

$$B_1 = -327.372$$

$$A_2 = -0.258304$$

$$B_2 = 44.5586$$

$$A_3 = -0.0889287$$

$$B_3 = -1.38092$$

$$A_4 = 2.520173 \times 10^{-3}$$

where $Z = \log_{10} [\text{N}_2]$ and is applicable only for the ranges $200 < T/K < 350$ and $16.3 < \log_{10} ([\text{N}_2]/\text{molecule cm}^{-3}) < 19.5$, with an estimated reliability in $\log k$ of ± 0.10 (reliability analogous to 1σ). Air is approximately 6 percent less efficient than nitrogen as a third body (i.e., the expression above may be used with $[\text{Air}] = 0.94 [\text{N}_2]$).

NOTES TO TABLE 1

- A1 $\text{O}_3 + \text{NO} \rightarrow \text{NO}_2 + \text{O}_2$ —This new recommendation is based on the measurements of Birks et al. (1976b), which cover the applicable temperature range. Earlier studies confirm the 300-K value. The temperature coefficient is appreciably different from that given by Hampson and Garvin (1975) (henceforth, noted as HG) and that used by the National Academy of Sciences, Panel on Atmospheric Chemistry (1976) (henceforth, noted as NAS).
- A2 $\text{O} + \text{NO}_2 \rightarrow \text{O}_2 + \text{NO}$ —This recommendation is the same as that given by HG and NAS. There may be a slight negative temperature coefficient, but the evidence at low temperatures is uncertain.
- A3 $\text{N} + \text{O}_2 \rightarrow \text{NO} + \text{O}$ —This new recommendation is based on the measurements of Becker et al. (1969) as being the most reliable in the low temperature region. The value at 300 K agrees with that selected by Baulch et al. (1973b) for higher temperatures, $k = 1.1 \times 10^{-14} T \exp(-3150/T)$. NAS recorded this incorrectly, omitting the minus sign in the exponential.

- A4 $\text{N} + \text{NO} \rightarrow \text{N}_2 + \text{O}$ —This new recommendation is based on the recent measurements of Clyne and McDermid (1975) over the temperature range 298 to 670 K. The uncertainty limits allow for extrapolation to lower temperatures. The earlier evaluation by Baulch et al. (1973b), cited by NAS, was based on 300-K data and high-temperature measurements on the reverse reaction.
- A5 $\text{OH} + \text{NO}_2 (+\text{N}_2) \rightarrow \text{HONO}_2 (+\text{N}_2)$ —This recommendation is a correlation of all recent data for this combination reaction in the presence of nitrogen (Anastasi and Smith, 1976; Davis, 1976; Anderson et al., 1974; Harris and Wayne, 1975; Howard and Evenson, 1974; and Atkinson et al., 1976). It emphasizes measurements at 220 K and approximately 300 K. The earlier recommendation in HG was based on data taken in the presence of other third bodies and corrected to nitrogen. The origin of the analytical expression cited by NAS is unknown.
- A6 $\text{OH} + \text{HNO}_3 \rightarrow \text{H}_2\text{O} + \text{NO}_3$ —This new recommendation is based on the measurements of Smith and Zellner (1975) over the temperature range 240 to 300 K. It is confirmed, above 270 K, by Margitan et al. (1975), whose data were cited by NAS.
- A7 $\text{N} + \text{NO}_2 \rightarrow \text{N}_2\text{O} + \text{O}$ —This new recommendation accepts the 298-K results of Clyne and McDermid (1975). The temperature coefficient has been estimated here. NAS used the same 298-K value but without a temperature coefficient.
- A8 $\text{NO} + \text{O} + \text{N}_2 \rightarrow \text{NO}_2 + \text{N}_2$ —This new recommendation is based on the recent measurements of Whytock et al. (1976). It supersedes the earlier recommendation by Baulch et al. (1973b), accepted by HG and cited by NAS, in which the negative temperature coefficient is nearly two times larger. Other recent experiments confirm the revision (Singleton et al., 1975; and Atkinson and Pitts, 1974).
- A9 $\text{N} + \text{O}_3 \rightarrow \text{NO} + \text{O}_2$ —This new recommendation is based on the only direct measurement, which was at 300 K (Phillips and Schiff, 1962). The temperature dependence has been estimated here by assigning a pre-exponential factor similar to that for the reaction of O_3 with O or Cl. NAS cited the same data, without a variation with temperature, based on the older evaluation by Baulch et al. (1973a). This new recommendation supersedes the January 1977 estimate, $k = 5 \times 10^{-12} \exp(-650/T) \text{ cm}^3 \text{ molecule}^{-1} \text{ s}^{-1}$.

- A10 $\text{NO}_2 + \text{O}_3 \rightarrow \text{NO}_3 + \text{O}_2$ —This recommendation is the same as that used by NAS and recommended by HG. It is based on an equally weighted least-squares fit to the 22 points in the studies of Davis et al. (1974), Graham and Johnston (1974), and Huie and Herron (1974), all of which include measurements below 273 K. The older evaluation by Baulch et al. (1973b) shows a much larger temperature coefficient, based on old data.
- A11 $\text{HO}_2 + \text{NO}_2 + \text{N}_2 \rightarrow \text{HO}_2\text{NO}_2 + \text{N}_2$ —Peroxynitric acid, HOONO_2 , is a potential sink for NO_x (and HO_x) in the atmosphere. Its rate of formation has been reported by Simonaitis and Heicklen (1977) and Howard (1977). Niki et al. (1977) have reported the infrared spectrum of the product of the above reaction.

A tentative recommendation is made here for this formation reaction. However, peroxynitric acid should not be introduced into atmospheric models until there is also kinetic information on its photolysis and reactions with atoms and free radicals; it may be an ineffective sink.

The tentative recommendation is that the rate constant to be used for $\text{HO}_2 + \text{NO}_2 \rightarrow \text{HO}_2\text{NO}_2$ be the expression developed by Zahniser et al. (1977) for $\text{ClO} + \text{NO}_2 \rightarrow \text{ClONO}_2$, with twice the uncertainty assigned to that reaction.

- A12 Reactions of $\text{O}(^1\text{D})$ —The recommendations adopt the time-resolved $\text{O}(^1\text{D})$ emission measurements at the National Oceanic and Atmospheric Administration (NOAA) Laboratories, Boulder, Colorado, for reactions with O_2 , O_3 , N_2 , N_2O , NH_3 , H_2O , CO_2 , CH_4 , and HCl (Streit et al., 1976; and Howard, private communication, 1976), which supersede earlier reports. The branching ratio for the reaction with N_2O is based on numerous earlier measurements. See Cvetanovic (1974) for a review. However, the ratio k_{12}/k_{13} may be slightly less than unity, based on earlier results of Simonaitis et al. (1972) and recent, unpublished results from the NOAA laboratories. The rate constant for $\text{O} + \text{N}_2 + \text{M} \rightarrow \text{N}_2\text{O} + \text{M}$ is taken from the recent study by Kajimoto and Cvetanovic (1976).

The reactions with CFCl_3 and CF_2Cl_2 have been studied only by the resonance absorption technique at 300 K, as part of a series of studies at the University of Cambridge (Fletcher and Husain, 1976a, b; Heidner and Husain, 1973; and Heidner et al., 1973). When these absorption studies overlap those of the NOAA Laboratories, there is

usually a systematic difference. The reported results have been scaled by multiplying them by 0.41, and a zero temperature dependence has been assigned by analogy to the other chemical reactions of O (¹D). The chlorocarbon rate constants are for total disappearance of O (¹D) and probably include physical quenching. The lower limit for the fraction in the reactive channel forming ClO is 0.39 (CFCl₃) and 0.47 (CF₂Cl₂) (Gillespie et al., 1977).

For CCl₂O, CFCIO, and CF₂O, the only reported values are relative to the value for O (¹D) + N₂O. The recommended values combine these relative values by Jayanty et al. (1976) with the value given here for O (¹D) + N₂O (1.1×10^{-10}). However, these values may be low, since earlier measurements by the same group with the same technique gave ratios for CFCl₃ and CF₂Cl₂ relative to N₂O that were a factor of 2 lower than the same ratios measured by Pitts et al. (1974) and also derived from the absolute values of Fletcher and Husain (1976a).

It must be emphasized that there exist two disparate sets of absolute rate data for O(¹D) reactions. Although we have chosen to accept as correct the results obtained by the O(¹D) → O(³P) emission measurements in the NOAA Laboratories, the possibility cannot be ruled out that the results of the resonance absorption studies at the University of Cambridge are correct.

- B1 In the January 1977 version of this report, we attempted to resolve the conflicting data obtained from ratio and direct measurements on reactions 29 through 31 (OH + HO₂ → H₂O + O₂ (29), HO₂ + HO₂ → H₂O₂ + O₂ (30), and HO₂ + NO → OH + NO₂ (31)) and to formulate a consistent set of rate constants. That procedure gave a great deal of weight to: (a) studies of k₂₉ and k₃₁ that did not involve k₃₀ (and obtained "low" rate constants), and (b) ratio determinations of k₂₉/k₃₀^{1/2} and k₃₁/k₃₀^{1/2}. It was decided that the existing data could be brought into agreement if a lower value of k₃₀ were adopted— 1×10^{-12} instead of 3.6×10^{-12} cm³ s⁻¹. Subsequent to that evaluation, Howard (1977) has measured k₃₁ directly in his laser magnetic resonance system and obtained a result nearly 30 times higher than the earlier recommendation (8×10^{-12} versus 3.5×10^{-13} cm³ s⁻¹). Because this measurement represents the best information available for any of these three reactions, it must form the nucleus for the new recommendations. The value recommended here is temperature-independent, consistent with its large magnitude and

the determination of Glanzer and Troe (1975) near 1500 K ($7.5 \times 10^{-12} \text{ cm}^3 \text{ s}^{-1}$).

The basis for the previous recommendation for k_{31} was primarily the study of Hack et al. (1975). In light of Howard's measurement, however, it appears that their study may be in error due to reaction 31 itself. They used the $\text{H} + \text{NO}_2 \rightarrow \text{OH} + \text{NO}$ reaction to form OH at concentrations of $\sim 3 \times 10^{13} \text{ cm}^{-3}$ and subsequently formed HO_2 via $\text{OH} + \text{H}_2\text{O}_2 \rightarrow \text{HO}_2 + \text{H}_2\text{O}$. The higher value for k_{31} makes it very likely that HO_2 was being reconverted to OH via reaction 31, using the NO formed in the OH formation step. Because the decay of OH was followed for less than a factor of 2 change, it is difficult to assess to what extent this back reaction decreased the apparent rate constant. Other indirect ratio measurements for k_{31} also need to be reevaluated to ascertain the extent to which their earlier assumptions are still realistic. For example, the new value for k_{31} is not compatible with the Simonaitis and Hecklen (1976a) determination of $k_{31}/k_{30}^{1/2}$ because a value of $k_{30} = 3 \times 10^{-10}$ would be required. Clearly, their study, as well as others, needs to be reexamined in light of the drastic change in k_{31} to determine if any of their kinetic assumptions have been invalidated.

Because the ratio determinations involving the $\text{HO}_2 + \text{NO}$ reaction are in question, there is no basis for the low value of k_{30} ($1 \times 10^{-12} \text{ cm}^3 \text{ s}^{-1}$). The recommendation is to now use the k/σ ratio of Hamilton and Lii (1976) and the σ measurement of Paukert and Johnston (1972). The resulting $k_{30} = 2.5 \times 10^{-12} \text{ cm}^3 \text{ s}^{-1}$ is somewhat lower than the Paukert and Johnston value and may indicate that their σ is also high by ~ 30 percent, although there is insufficient data to draw any firm conclusions. In view of the rather poor state of knowledge for this reaction, no temperature dependence is recommended.

The recommendation for k_{29} is unchanged from the earlier report ($3 \times 10^{-11} \text{ cm}^3 \text{ s}^{-1}$). This value is consistent with the upper limits of Chang and Kaufman (1976) and Howard (1977) and is within our estimate of the experimental uncertainty of the recent Burrows et al. (1977) result of $5.1 \times 10^{-11} \text{ cm}^3 \text{ s}^{-1}$. Clearly, additional unambiguous studies are sorely needed on all three reactions.

- B2 Both Simonaitis and Hecklen (1973) and DeMore and Tschuikow-Roux (1974) measured the ratio $\frac{k(\text{HO}_2 + \text{O}_3)}{[k(\text{HO}_2 + \text{HO}_2)]} 1/2$.

The average value for this ratio is $4.6 \times 10^{-8} \exp(-1275/T) \text{ cm}^{1/2} \text{ molecule}^{-1/2}$. Using this ratio and the value of $k(\text{HO}_2 + \text{HO}_2)$ recommended in this evaluation (see note B1), the value for $k(\text{HO}_2 + \text{O}_3)$ given in table 1 was obtained. This value must be changed if there are any changes in $k(\text{HO}_2 + \text{HO}_2)$. The tentative January 1977 value for $\text{HO}_2 + \text{O}_3$, based on the earlier $k(\text{HO}_2 + \text{HO}_2)$, was $1 \times 10^{-13} \exp(-1525/T) \text{ cm}^3 \text{ molecule}^{-1} \text{ s}^{-1}$.

- B3 The A-factor was decreased by 8 percent from that in Hampson and Garvin (1975) to correct O_3 absorption measurements to standard atmospheres. The activation energy is that of Anderson and Kaufman (1973), which is 500 calories/mole lower than the more recent DeMore (1975) work, but is preferred because of the larger temperature range (220 to 450 K) covered by them versus the more limited range (270 to 335 K) in the DeMore work.
- B4 There are no data on the temperature dependence of either reaction. The recommended value for $\text{O} + \text{OH}$ is the same as that of NBS TN866 since no new measurements are available. The recommended value for $\text{O} + \text{HO}_2$ is based on the recent measurements of Burrows, et al. (1977). The January 1977 values for both $\text{O} + \text{OH}$ and $\text{O} + \text{HO}_2$ were $1 \times 10^{-10} \exp(-250/T) \text{ cm}^3 \text{ molecule}^{-1} \text{ s}^{-1}$.
- B5 Although there is no evidence, products are most likely $\text{OH} + \text{HO}_2$, because the $\text{H}_2\text{O} + \text{O}_2$ requires a complex rearrangement. More work is needed, especially below room temperature. The present recommendation is the same as that of NBS TN 866.
- B6 This reaction is one of the few that does not require further work. New results are in excellent agreement with previously established values. The recommendation is the same as that of NBS TN 866.
- B7 More work is needed, especially below room temperature. The value here is a report by Clyne and Monkhouse (1977) measured over the 300- to 600-K range.
- B8 More work is needed, especially on the T dependence around and below room temperature. The recommendation is the same as that of NBS TN 866.
- B9 The value employed by NAS of $B = 2500 \text{ K}$ ($B = E/R$) is very large for a recombination involving four atoms. For comparison, $\text{OH} + \text{NO}$ and $\text{OH} + \text{NO}_2$ have $B \sim 900 \text{ K}$. In addition, $k(295) = 1.2 \times 10^{-29}$

- $\text{cm}^6 \text{s}^{-1}$ from the NBS expression, which is much larger than $2.5 \times 10^{-31} \text{ cm}^6 \text{s}^{-1}$ from Trainor and von Rosenberg (1974). The expression here fits their k (295) and uses $B = 900 \text{ K}$. Clearly, more work is needed, especially on temperature dependence.
- B10 More work is needed, especially below room temperature. This value is a composite of a recent Hack et al. (1975) measurement of $8 \times 10^{-12} \exp(-\frac{670}{T}) \text{ cm}^3 \text{ molecule}^{-1} \text{ s}^{-1}$ with earlier work of Greiner (1968). Although the two studies are in relatively good agreement, there are reasons to question both determinations. The Greiner work involved a large temperature increase due to absorption of flash energy. The Hack et al. study used radical densities of $3 \times 10^{13} \text{ cm}^{-3}$ and may have been complicated by the back reaction between the product HO_2 and residual NO from the OH formation step. The new value for k ($\text{HO}_2 + \text{NO}$) of 8×10^{-12} implies a very rapid reconversion. Additional studies are needed.
- B11 Several recent investigations of reaction 42 at atmospheric pressure in noninert gases have found an enhancement of k of about a factor of 2 (Sie et al., 1976; Cox et al., 1976; Chan et al., 1977; and Atkinson et al., 1977). There is virtually no pressure dependence with He or Ar. For stratospheric calculations, the pressure dependence may be disregarded; however, in tropospheric models it must be taken into account. In a recent paper, Smith (1977) explains the pressure effect, temperature independence, and low absolute magnitude as consistent with an energized HOCO radical as an intermediate. Clearly, more experiments are needed utilizing various M gases and both reactant and product identification.
- C1 All of the data used in this evaluation are tabulated in the reviews of R. T. Watson (1974, 1977) and the position paper entitled "Review of Halogen Kinetics."
- C2 This evaluation was based on data obtained from Watson et al. (1976), Zahniser et al. (1976), Kurylo and Braun (1976), and Clyne and Nip (1976a).
- C3 This expression is based on values of $5.0 \times 10^{-11} \text{ cm}^3 \text{ molecule}^{-1} \text{ s}^{-1}$ and $4.4 \times 10^{-11} \text{ cm}^3 \text{ molecule}^{-1} \text{ s}^{-1}$ at 298 and 230 K, respectively. These values were deduced from the experimental data of Bemand et al. (1973), Clyne and Nip (1976b), and Zahniser and Kaufman (1977).

- C4 The recommended rate constant is an evaluated expression that has a 298-K value equal to the average of two available experimental measurements (Clyne and Watson, 1974; and Zahniser and Kaufman, 1977), and that has a temperature dependence as measured by Zahniser and Kaufman (1977). The tentative January 1977 value was $2.2 \times 10^{-11} \text{ cm}^3 \text{ molecule}^{-1} \text{ s}^{-1}$.
- C5 This evaluation was based on the data of Anderson et al. (1974), Smith and Zellner (1974), and Ravishankara et al. (1977).
- C6 This value is based on the four recent direct studies that measured k at stratospheric temperature (Watson et al., 1976; Manning and Kurylo, 1977; Zahniser and Kaufman, 1977; and Whytock et al., 1977a). It does not consider the discharge flow-mass spectrometric results that determined k at and above 300 K (Clyne and Walker, 1973; Poulet et al., 1974; and DeMore and Leu*), and the competitive chlorination results that measured $B(\text{CH}_4) - B(\text{C}_2\text{H}_6)$ from 190 to 650 K (a recent study by DeMore and Lin† agrees with the literature value (Fettis and Knox, 1964) of 1400 K for $B(\text{CH}_4) - B(\text{C}_2\text{H}_6)$). It was recently reported by both Whytock et al. (1977a) and Zahniser and Kaufman (1977) that the $\text{Cl} + \text{CH}_4$ reaction exhibited a nonlinear Arrhenius behavior, which appeared to explain the differences in $B(\text{CH}_4)$ between the studies that determined B below 300 K and those above 300 K (even though it is acknowledged that the absolute values of k above 300 K in the mass-spectrometric studies and the resonance fluorescence studies are not in particularly good agreement). However, the competitive chlorination results indicate that the magnitude of $B(\text{CH}_4) - B(\text{C}_2\text{H}_6)$ is constant with temperature, which strongly indicates that the Arrhenius behavior of $\text{Cl} + \text{CH}_4$ is linear (the $\text{Cl} + \text{CH}_4$ and $\text{Cl} + \text{C}_2\text{H}_6$ reactions are unlikely to have identical nonlinear Arrhenius behaviors). The value of B for C_2H_6 has been reported to be 60 K, yielding a value of 1460 K for $B(\text{CH}_4)$. However, if the resonance fluorescence results have underestimated $B(\text{CH}_4)$, it is possible that the resonance fluorescence results for $B(\text{C}_2\text{H}_6)$ have been underestimated as well. In conclusion, it can be stated that no significant errors can be found in any particular study; therefore, the direct data collected at stratospheric temperatures will be used until further data are available. Note the unsymmetric error limits that allow for a wide range of k_{48} at 230 K.

*W. B. DeMore and M. T. Leu, Jet Propulsion Laboratory, Pasadena, California, unpublished data, 1977.

†W. B. DeMore and C. L. Lin, Jet Propulsion Laboratory, Pasadena, California, 1977.

- C7 These data were reported by Leu and DeMore (1976).
- C8 This is an evaluated expression put forward by Zahniser et al. (1977). It is consistent with the available low-pressure data (Leu et al., 1977; Zahniser and Kaufman, 1977; and Birks*). The pressure dependence is based on a theoretical RRKM model of Smith and Golden (1977). No experimental measurements of falloff behavior have been reported. The tentative January 1977 value was $5.1 \times 10^{-33} \exp(+1033/T) \text{ cm}^6 \text{ molecule}^{-2} \text{ s}^{-1}$, with no pressure falloff.
- C9 This is a composite expression derived by Kurylo (1977) based on his data combined with that reported by Molina et al. (1977). The January 1977 recommendation was $4.5 \times 10^{-12} \exp(-840/T) \text{ cm}^3 \text{ molecule}^{-1} \text{ s}^{-1}$.
- C10 This value was reported by Kaufman and Zahniser.†
- C11 This value is based on the data reported by Kurylo and Manning.‡
- C12 This evaluation is based on the results of Wong and Belles (1972), Brown and Smith (1975), Ravishankara et al. (1977), and Hack et al. (1976). The results of Balakhnin et al. (1971) have not been used.
- C13 This value combined the evaluation of k_{54} with the most recent thermodynamic data for $\Delta H_f^\circ_{298}$ and S°_{298} of HCl, O(³P), OH(²Π), and Cl(²P).
- C14 This value is based on the results obtained below 300 K in the recent studies reported by Watson et al. (1977) and Whytock et al. (1977b). However, if the data of Benson et al. (1969) and Westenberg and deHaas (1968) are included with all the data of Watson et al. (1977) and Whytock et al. (1977b), the overall expression is almost identical.
- C15 This expression is based on the activation energy reported by Michael et al. (1977) and an A-value that has been modified to yield the mean of the values reported for k_{57} at 298 K by Michael et al. (1977) and Leu and DeMore (1976). This value is in good agreement with that reported by Watson et al. (1976). Two reaction channels

*J. Birks, University of Illinois, unpublished data, 1977.

†F. Kaufman and M. S. Zahniser, University of Pittsburgh, unpublished results, 1977.

‡M. J. Kurylo and R. Manning, National Bureau of Standards, Washington, D.C., published data, 1977.

are exothermic; however, there is no experimental evidence for process (b).

- C16 This is the estimated pre-exponential A-value to yield the 298-K value reported by Leu and DeMore (1976).
- C17 The reliability of the published values of k_{62} are certainly questionable, and there is no experimental data for k_{63} . However, the photochemical models require only $K_{eq} = k_{62}/k_{63}$ and not individual values for k_{62} and k_{63} . Although K_{eq} can be calculated from thermochemical data, the best literature value for $\Delta H_f^\circ \text{ClO}$ is uncertain by $\pm 5 \text{ kJ mol}^{-1}$, leading to an uncertainty of a factor of 10 in the value of K_{eq} .
- C18 The rate constants are not well-defined for either channel. The value shown for channel (a) is that reported by Johnston et al. (1969), whereas the value for (b) is approximately an order of magnitude greater than that reported by Johnston et al. and is influenced by two factors: (1) the ratio of k_{64a}/k_{64b} reported by Nicholas and Norrish (1968), and (2) the rate constant for k_{72a} and thermochemical data, assuming that $E_a(64b)$ is zero.
- C19 There is no recommendation because there is no experimental data.
- C20 There is no experimental data. k_{66} has been assumed to be intermediate between $k(\text{HO}_2 + \text{HO}_2)$ and $k(\text{ClO} + \text{ClO})$.
- C21 These are estimated Arrhenius expressions based on the data reported by Clyne and Watson (1974).
- C22 Although the branching ratio between reactions 72a and 72b is not well-defined, the overall rate constant (72a + 72b) is accurately known at low pressures. It is assumed in this review that the branching ratio is 2:1. There is experimental evidence for reaction 72c, but this expression was derived by combining thermodynamic data with the value of k_{75} . The low precision is due to the uncertainty associated with the value of ΔH_f° for OClO at 298 K.
- C23 The experimental data base does not strongly support the presence of a third-order reaction channel for ClO decay.

- C24 The branching ratio between channels (a) and (b) is not well-defined but, for the present discussion, is assumed to be unity. The Arrhenius expressions were estimated on the basis of data reported by DeMore and Lin* at 298 K.
- C25 These are estimated Arrhenius expressions based on 298-K data.
- C26 These are evaluated expressions based on all available data, which are normally in good agreement.
- C27 This value was reported by Chang and Kaufman (1977).
- C28 Although all three studies of k_{86} are in excellent agreement at 298 K, there is some doubt as to the temperature dependence. However, the uncertainty limits adequately allow for any temperature dependence within the 200- to 300-K range.
- C29 These are the estimated upper limit Arrhenius expressions based on the 480-K data of Kaufman and Chang.†
- C30 This is the Arrhenius expression of DeMore and Leu.‡ There is excellent agreement between this work and that of Clyne and Watson (1975) at 298 K.
- C31 This value is based on data of Clyne et al. (1976).
- C32 This value is based on data of Clyne and Watson (1975).
- C33 This is the activation energy reported by Clyne and Cruse (1970), but the A-value has been modified to yield the value of k_{92} (298 K) reported by Clyne and Watson (1975).
- C34 This is the upper limit set by Clyne and Cruse (1970); there is no evidence for reaction.
- C35 This is the estimated Arrhenius expression based on the value of k_{94} (298 K) reported by DeMore and Leu.‡

*W. B. DeMore and C. L. Lin, Jet Propulsion Laboratory, Pasadena, California, unpublished data, 1977.

†F. Kaufman and J. S. Chang, University of Pittsburgh, unpublished data, 1977.

‡W. B. DeMore and M. T. Leu, Jet Propulsion Laboratory, Pasadena, California, unpublished data, 1977.

- C36 This is an estimate; there are no experimental data.
- C37 This value is based on the data of Takacs and Glass (1973a, b).
- C38 This evaluation is based on the data of Brown and Smith (1975) and Takacs and Glass (1973c).
- C39 This value is based on the data of Davis et al. (1976b).
- D1 This is the sole fate of CH_3 radicals in the atmosphere; reaction proceeds at the rate of reaction 43.
- D2 See Hampson and Garvin (1975).
- D3 This is the A-factor chosen and activation energy derived to fit room-temperature value in Hampson and Garvin (1975).

CROSS SECTIONS AND QUANTUM YIELDS

INTRODUCTION

This subsection is concerned with photoabsorption cross sections and with quantum yields for photodissociation in the visible and ultraviolet wavelength regions for molecules that are of importance in the stratosphere. Several excellent reviews on this subject have been published recently:

- "Absorption Cross Sections of Stratospheric Molecules," by Hudson and Kieffer (1975); Section 5.8 of the Climatic Impact Assessment Program (CIAP) Monograph I
- "Rate and Photochemical Data," by Hampson and Garvin (1975); Section 5.9 of CIAP Monograph I, which contains an extensive table providing information on quantum yields and absorption cross sections
- "Photodissociation Rates in the Atmosphere Below 100 Kilometers," by Turco (1975); includes a discussion on absorption cross sections and quantum yields
- "Rate Constants of ClO_x of Atmospheric Interest," by Watson (1977); reviews absorption cross sections and quantum yields for molecules containing chlorine atoms

Table 3 lists photochemical reactions of stratospheric interest, divided into two groups: (1) reactions referred to the foregoing reviews, and (2) reactions for which there are additional data not included in the earlier reviews. Only reactions pertaining to the second group are discussed here; reference is made only to those aspects of the reactions for which new or supplementary information is available. Details of measurements, analysis of errors, etc., are not repeated here; see Hudson (1971).

The absorption cross sections reported here are defined by the following expression of Beer's Law:

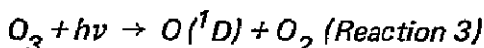
$$I = I_0 \exp(-\sigma c \ell)$$

where

$$\begin{aligned} I_0, I &= \text{incident and transmitted light intensity} \\ \sigma &= \text{absorption cross section, cm}^2 \text{ molecule}^{-1} \\ c &= \text{concentration, molecule cm}^{-3} \\ \ell &= \text{pathlength, cm} \end{aligned}$$

DISCUSSION OF PHOTODISSOCIATION REACTIONS

Species Containing N, H, and O Atoms



The photolysis of ozone at wavelengths near 300 nanometers to produce electronically excited oxygen atoms, $O(^1D)$, is a very important process in the atmosphere; the reaction of $O(^1D)$ with water is the principal source of hydroxyl radicals; and nitric oxide is produced in the stratosphere by the reaction of $O(^1D)$ with N_2O .

Several groups have reinvestigated the photodissociation of ozone since it was reviewed by Hampson (1973); table 4 (taken from Philen et al., 1977) summarizes the results of quantum yield measurements, $\phi(O^1D)$, at 313 nanometers. As table 4 shows, the disagreement is very significant: the reported $\phi(O^1D)$ values range from 0.1 to 1.0 at 298 K. The studies that report $\phi(O^1D)$ as a function of wavelength do not resolve these discrepancies.

The tentative recommendation for quantum yields at 235 K is given in table 5; this recommendation is based on the earlier work of Lin and

Table 3
Photochemical Reactions of Stratospheric Interest

1. $O_2 + h\nu \rightarrow O + O$ (a)	25. $ClO_3 + h\nu \rightarrow \text{products}$
2. $O_3 + h\nu \rightarrow O + O_2$ (a)	26. $HCl + h\nu \rightarrow H + Cl$ (c)
3. $O_3 + h\nu \rightarrow O(^1D) + O_2$	27. $HOCl + h\nu \rightarrow OH + Cl$
4. $NO + h\nu \rightarrow N + O$ (a)	28. $ClNO + h\nu \rightarrow Cl + NO$
5. $NO_2 + h\nu \rightarrow NO + O$	29. $ClNO_2 + h\nu \rightarrow \text{products}$
6. $NO_3 + h\nu \rightarrow NO + O_2$	30. $ClONO + h\nu \rightarrow \text{products}$
7. $NO_3 + h\nu \rightarrow NO_2 + O$	31. $ClONO_2 + h\nu \rightarrow \text{products}$
8. $N_2O + h\nu \rightarrow N_2 + O(^1D)$	32. $Cl_2 + h\nu \rightarrow Cl + Cl$ (c)
9. $N_2O_5 + h\nu \rightarrow \text{products}$	33. $Cl_2O + h\nu \rightarrow Cl + ClO$ (c)
10. $NH_3 + h\nu \rightarrow NH_2 + H$ (a)	34. $CCl_4 + h\nu \rightarrow \text{products}$ (c)
11. $HO_2 + h\nu \rightarrow \text{products}$ (b)	35. $CCl_3F + h\nu \rightarrow \text{products}$
12. $H_2O + h\nu \rightarrow H + OH$ (a)	36. $CCl_2F_2 + h\nu \rightarrow \text{products}$
13. $H_2O_2 + h\nu \rightarrow OH + OH$ (a)	37. $CClF_3 + h\nu \rightarrow \text{products}$
14. $HNO_2 + h\nu \rightarrow OH + NO$	38. $CHCl_2F + h\nu \rightarrow \text{products}$ (c)
15. $HNO_3 + h\nu \rightarrow OH + NO_2$ (a)	39. $CHClF_2 + h\nu \rightarrow \text{products}$ (c)
16. $SO_2 + h\nu \rightarrow SO + O$ (a)	40. $CH_2ClF + h\nu \rightarrow \text{products}$ (c)
17. $H_2S + h\nu \rightarrow HS + H$ (b)	41. $CH_3Cl + h\nu \rightarrow \text{products}$ (c)
18. $CO + h\nu \rightarrow C + O$ (a)	42. $CCl_2FCClF_2 + h\nu \rightarrow \text{products}$
19. $CO_2 + h\nu \rightarrow CO + O$ (a)	43. $CClF_2CClF_2 + h\nu \rightarrow \text{products}$
20. $CH_4 + h\nu \rightarrow \text{products}$ (b)	44. $CClF_2CF_3 + h\nu \rightarrow \text{products}$
21. $CH_2O + h\nu \rightarrow \text{products}$ (a)	45. $CH_3CCl_3 + h\nu \rightarrow \text{products}$
22. $ClO + h\nu \rightarrow Cl + O$	46. $CCl_2O + h\nu \rightarrow \text{products}$
23. $ClO_2 + h\nu \rightarrow \text{products}$ (c)	47. $CClFO + h\nu \rightarrow \text{products}$
24. $OCIO + h\nu \rightarrow O + ClO$ (c)	48. $CF_2O + h\nu \rightarrow \text{products}$

(a) Hudson and Kieffer (1975) and Hampson and Garvin (1975).

(b) Turco (1975).

(c) Watson (1977).

Table 4
Summary of Reported Quantum Yields for O(¹D) Production
from Photolysis of Ozone at 313 Nanometers

Investigator	ϕ O(¹ D)	Temperature (K)	Technique	Photolytic Source*
Castellano and Schumacher (1969; 1975)	0.75	248	Gas phase O ₃ ; decrease in O ₃ pressure	CW lamp
	1.0	298		
Kajimoto and Cvetanovic (1976)	0.53	313	Gas phase O ₃ , N ₂ O, increase in N ₂	CW lamp; chemical filter
	0.21	198		
Simonaitis et al. (1973)	0.35	298	Gas phase O ₃ , N ₂ O, increase in N ₂	CW lamp; chemical filter
Martin et al. (1974)	0.32	298	O ₃ , N ₂ O; NO ₂ chemiluminescence	CW lamp
Moortgat and Warneck (1975)	0.29	298	O ₃ , N ₂ O; NO ₂ chemiluminescence	CW lamp
Kuis et al. (1975)	0.29	293	Gas phase O ₃ , O ₂ , N ₂ O; increase in N ₂	CW lamp; chemical filter
	0.22	258		
	0.11	221		
Jones and Wayne (1970)	0.1	298	Decrease in O ₃	CW lamp
Lin and DeMore (1973/74)	0.08	235	O ₃ , isobutane	CW; monochromator
Philen et al. (1977)	0.12	298	O ₃ , N ₂ O; NO ₂ chemiluminescence	Pulsed dye laser

*CW = continuous irradiation (usually with medium pressure Hg lamp).

Table 5
 Quantum Yields for O(¹D) Production
 from Photolysis of Ozone at 235 K

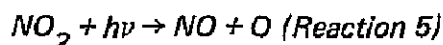
λ (nm)	ϕ O(¹ D)*	λ (nm)	ϕ O(¹ D)*
≤ 303	1.00	310	0.25
304	0.99	311	0.15
305	0.95	312	0.10
306	0.90	313	0.07
307	0.80	314	0.04
308	0.55	315	0.02
309	0.35	≥ 316	0

*Relative to $\phi = 1$ for $\lambda < 300$ nanometers.

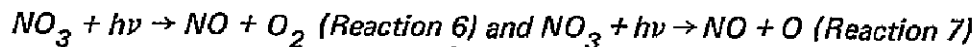
DeMore (1973), who measured quantum yields as a function of wavelength at 235 K, using a light source with a bandwidth of 1.6 nanometers. If the temperature effect is taken into account, their results are in good agreement with those of Philen et al. (1977), who determined quantum yields at 298 K as a function of wavelength, with a photolytic source having a much narrower bandwidth (about 0.1 nanometer).

The values shown in table 5 were estimated from the figure given by Lin and DeMore (1973). This recommendation is rather arbitrary; no explanation can be forwarded for the significant discrepancies at 313 nanometers between the value of 0.07 given in table 5 and the values reported by Kuis et al. (1975), Kajimoto and Cvetanovic (1976), Martin et al. (1974), and Moortgat and Warneck (1975), which are a factor of 2 to 3 larger. Further work is probably needed to resolve this issue.

The quantum yields noted in table 5 were based on the assumption that the quantum yield below 300 nanometers is unity. However, a recent study by Lawrence and Stone (private communication, 1976) has indicated that $\phi(O^1D)$ has a value between 0.87 and 0.93 for the wavelength region 274 to 300 nanometers. Therefore, if $\phi(O^1D)$ is less than unity at 300 nanometers, the relative measurements above 300 nanometers must be modified accordingly.



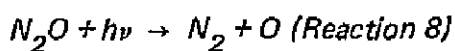
The absorption cross sections for nitrogen dioxide have been remeasured as a function of temperature by Bass et al. (1976), who report extinction coefficients every 1/8th nanometer between 185 and 410 nanometers at 298 K, and between 290 and 400 nanometers at 235 K. The effect of the dimer (N_2O_4) absorption was considered in detail, and the measurements are probably correct to within ± 10 percent. Table 6 lists these results for every 5 nanometers.



The photoabsorption cross sections of the nitrogen-trioxide radical, NO_3 , taken from Graham (1975) are included as table 7; these results supersede the earlier ones of Johnston and Graham (1974). The quantum yields, which are wavelength dependent for each of the channels (i.e., for reactions 6 and 7), are rather uncertain. For atmospheric calculations, it is recommended to use simply the photodissociation rates estimated by Graham (1975); for reaction 6, $J \cong 0.04 \text{ sec}^{-1}$; and for reaction 7, $J \cong 0.10 \text{ sec}^{-1}$ (at the Earth's surface, for overhead Sun).

Table 6
 NO_2 Absorption Cross Sections at 235 and 298 K

λ (nm)	σ (cm ²)		λ (nm)	σ (cm ²)	
	235 K	298 K		235 K	298 K
185		2.60 (-19)	300	1.09 (-19)	1.17 (-19)
190		2.93	305	1.67	1.66
195		2.42	310	1.83	1.76
200		2.50	315	2.19	2.25
205		3.75	320	2.35	2.54
210		3.85	325	2.54	2.79
215		4.02	330	2.91	2.99
220		3.96	335	3.14	3.45
225		3.24	340	3.23	3.88
230		2.43	345	3.43	4.07
235		1.48	350	3.11	4.10
240		6.70	355	4.37	5.13
245		4.35 (-20)	360	3.90	4.51
250		2.83	365	5.37	5.78
255		1.45	370	4.87	5.42
260		1.90	375	5.00	5.35
265		2.01	380	5.93	5.99
270		3.13	385	5.79	5.94
275		4.02	390	5.49	6.00
280		5.54	395	5.62	5.89
285		6.99	400	6.66	6.76
290	6.77 (-20)	8.18	405	5.96	6.32
295	8.52	9.67	410	5.32	5.77



The ultraviolet absorption spectrum of N_2O has been reinvestigated by Johnston and Selwyn (1975); their results agree with the previously measured ones in the range 210 to 235 nanometers (Hudson and Kieffer, 1975), but disagree with Bates and Hays (1967) for wavelengths above 260 nanometers. The significant new result of Johnston and Selwyn (1975) is that the cross sections at these longer wavelengths are vanishingly small, a result

Table 7
 NO₃ Absorption Cross Sections from 400 to 700 Nanometers*

λ	$10^{19} \sigma$								
400	0.0	460	3.9	520	14.4	580	29.9	640	9.8
402	0.1	462	3.5	522	17.2	582	31.0	642	6.8
404	0.2	464	4.1	524	15.0	584	24.7	644	7.1
406	0.3	466	4.5	526	13.7	586	27.5	646	5.6
408	0.3	468	5.0	528	17.9	588	44.8	648	4.3
410	0.6	470	4.9	530	20.9	590	56.7	650	3.2
412	0.3	472	5.4	532	18.1	592	48.3	652	3.9
414	0.7	474	5.6	534	17.7	594	39.2	654	5.7
416	0.3	476	6.4	536	23.2	596	41.6	656	8.9
418	0.6	478	6.6	538	21.1	598	35.4	658	16.8
420	0.9	480	6.4	540	18.1	600	24.5	660	51.2
422	0.8	482	6.3	542	16.8	602	28.4	662	170.8
424	1.2	484	6.2	544	13.9	604	40.0	664	115.4
426	0.9	486	7.4	546	20.4	606	33.8	666	48.6
428	1.2	488	8.0	548	27.5	608	15.9	668	17.5
430	1.2	490	9.3	550	22.4	610	13.5	670	7.5
432	1.4	492	8.9	552	21.6	612	16.9	672	5.7
434	1.7	494	8.8	554	24.5	614	22.4	674	3.6
436	2.1	496	10.4	556	29.5	616	17.4	676	3.1
438	1.8	498	10.8	558	31.7	618	18.3	678	5.5
440	1.9	500	9.8	560	32.3	620	24.7	680	4.9
442	2.0	502	9.1	562	26.8	622	76.1	682	2.5
444	2.1	504	10.5	564	24.8	624	116.6	684	0.9
446	2.3	506	11.9	566	25.8	626	70.0	686	0.3
448	2.8	508	10.6	568	25.7	628	68.9	688	0.4
450	2.7	510	13.0	570	25.3	630	64.1	690	0.1
452	3.1	512	16.1	572	24.8	632	32.7	692	0.0
454	3.4	514	14.1	574	25.5	634	13.2	694	0.1
456	3.2	516	14.0	576	29.2	636	12.3	696	0.4
458	3.7	518	12.1	578	30.3	638	17.6	698	0.4

* λ in nm, σ in cm².

that implies a negligible rate of photolysis of N_2O in the troposphere. This result has been corroborated by Stedman et al. (1976), who measured directly an upper limit to the N_2O photodissociation rate at ground level of $10^{-11} \text{ sec}^{-1}$.

$N_2O_5 + h\nu \rightarrow \text{Products (Reaction 9)}$

Table 8 lists data for N_2O_5 taken from Graham (1975), which supersedes the results from the review article by Johnston and Graham (1974). The quantum yields for photodissociation are unknown; possible products are $NO_2 + NO_3$ and $N_2O_4 + O$.

$HNO_2 + h\nu \rightarrow \text{Products (Reaction 14)}$

Absorption cross sections of HNO_2 have been measured in the region of 200 to 400 nanometers by Graham (1975) and Cox et al. (1976). Graham's original measurements gave relative numbers that should be multiplied by a factor of 2.4 (Graham, private communication, 1976) to bring them into agreement with the measurement of Zafonte (1975), which provides an HNO_2 photolysis rate relative to an NO_2 photolysis rate under conditions of broadband excitation (310 to 410 nanometers). The cross sections obtained in this way are at least a factor of 2 smaller than the data of Cox et al. (1976); no preferred values can be given. The two sets of data are listed in table 9.

Chlorine Containing Species

$ClO + h\nu \rightarrow Cl + O \text{ (Reaction 22)}$

The absorption cross sections of chlorine monoxide, ClO , have been reviewed by Watson (1974). Two recent calculations (Langhoff et al., 1976; and Coxon et al., 1976) indicate that photodecomposition (predissociation of the $A^2 \Pi_{3/2}$ state) of ClO accounts for at most 2 to 3 percent of the total destruction rate of ClO in the stratosphere, which occurs predominantly by reaction with oxygen atoms and nitric oxide.

$ClO_3 + h\nu \rightarrow \text{Products (Reaction 25)}$

Table 10 lists absorption cross sections of chlorine trioxide, ClO_3 , for the 200- to 350-nanometer range obtained by graphical interpolation between the data points of Goodeve and Richardson (1937). Although the quantum

Table 8
 N_2O_5 Absorption Cross Sections from 200 to 400 Nanometers

λ (nm)	σ (cm^2)	λ (nm)	σ (cm^2)	λ (nm)	σ (cm^2)
206	6.6 (-18)	246	4.3 (-19)	286	7.8 (-20)
208	5.9	248	3.8	288	7.1
210	5.2	250	3.5	290	6.3
212	4.4	252	3.0	292	5.7
214	3.7	254	2.72	294	4.9
216	3.0	256	2.55	296	4.4
218	2.48	258	2.33	298	3.8
220	2.06	260	2.12	300	3.2
222	1.71	262	1.97	302	2.7
224	1.41	264	1.86	304	2.4
226	1.23	266	1.7	306	2.1
228	1.06	268	1.64	308	1.8
230	9.3 (-19)	270	1.52	310	1.5
232	8.4	272	1.42	320	7.5 (-21)
234	7.5	274	1.31	330	4.0
236	6.9	276	1.2	340	2.7
238	6.3	278	1.15	350	1.8
240	5.7	280	1.07	360	1.0
242	5.3	282	9.9 (-20)	370	4.7 (-22)
244	4.7	284	8.9	380	1.3

Table 9
 HNO_2 Absorption Cross Sections from 200 to 400 Nanometers

1. 200- to 300-nanometer region ^(a)					
λ (nm)	$10^{20} \sigma$ (cm^2)	λ (nm)	$10^{20} \sigma$ (cm^2)	λ (nm)	$10^{20} \sigma$ (cm^2)
200	125	235	68	270	2.0
205	185	240	42	275	< 0.4
210	295	245	28	280	< 0.4
215	425	250	18	285	< 0.4
220	177	255	11	290	< 0.4
225	140	260	8	295	< 0.4
230	104	265	4	300	< 0.4
2. 300- to 400-nanometer region					
λ (nm)	$10^{20} \sigma$ (cm^2)		λ (nm)	$10^{20} \sigma$ (cm^2)	
	(a)	(b)		(a)	(b)
300	< 0.4	1.63	352	28	10.2
302		1.42	354	56	24.2
304		1.68	356	20	11.7
306		2.09	358	19	7.73
308		1.99	360	17	6.10
310	< 0.4	2.18	362	16	5.21
312	< 0.4	2.64	364	21	8.09
314	2.0	3.00	366	27	10.9
316	1.0	1.78	368	56	25.9
318	4.0	3.22	370	25	14.5
320	7.0	3.84	372	29	6.55
322	6.0	4.25	374	12	4.34
324	3.0	4.87	376	17	3.07
326	5.0	2.98	378	12	3.65
328	11.0	6.72	380	22	5.28
330	26.0	6.84	382	21	8.66
332	21.0	6.60	384	33	13.9
334	14.0	6.14	386	9	9.36
336	12.0	4.87	388	5	4.13
338	27.0	6.22	390	2	2.02
340	24.0	7.42	392	1	1.44
342	26.0	18.6	394	< 0.4	0.86
344	18.0	6.82	396	< 0.4	0.67
346	20.0	7.32	398	< 0.4	0.41
348	23.0	5.54	400	< 0.4	0.29

(a) Cox and Derwent (1976).

(b) Graham (1975) (original values $\times 2.4$).

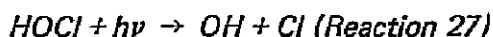
Table 10
 ClO₃ Absorption Cross Sections from 200 to 350 Nanometers

λ (nm)	$10^{18} \sigma$ (cm ²)	λ (nm)	$10^{18} \sigma$ (cm ²)
200	5.3	280	4.6
210	5.0	290	4.3
220	4.8	300	4.0
230	4.3	310	3.2
240	3.5	320	2.5
250	3.7	330	1.8
260	4.3	340	1.1
270	4.5	350	0.76

Table 11
 HOCl Absorption Cross Sections

λ (nm)	$10^{20} \sigma$ (cm ²)	λ (nm)	$10^{20} \sigma$ (cm ²)
290	6.3	380	2.4
300	9.5	390	1.6
310	11.5	400	0.8
320	13.5	410	0.6
330	11.9	420	0.5
340	9.5	430	0.4
350	7.9	440	0.3
360	4.8	450	0.2
370	2.8		

yield for decomposition has not been measured, the continuous nature of the spectrum indicates that it is likely to be unity.



The ultraviolet absorption cross sections of HOCl have been measured by Ferguson et al. (1936) and, more recently, by DeMore (1976). The recommended values, listed in table 11, are taken from the data of DeMore

(1976). The photodecomposition products have not yet been experimentally determined, although Cl atoms and OH radicals appear most likely. A theoretical study by Jaffe (1976) indicates that HCl formation is quite improbable.

$\text{ClNO} + h\nu \rightarrow \text{Cl} + \text{NO}$ (Reaction 28)

Nitrosyl chloride—a green gas—has a continuous absorption extending beyond 650 nanometers. There is good agreement between the work of Martin and Gareis (1956) for the 240- to 420-nanometer wavelength region, of Ballash and Armstrong (1974) for the 185- to 540-nanometer region, and of Illies and Takacs (1976) for the 190- to 400-nanometer region. These results indicate that the early data of Goodeve and Katz (1939) were seriously in error between 186 and 300 nanometers, whereas, at longer wavelengths, they are in good agreement with the more recent measurements.

The results of Ballash and Armstrong (1974) and of Illies and Takacs (1976) are listed in table 12. The two sets of measurements agree within 20 percent, except in the region near 240 nanometers, where the values of Ballash and Armstrong are about 60 percent higher. The recommended cross sections (also listed in table 12) were obtained by taking the mean of the two studies.

The quantum yield for the primary photolytic process (reaction 28) has been reviewed by Calvert and Pitts (1967); it is unity over the entire visible and near-ultraviolet bands.

$\text{ClNO}_2 + h\nu \rightarrow \text{Products}$ (Reaction 29)

The absorption cross sections of nitryl chloride, ClNO_2 , have been measured between 230 and 330 nanometers by Martin and Gareis (1956) and between 185 and 400 nanometers by Illies and Takacs (1976). The results are in good agreement. Table 13 lists the recommended cross sections, taken from Illies and Takacs (1976).

The photochemistry of ClNO_2 has not yet been studied. Likely photolysis products are Cl and NO_2 , and the quantum yield for decomposition is probably unity, due to the characteristics of the spectrum.

Table 12
ClNO Absorption Cross Sections from 190 to 400 Nanometers

λ (nm)	σ (cm ²)		
	(a)	(b)	Mean
190	5.34 (-17)	5.20 (-17)	5.27 (-17)
200	7.19	6.74	6.97
210	3.36	2.99	3.18
220	1.26	1.07	1.17
230	4.36 (-18)	3.17 (-18)	3.77 (-18)
240	1.91	7.68 (-19)	1.34
260	1.99 (-19)	1.61	1.80 (-19)
280	1.13	9.35 (-20)	1.03 (-20)
300	1.03	8.67	9.49
320	1.33	1.08 (-19)	1.21 (-19)
340	1.50	1.24	1.37
360	1.30	1.13	1.22
380	8.86 (-20)	7.78 (-20)	8.32 (-20)
400	5.12	5.15	5.14

(a) Ballash and Armstrong (1974).

(b) Illies and Takacs (1976).

Table 13
ClNO₂ Absorption Cross Sections from 190 to 400 Nanometers

λ (nm)	σ (cm ²)	λ (nm)	σ (cm ²)
190	2.69 (-17)	300	1.54
200	4.55 (-18)	310	1.32
210	3.39	320	1.02
220	3.42	330	7.11 (-20)
230	2.36	340	4.81
240	1.40	350	3.06
250	9.85 (-19)	360	1.82
260	6.37	370	1.07
270	3.73	380	0.62
280	2.31	390	0.38
290	1.80	400	0.21

ClONO + hν → Products (Reaction 30)

Measurements in the near-ultraviolet of the cross sections of chlorine nitrite (ClONO) have been made by Molina and Molina (1977). Their results are listed in table 14. The characteristics of the spectrum and the instability of ClONO strongly suggest that the quantum yield for decomposition is unity. The Cl-O bond strength is only about 20 kilocalories, so that chlorine atoms are likely photolysis products.

Table 14
ClONO Absorption Cross Sections at 231 K

λ (nm)	$10^{20} \sigma$ (cm ²)	λ (nm)	$10^{20} \sigma$ (cm ²)
235	215.0	320	80.3
240	176.0	325	75.4
245	137.0	330	58.7
250	106.0	335	57.7
255	65.0	340	43.7
260	64.6	345	35.7
265	69.3	350	26.9
270	90.3	355	22.9
275	110.0	360	16.1
280	132.0	365	11.3
285	144.0	370	9.0
290	144.0	375	6.9
295	142.0	380	4.1
300	129.0	385	3.3
305	114.0	390	2.2
310	105.0	395	1.5
315	98.1	400	0.6

ClONO₂ + hν → Products (Reaction 31)

The ultraviolet spectrum of chlorine nitrate has been examined in the 215- to 300-nanometer wavelength region by Martin and Gareis (1956) and in the 185- to 460-nanometer region by Rowland et al. (1976) and Birks et al. (1976a). The last two sets of measurements are in excellent agreement with each other, as well as with the earlier measurements in the shorter wavelength region. Table 15 lists the data of Rowland et al. (1976).

Table 15
ClONO₂ Absorption Cross Sections from 186 to 460 Nanometers

λ (nm)	$10^{20} \sigma$ (cm ²)	λ (nm)	$10^{20} \sigma$ (cm ²)
186	995.0	300	3.91
190	690.0	305	2.79
195	502.0	310	2.03
200	372.0	315	1.45
205	344.0	320	1.07
210	348.0	325	0.79
215	375.0	330	0.61
220	376.0	335	0.48
225	307.0	340	0.38
230	231.0	345	0.34
235	159.0	350	0.29
240	118.0	360	0.23
245	85.4	370	0.19
250	65.7	380	0.15
255	50.9	390	0.11
260	40.7	400	0.085
265	32.8	410	0.059
270	26.1	420	0.042
275	20.2	430	0.028
280	14.5	440	0.019
285	10.5	450	0.013
290	7.34	460	0.008
295	5.12		

Although the primary quantum yield for photodissociation of ClONO₂ has not yet been measured, it is very likely to be unity because of the continuous nature of the spectrum and the large excess of available energy over that needed for decomposition. Possible photolytic channels include the formation of ClO + NO₂, Cl + NO₃, and ClONO + O. The quantum yield for disappearance of ClONO₂ around 300 nanometers is about 4 for samples of pure ClONO₂ at pressures between 10 and 100 torr (Smith et al., 1977), a result that can be best explained by assuming that the primary quantum yield for photodecomposition is indeed unity.

Chlorinated Hydrocarbons

The primary process in the photodissociation of chlorinated hydrocarbons is well-established: absorption of ultraviolet radiation in the lowest frequency band is interpreted as an $n\text{-}\sigma^*$ transition involving excitation to a repulsive electronic state (antibonding in C-Cl), which dissociates by breaking the carbon-chlorine bond (Majer and Simons, 1964). As expected, the chlorofluoromethanes, which are just a particular type of chlorinated hydrocarbons, behave in this fashion (Sandorfy, 1976). At shorter wavelengths, two halogen atoms can be released simultaneously in the primary process. The quantum yield for photodissociation of chlorinated hydrocarbons is therefore expected to be unity; the studies that specifically show that this is the case for CF_2Cl_2 , CFCl_3 , and CCl_4 have been reviewed by Watson (1977). Only some recent measurements that pertain to the absorption cross sections of some chlorofluorocarbons and their temperature dependence are discussed here.

$\text{CFCl}_3 + h\nu \rightarrow \text{Products}$ (Reaction 35) and $\text{CF}_2\text{Cl}_2 + h\nu \rightarrow \text{Products}$ (Reaction 36)

The ultraviolet spectra of the chlorofluoromethanes have been examined by several groups. The results are in excellent agreement, as shown in table 16 for CFCl_3 (trichlorofluoromethane, or fluorocarbon 11) and table 18 for CF_2Cl_2 (dichlorodifluoromethane, or fluorocarbon 12), which include the room-temperature data of Chou et al. (1976a), Robbins et al. (1975), and Bass (private communication, 1976). The preferred value is the mean, listed in the last column of each table. The low-temperature data of Chou et al. (1976a) and Bass (private communication, 1976) are shown in table 17 for CFCl_3 and table 19 for CF_2Cl_2 ; the agreement is also very good. For simplicity, the recommended low-temperature values for CF_2Cl_2 are given by the following expression (Chou et al., 1976a):

$$\sigma_T = \sigma_{296} \exp [3.6 \times 10^{-4} (\lambda - 184.9) (T - 296)]$$

where σ_{296} are cross sections, $\text{cm}^2 \text{ molecule}^{-1}$, at 296 K (i.e., the last column in table 18); λ is the wavelength in nanometers; and T is the temperature in Kelvin.

Although no such simple expression is available for CFCl_3 , the temperature effect at stratospherically important wavelengths (near the 200-nanometer "window") is much smaller than for CF_2Cl_2 .

Table 16
 CCl_3F Absorption Cross Sections at 298 K

λ (nm)	ν (10^3 cm^{-1})	$10^{20} \sigma \text{ (cm}^2\text{)}$			
		(a)	(b)	(c)	Mean
186.0	54.0	255.0	247.0	226	243.0
187.8	53.5	227.0	218.0	206	217.0
189.6	53.0	197.0	186.0	175	186.0
191.4	52.5	164.0	160.0	152	159.0
193.2	52.0	141.0	134.0	125	133.0
195.1	51.5	115.0	112.0	105	111.0
197.0	51.0	93.2	93.3	84.5	90.3
199.0	50.5	74.3	74.2	70.6	73.0
201.0	50.0	59.0	58.0	55.0	57.3
203.0	49.5	45.7	44.0	46.0	45.2
205.1	49.0	34.1	32.9	33.0	33.3
207.3	48.5	24.8	23.0	23.8	23.9
209.4	48.0	17.3	16.2	16.8	16.8
211.6	47.5	11.6	11.2	11.8	11.5
213.9	47.0	7.8	7.3	7.8	7.6
216.2	46.5	4.9		5.0	5.0
218.6	46.0	3.0		3.2	3.1
221.0	45.5	2.1		1.9	2.0
223.5	45.0	1.2		1.2	1.2
226.0	44.5	0.8		0.8	0.8
	44.0				

(a) Chou et al. (1976a)

(b) Robbins et al. (1975).

(c) Bass (private communication, 1976).

$\text{CF}_3\text{Cl} + h\nu \rightarrow \text{Products}$ (Reaction 37) and $\text{CCl}_2\text{FCClF}_2 + h\nu \rightarrow \text{Products}$ (Reaction 42)

The absorption cross sections of CF_3Cl (fluorocarbon 13) and $\text{CCl}_2\text{FCClF}_2$ (fluorocarbon 113) have been measured at room temperature by Chou et al. (1976b); the results are listed in table 20.

$\text{CClF}_2\text{CClF}_2 + h\nu \rightarrow \text{Products}$ (Reaction 43) and $\text{CClF}_2\text{CF}_3 + h\nu \rightarrow \text{Products}$ (Reaction 44)

Two groups (Chou et al., 1976b; and Robbins, private communication, 1976) have examined the spectra of $\text{CClF}_2\text{CClF}_2$ (fluorocarbon 114) and CClF_2CF_3 (fluorocarbon 115). Table 21 lists the results; the recommended value is the mean, which is also listed in table 21.

Table 17
Low-Temperature Absorption Cross Sections for CCl_3F

λ (nm)	ν (10^3 cm^{-1})	$10^{20} \sigma (\text{cm}^2)$			
		252 K (a)	232 K (a)	213 K (a)	222 K (b)
186.0	54.0				233.0
187.8	53.5				202.0
189.6	53.0				176.0
191.4	52.5				143.0
193.2	52.0	164.0	161.0	161.0	143.0
195.1	51.5	141.0	137.0	137.0	120.0
197.0	51.0	114.0	110.0	110.0	97.0
199.0	50.5	91.3	88.5	88.5	79.8
201.0	50.0	72.1	69.1	69.1	62.6
203.0	49.5	56.6	54.3	53.1	50.8
205.1	49.0	43.0	41.1	40.2	38.9
207.3	48.5	31.7	30.0	28.6	28.6
209.4	48.0	22.6	21.1	19.8	19.6
211.6	47.5	15.2	14.2	13.3	13.5
213.9	47.0	9.9	9.1	8.5	8.7
216.2	46.5	6.4	5.7		5.4
218.6	46.0	3.9	3.4		3.3
221.0	45.5	2.3	2.0		1.9
223.5	45.0				1.2
226.0	44.5				0.68
	44.0				0.40

(a) Chou et al. (1976a).

(b) Bass (private communication, 1976).

$\text{CH}_3\text{CCl}_3 + h\nu \rightarrow \text{Products}$ (Reaction 45)

The absorption cross sections of trichloroethane, CH_3CCl_3 , are listed in table 22. The data are taken from Rowland (private communication, 1976). Christiansen et al. (1972) have studied the photochemical decomposition of this molecule in air. By analysis of the reaction products, the quantum yield for phosgene formation was determined to be 1.3, and the quantum yield for the primary process was assumed to be unity. An absorption spectrum from 190 to 220 nanometers was also reported in graphical form, but it is not suited for quantitative purposes. No information pertinent to this spectrum was provided, and the results are in poor agreement with those listed in table 22.

Table 18
 CCl_2F_2 Absorption Cross Sections at 298 K

λ (nm)	ν (10^3 cm^{-1})	$10^{20} \sigma (\text{cm}^2)$			
		(a)	(b)	(c)	Mean
186.0	54.0	105.0	108.0	104.0	106.0
187.8	53.5	86.5	84.5	85.1	85.4
189.6	53.0	66.1	62.8	64.8	64.6
191.4	52.5	51.4	46.0	48.7	48.7
193.2	52.0	36.7	34.0	35.3	35.3
195.1	51.5	24.9	24.3	24.3	24.5
197.0	51.0	16.8	16.5	16.6	16.6
199.0	50.5	10.9	11.0	10.5	10.8
201.0	50.0	6.96	7.00	6.65	6.87
203.0	49.5	4.37	4.40	4.32	4.36
205.1	49.0	2.66	2.60	2.52	2.59
207.3	48.5	1.53	1.50	1.47	1.50
209.4	48.0	0.90	0.87	0.90	0.89
211.6	47.5	0.53	0.49	0.50	0.51
213.9	47.0	0.32	0.27	0.28	0.29
216.2	46.5	0.19	0.17	0.16	0.17
218.6	46.0	0.10		0.089	0.095
221.0	45.5	0.05			0.05
223.5	45.0	< 0.05			< 0.05
226.0	44.5	< 0.05			< 0.05
	44.0				

(a) Chou et al. (1976a)

(b) Robbins et al. (1975).

(c) Bass (private communication, 1976).

Chlorofluorocarbonyls

$\text{CCl}_2\text{O} + h\nu \rightarrow \text{Products}$ (Reaction 46), $\text{CClFO} + h\nu \rightarrow \text{Products}$ (Reaction 47), and $\text{CF}_2\text{O} + h\nu \rightarrow \text{Products}$ (Reaction 48)

Table 23 shows the absorption cross sections of CCl_2O (phosgene), CFCIO , and CF_2O taken from the work of Chou et al. (1977). The spectrum of CF_2O shows considerable structure. The values listed in table 23 are averages over each 50-wavenumber interval. Preliminary photochemical studies (Chou et al., 1977) indicate unit quantum yield for photodissociation at 184 nanometers. The spectrum of CFCIO shows less structure, and the CCl_2O spectrum is a continuum; its photodissociation quantum yield is unity (Calvert and Pitts, 1967).

Table 19
Low-Temperature Absorption Cross Sections of CCl_2F_2

λ (nm)	ν (10^3 cm^{-1})	$10^{20} \sigma (\text{cm}^2)$		
		252 K (a)	230 K (a)	222 K (b)
186.0	54.0	103.0	102.0	99.7
187.8	53.5	83.0	80.4	81.7
189.6	53.0	61.5	58.8	60.7
191.4	52.5	46.3	44.2	42.1
193.2	52.0	32.3	30.1	29.3
195.1	51.5	21.2	19.4	19.2
197.0	51.0	13.9	12.6	12.4
199.0	50.5	8.72	7.85	7.49
201.0	50.0	5.36	4.80	4.39
203.0	49.5	3.28	2.84	2.58
205.1	49.0	1.94	1.65	1.46
207.3	48.5	1.07	0.90	0.76
209.4	48.0	0.61	0.50	0.44
211.6	47.5	0.35	0.28	0.25
213.9	47.0	0.21	0.16	0.13
216.2	46.5	0.12	0.09	0.07
218.6	46.0	0.06	0.05	0.04
	45.5			

(a) Chou et al. (1976a).

(b) Bass (private communication, 1976).

HETEROGENEOUS CHEMISTRY

The existence of aerosol particles in the stratosphere raises the possibility that heterogeneous processes may perturb the gas-phase chemistry. Much of the existing information concerning the properties of stratospheric aerosols has been summarized in CIAP Monographs I and III.

The situation with regard to chemical effects is characterized in general by a lack of specific rate data for possible surface reactions, owing largely to the difficulty of carrying out such experiments and the fact that surface

Table 20
Absorption Cross Sections for CClF_3 and $\text{CCl}_2\text{FCClF}_2$

λ (nm)	ν (10^3 cm^{-1})	$10^{20} \sigma$ (cm)	
		CClF_3	$\text{CCl}_2\text{FCClF}_2$
184.6	54.0	0.36	116.0
186.0	53.5	0.31	105.0
187.8	53.0	0.23	85.0
189.6	52.5	0.168	68.9
191.4	52.0	0.126	53.8
193.2	51.5	0.090	41.0
195.1	51.0	0.064	30.0
197.0	50.5	0.041	21.3
199.0	50.0	0.026	14.9
201.0	49.5	0.017	10.4
203.0	49.0	0.012	7.0
205.1	48.5		4.7
207.3	48.0		3.2
209.4	47.5		2.05
211.6	47.0		1.26
213.9	46.5		0.78
216.2	46.0		0.47
218.6	45.5		0.29
221.0	45.0		0.18
223.5	44.5		0.11

properties of the aerosols are not well-defined. Fortunately, however, most of the hypothetical surface effects can be ruled out by upper limit arguments. Three categories of possible surface effects are reviewed in the following subsections.

REMOVAL OF CHLOROFLUOROMETHANES (CFM'S)

This question was considered in detail in the NAS report. To summarize, it was shown that no known heterogeneous processes, including absorption, adsorption, or chemical reaction, can account for significant rates of CFM loss due to aerosols.

Table 21
Absorption Cross Sections for CClF_2 , CClF_2 and CClF_2CF_3

λ (nm)	ν (10^3 cm^{-1})	$10^{20} \sigma \text{ (cm}^2\text{)}$					
		CClF_2			CClF_2CF_3		
		(a)	(b)	Mean	(a)	(b)	Mean
186.0	54.0	10.0	10.5	10.0	0.67	0.54	0.61
187.8	53.4	7.71	8.10	7.91	0.58	0.40	0.49
189.6	53.0	5.84	6.10	5.97	0.44	0.28	0.36
191.4	52.5	4.36	4.52	4.44	0.33	0.20	0.27
193.2	52.0	3.18	3.08	3.13	0.24	0.15	0.20
195.1	51.5	2.81	2.22	2.52	0.17	0.10	0.14
197.0	51.0	1.44	1.63	1.54	0.11	0.075	0.093
199.0	50.5	0.97	1.03	1.00	0.077	0.055	0.066
201.0	50.0	0.66	0.67	0.67	0.050		
203.0	49.5	0.43	0.45	0.44	0.032		
205.1	49.0	0.28	0.31	0.30			
207.3	48.5	0.18	0.18	0.18	0.012		
209.4	48.0	0.12	0.10	0.11			
211.6	47.5	0.070	0.055	0.063			
213.9	47.0	0.044	0.041	0.043			
216.2	46.5	0.027					
218.6	46.0	0.015					
	45.5						

(a) Chou et al. (1976b).

(b) Robbins (private communication, 1976).

REMOVAL OF Cl_x

In principle, some of the more reactive forms of chlorine, such as HCl, ClO, or Cl, might be removed at significant rates from the stratosphere by incorporation into aerosols. There is evidence, however, that this is not the case. Wofsy (private communication, 1976) has shown that, on the basis of vapor-pressure data, HCl-H₂O aerosols are not stable under stratospheric conditions. Similar results probably hold for HCl-sulfuric-acid aerosols. Therefore, it is not expected that significant fractions of stratospheric HCl would be present in aerosol droplets. This conclusion is supported by measurements of aerosol composition that indicate low or zero chloride content (Lazrus et al., 1975; and Bigg et al., 1974).

For a typical aerosol concentration of 1 per cubic centimeter (assuming 0.3-micrometer radius and 2-gram-per-cubic-centimeter density), the aerosol mass concentration is about 2×10^{-13} grams per cubic centimeter.

Table 22
Absorption Cross Sections for CH_3CCl_3

λ (nm)	ν (10^3 cm^{-1})	$10^{20} \sigma$ (cm^2)	λ (nm)	ν (10^3 cm^{-1})	$10^{20} \sigma$ (cm^2)
186.0	54.0	325.0	205.1	49.0	80.5
187.8	53.5	284.0	207.3	48.5	63.9
189.6	53.0	246.0	209.4	48.0	51.1
191.4	52.5	215.0	211.6	47.5	39.4
193.2	52.0	189.0	213.9	47.0	28.1
195.1	51.5	168.0	216.2	46.5	19.6
197.0	51.0	148.0	218.6	46.0	12.5
199.0	50.5	128.0	221.0	45.5	8.3
201.0	50.0	111.0	223.5	45.0	5.1
203.0	49.5	95.4	226.0	44.5	2.9
	49.0			44.0	

This quantity is comparable to the mass concentration of Cl_x in lower regions of the stratosphere. On the basis of the aerosol composition measurements mentioned above, it follows that significant fractions of the stratospheric Cl_x are not present in the aerosol particles.

Of course, even a very small aerosol chloride content could correspond to large loss rates if there were a rapid flux of aerosols out of the stratosphere. However, the residence time of aerosols is comparable to that of gaseous species. It is therefore unlikely that aerosols provide a significant sink of Cl_x in the stratosphere.

CATALYTIC PROCESSES

Aerosols might also perturb stratospheric chemistry by surface catalysis of reactions that are slow in the gas phase. For an aerosol concentration of 1 per cubic centimeter, the collision frequency for gaseous species with the surface is of the order of 10^{-5} sec^{-1} , with some uncertainty due to the size and geometry of the particle. (In most regions of the stratosphere, the aerosol density is probably less than 1 per cubic centimeter, so that the figure 10^{-5} sec^{-1} is an upper limit.) The frequency of 10^{-5} sec^{-1} thus constitutes a reference value against which the rates of gas-phase processes are to be compared. If, as is often the case, the gas reaction that accomplishes the same net effect is much faster, the heterogeneous process can be neglected. A possible example of a significant surface process would be the catalytic conversion of active forms of chlorine (Cl or ClO) to inactive

Table 23
Absorption Cross Sections for CCl_2O , CClFO , and CF_2O

λ (nm)	ν (10^3 cm^{-1})	$10^{20} \sigma (\text{cm}^2)$		
		CCl_2O	CClFO	CF_2O
184.9		204.0		4.7
186.0	54.0	189.0	15.6	5.5
187.8	53.5	137.0	14.0	5.2
189.6	53.0	117.0	13.4	4.5
191.4	52.5	93.7	12.9	4.0
193.2	52.0	69.7	12.7	3.3
195.1	51.5	52.5	12.5	2.8
197.0	51.0	41.0	12.4	2.3
199.0	50.5	31.8	12.3	1.9
201.0	50.0	25.0	12.0	1.4
203.0	49.5	20.4	11.7	1.1
205.1	49.0	16.9	11.2	0.86
207.3	48.5	15.1	10.5	0.65
209.4	48.0	13.4	9.7	0.48
211.6	47.5	12.2	9.0	0.36
213.9	47.0	11.7	7.9	0.26
216.2	46.5	11.6	6.9	0.21
218.6	46.0	11.9	5.8	0.15
221.0	45.5	12.3	4.8	0.12
223.5	45.0	12.8	4.0	0.10
226.0	44.5	13.2	3.1	0.08

reservoirs (such as HCl). It can be shown, however, that these processes are unlikely to be important. The frequency of Cl conversion to HCl by the gas-phase reaction, $\text{Cl} + \text{CH}_4 \rightarrow \text{HCl} + \text{CH}_3$, is about 10^{-2} sec^{-1} under stratospheric conditions. Thus, the surface process could not possibly compete with the homogeneous reaction, even in the unlikely case of unit collision efficiency.

For ClO, the situation is slightly different because the frequency for ClO conversion to HCl (by the sequence of reactions $\text{ClO} \rightarrow \text{Cl} \rightarrow \text{HCl}$) is about 10^{-6} sec^{-1} . This figure is obtained by multiplying the frequency of

ClO conversion to Cl (about 10^{-2} sec^{-1} through reaction with O and NO) by the fraction of those Cl atoms that react with CH_4 rather than with O_3 (about 1 in 10^4). Since this rate is comparable to the surface collision rate, an appreciable effect might arise in the event of a high collisional efficiency for reduction of ClO to HCl. However, as pointed out in the NAS report, ClO is known to survive 10^4 to 10^5 collisions with aqueous acidic surfaces similar to those expected for the sulfate aerosols. Therefore, there is no reasonable expectation that ClO would be converted to HCl on stratospheric aerosols at a rate sufficient to perturb the gas-phase chemistry.

Perhaps heterogeneous conversion of ClO to HOCl should also be considered, although there is no evidence that the efficiency of such a process would be high. Moreover, HOCl is not an effective reservoir for stratospheric chlorine because it photolyzes with a J-value of the order of 10^{-3} sec^{-1} .

A surface process that may play a significant role in the stratosphere is the hydrolysis of chlorine nitrate. This compound can be considered to be the mixed anhydride of nitric and hypochlorous acid. The reaction, $\text{ClNO}_3 + \text{H}_2\text{O} \rightarrow \text{HOCl} + \text{HNO}_3$, might have a high collision efficiency on the surface of aerosol particles, in which case the collision frequency of 10^{-5} sec^{-1} would be competitive with the photolysis of chlorine nitrate, which has a J-value of about $5 \times 10^{-5} \text{ sec}^{-1}$ (Rowland et al., 1976). The formation of HOCl by this route would probably not be significant for reasons already given. However, production of HNO_3 by this path could be competitive with the gas-phase process, $\text{OH} + \text{NO}_2 + \text{M} \rightarrow \text{HNO}_3 + \text{M}$, as can be shown by approximate calculations. For these reasons, additional experimental studies of the rate of surface hydrolysis of chlorine nitrate (and N_2O_5) are needed.

The stratospheric H_2O_2 concentration may be reduced by surface destruction if the collision efficiency is high. This follows from the fact that the frequency of H_2O_2 destruction by reaction with OH (the dominant gas path) is about 10^{-6} sec^{-1} , which is lower than the maximum surface collision frequency.

Loss of odd oxygen by surface destruction of either atomic oxygen or ozone cannot compete with the gas-phase rates at which these species are converted to O_2 . Similarly, surface loss of OH or HO_2 cannot compete with homogeneous termination reactions of these species.

CHAPTER 2

MEASUREMENTS AND ANALYSIS OF OZONE VARIATIONS

INTRODUCTION

Variations in atmospheric ozone result from a number of interacting photochemical and meteorological processes; therefore, changes in the concentrations of some of the gases that are active in the ozone production/destruction cycle could significantly alter the amounts of ozone at various levels in the atmosphere and thus produce a net change in the total-ozone amount in a vertical column. It has been suggested that chlorofluoromethanes (CFM's) that are transported upwards from the troposphere to the stratosphere act as a significant agent for such a destruction process. It is shown in Chapter 4 of this document that the largest reduction of the ozone concentration (about 60 percent) resulting from CFM input to the stratosphere would be at about 40 kilometers with a net decrease of about 3 percent in the total amount in a time frame of about 40 to 50 years. It is therefore of particular interest to determine the natural ozone variations that occur above the ozone maximum where the most pronounced effects of the CFM's are expected to be manifested, as well as to determine natural changes in total ozone that have been observed to occur during time intervals of several years or more.

The total amount of ozone in a unit vertical column (usually referred to as "total ozone") is of the order of 300 milliatmosphere centimeters (m-atm-cm) or 0.3 centimeter at standard temperature and pressure. This amount varies typically from about 250 m-atm-cm near the Equator to about 400 m-atm-cm at high latitudes. There are large daily and seasonal variations, particularly at mid-to-high latitudes where day-to-day changes can be as high as 40 m-atm-cm per day, and the seasonal variation can be about 140 m-atm-cm. The mean surface-ozone concentration in clear air is about 3 parts per hundred million by volume (pphmv). Surface-ozone variations do not indicate a significant diurnal cycle, although the annual cycle is prominent at all latitudes. Observations of the vertical ozone distribution show maximum ozone concentrations at about 25 kilometers over the Equator and at 16 to 18 kilometers in polar regions during the spring. There is a strong correlation between the total-ozone amount and the level and strength of the maximum concentration. Large total amounts are associated with large values of the maximum concentration situated at low atmospheric levels.

Pronounced seasonal variations are present in the lower stratosphere and in the middle and upper stratosphere above the ozone maximum, particularly at high latitudes. The existence of a quasi-biennial oscillation in ozone has also been well documented, and it has been suggested that there may be a solar-cycle variation. Analysis of long-term ozone data at a number of observing stations does not indicate any clearly defined relationship between volcanic eruptions and/or nuclear explosions and ozone variations. Discussions of the distribution of ozone and its "natural" variations are contained in the Climatic Impact Assessment Program (CIAP, Volume 1, 1975).

Knowledge of the data base, including the various techniques of observations in current and planned use, is essential for detecting anthropogenically caused ozone variations. This chapter briefly discusses the techniques that have been used for total-ozone and vertical distribution, including measurement accuracy and precision. A description of data availability is provided, and sample total-ozone and stratospheric data are presented that illustrate the trends that have been deduced from the data. Comments on the problem of the analysis of ozone variations are contained in the final subsection.

MEASUREMENTS

TOTAL OZONE

Ground-Based Measurements

Observations of total ozone are currently made at about 75 locations over the Earth, with the majority (85 percent) of the stations located in the Northern Hemisphere. Dobson ozone spectrophotometers (Dobson, 1957) are used at 53 of the stations, while other instruments, generally broad-band filter ozonemeters (Gushchin, 1963) are used at 22 stations, principally in the Union of Soviet Socialist Republics (USSR). Other types of instruments are used at six stations. Two new types of instruments are presently being developed for total-ozone measurements: a grating ozone spectrophotometer (Brewer, 1973) and a narrowband filter ozonemeter (Matthews et al., 1974).

The Dobson spectrophotometer is a prism double monochromator that yields atmospheric total-ozone data from measurements of relative intensities of pairs of direct Sun or zenith sky scattered solar radiation at wavelengths in the 300- to 340-nanometer wavelength region where ozone

absorption changes greatly with wavelength. In principle, measurements on single wavelength pairs, designated as the A, B, C, and D pairs, are possible. However, in practice, observations are generally made on double-pair wavelengths, such as AD or CD, because, in this way, the effect on the measurements of light scattering by particulates is minimized. Of the various instrument types, Dobson spectrophotometers are currently considered to yield the most reliable data. Performance of the USSR filter ozonemeters has been discussed elsewhere (Bojkov, 1969; and Gushchin, 1972). Gushchin (1970) has described improvements made to the meters since 1969, and a program is currently underway in Boulder, Colorado, to assess the performance of a USSR filter ozonemeter in relation to measurements made with a United States' (U.S.) Dobson spectrophotometer.

The uncertainty ($\pm 1\sigma$) associated with the absolute calibration (accuracy) of Dobson spectrophotometers for AD wavelength observations on the direct Sun is estimated to be ± 5 percent and stems primarily from uncertainties in the ozone absorption coefficients used in reducing the observational data. Systematic errors may be incurred through assumptions made about aerosol scattering effects and the constancy of the extraterrestrial solar flux (L_0) at the spectrophotometer wavelengths. Because observations on different wavelength pairs have been found to yield somewhat different results, the International Ozone Commission has adopted AD direct-Sun observations as standard, since absorption coefficients for AD wavelengths are believed to be the least in error. For Dobson measurements made on clear or cloudy zenith skylight, relative uncertainties associated with the data compared to AD direct-Sun measurement data uncertainties are estimated to amount to ≤ 3 percent for 90 percent of the observations (Komhyr, 1961) if adequate care has been taken in devising empirical charts for reduction of the zenith-sky data. Such charts are ordinarily constructed from a substantial body of quasi-simultaneously obtained direct-Sun and zenith-sky data. Because the spectral composition of light scattered from the zenith sky depends on atmospheric aerosol loading, ozone vertical distribution, and ground albedo (which may all vary at a particular station during the course of a year), zenith-sky observations do not yield as reliable total-ozone data as do direct-Sun measurements.

Within the operational Dobson station network, larger discrepancies than those previously indicated have been found in comparisons among different instruments. For example, during an intercomparison of Eastern European Dobson instruments held in Hungary (Gushchin, 1972), differences in calibration of up to 20 percent were observed. An inter-

national comparison of Dobson spectrophotometers held in Poland (Dziewulska-Losiowa and Walshaw, 1975) revealed calibration differences among 10 instruments of up to 17 percent, although, for 7 of the 10 instruments, the calibration levels did not differ by more than 8 percent.

For a total-ozone-trend determination, the long-term Dobson spectrophotometer measurement precision is of relevance rather than the absolute measurement accuracy. Factors affecting the measurement precision are uncertainties associated with determinations of the instrument extra-terrestrial constants, the transferring of calibrations from calibrated to noncalibrated spectrophotometers, and instrument drift corrections, as well as absorption and scattering coefficient errors and errors associated with the temperature dependence of the ozone-absorption coefficients. It is estimated from a root-mean-square error analysis that, for a carefully operated worldwide Dobson instrument network with good quality control, the maximum possible long-term measurement precision corresponds to uncertainties in direct-Sun measurement data of about ± 1.5 percent and uncertainties in zenith-sky measurement data of approximately ± 3.5 percent. However, it is not likely that this can be achieved, and a practical measurement precision goal for such a station network might be uncertainties of ± 2 to ± 3 percent for direct-Sun data and ± 5 percent for zenith-sky data. These measurement precision uncertainties would be essentially random if appropriate instrument drift corrections were applied when needed. Therefore, they would not contribute significantly to uncertainties in trend determinations from data sets consisting of more than several years observations.

Within the U.S. 12-station Dobson spectrophotometer network operated during the past 15 years, uncertainties associated with the direct-Sun observations on AD wavelengths are estimated to be ± 2 to ± 3 percent, while those for zenith-sky observations are estimated to be ± 5 to ± 6 percent. Improvement in the quality of the existing data body can be made by applying final corrections to the data and reprocessing them.

The attainment of long-term, high-precision total-ozone measurements within the global total-ozone station network will require periodic (3- to 5-year interval) intercalibrations of primary standard and secondary standard spectrophotometers and an ongoing program of intercalibrations of secondary standard and field instruments. At a recent meeting in Dresden, German Democratic Republic, the International Ozone Commission recommended that U.S. Dobson spectrophotometer No. 83 be designated by the World Meteorological Organization (WMO) as the Primary Reference Standard Instrument for total-ozone measurements

and that Dobson spectrophotometers Nos. 41 and 64 (Europe), No. 77 (Canada), No. 108 (USSR), No. 112 (India), and instruments from Japan, Australia, Africa, and South America be designated as Secondary Reference Standard Instruments. Plans are currently underway for an international comparison of secondary standard Dobson spectrophotometers with U.S. instrument No. 83 to be held at the National Oceanic and Atmospheric Administration (NOAA), Boulder, Colorado, in July 1977.

The question of whether or not significant variations in L_o , the extra-terrestrial solar flux at Dobson spectrophotometer wavelengths occur during the course of a solar sunspot cycle remains unanswered. Although such variations, if any, are not expected to affect the precision of total-ozone measurements beyond the ± 1 -percent level, an optimum monitoring program requires that L_o variations be monitored by the standard Dobson spectrophotometer on a continuous basis and that any detected changes in L_o values be transferred to the field instruments by the secondary standard spectrophotometers, as required. An ongoing program to monitor L_o variations with U.S. Dobson spectrophotometer No. 83 should therefore be implemented at Mauna Loa Observatory as soon as possible. Mauna Loa Observatory is especially suited for such measurements because of the clarity of the atmosphere at that site and the relatively small day-to-day variations in total ozone that occur there during the course of a year.

In the future, satellite observations will play an important role in global total-ozone measurements and the monitoring of secular changes in ozone on a global scale. The satellite-based measuring instrumentation will require calibration data from a select set of ground-based total-ozone measuring instruments. Conversely, satellite observations of total ozone may play a useful role in identifying instruments within the worldwide Dobson spectrophotometer station network that require recalibration.

Satellite Measurements

Remote sensing from satellites permits observations over most of the globe with a uniformity of space and time sampling that is not obtainable with any other kind of observing network. Obtaining the coverage with a single instrument results in improved measurements of gradients and trends, and eliminates the requirement of intercomparing the results obtained from a large number of instruments. Satellite sounding is also cost-effective because, although the initial investment is large, the cost per datum is extremely small.

Backscattered Ultraviolet

This technique utilizes measurements of the ratio of the backscattered ultraviolet radiation to the incident solar flux in the long wavelength end of the Hartley-Huggins bands. An additional measured radiance in an absorption-free spectral region adjacent to the band is used to determine the required lower boundary reflectivity, whereas a weak dependence on vertical distribution is accounted for in a statistical sense through the use of average profiles in precalculated lookup tables. Estimates of ozone are obtained for a lower boundary either of clouds or the planetary surface, with the decision and any interpolation based on the measured albedo in the spectral region outside the absorption band.

Dave and Mateer (1967) have studied the sensitivity of ozone estimates to instrument noise and errors in lower boundary reflectivity and pressure. A 1-percent error in the measurement of the ratio of backscattered radiance to incident solar radiance is found to propagate into an error of approximately 1 percent in ozone-column amount. The major sources of error are associated with the necessity of modeling the lower boundary. Because of the wavelength dependence on the reflective properties of natural surfaces, clouds, and aerosols, the reflectance measured outside the absorption band must be extrapolated to wavelengths within the band. This can contribute to the overall error, since a 5-percent error in reflectance is found to propagate typically into ozone errors of 2 to 3 percent. Uncertainties due to lower-boundary pressure errors are found to be of the same order. Detailed estimates of sensitivity to other factors, such as aerosols and non-Lambertian and nonhomogeneous lower boundaries, have not yet been made; however, efforts are underway to address these problems.

Comparisons between total-ozone estimates from the Nimbus-4 backscattered ultraviolet instrument (BUV) and ground-based Dobson measurements have been made. Mateer et al. (1971) analyzed a heterogeneous sample of 320 near-coincident Dobson and Nimbus-4 BUV measurements and found the satellite values to be smaller than the Dobson values for low total ozone and larger than the Dobson values for high total ozone. The standard error of estimate was found to be approximately 6 percent. Similar comparisons are now being made for individual stations as a function of time, but results are not available.

Nadir-Viewing Infrared

The nadir-viewing infrared technique utilizes measurements of upwelling radiation within the 1042 cm^{-1} ozone-absorption band. Ozone-column amounts are determined from the alteration of surface radiation after corrections are made for emission by the atmosphere itself. An important limitation of the method is the need for a strong temperature contrast between the underlying surface and the ozone layer—a condition that is often poorly met at high latitudes in winter.

Prabhakara et al. (1970) compared Nimbus-3 infrared interferometer spectrometer (IRIS) ozone measurements with Dobson spectrophotometers for 23 stations and found a standard deviation of the differences of 0.020 centimeters or 5.8 percent of the mean Dobson total. A comparison of results from the higher spectral-resolution Nimbus-4 IRIS with Dobson measurements at Arosa, Switzerland, and Macquarie Island (Prabhakara et al., 1976) shows good agreement in day-to-day ozone fluctuations with a random difference of about 6 percent. However, on a seasonal time scale there are systematic differences, as large as 20 percent at high northern latitudes.

Programs to evaluate the overall accuracy and precision have not been established for either of the foregoing satellite techniques; therefore, at the present time, it is difficult to establish a quantitative error estimate for the determination of ozone trends from satellite measurements. However, as discussed in the preceding subsection, it is anticipated that, for analysis of ozone trends, satellite and Dobson data will be combined in a complementary fashion to provide results of better quality than could be achieved with either approach alone. Further work is required for determining the most effective way of combining these data. The desired outputs include not only the link between the two systems but also a characterization of the individual precisions and long-term stabilities.

OZONE VERTICAL DISTRIBUTION

Ground-Based Measurements

Dobson spectrophotometers have been used to determine ozone profiles by a method developed by F. W. Gotz in 1929 (see, for instance, Craig, 1965). This method involves observation of the ratio of the intensities of

downward scattered zenith radiation at two wavelengths in the Huggins bands (one strongly absorbed, the other weakly absorbed) as the solar zenith angle varies from about 60° to 90° . As the solar zenith angle increases, the shorter wavelength radiation is absorbed more and more compared to the longer wavelength radiation, but, at a zenith angle of about 85° , this relation tends to be reversed (hence, the name Umkehr, which means "turnaround") because relatively more of the shorter wavelength radiation is scattered vertically downward through the ozone layer. An estimate of the vertical ozone distribution can be obtained from the ratio of the radiation intensities at the two wavelengths as a function of solar zenith angle. The mean ozone concentration is calculated for nine layers (each about 5 kilometers deep) up to about 45 kilometers.

Umkehr observations are sensitive to the normal factors involved in all inversion evaluations; namely, measurement errors and errors in *a priori* statistics. In addition, however, changes in optical effects due to aerosols, temperature dependence of ozone absorption in the Huggins bands, and the effects of surface reflectivity all add to uncertainties in the application of the Umkehr method. Nevertheless, Umkehr observations represent the only long-term data base (approximately 20 years for some stations) for variations above the level of ozone maximum (see, for instance, Dutsch, 1974).

Attempts to evaluate the accuracy of the Umkehr results using simultaneous direct ozone observations have shown that the Umkehr measurements give less ozone at the level of the major maximum and more at the upper and lower levels than observed by the ozonesonde. This is due, in part, to deficiencies in the first-guess statistics used in the inversion procedure, and probably to a lesser extent to the other error sources discussed previously. Evaluation of data from Tallahassee, Florida; Aspendale, Australia; and Arosa, Switzerland, indicate that, in the low levels, the average difference is on the order of 20 to 40 percent, 10 to 20 percent at the ozone maximum, and 10 to 30 percent at the maximum altitude of the balloon observations (approximately 30 kilometers). It should be noted that accuracy of the balloonsonde decreases above about 25 kilometers. Vertical ozone-profile Umkehr observations are more sensitive to ozone changes at the higher levels (greater than 25 kilometers), and increasingly better results would be expected with altitude above that level. If random errors in the observations tend to cancel for a large number of observations, the average profiles become meaningful, and a large number of observations may be quite useful in determining time changes in gross features of the vertical ozone profile.

Rocket, Balloon, and Aircraft Measurements

Direct ozone soundings are a desirable part of any comprehensive program to test model predictions at the levels of greatest sensitivity to CFM effects (35 to 45 kilometers). These measurements can be used to determine long-term changes either directly, or indirectly used as ground-truth data for satellite remote sensors. Sounding instruments have been developed using optical, chemical, and chemiluminescent methods (table 24).

Optical Methods

Optical methods that use the height varying differential absorption of sunlight in the Hartley and Huggins bands of ozone are absolute. Results are generally reported as the integrated ozone concentration in layers 1 or 2 kilometers thick. Because the product of height resolution and precision is proportional to the signal-to-noise ratio, precision is improved by degrading the height resolution. The optimum height region for optical ozone soundings is from 25 to 55 kilometers, where the optical depth is a rapidly varying function of height. Several wavelength bands can be used to maintain good precision, as well as to produce redundant data to test internal consistency. The methodology for routine optical soundings was devised by Kulcke and Paetzold (1957), who produced a two-band filter wheel radiometer for balloons. Optical methods for inexpensive rockets were later developed in the United States by Krueger and McBride (1968), in Australia by Sissons (1968), and in Japan by Nagata et al. (1971). The U.S. instrument uses four filters at wavelengths between 250 and 320 nanometers to obtain the dynamic range for the ozone changes in the height range from 25 to 60 kilometers. The measurement precision is better than 5 percent for 2-kilometer layers, and the accuracy is estimated to be between 5 and 15 percent. Closed optical-absorption cells for surface-ozone measurements have been modified by Hilsenrath and Ashenfelter (1976) for balloon applications and by Falconer and Holdeman (1976) and Loewenstein et al. (1975) for aircraft use. The accuracy is potentially quite high, although the present altitude limit is about 35 kilometers.

Chemical Methods

Chemical methods are ideal for measurements in the troposphere and the lower stratosphere. Brewer and Milford (1960) developed an instrument based on the reaction of ozone with potassium iodide (KI) that is capable

Table 24
Direct Ozone Measurement Techniques

Technique	Reference	Data Type	Height Range (kilometers)	Advantages	Disadvantages
Chemical					
Balloonsonde	Brewer and Milford (1960)	KI bubbler	0 to 30	Good vertical resolution	Height limited by solution boiling point; subject to contamination; air-pump errors at high altitudes, requires correction to Dobson total ozone; measures total oxidant
	Komhyr and Harris (1971)	KI electro-chemical concentration	0 to 30	Good vertical resolution	
Chemiluminescence					
Balloonsonde	Regener (1960)	Dye chemiluminescence	0 to 30	High sensitivity, good vertical resolution	Calibration stability problems
Rocketsonde	Hilsenrath et al. (1969)	Self-pumping dye chemiluminescence	35 to 70	High sensitivity; good vertical resolution	Long calibration procedure; cost high
	Randhawa (1966)	Self-pumping dye chemiluminescence	20 to 60	Good vertical resolution	Calibration stability problems

Table 24 (Continued)

Technique	Reference	Data Type	Height Range (kilometers)	Advantages	Disadvantages
<u>Optical</u>					
Balloonsonde	Paetzold and Piscolar (1961)	Differential absorption of sunlight	15 to 30	Absolute	Limited vertical resolution response, day only; diffuse skylight problems at heights less than 20 kilometers; interference by other absorbers could exist
Rocketsonde	Krueger (1965)	Differential absorption of sunlight	20 to 65	Absolute; internally redundant	
	Sissons (1968)	Differential absorption of sunlight	20 to 65	Absolute, internally redundant	
	Nagata et al (1971)	Differential absorption of sunlight	20 to 65	Absolute; internally redundant	
Balloon/aircraft	Hilsenrath and Ashenfelter (1976), Loewenstein et al (1975)	Absorption cell	0 to 35	Absolute	

of fast response and that has demonstrated repeatability within a few percent. A variation of the KI technique was developed by Komhyr and Harris (1971). This instrument shows better agreement with Dobson total-ozone data than does the Brewer instrument.

Chemiluminescent Methods

The use of dry chemiluminescent methods for balloon ozonesondes was developed by Regener (1960). The primary advantages are high sensitivity (needed for measuring tropospheric ozone), specificity to ozone, and inherent simplicity. Unfortunately, production instruments exhibit instabilities, and the technique is no longer used on balloons. The high sensitivity and simplicity have continued to be attractive for rocket purposes. Hilsenrath et al. (1969) and Randhawa (1966) have pioneered this development, which uses self-pumping into an evacuated chamber for air flow. By careful attention to calibration detail, Hilsenrath (1969) obtains close agreement in ozone profiles with other techniques from 25 to 65 kilometers. He computes uncertainties of 20 percent between 25 and 55 kilometers.

Data Quality and Accuracy

The WMO and the International Association of Meteorology and Atmospheric Physics (IAMAP) have acted to maintain the quality of ozone measurements by sponsoring instrument intercomparisons through the International Ozone Commission.

Balloon Intercomparisons—In 1970, international tests compared data from the Brewer and Komhyr instruments, and Japanese, Indian, Italian, and East German (GDR) versions thereof (Attmannspacher and Dutsch, 1970). This flight series demonstrated that the operational instruments generally determined the fine structure reproducibly up to at least 30 millibars (~25 kilometers) and that adjustment factors were required to obtain agreement with Dobson total-ozone amounts.

The adjustment factors, which depended on the instrument type, were constant within a standard deviation of 5 to 9 percent. If the data are averaged over 4.5-kilometer layers, the instruments differ from the mean by less than 5 percent in the stratosphere, but errors of up to 25 percent are found in the troposphere.

The balloonsonde intercomparisons have been productive in determining instrument precisions and accuracies and in eliminating unstable instruments. Contemporary production wet-chemical ozonesondes are internally consistent within 10 percent (better if coincident total-ozone data are available) and can detect fine structure from the surface to at least 30 millibars. The accuracy at upper levels (25 to 35 kilometers) has not been tested. At these levels air-pumping errors and solution freezing can be significant problems. WMO and IAMAP are planning a new balloonsonde intercomparison series for 1977.

Rocket Intercomparisons—Regular intercomparisons of different rocket ozonesondes have not been conducted; however, several *ad hoc* comparisons have been made between U.S. instruments so that relative merits can be assessed. In 1968, the Hilsenrath chemiluminescent and Krueger opticalsondes were compared and showed no differences greater than 10 percent between 30 and 50 kilometers, including small-scale structure. In 1975, the latest comparisons of these instruments show agreement within 10 percent above 40 kilometers, but differences are greater than 20 percent at lower altitudes. Additional comparisons of these and other rocket instruments would serve to resolve these differences. Prior to this, experimenters should be encouraged to conduct repeatability flights to determine internal consistency.

The optical techniques are capable of better than 5 percent accuracy when properly applied at altitudes between 25 and 55 kilometers. With careful testing for calibration stability, the chemiluminescent techniques should be capable of similar accuracies.

Rocket and Balloon Comparisons—Few comparisons have been held. Limited experience with Komhyr chemicalsondes and Krueger opticalsondes indicates agreement within 5 percent at 25 kilometers but 20-percent differences at 30 kilometers and above.

Satellite Measurements

Backscattered Ultraviolet

The backscattered ultraviolet technique has been employed in experiments flown on Nimbus-4 (Heath et al., 1973), Orbiting Geophysical Observatory-4 (OGO-4) (Anderson et al., 1969), and Atmosphere Explorer-E (AE-E). This method makes use of radiance measurements within an

ozone-absorption band at several different wavelengths corresponding to scattering layers that cover a range of heights in the stratosphere. "Top-side" profiles can be retrieved from these data between approximately the 0.5- and 10-millibar levels. The information content of the measurements is limited by both the nature of the radiative transfer process and by the instrumental measurement errors. Analyses indicated that, for measurement errors of 1 percent, the mixing-ratio profile can be retrieved with a formal root-mean-square error of about 10 percent and a vertical resolution of approximately one pressure-scale height (about 7 kilometers). Little profile information can be extracted below 10 millibars; in this region, the profile can probably be better estimated through statistical correlation with the total column abundance (Sellers and Yarger, 1969).

Assumptions that are generally made in retrieving topside ozone profiles include molecular scattering and horizontal homogeneity. For instruments such as the Nimbus-4 BUV, in which the field of view is slightly offset between measurements at successive wavelengths, the profile is representative of spatially averaged conditions with the upper part of the profile representative of a region slightly different from that of the lower part. The assumption of molecular scattering is violated when stratospheric aerosols are present, and high-level dust layers may result in significant scattering contributions that can affect high-level retrievals (Elliott, 1971; and Cunnold et al., 1973). However, nearly simultaneous rocket and satellite retrieval profiles indicate little or no aerosol effect during 1970 and 1971.

Long-term stability of profile determinations necessitates the periodic measurement of incident solar flux. Practically, this requires that a spectrally stable transfer device be inserted in the optical train to fill the field of view. If stability is in doubt, measurements of ozone profiles to above 50 kilometers by another technique could be used to assess the solar flux.

Infrared Limb Viewing

Ozone distributions can be determined from measurements of the profiles of emission by the 1042-cm^{-1} band of ozone, as viewed at the Earth's limb (Gille et al., 1970). One of the advantages of this approach is the high vertical resolution (3 to 5 kilometers) that is possible. Other advantages are the reduction in ambiguity in data interpretation when viewing the emission against the cold background of space and nightside,

as well as dayside, operation. Data have now been obtained from the Limb Radiance Inversion Radiometer (LRIR) (Gille et al., 1975), which was launched on Nimbus-6 in June 1975.

From a noise of $0.01 \text{ W m}^{-2} \text{ sr}^{-1}$ determined for the LRIR, prelaunch calculations suggest a precision of 23 percent in the altitude range of 15 to 21 kilometers, 5 percent between 30 and 36 kilometers, and 18 percent from 45 to 51 kilometers, with an average of 12 percent over the entire 15- to 51-kilometer interval. Modified inversion procedures should improve these results.

A comparison of an LRIR retrieval and an optical rocket measurement at Wallops Island in summer (figure 1) gave a root-mean-square percentage difference of 14 percent between the satellite and rocket over the 20- to 55-kilometer range (Gille et al., 1976a and 1976b). This value is very close to the precision claimed for the rocket flight, as well as to the overall value noted previously. The conclusion is that the LRIR retrieval and the rocket measurement cannot be distinguished in quality.

The LRIR data cover the globe from 80°N to 65°S for the 7 months of operation. The reduction is now proceeding rapidly, and the data look very promising. Further comparisons of retrievals with rockets and the Nimbus-4 and AÉ BUV results are planned.

Occultation Measurements

Hays et al. (1972) and Reigler et al. (1976 and 1977) have shown that ozone profiles above about 50 kilometers can be determined by observing the occultation of stars by the ozone atmosphere at wavelengths in the Hartley band. Differences among the various observational results and between observations and theoretical calculations for the ozone densities in the tropical mesosphere and lower thermosphere suggest the need for improvements in the theory and a continued program of ozone observation at these altitudes. Pepin plans to determine ozone profiles from solar occultations in the Chappuis band during the Stratospheric Aerosol and Gas Experiment (SAGE), planned for a 1978 launch. Studies of occultation determination in the near-infrared have been performed by Drayson et al. (1972). Because no extensive body of occultation data exists at this time, no further discussion of this technique will be given.

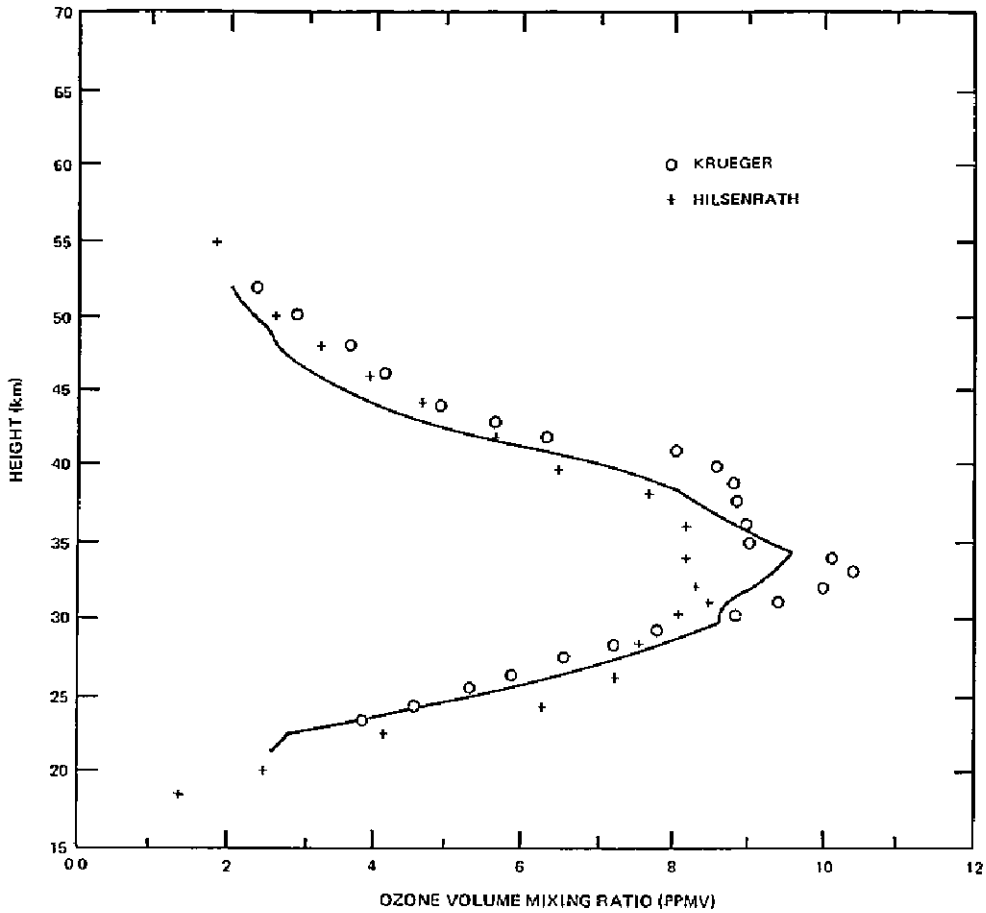


Figure 1. Ozone profile in the stratosphere over Wallops Island, Virginia, on July 29, 1975, determined by three different techniques. The solid line is a preliminary retrieval from measurements by the LRIR aboard the Nimbus-6 satellite. Symbols show *in situ* measurements from rockets by the Krueger optical ozonesonde and the Hilsenrath chemiluminescent-sonde.

Additional Measurement Techniques

Several additional measurement techniques either have been proposed or are under development. Because no body of data applicable to the CFM

problem has been produced by these techniques, they will not be discussed in detail. For completeness, differential absorption of laser radiation, laser heterodyne spectroscopy, ground-based microwave radiometry, and limb scanning at visible and microwave frequencies are noted.

ANALYSIS OF OZONE VARIATIONS

DATA AVAILABILITY

Ground-Based Observations

As previously mentioned, ground-based total-ozone observations are currently made in a global network employing Dobson ozone spectrophotometers (at about 53 stations), and broadband filter ozonemeters (at about 22 stations). Data from the stations are routinely published by the Canadian Atmospheric Environment Service, Department of the Environment (Ozone Data for the World (ODW)), in cooperation with the World Meteorological Organization. Figure 2 is a plot of the global distribution of total-ozone observing stations with an indication of those in current operation. As can be seen, most of the stations are at mid-latitudes in the Northern Hemisphere and on land.

A few Umkehr observations were made prior to the start of the International Geophysical Year (IGY). However, quasi-regular data have been available only since 1958. The present network consists of four stations in Europe, four in Japan, five in India, and four in Australia. Any Dobson station has the capability of making Umkehr measurements.

Balloons

Although many balloon data have been accumulated by limited flight programs and published independently, a few synoptic networks have been operated. The U.S. Air Force Cambridge Research Laboratory derived synoptic results from a North American network from 1964 to 1966. At about the same time, the Environmental Sciences Service Administration (now known as the National Oceanic and Atmospheric Administration) established a meridional array of sounding stations in both hemispheres. An international European network of four stations was established in the late 1960's. Long-term soundings have been made at a few stations (e.g., Thalwil, Switzerland; Weissenau, Hohenpeissenberg, and Berlin, Germany; Wallops Island, Virginia; and Aspendale, Australia). The results from the networks and time series are generally available as in-house documents and special reports. The more recent results are published in *Ozone Data for the World*.

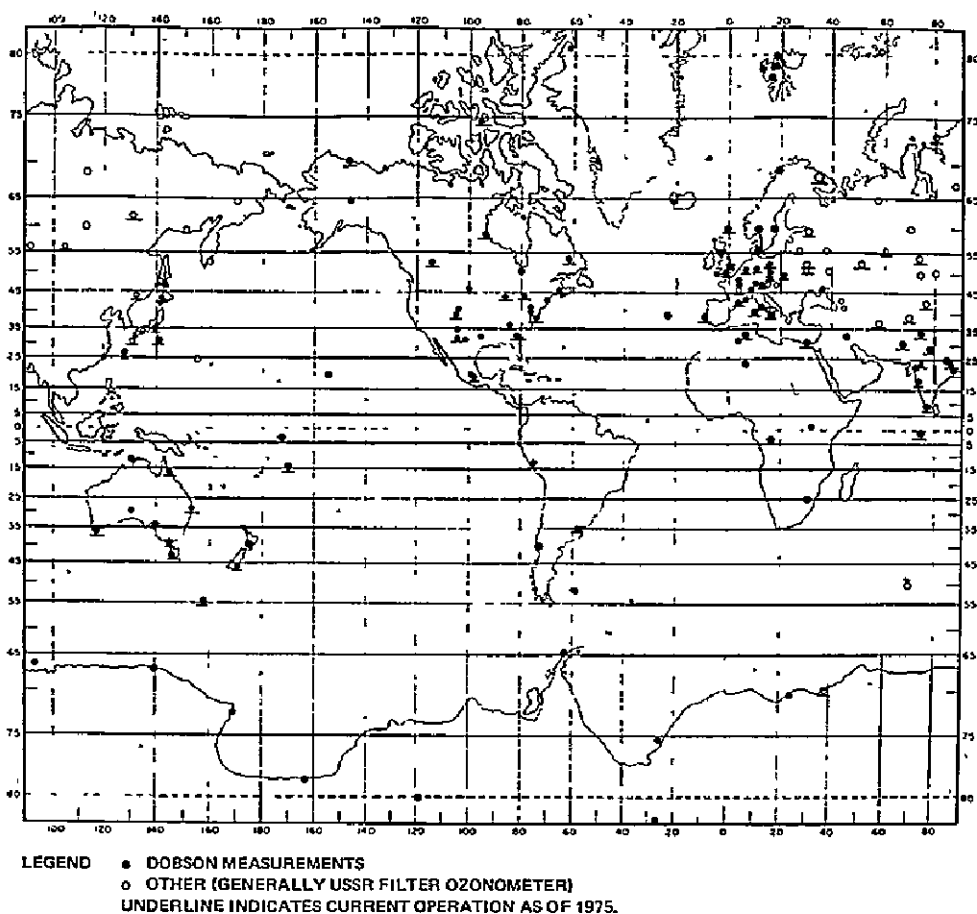


Figure 2. Global distributions of total-ozone stations.

Additional ozone measurements, originally conducted under CIAP sponsorship, were carried out on balloons by the University of Wyoming at 10 sites from the ice island, T-3, to the South Pole and by NOAA and National Center for Atmospheric Research (NCAR) (aircraft measurements using a WB 57-F). The results of these efforts are available in reports by the investigators. It should be noted that balloonborne ozone sondes provide the greatest amount of information on ozone concentrations up to the level of ozone maximum (about 25 kilometers). This is the region of most of the natural variability of ozone. These observations are therefore essential for understanding the model simulations of the nonperturbed ozone atmosphere.

Rockets

The number of rocket soundings is much smaller than the number of balloon soundings because rocket flights are generally made for special

experiments rather than for climatological purposes. The cooperative Meteorological Rocket Network is considering a program of routine flights, and the National Aeronautics and Space Administration (NASA) is conducting a series of monthly soundings from a few stations. Existing rocket data are available in individual publications, and Krueger and Minzner (1976) have constructed a "standard 45°N ozone atmosphere" from these data.

The distribution of routine stratospheric ozone measurements (Umkehr, ozonesonde, and rocketsonde) both past and present is shown in figure 3. Again it can be seen that most of the stratospheric ozone observations are currently being made over land areas in midlatitudes of the Northern Hemisphere.

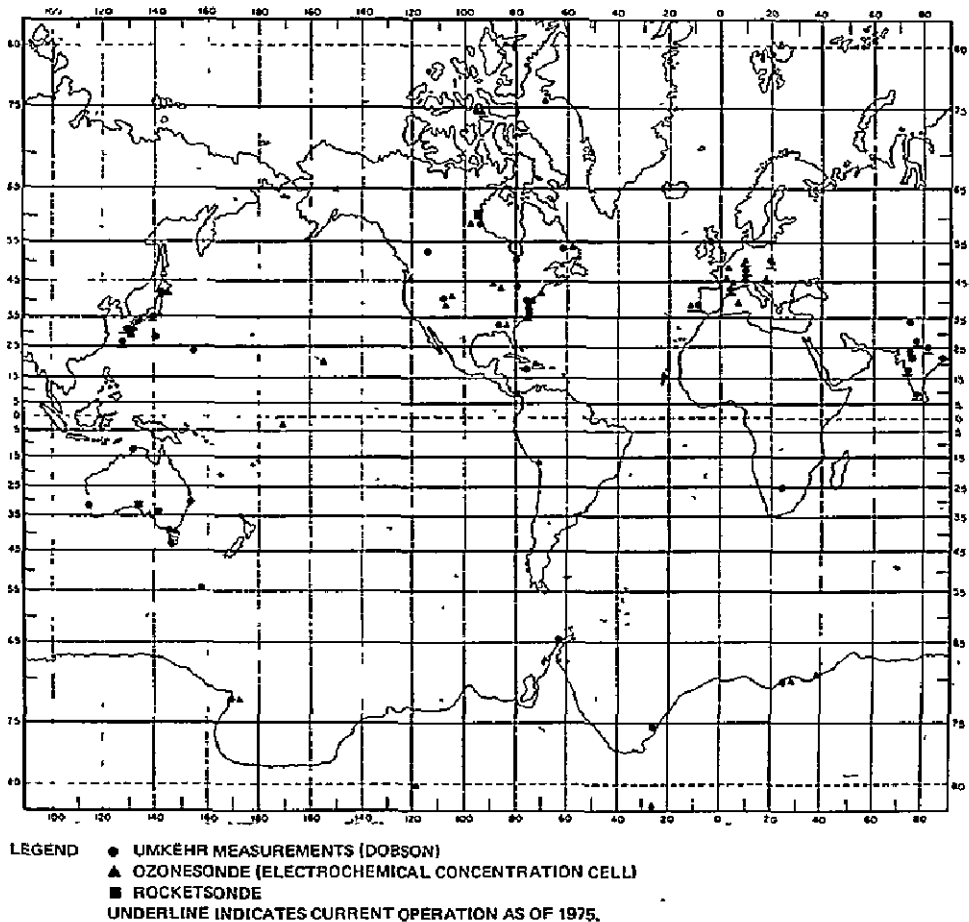


Figure 3. Observations of stratospheric ozone (1957-1975).

Satellites

By far, the most extensive satellite data set currently in existence is that obtained with the BUV experiment carried on Nimbus-4 (Heath et al., 1973). Data have been taken over approximately the past 7 years (since April 1970) and are still being acquired on a limited basis. Both high-level profiles and total-column amounts can be retrieved from these data. The latitude coverage is 80°S to 80°N , and all data are acquired at approximately local noon. Although only small samples have been reduced and published thus far, an intensive effort is currently underway to process the entire body of data and make it available to the scientific community. This task is scheduled for completion by mid-1978.

A spare Nimbus-4 BUV instrument was flown on the AE-E satellite that was launched in December 1975. Again, total-ozone and upper-level profiles are obtained by this instrument. Although the latitude range covered is only 20°S and 20°N , more nearly complete coverages in longitude and local time are possible than could be achieved with the Nimbus orbit. Preliminary reduction of limited samples of data have thus far been carried out.

Observations made on the polar orbiting satellite, OGO-4, have provided data for calculating the global distributions of the vertical ozone profiles in the range 10 millibars to 0.4 millibar. Measurements are available for the period September 1967 to January 1969. The distributions for the period September 1967 to February 1968 have been calculated (London et al., 1977), and the remaining data are now being processed.

The Nimbus-6 LRIR experiment (Gille et al., 1975) has provided limb-radiance measurements in the 1042-cm^{-1} band over a 7-month period from June 14, 1975 to January 7, 1976 (when the subliming cryogenic material was exhausted as anticipated). These data cover the globe from approximately 80°N to 65°S , with most daytime observations at approximately 1330 local time and night observations at about 2230 local time. Preliminary profiles have been retrieved from these data, and a finalized data set is expected by mid-1977.

More than 3 months of data (April through July 1969) were obtained from the Nimbus-3 IRIS, and approximately 9 months (April through December 1970) of total-ozone estimates were obtained from the Nimbus-4 IRIS experiment. These data, taken either at local noon or local midnight and covering the latitude range from 80°S to 80°N , have been described in detail by Prabhakara et al. (1976).

Future Satellite Data

In early 1977, a meteorological sounder on a Block 5 satellite began returning measurements of, among other things, upwelling radiation in the 1042-cm^{-1} band. This series is planned to maintain two satellites in orbit into the 1980's.

The Nimbus-G research satellite, to be launched in 1978, will carry improved instrumentation for obtaining both backscattered ultraviolet measurements and horizon-emission measurements of ozone.

The SAGE will measure high-resolution ozone profiles by observing solar occultations in the Chappuis band. A 1978 launch is planned for an Applications Explorer Mission (AEM) satellite.

It should be noted that there are currently no long-term plans to monitor either the ozone profile or the total ozone by satellites.

LONG-TERM VARIATIONS

Total Ozone

Ground-Based Data

In discussing total-ozone trends derived from the Dobson instruments, two basic limitations of these instruments for estimating hemispheric or global variations should be emphasized. First, the instruments may go badly out of calibration every few years, and the lack of calibration has been a continuing problem with this network. Second, the distribution of Dobson stations is not adequate for accurately estimating hemispheric or global variations, mainly because the stations were established regionally (mostly during the IGY) for studying the synoptic variability in total ozone. The problem of using a heterogeneous network has been compounded by frequent activation and deactivation of Dobson stations, and it is therefore difficult to estimate the representativeness and reliability of these data for determining total-ozone trends. The best Dobson network is to be found in the north-temperate latitudes, in which there are two regions with good Dobson coverage (Europe and North America) and two regions with adequate coverage (Japan and India).

Investigators using different methods of statistical analysis have inferred an increase in total ozone during the 1960's and generally some decline

following 1970. Komhyr et al. (1971), using a regression analysis, showed that total ozone increased by about 5 percent at most North American stations during the 1960's. Although it was initially considered possible that this was strictly a regional effect due to a shift in the long-wave pressure pattern (the total-ozone amount tends to be higher in troughs than in ridges), London and Kelley (1974), using grid-point data from mean monthly maps, showed that an increase of this magnitude occurred over much of the Northern Hemisphere during this period. Goldsmith et al. (1973), Christie (1973), and Johnston et al. (1973), using diverse analysis techniques, also detected an increase of total ozone during this period. Figure 4 shows the total-ozone variation (expressed as a percentage deviation from the record mean) in climatic zones, based on the analysis of Angell and Korshover (1976).

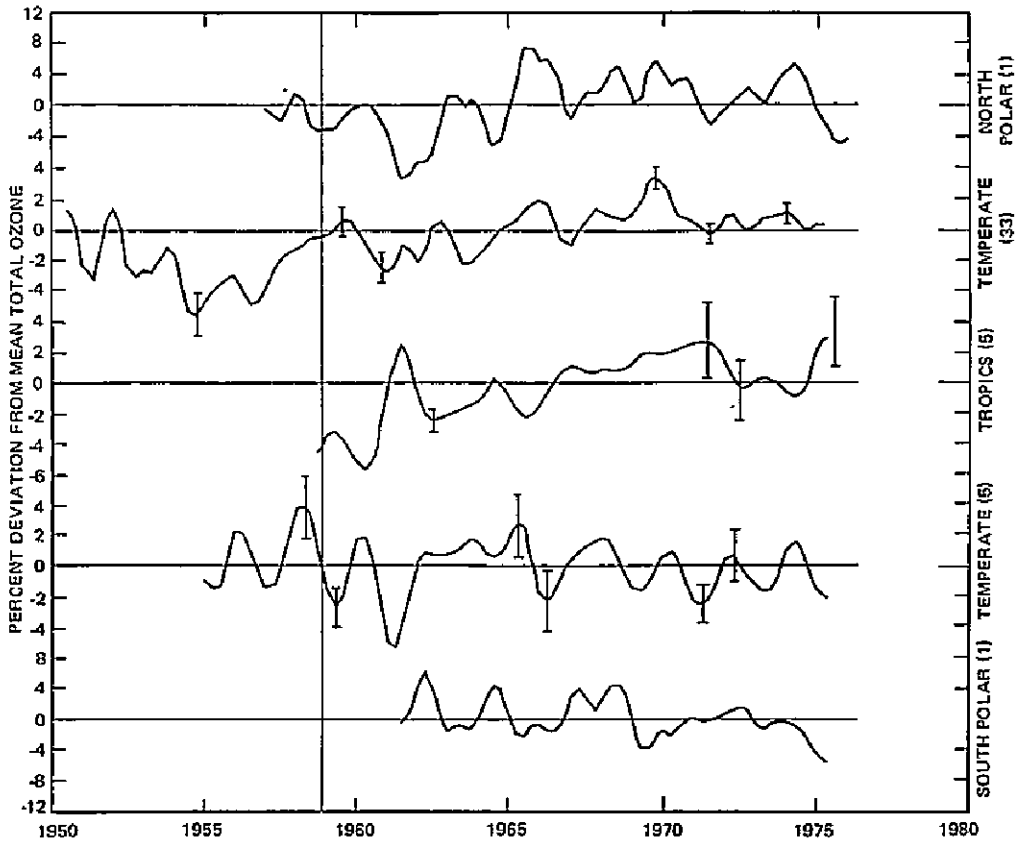


Figure 4. Time variation in total ozone for various climatic zones. Variation is expressed as a percentage deviation from the mean for the length of record. The annual oscillation has been eliminated and a 1-2-1 smoothing applied to the successive seasonal values. The vertical bars extend two standard deviations of the mean on either side of the mean, whereas the number of Dobson stations is indicated in parentheses at right.

Note that the annual oscillation has been eliminated by taking deviations from the long-term seasonal means and that the vertical bars embrace two standard deviations from the mean. If the vertical bars do not overlap, the total-ozone variation is assumed to be significant at the 5-percent level. In north-temperate latitudes, the total-ozone amount is seen to have increased by about 5 percent between 1963 and 1970, and, since 1970, it has increased by about half this amount. This variation is mostly the result of rather large variations in Europe and North America, with only a slight long-term trend in Japan and India after 1960. In the USSR, the increase in total ozone during the 1960's was about four times as great as that indicated by European and North American stations, and, accordingly, the Soviet filter ozonemeter data were not included in the north-temperate latitude average. The single north-polar station (Resolute, Canada) exhibits a trend similar to that found for north-temperate latitudes.

The Dobson network in the tropics is rather sparse and now consists of only Huancayo, Peru (in need of calibration); Mauna Loa, Hawaii (more a subtropical than tropical station); and Kodaikanal, India. The inadequacy of the tropical Dobson network is especially unfortunate because, if CFM does affect the ozone, the effect should be first noted near the Equator where the synoptic and annual variations in total ozone are small, where the photochemical effects dominate the atmospheric transport effects, and where CFM's are apparently transported upwards through the tropical tropopause by means of the Hadley cell circulation (toward the region above 30 kilometers in which the CFM's are dissociated by ultraviolet radiation). Establishment of an adequate Dobson network in the tropics is of utmost priority, as indicated by recent WMO recommendations. In the meantime, the total-ozone variation in the tropics illustrated in figure 4 should be accepted with great caution, as emphasized by the lengths of the vertical bars.

In south-temperate latitudes (Australian stations and Buenos Aires) and south-polar latitudes (Amundsen-Scott or South Pole), the total-ozone trend has been slightly downward during the period of record. Superimposed on this trend is a pronounced quasi-biennial oscillation in total ozone at the Australian stations. It is obvious that the Dobson network is also inadequate in south-temperate and south-polar latitudes, and there are recent WMO recommendations in this respect.

Figure 5 shows the derived variation in global total ozone obtained by weighting the climatic zones (figure 4) by the area of the Earth's surface

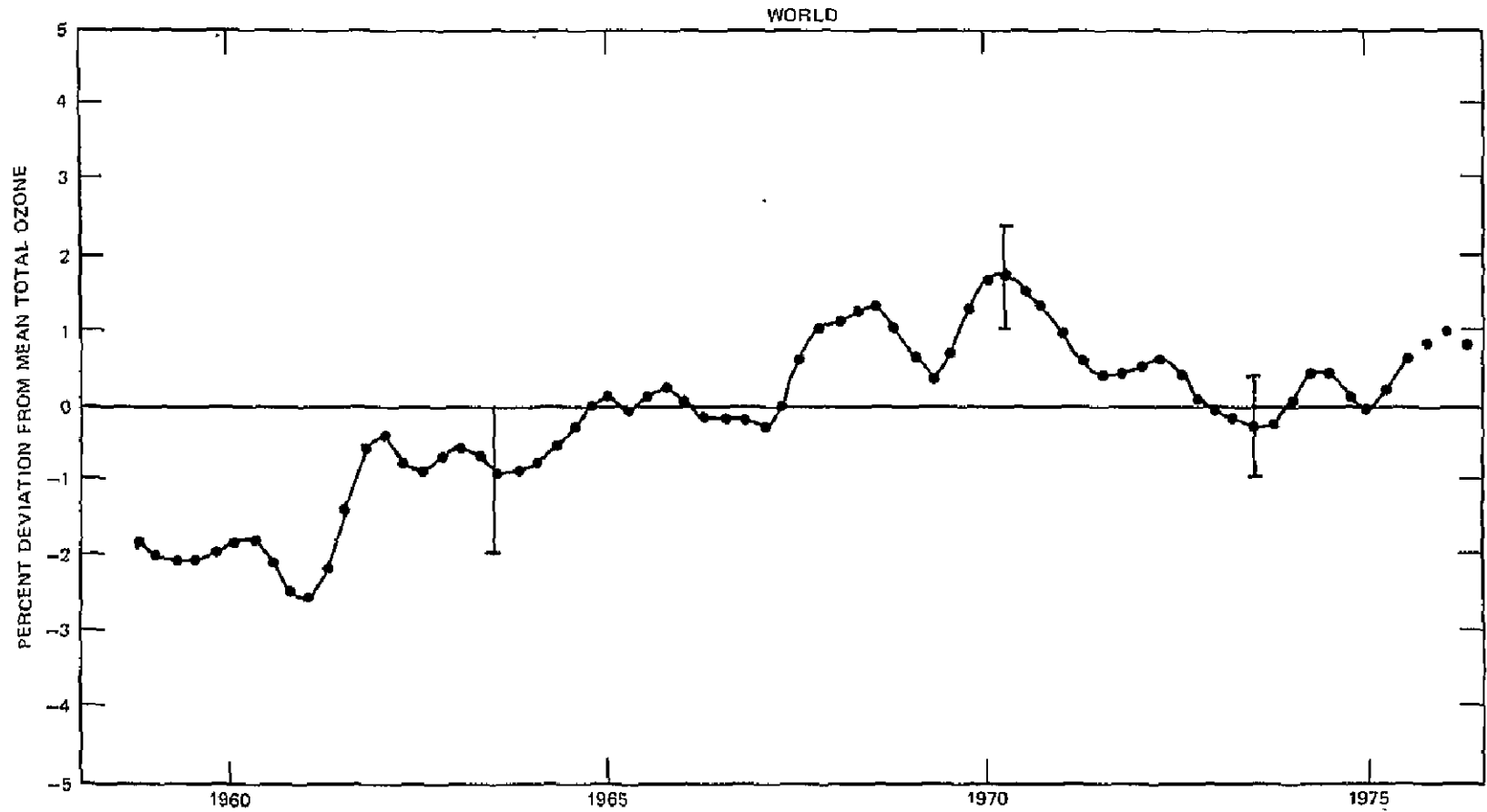


Figure 5. Time variation in total ozone for the world. Variation is obtained by weighting the climatic zones by the approximate area of the Earth's surface that they represent.

that they represent. The resulting global trends move significantly upward during the 1960's, move significantly downward during the early 1970's, and tend to zero during the mid-1970's. The slight (and provisional) increase indicated for 1976 results from the dominating effect (because of the relatively large area involved) of the tropical trend; as previously mentioned, the sparseness of data in this region make the analysis somewhat doubtful.

It is of interest to compare the global total-ozone trend in figure 5 with the trend obtained by London (unpublished) by averaging individual station values in latitude bands and then weighting these bands by the area of the Earth's surface that they represent. London obtained about a 5-percent increase in global total ozone between 1963 and 1970 in comparison with the 3-percent increase noted in figure 5 and a decrease between 1970 and 1973 of about 1.5 percent in comparison with the 2-percent decrease indicated in figure 5. This illustrates the relatively small difference in total-ozone trends obtained by applying different analysis techniques to the same data. A noteworthy feature of London's results is the increase in trend magnitude with increasing latitude, as well as the increase in shorter term variability with increasing latitude.

A factor to be considered in deducing total-ozone trends from data obtained at stations located in industrial regions of the globe is the effect of anthropogenic influences on the measurements. White et al. (1976) have reported that ozone concentrations in excess of 20 pphmv have been observed in urban pollution plumes that extend several hundred kilometers. Since background surface-ozone concentrations in clean air amount to 3 pphmv, the bulk of the observed surface ozone must be produced photochemically within the plume. Assuming a mean vertical height for a plume of 1 kilometer, a concentration of 20 pphmv of anthropogenically produced ozone amounts to an ozone contribution to the total atmospheric ozone column of 20 m-atm-cm (or 6 percent of the ozone for a total-ozone amount of about 300 m-atm-cm). At Dobson spectrophotometer stations located in areas subject to pollution, therefore, it appears worthwhile to make measurements of surface ozone along with observations of total ozone in order to estimate the contribution of photochemically produced surface-ozone variations to variations in background total-ozone amounts.

Satellite Data

As mentioned in the section on availability of satellite data, only a small amount of satellite-derived total-ozone data have been reduced and published. At the present time, comparison of absolute concentrations of

ozone determined from satellites of nonoverlapping time periods is not particularly useful for ascertaining trends, because there can be a larger uncertainty in the absolute calibrations than the likely amplitudes of the trends. The potentially most useful of the present data sets, that from Nimbus-4 BUV, has been reduced for the first 2 years of operation. For this period, the total-ozone measurement indicates a decrease of about 0.30 percent, which is in qualitative agreement with the trend deduced from the ground-based data (see figure 4). Intercomparison of results from Nimbus-4 with those from different satellites at overlapping times (e.g., AE-E) and with the Dobson network will lend confidence to the absolute values over the period through 1976.

Stratospheric Ozone

Umkehr Data

Relative to measurements of total-column abundance of ozone, stratospheric measurements of ozone density are probably of greater importance in early detection of ozone depletions attributable to CFM's. It is shown in Chapter 4 that the reduction in ozone attributable to the effect of CFM's would preferentially occur near the region where the CFM's are photodissociated, and, in this region (35 to 45 kilometers), the percentage ozone reduction would be almost nine times the reduction observed in total ozone. The satellite BUV and limb-scanning measurements should be excellent for this purpose in the future, but somewhat less precise data are now available from the Dobson instruments using the Umkehr method.

Figure 6 shows the ozone trends in the layers 32 to 37 kilometers, 37 to 42 kilometers, and 42 to 47 kilometers for the four regions (Europe, Japan, India, and Australia) over which Umkehr measurements have been obtained. The following can be seen:

- The ozone trends at these high levels are similar to the trends in total ozone. (Some similarity might be expected *a priori* because the Umkehr measurements are forced to sum to the Dobson measurements of total ozone.)
- The amplitudes of the ozone trends appear to increase with height. It is uncertain whether this variation with height is real or is somehow inherent in the Umkehr technique. (Rocketsonde data do not suggest such an increase with height.)

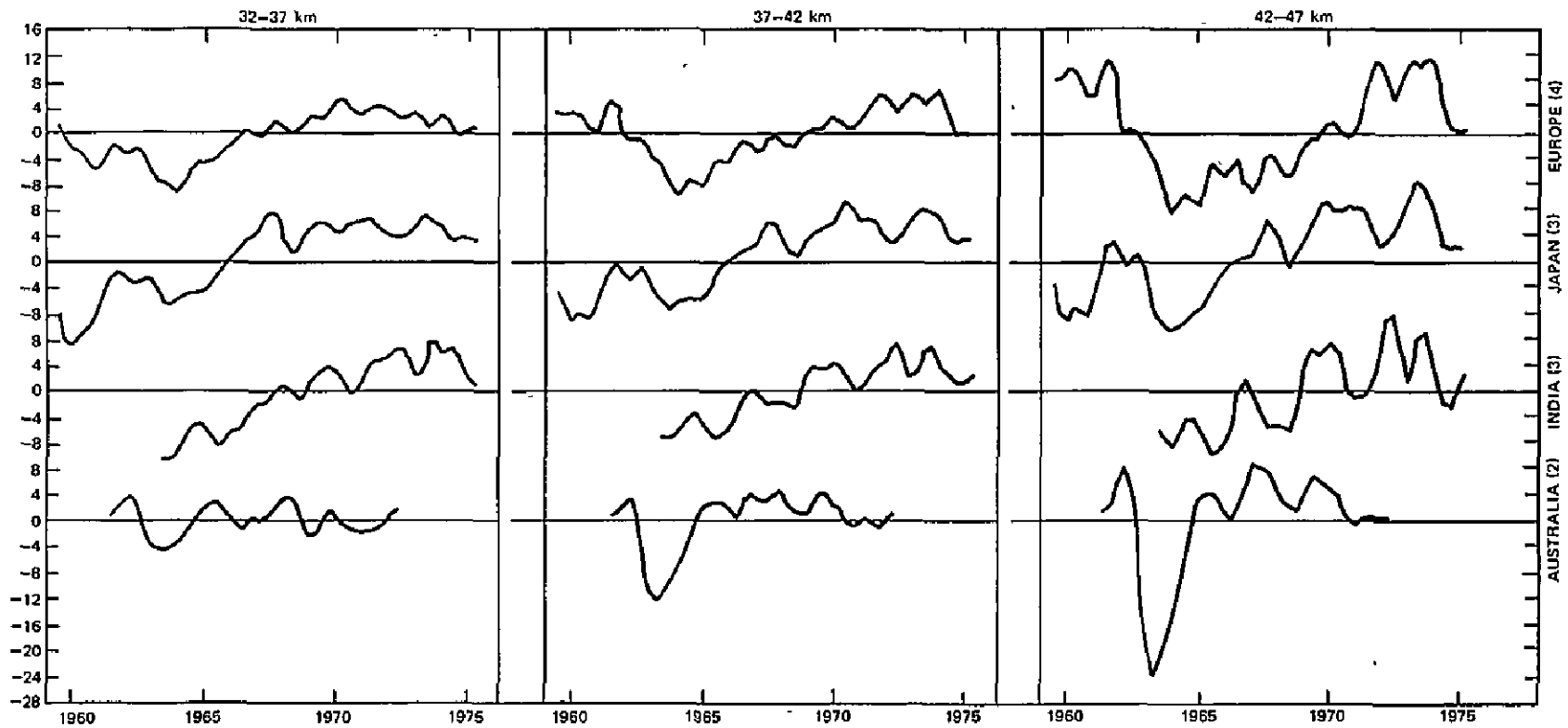


Figure 6. Time variation in ozone amount at heights of 32 to 37 kilometers (left), 37 to 42 kilometers (middle), and 42 to 47 kilometers (right) for various regions (from Dobson Umkehr measurements).

- A large ozone depletion was indicated by the two Australian stations at heights above 40 kilometers following the eruption of Mt. Agung in 1963. A more detailed analysis shows that the decrease occurred later in time the further away in latitude the stations were from the eruption site, as if a haze cloud were dispersing poleward from the volcano. Because the volcanic debris could hardly have exceeded 30 kilometers in height but the implied effect on ozone increases up to 45 to 50 kilometers, it is likely that the indicated ozone depletion is fictitious (or mostly fictitious) and attributable to the effect of volcanic aerosols on the Umkehr measurement technique.
- Between 1974 and 1975, a rather abrupt decrease in ozone occurred at the higher levels above Europe and Japan, somewhat similar to the total-ozone decrease noted in North America in 1976.

It is of interest to compare these Umkehr trends with the trends observed from ozonesonde measurements in Switzerland (London and Dutsch, 1976). They show that the increase in total ozone between 1966 and 1970 in this area was associated with an increase in ozone in the layer at 20 to 25 kilometers, but that there was very little trend at higher levels. This is somewhat inconsistent with the Umkehr results for Arosa, Switzerland, as discussed by Dutsch and Ling (1973), and comparison of the results of these two methods needs to be pursued further.

Balloon and Rocket Data

Flight platforms available for sounding this region are balloons, rockets, and satellites. The ozone profile from 2 to 74 kilometers shown in figure 7 is a composite of rocket and balloon data from the midlatitudes (Krueger and Minzner, 1976). The rocket data were taken over a period of 7 years by diverse techniques and thus give an upper limit to the variability. The mean variability between 30 and 50 kilometers is about 15 percent, in contrast to values approaching 100 percent below 20 kilometers. The low variability near 40 kilometers, combined with the greater response of ozone to CFM's at these levels, suggests an improved signal-to-noise ratio for detection of changes in this region.

Satellite Data

Measurements from the LRIR and BUV that have not yet been analyzed will give many more determinations of ozone in this region, from which

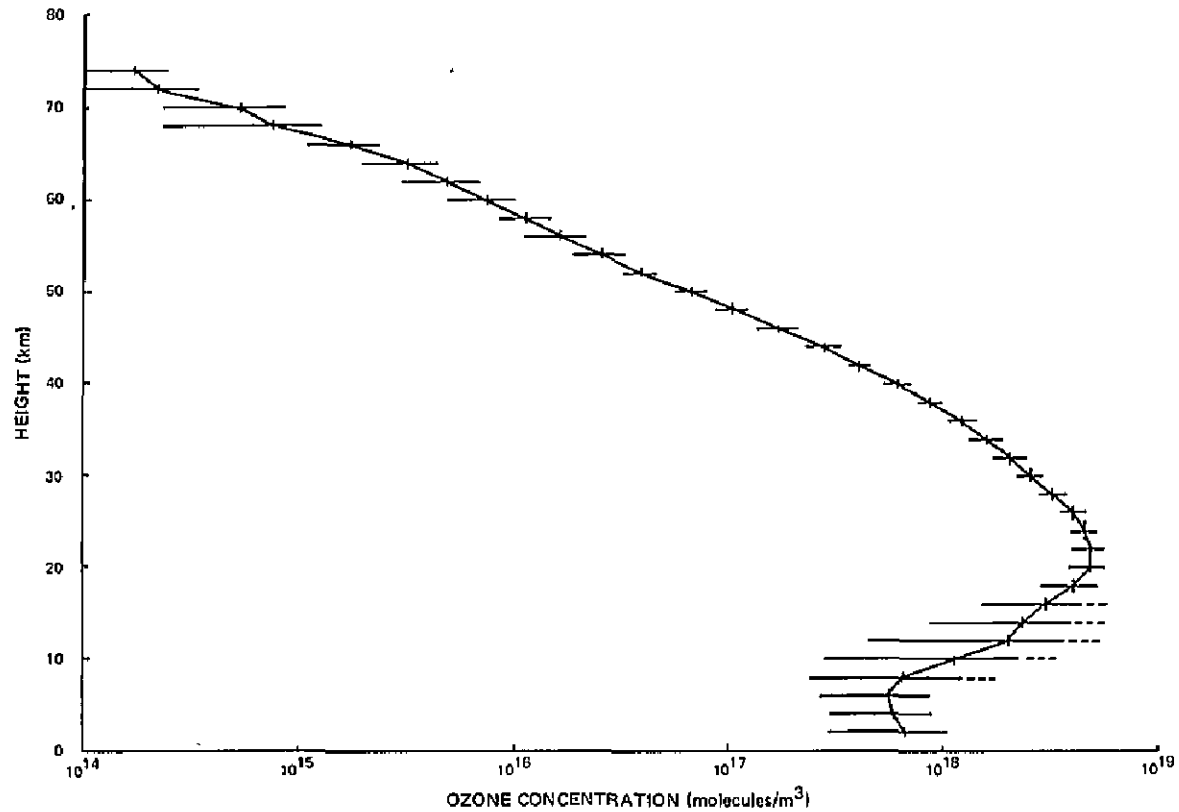


Figure 7. Model of the midlatitude vertical ozone distribution and its variability based on balloon and rocket data. The variability indicated by horizontal bars shows lower values between 30 and 50 kilometers than at other altitudes.

seasonal variation may be determined and the unexplained variability reduced. Existing measurement programs can only marginally detect predicted changes in stratospheric ozone at this time, as in the case of total ozone. However, because increased depletion is expected and because of improved satellite and rocket programs, a conclusive measurement can be expected by 1980. An improved BUV instrument and a slightly modified LRIR (denoted Limb Infrared Monitor of the Stratosphere (LIMS)) will be flown on Nimbus-G in 1978. Rockets are being systematically launched to bridge the data gap between Nimbus-6, AE-E, and Nimbus-G. This coordinated effort is capable of early detection of changes.

SOME INFERENCES ON PHOTOCHEMICAL MODELS DERIVED FROM OZONE-VARIATION OBSERVATIONS

Observations of ozone variations in the middle and upper stratosphere, in which photochemistry is dominant in determining the ozone concentration, can be used to further the understanding of the ozone chemistry in this region. The following subsections describe two examples (of many) in which such comparisons have been particularly useful.

Relationship Between Ozone Concentration and Temperature

By combining temperature observations and BUV ozone concentrations measured from the Nimbus satellite during a stratospheric warming at levels above 2 millibars, Barnett et al. (1975) found an inverse correlation between temperature and ozone concentration. Using simple photochemical theory, they showed that oxygen (and odd nitrogen) chemistry gave a much larger temperature dependence than odd hydrogen chemistry. Comparison between the calculated and observed temperature dependence showed values between the pure oxygen and odd-hydrogen chemistry values. This could indicate that the odd-hydrogen chemistry does not operate as effectively as believed or that the temperature dependence of the rate coefficients may not be correct.

Solar-Proton Events

The effects of continuous injections of ozone catalysts in the stratosphere should be detectable as long-term changes in total ozone or its

vertical distribution. These slow trends tend to be obscured by other sources of ozone variability, such as changes in atmospheric circulation. However, transient injections may be uniquely identified by their spatial and temporal signatures. In early August 1972, a sudden decrease in the density of upper stratosphere ozone at high geomagnetic latitudes was observed with the Nimbus-4 BUV (Heath et al., 1977) (figure 8). This change was coincident with a major solar-proton event, which should have enhanced the nitric-oxide concentration. The altitude distribution and amplitude of the ozone decrease were substantially as predicted in calculations by Crutzen et al. (1975). Thus, the catalytic effect of nitric oxide within the stratosphere was quantitatively supported by this observation.

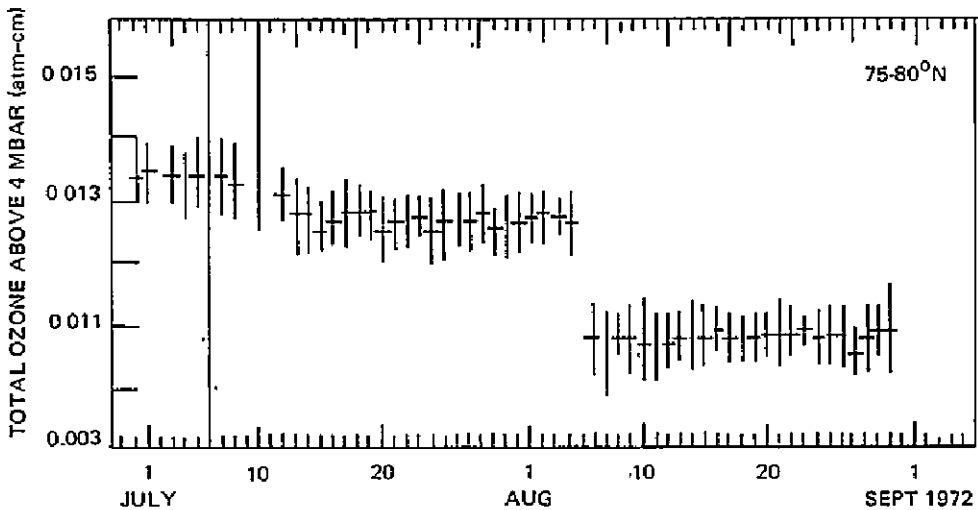


Figure 8. Decrease in the zonally averaged integral amount of ozone above the 4-millibar surface for the 75 to 80°N zone associated with a solar-proton event on August 4, 1972, as observed with the Nimbus-4 BUV. The sudden decrease in total ozone in early August 1972 was coincident with a major solar-proton event.

COMMENTS ON THE ANALYSIS OF OZONE DATA

DISTINGUISHING BETWEEN NATURAL AND ANTHROPOGENIC TRENDS

A major concern involving determination of CFM-produced ozone variations deals with the threshold of detectability, if indeed there is (and/or has been) a significant effect on the ozone concentration of past, present, and future CFM releases.

The problem of the threshold of detectability is made particularly difficult because of the high natural variability of the observed data. As pointed out in the foregoing discussion, ozone measurements exhibit many periodic variations (e.g., seasonal and quasi-biennial) and are strongly related to meteorological variabilities that tend to mask or obscure long-period ozone changes. Thus, the early effects of any anthropogenic perturbation could be so small as to be indistinguishable from the natural variations. Statistical techniques need to be used that will minimize the difficulty of distinguishing between natural and anthropogenic variations. In addition, it is necessary to determine if changes that are observed in the ozone concentration are global in extent or simply the result of a redistribution of ozone due to meteorological variations (e.g., shifting of atmospheric circulation patterns).

Total ozone* at a particular location can be considered a random or stochastic function of time, $O_3(t)$, made up of two distinct components: periodic oscillations and a nonperiodic component. The observed time variation of ozone is then given by:

$$O_3(t) = O_3 + \sum_i F_i O_3(t) + X'(t)$$

where

O_3 = the long-term average

$F_i O_3(t)$ = the *i*th periodic component

$X'(t)$ = the residual nonperiodic component

*Reference to total ozone could be just as well applied to ozone concentration at some level.

The periodic part can be modeled as the sum or superposition of several periodic functions of time, each with a different amplitude, phase, and period. These amplitudes, phases, and periods may be random processes themselves so that the periodic variations may be called "quasi-periodic." Without loss of generality, it can be assumed that the time average (averaged over all time) of the periodic component of $O_3(t)$ is zero.

The nonperiodic component can then be reduced to a function of time, $X(t)$, plus white noise, $E(t)$, having a variance, $\sigma_X^2(t)$. For the purposes of discussion, assume that $\sigma_X^2(t) = \sigma_X^2$, (i.e., the variance of the white noise does not change with time). Thus, the nonperiodic component of $O_3(t)$ might look like the graph in figure 9.

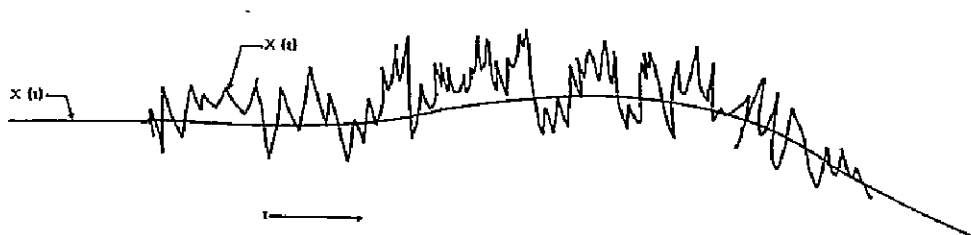


Figure 9. Time variations of the nonperiodic component of ozone (schematic).

$X'(t)$ can be filtered by various standard methods to give $X(t)$ a smooth function of time. The total ozone will be said to have no trend if $X(t) = \text{constant}$ (that is, if $X(t)$ is stationary). A variation of $X(t)$ with time will be a trend. In this definition, nothing is said about the cause of the trend—whether it is "natural" or a result of man's intervention—or how long it persists.

Note that the definition of the periodic variations as having a zero time average presupposes a knowledge of $O_3(t)$ for all time. In practice, only some finite interval of time, T , can be observed. In the case of total ozone, the largest value of T , that at Arosa, Switzerland, is less than 50 years, whereas most observing stations have less than 20 years of data. This implies that some natural oscillatory waves may have periods that cannot be distinguished from nonperiodic trends. Thus, apparent trends in a data set can, in fact, be parts of long-wave natural oscillatory variation.

STATISTICAL ANALYSIS APPLIED TO PRESENT DATA SETS

Virtually every statistical analysis seeking to detect a trend attempts in one way or another to remove or "filter out" the oscillatory component of the data and to isolate the nonperiodic component.

Three basic steps are usually taken. The first involves data smoothing in which "raw" data are replaced by averages of data that are close together in time and space. This smoothing removes some of the high-frequency variations and some of the white noise. The next step is to determine the different periodic variations. Any oscillatory variation that is not removed in this process remains as a part of the "residual." The third step is an examination or modeling of these residuals in an effort to estimate $X'(t)$ and $X(t)$. The consequence of leaving unevaluated periodicities in the residuals is that the estimate of S_x (the standard error of the estimate) becomes inflated. Since the errors made in estimating $X(t)$ are proportional to S_x , a goal of any trend analysis should be to remove as much significant periodic variations as possible to reduce the variance in the residuals.

A method that reportedly reduces S_x significantly is the time-series analysis discussed by Hill and Sheldon (1975). According to their analysis, residuals in the total-ozone data from Arosa, Switzerland, appear to be white noise, and there is no significant trend for the entire data period (1932 to 1974). It should be noted, however, that a significant upward trend of total ozone was noted by Komhyr et al. (1971) in the data for Arosa for the period 1960 through 1970. As Birrer (1974) has shown, trends in past Arosa data lose their significance with an increase in the period for which the trends are calculated. A model of the Arosa data prior to 1970 was used by Hill and Sheldon (1975) to predict the observed downward trend through 1974. This prediction is largely a consequence of the continued propagation of the unexplained 133-month period in the ozone record at Arosa as described by them.

THRESHOLD OF DETECTABILITY

Errors made in estimating the slope, β , of a linear trend are proportional to S_x/\sqrt{n} , where n is the number of independent observations. For any S_x , the minimum detectable slope can be determined as a function of n . Since this "minimum detectable trend" is also dependent on S_x , the result is dependent on the statistical method used to remove the periodic components of $O_3(t)$.

Using their model involving data from a sample of nine globally distributed stations, Hill et al. (1977) estimated that a trend producing a 1.56-percent change over 6 years would be statistically significant. This means that if a linear trend with slope $\beta = 0.26$ percent per year begins at time t_0 , then, by time = 6 years, this linear trend will be recognizable from the zero trend observed in the larger data set prior to time t_0 (shown in figure 10).

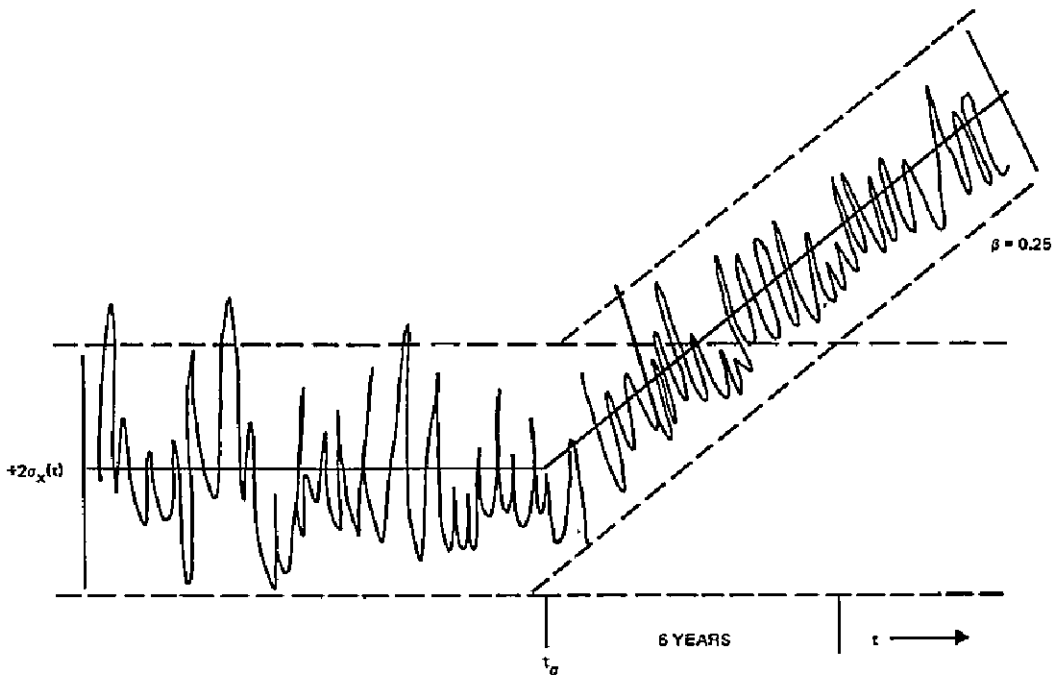


Figure 10. Schematic representation of the time variation of the non-periodic variation resulting from an arbitrary perturbation.

As mentioned previously, the ability to obtain this high sensitivity is based on how well S_x (a function of the residual statistics of the large data set prior to time t) can be reduced. The level of detectability claimed by Hill et al. (1977) is lower than that previously estimated by Pittcock (1974) for a global network. A large part of the difference in the two estimates is probable due to the fact that the statistical analysis used by Hill et al. (1977) resulted in smaller residual variances. Pittcock did not remove the variance due to the mean annual cycle from his data.

If a "statistically significant" trend is observed, it could indicate that $X(t)$ is changing due to some disruption in the equilibrium that existed prior to time t , or that the model used to remove periodic components is breaking down due to shifts in periods, amplitudes, or phases that may themselves be random.

SUMMARY AND CONCLUSIONS

The present estimate of the effect of CFM's injected into the stratosphere is a long-term reduction of total-column abundance of ozone of about 7 percent with a maximum reduction of the order of 60 percent in ozone concentration in the middle and upper stratosphere (35 to 45 kilometers). A careful analysis of the past records of total ozone and its vertical distribution contributes to an understanding of the origin of natural variations of ozone (both periodic and nonperiodic) and therefore should aid in detecting ozone variations that are related to the predicted reduction.

The data base for determining perturbations in the ozone series is best documented in the observations of the total amount. However, because the largest percentage of reduction in ozone is expected to occur at about 40 kilometers and to occur earlier at this level than in the total amount, special efforts should be made to provide information on the natural variations at this height and to detect the predicted CFM effects.

Many measurement techniques are available for determining total ozone with the use of ground-based and/or satellite platforms. An obvious and important advantage of satellite observations is the potential for global coverage, and continued satellite total-ozone monitoring programs need to be assured. The ground-based measurements have the benefit of a long history of observations with about 75 observing stations operating in the present international network, some of which have taken observations more or less continuously for 20 years or more. Although the precision of these techniques varies somewhat, it is of the order of ± 3 to ± 5 percent for ground-based methods and about ± 5 percent for satellite determinations of total ozone. It should be emphasized that a coordinated program of complementary ground-based and satellite measurements is capable of providing better quality determinations of total ozone than those that can be obtained with either technique alone.

The best methods for determining long-term trends in the vertical ozone distribution are through Umkehr observations because they provide a relatively long-term data base or through the use of balloonborne and rocketborne or satellite platforms, with the latter two the more promising for the region above 30 kilometers. In addition, rocket observations present an excellent way to calibrate the satellites, and a coordinated program of *in situ* and satellite measurements holds the best promise for obtaining good-quality profile information.

The variability and long-term trends in total ozone are closely related to the variability and long-term trends at and just below the level of ozone maximum. Indications are that the natural variability of the ozone concentration decreases above the ozone maximum in the tropics and mid-latitudes. At high latitudes during winter, however, the variability is quite large with evidence of large fluctuations associated with meteorological perturbations (e.g., sudden warmings). Thus, observing systems designed for determining the presence of CFM-induced trends in the middle stratosphere should be planned to focus on those atmospheric regions in which the natural periodic and nonperiodic variations are smallest and in which photochemistry is the dominant process that produces ozone variations.

Analysis of past total-ozone data indicate the broad features of the temporal ozone changes (i.e., seasonal variations), as well as the general increase in ozone in the Northern Hemisphere during the 1960's. However, the seasonal variations and long-term trends in the stratosphere, particularly above the level of maximum ozone are not nearly as well-documented. Extension of the ozonesonde network would contribute important information on ozone variability in regions of the largest concentrations. However, it is essential that provisions for a long-term stable satellite and rocketsonde program be made to fill the gap of ozone information in the stratosphere.

Although presently available statistical techniques appear to be adequate for filtering the various "natural" periodicities in the ozone records and for giving estimates of the variance of the residual data, work now in progress gives promise that statistical analysis of long-term ozone trends can be improved to give more definitive results of possible interruptions (or modulation) of the present patterns by CFM inputs to the atmosphere. However, it is clear that a larger data set (based on more precise observational techniques) than is currently available is needed to verify the rate of ozone destruction by CFM's postulated by the models discussed in this document.

Regarded as being generally correct and timely is that part of the general statement contained in the report of the Committee on Impact of Stratospheric Change (Tukey Report), which states that studies must be conducted dealing with:

- “ . . . Development and general acceptance of standard methods for routine mapping and summarization of the measurements of the distribution in space and time of ozone and other low-concentration constituents. The reduction of such measurements is far from

trivial and requires well-chosen allowances for fluctuations both in smoothing and in stating the uncertainties of the results.”

- “. . . Processes and mechanisms determining the natural variations of ozone, particularly the longer-term changes. As we improve our understanding of natural ozone changes, we will be able much more easily to interpret observed changes, to identify human-produced changes, and to give guidance to the assessment of historical changes in UV-B intensity.”

CHAPTER 3

MINOR SPECIES AND AEROSOLS

INTRODUCTION

In the present state of the art, stratospheric measurements are available only for some of the most critical species. In some cases, successful techniques have not yet been developed. Nevertheless, a variety of species have been measured and the existence of critical species in the stratosphere has been established. In this chapter, an attempt is made to establish some order to the measurements that have been made and in the type of problems that exist.

A measurement of the species that represent sources and sinks as a function of latitude can be of considerable help in tying together the efforts of one-dimensional (1-D) and multidimensional models. Given appropriate information on latitude variations, boundary-value terms for the equations can be developed. In this case, efforts to enhance the precision and cross-correlation of results among various investigators are important.

In the evaluation of sinks and sources in the troposphere, the limiting factor is the accuracy with which measurements can be made. At present, there are no standards by which various groups can verify the absolute accuracy of their techniques. The development of such standards is necessary if accurate estimates of tropospheric sinks are to be possible.

Another type of constituent measurement is that which checks models involving the creation and destruction of radicals. For these models, measurements with high accuracy are not as important as good precision and the availability of a variety of correlated measurements. Each of these requirements will be discussed later in this chapter.

The physical and chemical processes that occur in the stratosphere are so complex and coupled that measurements of the chemical species and physical parameters involved are necessary for obtaining an understanding of this region of the atmosphere. These measurements can, and do, provide the knowledge required for identifying individual phenomenon, for assessing their importance, and for providing necessary quantitative checks and constraints on theoretical descriptions of the processes involved. These checks assume increased importance when theoretical descriptions are used for prognostication, as in the case of the evaluation of chloro-fluoromethane (CFM) influence on stratospheric ozone.

The ultimate interest in this assessment is whether total-ozone column density and ozone distribution is changed by the release of CFM's into the lower atmosphere. This interest necessarily involves the identification and consideration of the processes responsible for ozone loss and production. It involves a scale that is global, evaluation of photochemical processes involving species that exist in the stratosphere, and interaction of the production and loss of trace species with the general circulation and other transport processes that occur in the atmosphere. The state of empirical and theoretical knowledge concerning many of these species and processes is at a rudimentary level.

Many species are important to the calculation of ozone destruction. Those species that have been identified as being most important are listed in table 25 along with pertinent data concerning the extent to which they have been measured. In addition, a variety of ratios are important in the chemistry of ozone. In some instances, these ratios can be shown to be determinable from relatively simple measurements. Chief among them are the O/O_3 ratio, the NO/NO_2 ratio, and perhaps the Cl/ClO ratio. In almost all instances, these ratios depend strongly on the solar-flux value that dissociates the principal molecule. The solar flux from about 180 to 600 nanometers is the region of most importance for a variety of stratospheric species. It is well known that the flux in the region below about 130 nanometers varies with solar activity. It is also known that the solar constant appears to be constant to a few percent when measured from the ground. The spectral region between about 150 and 350 nanometers is not easily monitored, and less is known about the constancy of the Sun in this region. In the past, it was generally assumed that the critical region between 200 and 300 nanometers did not vary in time. Recent results indicate that this assumption may be in error (Heath and Thekaekara, 1976). At present, no solid experimental data exist on which either the constancy or the variability of the Sun in this spectral region can be determined.

A parameter that has only recently been considered is the error introduced by assuming single scattering models (Callis et al., 1975; Luther and Gelinis, 1976; and Luther and Wuebbles, 1977). At present, few experimental data exist that can be used to establish the validity of single versus multiple scattering models. This is an area in which experimentation is needed.

In the discussion of photochemistry, a phenomenon often referred to is mixing or transport. The effects of these phenomena and the ways in which they are parameterized in models are extensively discussed in other

Table 25
Important Species

Species	Meas	No. of Meas	Technique*	Height Profile	Latitude Profile	Seasonal Variations	Temporal Variations	Hemispheric Variation
CFCl ₃	Yes	Many	a	0-35	Yes	?	?	Yes
CF ₂ Cl ₂	Yes	Many	a	0-43	Yes	?	?	Yes
CCl ₄	Yes	Many	a	0-21	Yes	-	-	Yes
N ₂ O	Yes	≥ 10	a, b, d	5-35	-	-	-	-
CH ₄	Yes	> 10	a, b	12-50	-	-	-	-
NO	Yes	Many	c, b	17-60	Yes	Yes	Yes	-
NO ₂	Yes	~ 10	h, b	10-37	Yes	Yes	Yes	-
HNO ₃	Yes	~ 5	d, b	12-39	Yes	?	Yes	-
Cl	Yes	2	g	35-44	-	-	-	-
ClO	Yes	3	h, e, g	23-42	-	-	-	-
Cl ₂	No							
ClONO ₂	Yes	2	b	No	-	-	-	-
HCl	Yes	~ 10	d, b	12-32	Yes	-	-	-
HO	Yes	> 6	g, i	0-70	-	-	Yes, column abundance	-
HO ₂	No							
H ₂ O ₂	No							
H ₂ O	Yes	Many	e, f, h	-	-	-	-	-
HBr	Yes		d	Yes	-	-	-	-
HF	Yes	~ 4	b, d	No	Yes	No	-	-
O	Yes	2	g	45-27	-	-	-	-
H ₂	Yes	7	a	15-50	-	-	-	-
Total chlorine	No							

a = a sample
b = infrared spectra
c = chemiluminescence
d = altimeter
e = thermal radio emission
f = hygrometer
g = *in situ* response fluorescence
h = visible and/or ultraviolet absorption spectra
i = fluorescence

chapters of this report. In this chapter the few measurements that are now available are discussed.

In considering the mixing processes in the stratosphere, it should be noted that most height and many horizontal profiles of trace constituents present large variability over apparently very small scales. The term "transport" is usually invoked to explain these variations. Mechanisms are rarely discussed, however, by which processes that move air can alter the concentration of a trace constituent. If such mechanisms do not exist, then air must have been moved in from another altitude at which the observed concentration is prevalent. At present, few data sets exist that are complete enough to permit an accurate description of such processes, especially on a mesoscale.

SUMMARY OF ATMOSPHERIC MEASUREMENTS

The strong chemical link among the chlorine, nitrogen, hydrogen, and oxygen photochemical systems in the stratosphere dictates that discussions of the field measurements be divided not according to chemical identity, but rather according to: (1) whether the species constitutes a chemical source that in general enters the stratosphere through the tropopause, is destroyed by reaction or photolysis, and is not reformed in a further photochemical step; (2) whether the species is a chemical sink or "reservoir" term that is a product of the photochemical reactions taking place in the stratosphere and that is carried downward out of the stratosphere into the troposphere; or (3) whether the species is a reactive fragment or radical that is produced from the source term by photolysis or oxidation and that recombines to form the sink terms. Advancements since the National Academy of Sciences (NAS) report in each of these areas are discussed in the following sections.

SOURCE SPECIES

Table 26 presents an inventory of the tropospheric mixing ratio of molecules believed to be of importance to the photochemical budget of the stratosphere. Particular attention is given to the question of uncertainties and discrepancies among the measurements. The quality of data is graded from A to F as follows:

- A Excellent statistical data base providing a clear picture of the global distribution of the particular species with uncertainties of 5 percent or better

Table 26
Tropospheric Sources

Compound	Source	Quality	Mixing Ratio
N_2O	N	B	290-330 ppbv
CH_3Cl	N	C	500-750 pptv
CF_2Cl_2 (F12)	A	B	200-230 pptv
$CFCl_3$ (F11)	A	B	110-140 pptv
CCl_4	A	C	100-150 pptv
$C_2H_3Cl_3$	A	C	~ 100 pptv
$CHCl_2F$ (F21)	A	C	< 10 pptv
$C_2Cl_3F_3$ (F113)	A	C	~ 20 pptv
$CHCl_3$	A	C	~ 20 pptv
CH_3I	N	C	~ 10 pptv
CH_3Br	N	C	< 10 pptv
C_2Cl_4	A	C	~ 30 pptv
C_2HCl_3	A	C	~ 20 pptv
SF_6	A	C	~ 0.2 pptv
CH_4	N + A	B	~ 1.6 ppmv
CO_2	N + A	A	320-331 ppmv
C_2H_6	N + A	B	< 50 ppbv
H_2O	N	A	Highly variable
CO	N + A	B	< 100-400 ppbv
H_2	N	A	0.4-1.3 ppmv

A = anthropogenic
N = natural

ppbv = parts per billion per volume
pptv = parts per trillion per volume
ppmv = parts per million per volume

- B Fair data base yielding statistically useful results, but with uncertainties equal to or exceeding 15 percent
- C Fragmentary information with incomplete coverage
- D Single observations
- F No measurements

Recent developments of importance are:

Continuing research by groups such as those of Schmeltekopf at the Aeronomy Laboratory, National Oceanic and Atmospheric Administration (NOAA); Rasmussen at Washington State University (WSU); Inn at the Ames Research Center; National Aeronautics and Space Administration (NASA); and Singh at Stanford Research Institute (SRI) has solidified the tropospheric data base significantly.

The lifetime of CH_3CCl_3 in the troposphere determined by measured mixing ratio and known source strengths is a factor of 5 greater than the lifetime inferred from 1-D model OH concentrations and the rate constant for $\text{OH} + \text{CH}_3\text{CCl}_3$ (Singh, 1977). This suggests that the average tropospheric level of OH is $3 \times 10^5 \text{ cm}^{-3}$ to $5 \times 10^5 \text{ cm}^{-3}$ which is significantly lower than that calculated from existing models (Singh, 1977). Measured values of OH range from $7 \times 10^6 \text{ cm}^{-3}$ to less than $2 \times 10^6 \text{ cm}^{-3}$ (Wang et al., 1975; Perner et al., 1976; and Davis et al., 1976). When the results of Davis et al. (1976) are scaled for seasonal and diurnal effects, a value of $9 \times 10^5 \text{ cm}^{-3}$ is obtained for the globally averaged OH concentration (National Academy of Sciences, Appendix C, 1976). When consideration of possible uncertainties in the OH measurements is made, it is unclear whether a real difference exists between the reported global values of OH concentration. However, the lower value for the global OH concentration might be significant because current assumptions regarding the troposphere's ability to eliminate moderately reactive chlorofluorocarbons, and theories regarding CO_2 , N_2O , and methane would require reexamination.

Uncertainties in the average mixing ratio of CCl_4 , CH_3Cl , and CH_3CCl_3 are unacceptably high, making an accurate appraisal of the total chlorine budget in the stratosphere difficult or impossible.

A convergence of N_2O data on a mixing ratio of 270 to 350 parts per billion per volume (ppbv) has significantly narrowed previous uncertainties. However, details of the global distribution of N_2O are crucial for determining the tropospheric lifetimes of this molecule, and, although adequate data are not available, they are of major importance. The measurement of source terms in the stratosphere is progressing, but the data are sparse. Table 27 represents the inventory of source terms that have been observed. Several facts have begun to emerge:

- The latitude studies of the vertical distribution of N_2O , $CFCl_3$, and CF_2Cl_2 by groups at NOAA and NASA using aircraft have begun to define major differences in the upward transport of the stratosphere as a function of latitude. This emphasizes the difference between: (1) small-scale "diffusion" driven only by a density gradient, and (2) a velocity field that represents macroscopic transport independent of density gradients. It is also clear that an apparent upward diffusion coefficient cannot be applied to the apparent downward diffusion of, for example, a sink term.
- It is desirable to extend the measurements a significant distance above the tropopause in order to clearly establish the mixing-ratio gradient as a function of altitude.
- Accuracy is limited by the absence of careful cross-calibration of gas chromatograph detectors.
- More data on methane through the stratopause are needed if improved vertical eddy-diffusion coefficients are to be inferred from such information.

SINK TERMS

The major stratospheric photochemical sink terms are HCl , HNO_3 , H_2O , N_2O_5 , $ClONO_2$, $COCl_2$, $COFCl$, and HF . Note that, although some of these species can be regarded as a source term under certain conditions (e.g., H_2O and HCl), in a time-integrated sense, continuity requires the net downward transport of these species from the stratosphere. By definition, all sink terms are the product of radical recombination steps and are at the same time the reservoir from which the atoms and radicals are formed by photolysis and/or oxidation.

Table 27
Stratospheric Sources

Compound	Quality	Altitude Range
N_2O	B	Troposphere-43 km
CH_3Cl	C	Troposphere-19 km
CF_2Cl_2 (F12)	B	Troposphere-43 km
$CFCl_3$ (F11)	B	Troposphere-43 km
CCl_4	C	Troposphere-19 km
CH_4	C	Troposphere-43 km
CO_2	C	Scattered
H_2O	B	Troposphere-32 km
CO	C	Scattered
H_2	C	Troposphere-43 km

Figure 10 summarizes the available HCl data that result from infrared observations and filter experiments. In brief, the measurements show the HCl mixing ratio (by number) to increase from approximately zero parts per billion (ppb) at the tropopause to 1.0 to 1.5 ± 0.5 ppb at 28 to 30 kilometers. Uncertainties in the infrared (IR) measurements increase from ± 25 percent in the lower stratosphere to ± 50 percent at 28 kilometers, resulting primarily from diminished absorption. Uncertainty remains regarding the absence of the R5 line of $H^{35}Cl$ absorption spectrum. The average of four seasonal determinations of HCl by the impregnated-filter method yields results in reasonable agreement with results from spectroscopic techniques, although it is generally slightly lower.

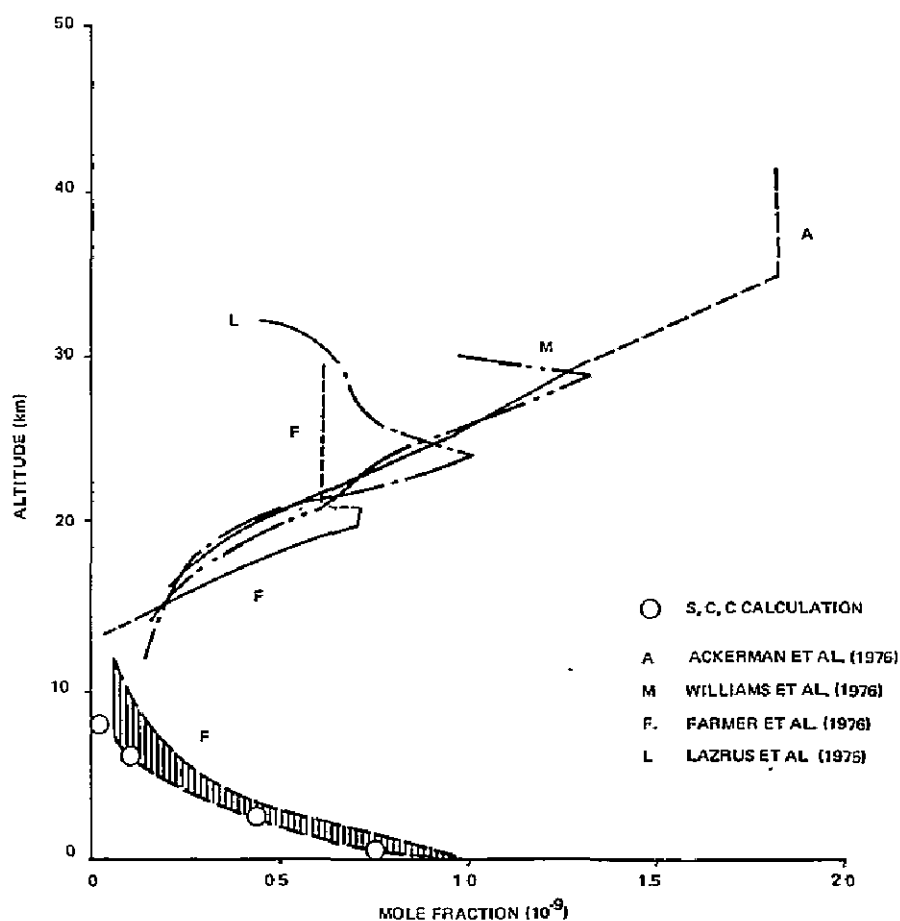


Figure 10. Measured hydrochloric-acid mixing ratios.

Data of Lazrus et al. (1975 and 1976) above 25 kilometers show a decrease in HCl to 0.49 ppbv at 31 kilometers that increases to 0.99 ppbv at 36 kilometers. An assessment of the experimental accuracy (as distinct from precision) of these results is currently under study and involves establishing the sensitivity of the technique to species such as ClO, ClONO₂, and COFCl. If such species are contributing to the observed acidic chlorine, the effect would be to decrease the apparent HCl densities. Filter collection efficiencies for acidic Cl have been tested by tandem filters, and no acid chlorine is observed on the second filter. In addition to midlatitude vertical profiles of HCl, its latitude distributions are being studied by using the impregnated-filter method aboard aircraft. From these data, stratospheric inventories are obtained that are used to compute the fluxes of HCl out of the stratosphere. Initial measurements at different latitudes indicate that concentrations of HCl are lower in equatorial regions, at least during spring.

Nitric-acid profile and column measurements have been made by filter-paper absorption (Lazrus and Gandrud, 1974a), by IR and submillimeter emission (Murcray et al., 1975; Harries et al., 1974; and Evans et al., 1976c); and by infrared absorption (Fontanella et al., 1975). Stratospheric altitude profile measurements usually display a more sharply peaked or multipeaked distribution in the lower stratosphere than that of model simulations. Various profile and total-column measurements made over a few days often exhibit differences on the order of a factor of 2, which 1-D models cannot simulate. On the other hand, data obtained from balloon platforms in summer at 51° to 59°N for 3 successive years demonstrate remarkable consistency with only slight changes in the altitude of the peak mixing ratio (Evans et al., 1976c). Although profile measurements show no unequivocal seasonal trends, the existing data may suggest larger amounts of HNO₃ during winter/spring than during summer/fall. Winter measurements at northern and southern latitudes are needed to substantiate this possible trend.

Stratospheric column measurements of HNO₃ (Murcray et al., 1975) indicate strong increases as polar latitudes are approached in both hemispheres during January and April. Profile measurements (Lazrus and Gandrud, 1974a; and Murcray et al., 1975) in early spring and late fall are usually not inconsistent with these observations. In contrast, column measurements by Harries et al. (1974) exhibit no obvious dependence on latitude or season. The reason for these differences is not known. However, the latter measurements were generally made over a small latitude range at widely spaced times so that short-term fluctuations may have masked the trends observed by Murcray et al. (1975). One flight of Harries et al. (1974) in June between 50°S and 50°N indicates no latitude dependence. Perhaps the latitude dependence of HNO₃ is strong only during January to April. Further measurements are needed to clarify this situation.

Nitric acid is not expected to have a very significant diurnal variation (Evans et al., 1976a).

For comparison of observations with 1-D model simulations, most of the available profile data have been grouped between latitudes approximately 30° to 45°N and approximately 51° to 64°N and have been averaged to give figure 11. All of the data were determined between mid-April and mid-November. Because the altitude of the peak mixing ratio varies, the

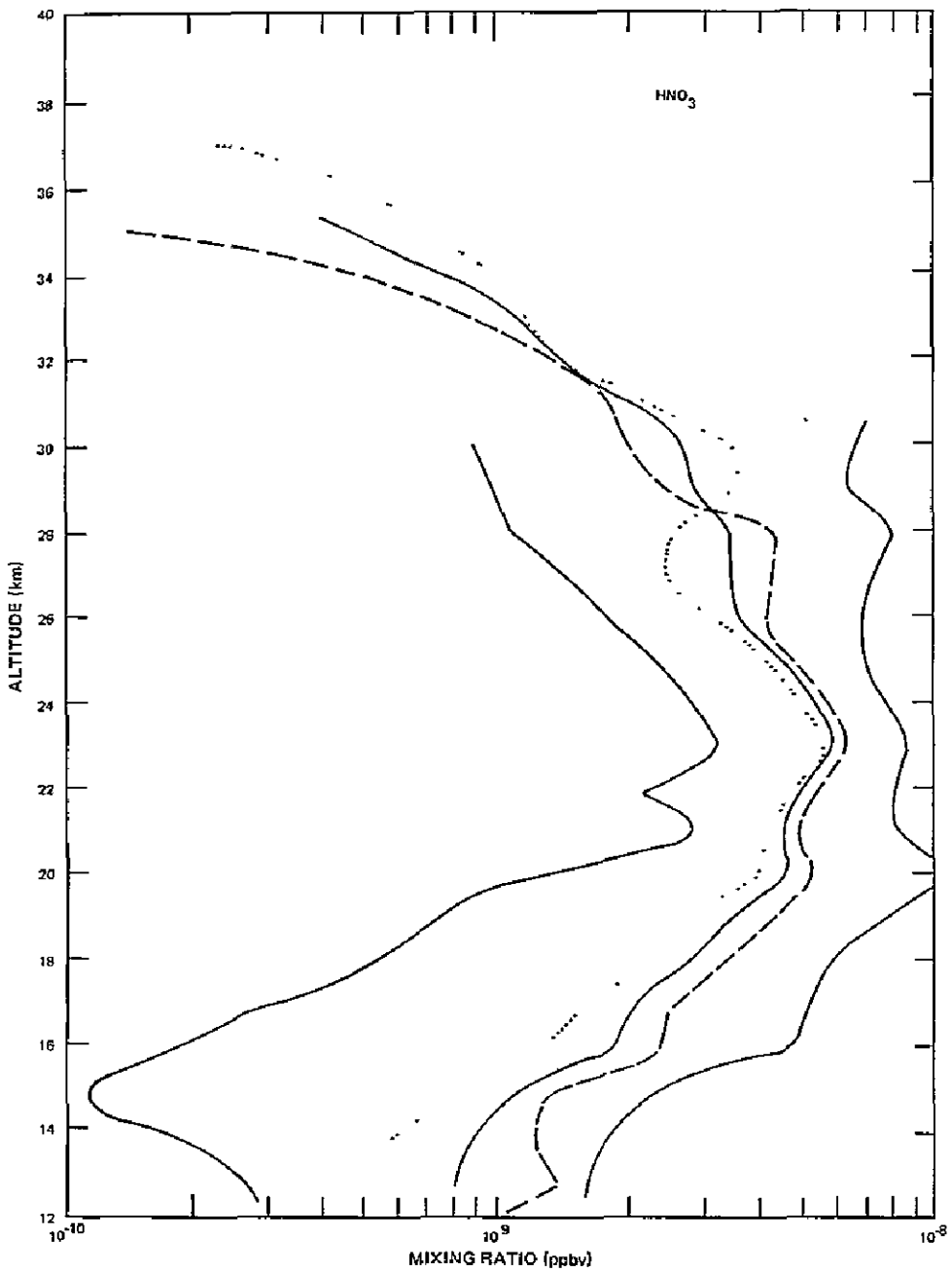


Figure 11. Calculated average of stratospheric measurements of nitric-acid mixing ratios (Ridley and Wuebbles, 1977).

averaging procedure smears the rather sharp layer structure observed in individual profiles. It is also evident that the average results show no strong latitude dependence despite the two rather wide latitude groupings. In contrast, profile measurements near the Equator are generally significantly lower than higher latitude measurements (Lazrus and Gandrud, 1974a). It would be more appropriate to form these averages referenced to the height of the tropopause. This was not done, however, because the tropopause information is not always reported for the NO_x measurements.

King et al. (1976) were unable to identify absorption features attributable to N_2O_5 in the twilight absorption spectra of Murcray et al. (1969), but assigned upper limits of approximately 0.5 ppbv at 30 kilometers, decreasing to approximately 0.1 ppbv at 20 kilometers. On the basis of radiometric observations in 1974, Evans (private communication, 1977) assigned an upper limit of 0.5 ppbv below 30 kilometers. Both observations were attempted (for other reasons) late in the afternoon when N_2O_5 is expected to be at a minimum in the diurnal cycle. More recently, Evans (private communication, 1977) has assigned an upper limit of 0.5 ppbv below 30 kilometers from a balloon ascent just after noon. This would indicate a high quantum yield for N_2O_5 photolysis.

If the difference between the NO_2 sunset and sunrise profiles of Kerr and McElroy (1976) is attributed to the change in N_2O_5 abundance at night, then $\Delta\text{N}_2\text{O}_5 = \Delta\text{NO}_2/2 \approx 1$ ppbv in the 24- to 32-kilometer region at 51°N in summer. Combined with the upper limit measurements, the maximum expected N_2O_5 mixing ratio would be approximately 1.5 ppbv.

Chlorine nitrate remains at the center of controversy. Infrared spectroscopy appears to be the most promising method for establishing the mixing ratio of ClONO_2 between 20 and 30 kilometers, which is the expected altitude interval of its peak mixing ratio. Upper limits have been placed on the amount of ClONO_2 present in the stratosphere by Murcray et al. (1977). Without an accurate knowledge of the ClONO_2 mixing ratio between 25 and 30 kilometers, it is difficult to interpret the observed HCl concentrations in terms of total chlorine mixing ratios.

Extensive work on H_2O has been recently reviewed by Harries (1977), who offered the following conclusions:

- Measured water-vapor mass mixing ratios are generally found to lie in the range 0.5 to 5 mg kg^{-1} for all levels in the stratosphere up to about 40 kilometers. Higher values have been reported on a few occasions that, if they are corroborated, may be an indication of temporal variations. Some evidence exists that the mixing ratio increases slowly with height between the tropopause and this level.
- Within the quoted range, however, there exists considerable divergence among the results of different workers for apparently similar locations and times of observations. At least part of these differences would appear to be instrumental in origin.
- It therefore seems imperative that workers, either by personal initiative or under an international program, should combine to compare their instrumental sensitivities and errors so that some standardization of results may be achieved. Without such standardization, much information about the real nature and behavior of stratospheric humidity is being lost. The purpose of an experiment should no longer be to decide whether or not the stratosphere is "dry," but should be to identify small variations of an already small relative humidity in order to study the detailed life cycle of the vapor.
- By adopting a pragmatic approach, current summaries have been produced of the variations of stratospheric humidity with height, season, latitude, and time from the data available in the literature. The results are as follows:
 - In midnorthern latitudes, the vertical profile of humidity shows a fairly constant mixing ratio between 13 and 30 kilometers of about $2.5 \pm 0.7 \text{ mg kg}^{-1}$. Some evidence for a small increase above 30 kilometers exists, to about 2.9 mg kg^{-1} on the average, but perhaps as high as 4 or 5 mg kg^{-1} on occasion.

- Certain results indicate very low mixing ratios in north polar air, but these require confirmation. Other data indicate, on the average, lower mixing ratios in the lower stratosphere at the southern winter pole than at the northern summer pole.
- Similarly, limited evidence of weak, shallow layers of water vapor at about 25 to 30 kilometers (within which the mixing ratio rises to approximately 4 mg kg^{-1} over 1 or 2 kilometers) exists but requires independent confirmation. These layers are much too high to be associated with the midlatitude tropopause breaks.
- The latitudinal distributions of lower stratospheric water vapor obtained by several workers show a general trend to a maximum near the Equator, the mixing ratio decreasing at higher latitudes in both hemispheres. There is considerable uncertainty, however, as to the absolute levels of humidity and also as to trends at latitudes greater than 30°N and 30°S . Data are particularly sparse in the Southern Hemisphere.
- The temporal variations of water vapor at various levels above single locations show marked annual cycles: the amplitudes of such cycles obtained by different workers seem to be in fair quantitative agreement. Such cycles may be related to annual variations in the tropical cold-trap temperature. In addition, three independent sets of observations show linear increases in the mean level of the mixing ratio between 0.1 and $0.25 \text{ mg kg}^{-1} \text{ yr}^{-1}$, which may possibly be related to long-term changes of temperature at the tropical tropopause.

The use of experimentally measured values of stratospheric humidity in atmospheric models has been investigated. It has been shown that extreme care must be exercised in the choice of values to use and that such considerable uncertainties exist that quantitative arguments that are based on these values may contain considerable uncertainties themselves. This is acceptable only as long as the implications of adopting a real experimental result, and the hidden errors that it may contain are fully appreciated.

The variability in OH observed by Burnett (1976) has now made it necessary to determine the *in situ* OH/H₂O ratio in order to determine if fluctuation in H₂O or if some other species (perhaps O₃) is responsible.

The HF molecule has a strong infrared absorption feature at 4039.0 cm^{-1} , which is a region that is relatively free from interference by other atmospheric absorption features. Zander (1975) observed this region of solar spectra from a balloon platform. This spectrum was obtained at a relatively high solar-elevation angle. As a result, it is possible that solar HF may be contributing to the absorption. Zander has also observed the absorption in spectra obtained from the ground at low solar-elevation angles. These spectra are obtained under conditions in which any solar contribution would be insignificant. However, the data yield only total-column density. By comparing the two spectra, Zander estimates a mixing ratio of 0.3 ppbv near 28 kilometers. These results were recently confirmed by Zander et al. (1977) from a second balloon flight. However, if solar absorption is occurring in the observed spectra, then the mixing ratios should be considered to be an upper limit.

Although this same spectral region has also been observed during sunset by Buijs (private communication, 1976) on several flights made in 1976, results have not yet been analyzed.

Lazrus (private communication, 1976) has also measured HF using impregnated-filter techniques. These measurements yield HF mixing ratios on the order 0.1 to 0.2 ppbv. Recent measurements should yield latitude and altitude profiles in the Northern Hemisphere for HF. Reduction of these data is in progress.

RADICAL SPECIES

A major movement is underway, shifting from the problem of verifying the existence of the major stratospheric radicals (which are here taken to include NO, NO₂, OH, HO₂, Cl, and ClO) to the simultaneous observation of these species. This change of emphasis results from rapidly expanding measurement techniques, observed variability of these short-lifetime species, and a continuing appreciation for the strong chemical coupling among the NO_x, HO_x, and ClO_x systems. Several other atoms and radicals are of importance—NO₃, N, H, $\dot{\text{O}}\text{ClO}$, and ClO₂; but, given finite resources, those species that are believed to control the rate of odd-oxygen destruction must receive priority consideration for the limited task of CFM ozone-depletion assessment.

Surprisingly few profile measurements of NO₂ have been made from stratospheric platforms, considering the availability of quite clean absorption lines in the ultraviolet (UV) and IR. No *in situ* measurements have

been reported. Instead, profiles have been derived from long-path twilight absorption measurements predominantly at sunset (Kerr and McElroy, 1976; Ackerman and Muller, 1972; Ackerman et al., 1975; Fontanella et al., 1974; and Murcraay et al., 1974) and from radiometric measurements (Chaloner et al., 1975). Column measurements using the Sun, Moon, and zenith sky have been made from the ground and from aircraft (Brewer et al., 1974; and Noxon, 1975 and 1976).

Profile measurements of NO_2 fall into two fairly distinct groups. Pressure modulation (Chaloner et al., 1975) and submillimeter (Harries et al., 1976) radiometric methods give substantially larger NO_2 mixing ratios during the day than those of UV and IR absorption methods at sunset (Kerr and McElroy, 1976; Ackerman and Muller, 1972; Ackerman et al., 1975; Fontanella et al., 1974; Murcraay et al., 1974). The disparity is larger at night, a few hours before sunrise, when the radiometric methods yield mixing ratios in the 20- to 35-ppbv range between 25 and 35 kilometers. Current theory suggests even larger values at night after sunset to allow for N_2O_5 formation. Thus, the long-path IR or UV absorption methods are generally three to four times lower at comparable times. The daytime NO_2 values determined radiometrically are larger than would be calculated from NO measurements, and the nighttime values are larger than the total NO_x predicted by current atmospheric models. The nighttime radiometric profile measurements give much larger total column NO_2 than those measured directly by Noxon (1975 and 1976). Either systematic errors in the different techniques or in data reduction are suspected, and in-flight NO_2 instrument intercomparisons are required.

If the radiometric measurements are neglected for the moment, the remaining published NO_2 profiles do not exhibit the order of variability observed for HNO_3 and NO. This may be attributable to the more limited data base. Variations in total-column NO_2 by a factor of 2 or so during a month are not uncommon (Noxon, 1975 and 1976). However, changes in the lower stratosphere strongly weight column measurements; a 1-kilometer layer of 0.2 ppbv at 15 kilometers is equivalent to one at 30 kilometers containing about 2 ppbv.

Profile measurements have been insufficient to determine if seasonal and latitudinal trends persist at all altitudes. However, stratospheric column measurements by Noxon (1976) indicate a summer-to-winter ratio of about 2 south of 50°N , and about 6 north of 55°N . During the summer, little change in total NO_2 occurred between 35° and 80°N . During winter months, in contrast, the latitude dependence is very strong with about a factor of 6 decrease in total NO_2 above about 50°N . Similarly, unpublished

experiments by McElroy and Kerr (private communication, 1976) indicate significantly lower total NO_2 in Arctic air masses that have reached southern Ontario. It has been argued qualitatively that this winter decrease is attributable to conversion of NO_2 into N_2O_5 and/or HNO_3 during the long winter nights. However, a 1-D diurnal model has been used to attempt a simulation, but the calculated column decrease was not nearly as great as that observed even when the unknown quantum yield of N_2O_5 photolysis was decreased to a reasonably low value (McConnell and Ridley, unpublished study). By default, then, the tentative conclusion was reached that macrotransport processes are responsible.

Altitude profile measurements of NO have been made by long-path IR absorption at sunset (Ackerman et al., 1975 and 1973), by long-path emission (Chaloner et al., 1975), and by *in situ* chemiluminescence instruments (Ridley et al., 1974, 1975, 1976 and 1977; and Ridley and Bruin, 1977). Particular altitudes have been sampled by a laser absorption method (Patel et al., 1974; and Burkhardt et al., 1975) and also by chemiluminescence methods (Loewenstein and Savage, 1975; and Loewenstein et al., 1975). As is the case for HNO_3 data, *in situ* and long-path techniques exhibit a spread between individual measurements of up to an order of magnitude in the 17- to 30-kilometer region between about 30° and 45°N . Short-term fluctuations of several fold are observed in aircraft measurements. In contrast, five balloon profiles in summer between 51° and 59°N are quite consistent, as were NO_2 , HNO_3 , and O_3 profiles (Evans et al., 1976a; and Ridley and Bruin, 1977).

Recently, NO chemiluminescence methods have extended measurements to 60 kilometers. In June, Drummond et al. (1976) obtained 10.5-ppbv constant between 40 and 45 kilometers. In April, Mason and Horvath (1976) obtained upper limits roughly two to three times lower in the same altitude range. This would be consistent with the observed seasonal changes in the 30° to 45°N region at lower altitudes, although more measurements are required to determine if the differences are not due to natural variability.

Aircraft measurements (Loewenstein and Savage, 1975; and Loewenstein et al., 1975) near 18 and 21 kilometers indicate typical summer values two to three times greater than in winter in the 30° to 45°N range. Whether this trend extends to higher altitudes is not determinable from the balloon measurements.

The latitude trends are also known only in the 18- to 21-kilometer region. Between the Equator and approximately 50°N , the data of Loewenstein and Savage (1975) obtained during summer and fall exhibit only small changes. Above approximately 50°N , there is a reasonably clear increase of up to a factor of about 3. Because profile measurements indicate a substantial increase in mixing ratio with increasing altitude, the latitude observations may be primarily due to deeper penetration of the stratosphere at northern latitudes.

The spread in measurements in the range of 30° to 45°N latitude now appears uncomfortably large. In general, the chemiluminescence measurements (Ridley et al., 1974 and 1975) are lower than those obtained by other techniques, although some measurements are in agreement with the seasonal trends at lower altitudes. In terms of the present data base, the variations appear much greater between 30° to 45°N than between 51° to 59°N , and this may be partially associated with changes in the strong jet stream at lower latitudes. Most of the balloon chemiluminescence results were obtained well before local noon, and it is now known that NO can continue to increase by varying amounts as the solar zenith angle decreases from about 90° to the value at local noon (Ridley et al., 1977; and Patel et al., 1974). In summary, if systematic errors between various techniques are not discovered, seasonal, diurnal, and transport changes may be responsible for the dispersion in the data. Certainly, the major NO_x constituent below about 25 kilometers is HNO_3 , and separate experiments made over a short period of time exhibit large differences. Thus, it is not unexpected that NO also exhibits large variability.

NO_3 is expected to have a strong diurnal variation with maximum concentrations during the night. However, nighttime and daytime total-column measurements by Noxon (1975) and Davies (1974) failed to identify absorption attributable to NO_3 , and only an upper limit of about 5 percent of NO_2 was set. This is consistent with model simulations; NO_3 is rapidly photolyzed during the day and slowly converted to N_2O_5 during the night.

Strong diurnal variations are expected in the concentrations of NO_2 , NO, NO_3 , and N_2O_5 , but this has been confirmed directly by experiment only for NO and NO_2 . Indirect evidence exists for the behavior of N_2O_5 .

For solar zenith-angle (χ) variation between approximately 90° and 95° , NO_2 is rapidly converted to NO during sunrise and NO is converted to NO_2 during sunset so that $\text{NO} + \text{NO}_2$ should be essentially constant. At sunset and below about 40 kilometers, for example, the decay of NO is

governed by the time constant, $t = 1/(J_{\text{NO}_2} + k_{\text{O}+\text{NO}_2} [\text{O}])$, where J_{NO_2} is the photodissociation coefficient for NO_2 . J_{NO_2} dominates this expression so that net NO -to- NO_2 conversion essentially parallels the attenuation of the UV flux. For NO , the rapid disappearance at sunset and appearance at sunrise has been measured with a time resolution that is shorter than t in the range $\chi = 90$ to 95° (Ridley et al., 1976 and 1977; Ridley and Bruin, 1977; Patel et al., 1974; and Burkhardt et al., 1975). When local ozone and temperature data are available, diurnal models can simulate the NO behavior quite well (Ridley et al., 1976 and 1977). This type of experimental data provides a stringent test of model chemistry since large-scale transport is negligible over the time scale of the experiments.

The variation of NO has not been measured for a 24-hour period during a single balloon flight. However, Burkhardt et al. (1975) have covered the period from before UV sunrise until about local noon and from before noon until UV sunset with two balloon flights near 28 kilometers at different times of the year. After the initial rapid increase in NO due to NO_2 photolysis at sunrise, the laser absorption measurements exhibit a further strong increase in NO until about noon. Similar results were mentioned by Chaloner et al. (1975).

Chemiluminescence measurements (Ridley et al., 1977) during sunrise until before noon also showed an increase of NO as χ decreases from about 90° , but the increase was considerably smaller than that of the laser measurement. However, a diurnal model that attributes the morning increase in NO to N_2O_5 photolysis can explain both sets of data if a judicious choice of O_3 concentration and total NO_x is made (Ridley et al., 1977). Measurements of O_3 were not made on either flight. For the period of several hours after local noon, the NO concentration remains quite constant according to the results of Burkhardt et al. (1975). Chemiluminescence measurements on four flights near 35 kilometers have established that, at this altitude, the net decay of NO at sunset begins abruptly as χ increases beyond about 90° (Ridley et al., 1976; and Ridley and Bruin, 1977). Only a slight decrease in NO is observed as χ increases from $\sim 80^\circ$ to 90° in agreement with only a slight decrease in J_{NO_2} at this altitude. This is in apparent disagreement with the afternoon flight of Burkhardt et al. (1975) on which they observed a large reduction in NO beginning near $\chi = 67^\circ$. However, their observations are perturbed by a severe loss in balloon altitude beginning several hours after local noon, and it appears that their data are essentially profile measurements intermixed with the diurnal decay as sunset approaches. Consequently, there remains a period from mid-afternoon until a short time before sunset in which the diurnal behavior of

NO was not observed. This is unfortunate because these observations of NO could contribute to resolving the controversy concerning the possibility of a strong afternoon maximum reported for NO₂ (Brewer et al., 1973 and 1974).

The diurnal variation of NO₂ is less clear because of conflicting reports. Long-path solar absorption measurements of NO₂ have been made by Kerr and McElroy (1976) from a balloon near 35 kilometers during morning and evening twilight. These measurements are weighted toward $\chi \approx 90^\circ$ and show from approximately 0.5 to 2 ppbv more NO₂ at sunset than at sunrise over the tangent altitude range of 16 to 30 kilometers. Total-column measurements by Noxon (1976) are consistent with this observation. These observations alone can be explained by slow conversion of NO₂ to N₂O₅ via NO₃ at night, followed by N₂O₅ photolysis to NO₂ during the day.

The daytime behavior of NO₂ remains in a state of controversy. Ground-based measurements (Brewer et al., 1973 and 1974) that have been reduced to give vertical profiles indicate a strong afternoon maximum with NO₂ being 3 to 4 times either sunrise or sunset values at all altitudes. In contrast, Noxon (private communication, 1976) cannot confirm this although the basis of the experimental method is the same. On the other hand, Chaloner et al. (1975) report that daytime NO₂ concentrations are lower than those after sunrise by up to a factor of 2 at 35 kilometers. Their daytime NO + NO₂ values are also much lower than the NO₂ measured several hours before sunrise. Both of these observations are inconsistent with morning measurements of NO and cannot be explained by current stratospheric chemistry. Their nighttime observations would require an additional source of NO₂ or NO_x. Substantiation of even the relative trends observed with this technique is necessary. Clearly, the diurnal behavior of NO₂ requires further investigation by independent measurement techniques. Present NO_x diurnal models below ~40 kilometers show NO₂ decreasing during the night by conversion to NO₃ and N₂O₅, a rapid decrease during sunrise due to photolysis, a slow growth during the day as a result of N₂O₅ photolysis, and a rapid increase during sunset as NO is oxidized to NO₂. The growth during the day depends on the assumed photolysis rate of N₂O₅. Noxon's (1976) column measurements and NO measurements are generally consistent with this scheme. Both daytime profile observations of NO₂ cannot be correct. However, if either one is substantiated, there must be missing chemistry in the model simulations.

Simultaneous measurements of at least O_3 , temperature, and several NO_x constituents provide stringent tests for model simulations. Few such measurements have been made. Using their absorption technique at sunset, Ackerman et al. (1975) obtained vertical NO and NO_2 profiles in May near $44^\circ N$. This permits a determination of the NO_2/NO ratio that is expected to be in photochemical steady state. However, this ratio is quite sensitive to local O_3 and temperature, and, unless these are measured during the flight in the neighborhood of the tangent altitude, a strict model comparison is not possible. Chaloner et al. (1975) also determined NO and NO_2 profiles during the day. If possible systematic errors in their technique cancel, they observe an NO_2/NO ratio of about 1.6 to 2 in the 20- to 33-kilometer region. Again, O_3 and temperature data were not reported.

Simultaneous measurements of O_3 , temperature, NO, NO_2 , and HNO_3 have been made yearly during the summer since 1974 (Evans et al., 1976b and 1976c). Profile measurements have been compared with a 1-D model that did not include ClO_x (Evans et al., 1976a). Although the comparison is reasonable, differences of a factor of 2 to 3 exist between the measured and calculated NO_2/NO , HNO_3/NO_2 , and HNO_3/NO ratios at some altitudes. Because the latter two ratios depend on the rate coefficient for the $OH + HO_2$ reaction, which is not well-known, the differences are not unexpected. More disturbing is the measured NO_2/NO ratio, which is roughly a factor of 2 greater than that of the model ratio at most altitudes. This could be due to several factors. First, either or both measurements may have unrecognized systematic errors. Secondly, the model-calculated photodissociation coefficients may not reproduce those of the flight, or they may have insufficient chemistry. Indeed, if recent ClO measurements (J. G. Anderson, private communication, 1977) are substantiated, the calculated NO_2/NO ratio would be significantly increased over that calculated with the measured amounts of ClO neglected. Thirdly, the measured NO_2/NO ratio is a combination of results from an *in situ* and long-path technique. Thus, the NO measurements were made in an air mass in which temperature and O_3 were measured, whereas the NO_2 measurements were made in different air masses that extend farther and farther from the balloon environment as the zenith angle increases beyond 90° .

Several independent methods are now being applied to the measurement of "reactive" chlorine, designated here as ClO_x , which is taken to include Cl, ClO, OClO, and ClO_2 . Of those four species, only the first two are believed to play a major part in the definition of stratospheric chlorine photochemistry, and thus they will receive the major amount of attention. However, it must be realized that no measurements of OClO or ClO_2 exist,

and thus their exclusion from further comment is not based on empirical information.

Chlorine monoxide is now under investigation by four independent methods: (1) solar ultraviolet absorption, (2) microwave emission, (3) cryogenic entrapment, and (4) *in situ* chemical conversion-resonance fluorescence. Atomic chlorine has been studied by using *in situ* atomic resonance fluorescence only. For chlorine monoxide, techniques (1) and (2) have yielded upper limits; technique (4) has been used to observe the altitude distribution.

Three simultaneous observations of Cl and ClO have been performed using the *in situ* resonance fluorescence technique, the first on July 28, 1976, at 12:00 noon Central Daylight Time (CDT) (local solar zenith angle 16°), the second on October 2, 1976, at 12:00 noon CDT (local zenith angle 35°), and the third on December 8, 1976, (local solar zenith angle 50°). In all cases, a 1.5×10^7 ft³ helium balloon, launched at dawn from Palestine, Texas, 32° N latitude, bore the experimental package to an altitude of 43 kilometers (141,000 feet). After activation and stabilization of instruments, the measurement phase began on deployment of the "guide-surface" parachute, which controlled both the velocity and attitude of the package during descent. The concentrations of both Cl and ClO were successfully measured on each flight with the results shown in figure 12. Significant vertical structure was apparent, particularly in the ClO profile for which the signal-to-noise ratio exceeded 10^2 throughout the region between 25 and 40 kilometers. In the case of atomic chlorine, the signal-to-noise ratio exceeded 3 above 40 kilometers, decreasing to 2 at 35 kilometers, below which contributions to the background count rate in the absence of Cl exceeded the fluorescence signal. It is expected that data extending to concentrations less than 10^5 cm⁻³ for Cl (²P) will be feasible on future flights. An experimental uncertainty of ± 40 percent is assigned to these data based partially on laboratory absolute calibration uncertainties (± 20 percent) and partially on a subjective appraisal of difficulties inherent in the control of any such field experiment.

Figure 13 presents a comparison between the data and four theoretical predictions of Cl and ClO appropriate to conditions during the flights. The difference in solar zenith angle between the July and October data is not a significant consideration, although it may be important with respect to the December data. It is impossible to compare these experimental results with all the available theoretical predictions; the foregoing four models were selected because: (1) they represent a cross section of the major

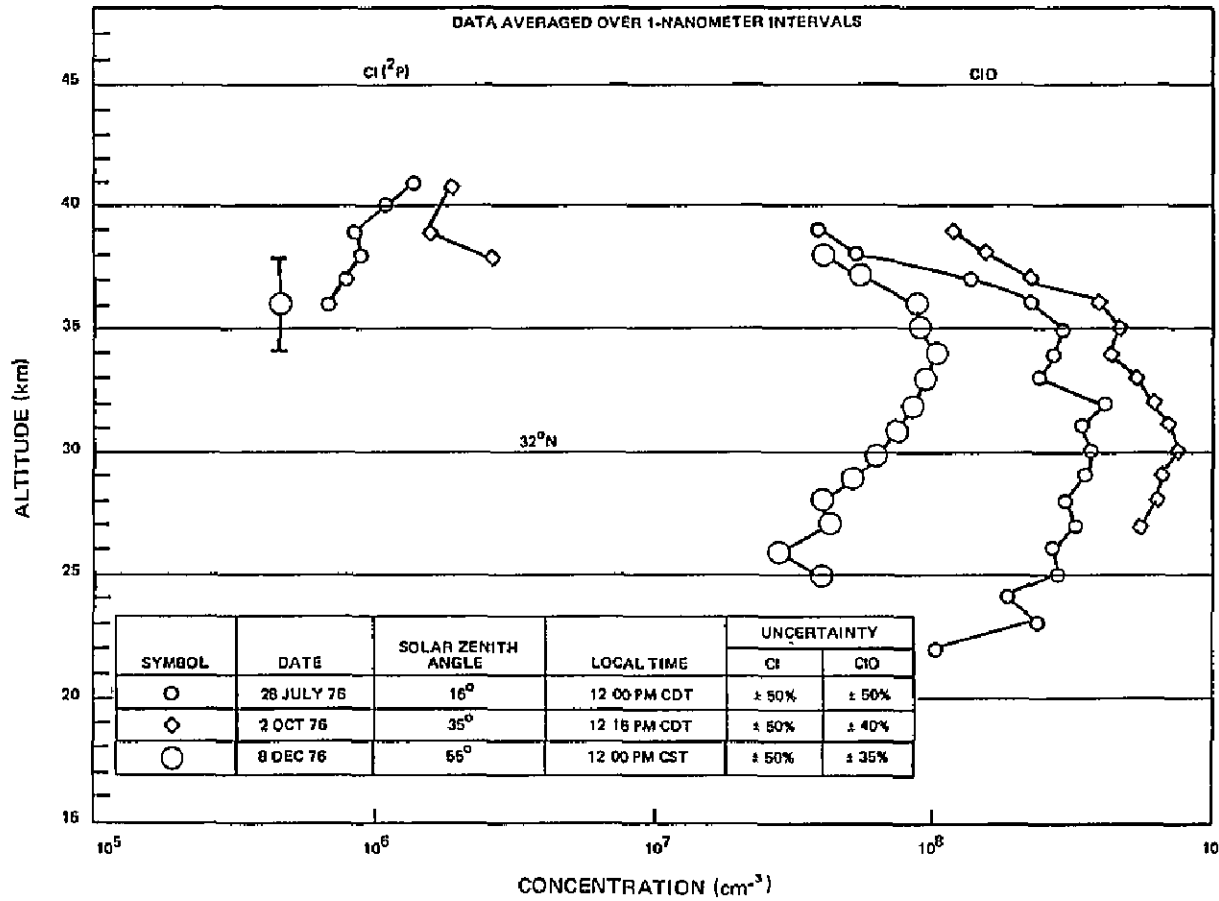


Figure 12. Measured concentrations of atomic chlorine and chlorine oxide.

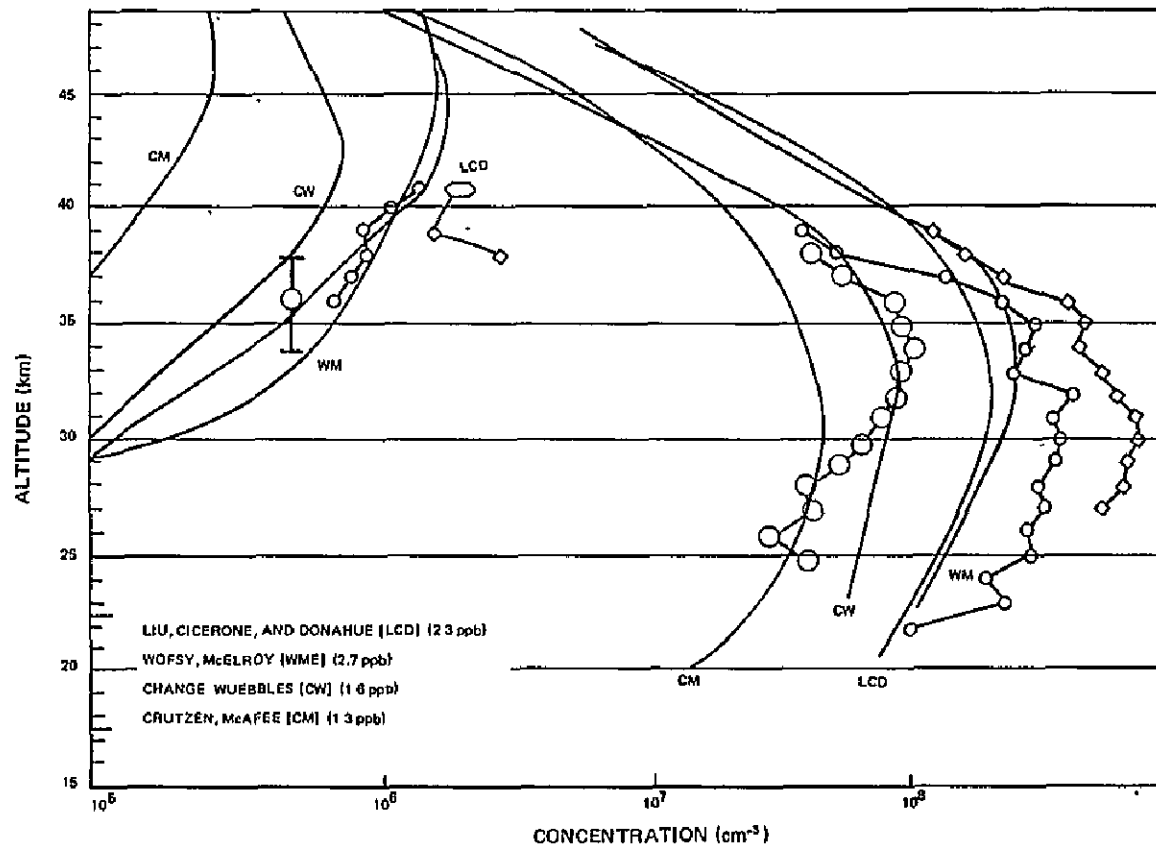


Figure 13. Comparison of measured and theoretical concentrations of atomic chlorine and chlorine oxide.

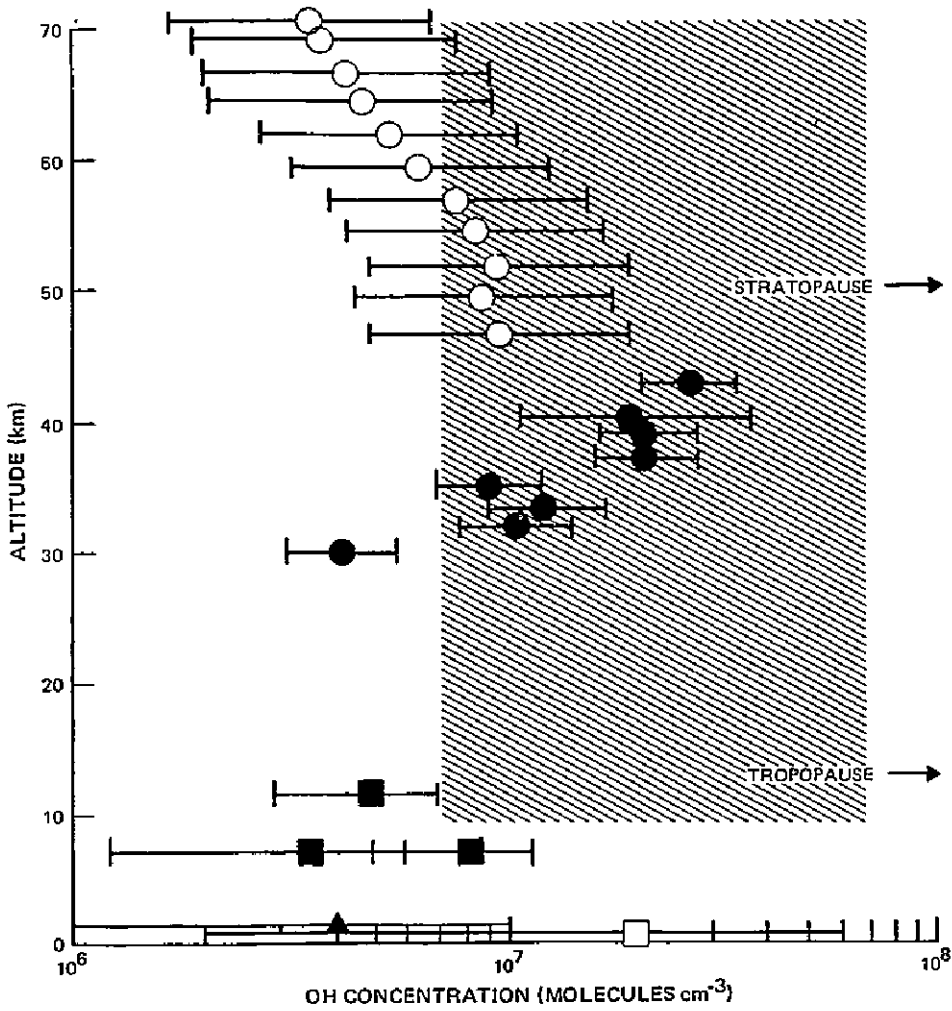
theoretical efforts to quantitatively predict chlorine catalyzed ozone depletion, and (2) they adequately encompass the range of theoretically predicted Cl and ClO concentrations. These determinations were made prior to the new determination of Howard (1977) for the reaction of $\text{HO}_2 + \text{NO}$. The theoretical consequences of employing the new rate are discussed in Chapter 4.

Several conclusions can be drawn from figures 12 and 13:

- Cl (^2P) and ClO exist in the stratosphere.
- Significant variability in the ClO and Cl concentrations exists throughout the stratosphere.
- Significant local structure is apparent in the ClO densities for which the signal-to-noise ratio is approximately 10^2 .
- The ratio of ClO to Cl is approximately 10^2 at 40 kilometers and 10^3 at 35 kilometers.
- Cl and ClO densities are equal to or greater than those predicted by theory. (A full discussion of these results appears in Chapter 4.)

Although several oxygen-hydrogen radicals exist, OH is the only species for which measurements have been reported in the troposphere and the stratosphere. OH is generally considered to be a key hydrogen radical linking the NO_x , HO_x , and ClO_x families. Since the NAS report, ground-based, column-density measurements of Burnett (1976) have become available.

Burnett's (1976) results may be summarized by noting that he observed column-OH concentrations as high as $4.4 \times 10^{14} \text{ cm}^{-2}$ and fluctuations in the column greater than factors of 3 in a few hours. Figure 14 summarizes all existing OH measurements to date. The tropospheric measurements of Wang et al. (1975) and Perner (1976) may not be representative of the natural troposphere because they are made at ground level. Taking the maximum value inferred from the Davis (1976) measurements, the column content contribution from the troposphere is less than $2 \times 10^{13} \text{ cm}^{-2}$. This means that Burnett's (1976) integrated column content of 4.4×10^{14} must arise principally from the stratosphere and mesosphere. J. G. Anderson (1971 and 1976) has recently revised his rocket data using new values



NOTE DATA SOURCES ARE AS FOLLOWS

- ANDERSON (1971), BY MONITORING SCATTERED 306.4-NANOMETER SUNLIGHT OVER WHITE SANDS, NEW MEXICO, IN APRIL WITH THE SOLAR ZENITH ANGLE AT 86°
- WANG ET AL (1975), BY DETECTING LASER-INDUCED FLUORESCENCE CENTERED AT 309 NANOMETERS AT THE GROUND NEAR DEARBORN, MICHIGAN, DURING 4 DAYS IN AUGUST
- ANDERSON (1976), BY MEASURING RESONANCE FLUORESCENCE AT ABOUT 309 NANOMETERS OVER PALESTINE, TEXAS, IN JULY (S) AND JANUARY AT A ZENITH ANGLE OF 80°
- ////// BURNETT (1976), BY COLUMN-INTEGRATED RESONANCE ABSORPTION OF 308-NANOMETER SUNLIGHT FROM THE GROUND AT FRITZ PEAK OBSERVATORY IN SEPTEMBER AND DECEMBER (THE INTEGRATED OH COLUMN HAS BEEN UNIFORMLY DISTRIBUTED BETWEEN 10 AND 70 KILOMETERS)
- DAVIS ET AL (1976), BY OBSERVING LASER-INDUCED FLUORESCENCE AT 309.5 NANOMETERS AT 21° AND 31° NORTH LATITUDES IN OCTOBER IN DAYLIGHT
- ▲ FERNER ET AL (1976), BY LASER LIGHT ABSORPTION AT 307.995 NANOMETERS IN THE AIR OVER JULICH, GERMANY (51° NORTH LATITUDE), IN LATE SUMMER AND FALL

Figure 14. Observed atmospheric hydroxyl radical concentrations.

for the rate of quenching of $A^2\Sigma^+$ with N_2 and O_2 (Becker, 1972). Applying this revision, plus a factor to account for the time of day, satisfactory agreement can be obtained between Burnett (1976) and J. G. Anderson's (1971 and 1976) values.

Several conclusions follow:

- Column densities of the hydroxyl radical are observed to vary by factors of 3 from day to day.
- Column and *in situ* measurements are in reasonable agreement.
- The determination of other radical concentrations that are known to depend on OH should be made simultaneously with that of OH. Also, OH itself should be measured simultaneously with O_3 and H_2O in order to determine the nature of the observed variability.

SOLAR FLUX AND O/O_3 RATIO

Three different types of information related to solar-flux measurements are required for a detailed knowledge of the photochemistry of the stratosphere: (1) the solar flux that reaches the top of the terrestrial atmosphere, (2) the solar flux at specific altitudes, and (3) the integrated effect in terms of the concentrations of photochemical species with short lifetimes.

The ultraviolet solar flux in the region from 160 to 300 nanometers is responsible for the photochemistry and heating of the stratosphere, which, in turn, is an important driving function for stratospheric transport processes. This wavelength region is noted for its complexity in terms of both terrestrial atmospheric and solar processes. During the early years of measurements of ultraviolet solar flux, it was not uncommon for measurements by independent groups to differ by factors of 2 to 3. Since that time, the techniques for measurement and absolute spectroradiometric calibrations have improved enormously.

Physical processes on the Sun that give rise to this radiation are extremely complex because the solar spectrum changes from a continuum with superimposed absorption lines at long wavelengths to a continuum with superimposed emission lines at the shorter wavelengths. Correspondingly, observations of the solar disk change their character from limb darkening to limb brightening at the shorter wavelengths.

Of great importance to understanding the physics and chemistry of the stratosphere and climatic trends is determining what the values of the ultraviolet solar spectral irradiance are and whether it has varied with time.

A current tabulation of some major sources of data on solar spectral irradiance may be found in Heath and Thekaehara (1976). Figures 15 and 16 graphically show these data sets. Not included in these figures are the data by Detwiler et al. (1961), which differ significantly from all later measurements. Figures 15 and 16 include data from Ackerman (1971), Simon (1975), and Heath (1973).

The other important aspect of the ultraviolet solar flux is the nature of its temporal variability. The effects of solar-flux variability for wavelengths less than 120 nanometers have been established from the analysis of satellite drag measurements for both the 27-day solar rotational period and the 11-year sunspot cycle by King-Hele and Quinn (1965) and Jacchia (1963), respectively. Although the 27-day variability in the ultraviolet solar flux below 120 nanometers has been observed directly, the variability for the flux for the 11-year period has not.

Observations of the 27-day variability of the solar flux in the region of 160 to 300 nanometers have been reported by Heath (1974) and Hinteregger (private communication, 1975). The maximum variability for this wavelength region appears to be less than 10 percent per solar rotational period.

Although it is generally accepted that the solar flux varies over the 27-day solar rotational period below 200 nanometers, this is not the case concerning questions of variability of this wavelength region over the 11-year sunspot cycle. Evidence for an 11-year variability of the Sun from 160 to 300 nanometers has been given by Heath and Thekaekara (1976). However, questions as to the reality of the effect have been raised. Evidence for the existence of a solar-cycle effect is derived from measurements on a rocket in 1966, on Nimbus-3 in 1969, on Nimbus-4 in 1970, and on Atmosphere Explorer-E (AE-E) in 1975. The ratio of solar flux measured at solar minimum to that at solar maximum (shown in figure 17) is approximately 0.5 at 177 nanometers and approximately 0.8 at wavelengths near 290 nanometers. The solar-flux values were derived from both broadband photometric observations and from measurements with a double monochromator with a 1.0-nanometer spectral bandpass. There were no measurements at 210 nanometers over the solar cycle. The validity of this curve needs to be established by other investigators, particularly in the atomic oxygen production region in the stratosphere at approximately 210 nanometers.

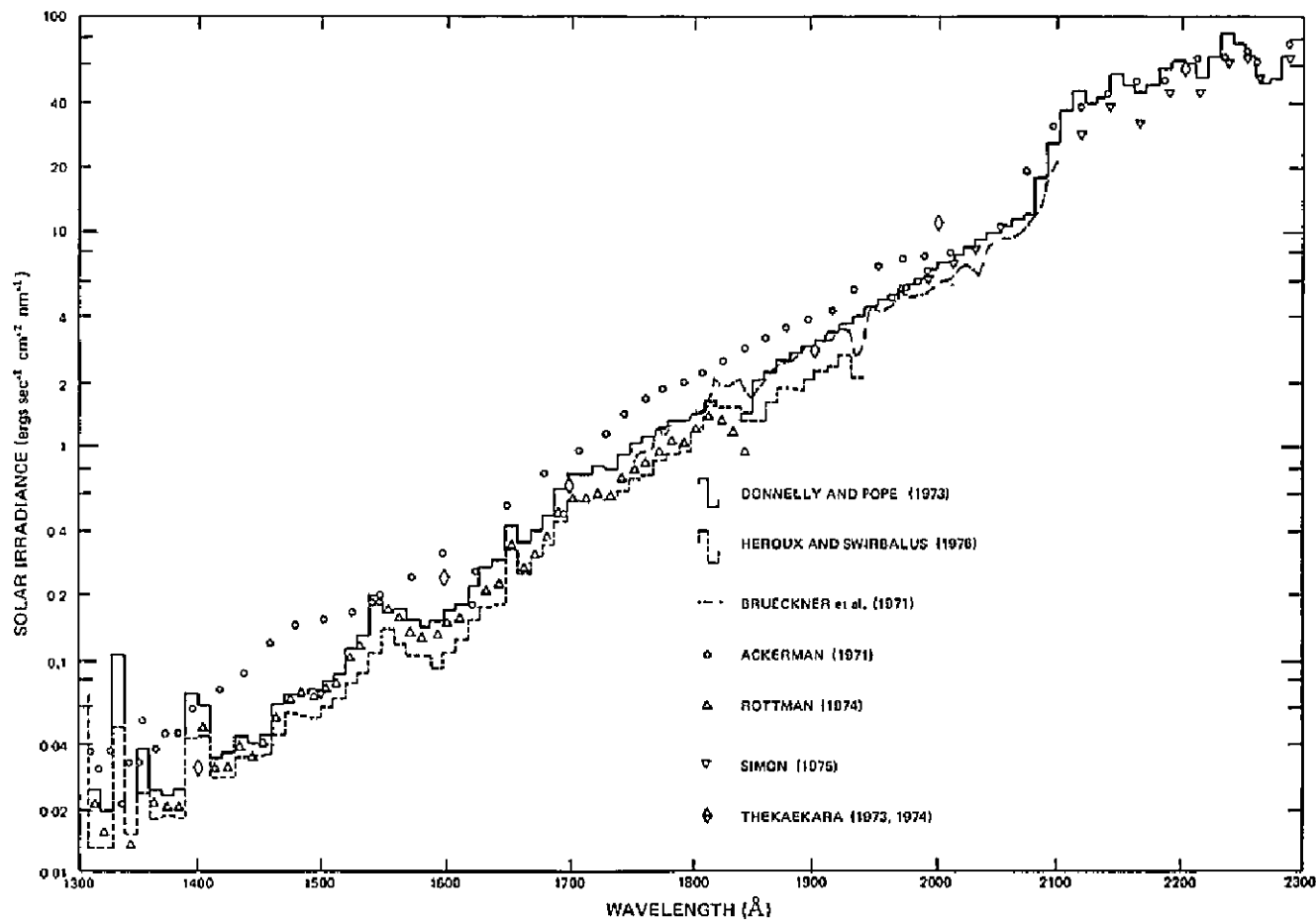


Figure 15. Solar spectral irradiance in the wavelength interval 1300 to 2300 Å.

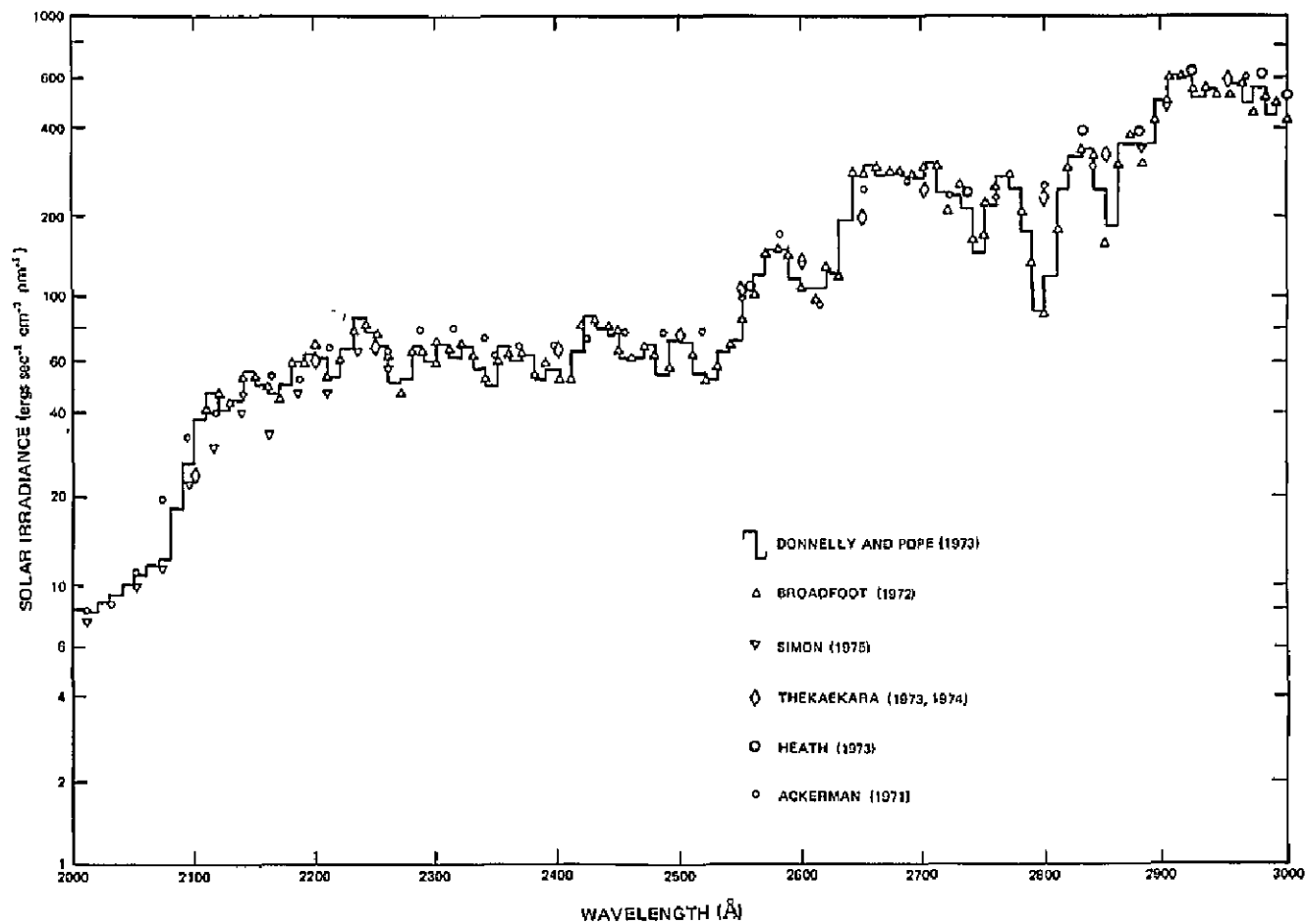


Figure 16. Solar spectral irradiance in the wavelength interval 2000 to 3000 Å.

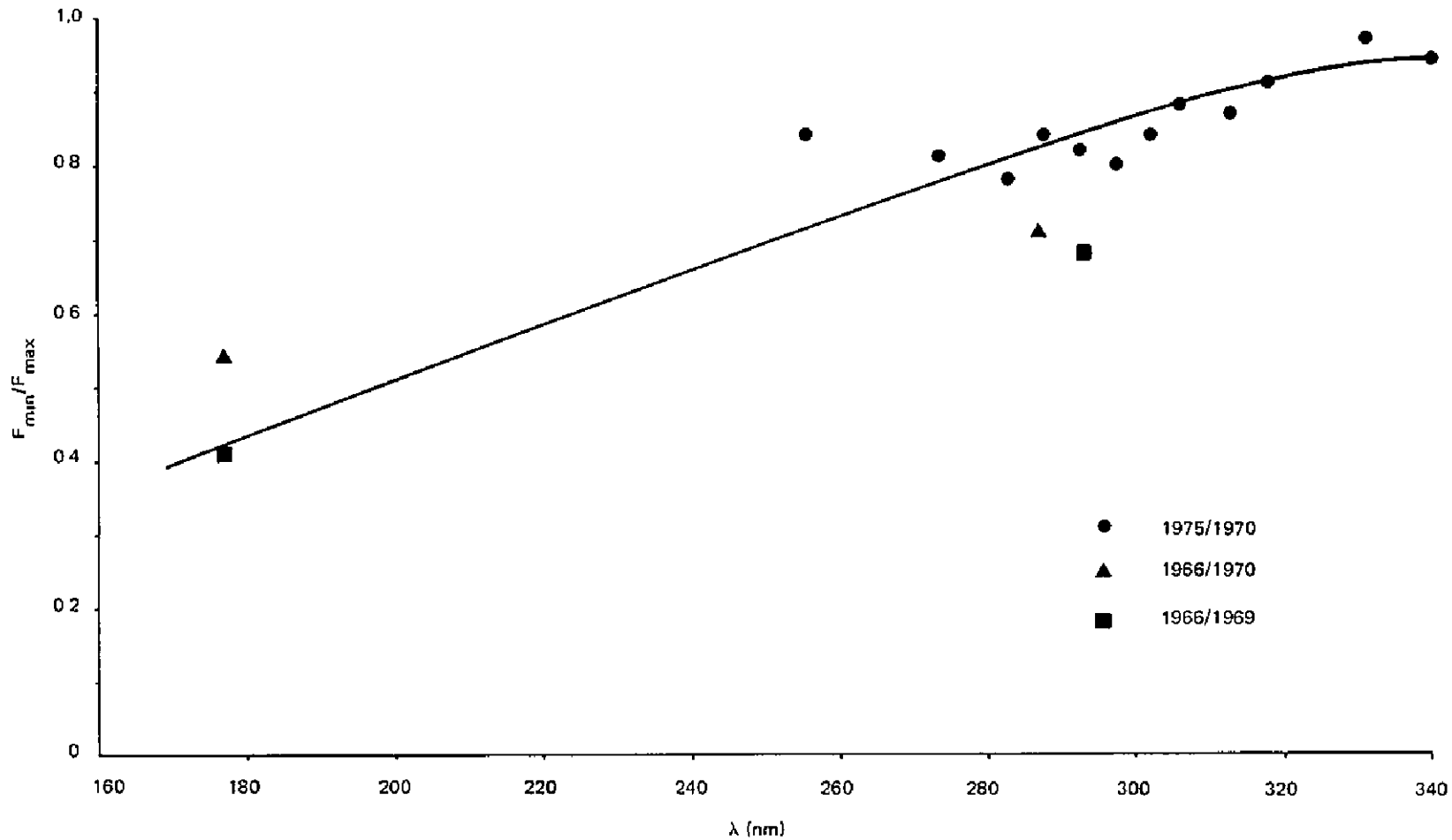


Figure 17. Ratio of solar flux measured near solar-cycle minimum to that measured near solar-cycle maximum versus wavelength.

Unfortunately, not enough is known about the global scale structure of the stratosphere over the sunspot cycle to permit the assessment of long-term solar variability on the stratosphere from atmospheric observations.

In summary, the current measurements of solar spectral irradiance from 160 to 300 nanometers appear to be in reasonably good agreement for the period of solar minimum. A concerted effort should be made to greatly increase the number of spectral irradiance measurements as the Sun goes from sunspot minimum to sunspot maximum. Emphasis should be placed on improving the accuracy of the absolute spectroradiometric calibration of the instruments that are used because it is extremely important to establish whether or not long-term changes are taking place in the ultraviolet solar flux.

Experimental measurements of the solar flux at specific altitudes in the stratosphere are required for verifying the calculated attenuated solar flux at that altitude. This is particularly desirable in the Schumann-Runge bands. Evens (private communication, 1977) has begun to obtain direct integrated solar-flux measurements in the spectral region 180 to 200 nanometers. Megill et al. (private communication, 1977) have obtained solar-flux data as a function of wavelength and angle with respect to the line of sight with the Sun.

The measurement of photochemically generated short-lived species provides information on the integrated effect of solar flux, photodissociation cross sections, and the column densities of major light absorbing species. These measurements are important as both altitude-concentration profiles and ground-based column densities. Atomic oxygen is a good candidate for altitude-concentration profiles. The excited molecular-oxygen species, $O_2(^1\Delta_g)$ and $O_2(^1\Sigma)$, are desirable for both column densities and altitude-concentration profiles.

The photochemical decomposition of ozone in the 50- to 30-kilometer region can be described quite accurately compared to other species. Scattering effects and albedo are calculated to have little influence on this process. The three-body recombination rate constant for forming ozone is also one of the better-known kinetic rate constants. The problem in accurately calculating the ozone profile in this region involves the rapidly changing lifetimes (2 hours to 10 days) and the destruction by minor species (NO_x , ClO_x , and HO_x). For these reasons, simultaneous experimental altitude-profile measurements of the local ozone are essential for the determinations of solar flux ($\lambda > 200$ nanometers), O atoms, $O_2(^1\Delta_g)$, and $O_2(^1\Sigma)$.

TRANSPORT MEASUREMENTS

Transport plays an important role in the stratosphere through the mixing processes and the circulation patterns. Transport processes are too often included only during the hand-waving stage of explaining differences between measurements and theory. Knowledge of these processes is essential to the development of useful transport parameters invoked in models. Understanding of the stratosphere has reached the point at which transport measurements should be made simultaneously with measurements of stratospheric composition.

This subsection describes the types of transport processes that affect composition measurements, the types of transport measurements that can be performed, and their accuracy.

Altitude-profile measurements of stratospheric constituents are performed on a mesoscale basis (100 kilometers to 100 meters). At this scale, large variability exists due to localized transport processes. The danger exists that the constituent measurements are accepted as representative of a global scale, which in fact they are not. Furthermore, no attempt is currently being made to understand or parameterize the mesoscale variations. Until these mesoscale variations are understood, it will be impossible to derive representative averages of constituent densities and eddy-diffusion coefficients for 1-D and 2-D models. It is established that tropospheric folding is a dominant mechanism for troposphere/stratosphere interchange at mid-latitudes. Midlatitude measurements of constituents may vary significantly if a tropopause folding occurs at the measurement location and times. Similarly, in the tropics where Hadley cell circulation dominates the lower stratosphere, altitude profiles alone should not be used to infer an eddy-diffusion coefficient. It is necessary to separate the effects of convective transport on a constituent profile before attempting to estimate the diffusive transport. This requires knowledge of the velocity field or, in some instances, the flux of an effective tracer (such as ozone). Such information is not readily available. Horizontal variability on the mesoscale is a result of irregular mixing and wind shear. At one altitude, the composition may be transported from the southwest, whereas, at another altitude, it is from the northwest. Hence, a single altitude-profile measurement can represent chemical processes occurring at widely separated locations. Thus, it is necessary to perform a meteorological analysis to trace the origin of the constituent as a function of altitude.

Frequently, the midlatitude tropopause is not sharply defined and consists of multiple temperature minimums with associated sharp increases in the ozone mixing ratio. Measurements of ozone taken simultaneously with other measurements are extremely useful in defining the tropopause structure and the transport processes above the tropopause.

The location of measurements is important, and a particular local feature can affect the data (e.g., measurements conducted near mountains). High Altitude Clear-Air Turbulence (HICAT) program data clearly indicate enhanced turbulence effects near mountains, probably because of breaking waves (see Climatic Impact Assessment Program (CIAP) Monograph I, Chapter 6). Certain latitudes pose problems attributable to the confluence of different circulation patterns.

Measurements can be conducted at specific locations to minimize or maximize one or the other circulation patterns. Measurements conducted in New Mexico and Texas are in the transition region between tropical effects and midlatitude effects (i.e., at the tropopause gap). A more effective procedure would be to conduct measurements farther south, such as in Panama, to isolate tropical transport effects and farther north to examine midlatitude transport.

Frequently, logistics considerations demand that balloon flights be conducted during the spring or fall turnaround. Unfortunately, these are times of rapidly changing circulation conditions, and measurement results are difficult to interpret in terms of being representative of a particular season.

WINDS AND DYNAMICS

The measurement of vector winds and dynamical processes in the stratosphere is significantly more difficult than measurement of scalar quantities, such as temperature, composition, or density. Because this difficulty has limited the number of measurements, present knowledge of the winds and dynamics is poor in quantitative accuracy in spite of the fact that transport plays a dominant role in the variation of trace constituent densities about the globe and the small-scale structure observed in ozone-density profiles (Dütsch, 1969). The general features of transport are known on a large scale such as geostrophic flow, two-cell meridional flow, and quasi-biennial oscillations. However, detailed measurements of the winds on the synoptic and mesoscales are not accurately known over the surface of the globe. Assuming that there is a need for detecting a perturbation in the stratospheric environment within a short period of a few years, it will be necessary to improve the present measurements of winds and dynamics.

The present measurement techniques can be grouped as either direct measurements or indirect measurements, the latter using numerical models to infer a transport term from known distributions of tracers. Most of the direct measurements of winds have been performed with rawinsondes and rocketsondes, small payloads that are tracked in ascent or descent to deduce a wind velocity from displacements of their horizontal position with time. These sondes are launched on a regular schedule as part of the Cooperative Meteorological Rocket Network (CMRN). Additional high-altitude data have been obtained from observations of improved radiosondes (jimspheres) and grenade experiments. Winds are also deduced from changes in position of balloons, ribbon chaff, falling spheres, and smoke trails. Direct measurement of circulation patterns are observed in the patterns of atmospheric tracers such as radioactive debris and ozone. Descriptions of these measurements and typical results can be found in the excellent summaries in the CIAP Monographs I and III. Direct measurement of small-scale turbulence has recently been conducted with anemometers suspended below balloons (Cadet, 1975; and Barat, 1975). Projects HICAT and Coldscan (see CIAP Monograph I, Chapter 6), conducted between 1964 and 1970, used aircraft to measure clear-air turbulence (CAT). These data are significant in describing the probabilities of occurrence, scale, and intensity of turbulence and in correlating the CAT with synoptic structure.

The primary source of wind measurements in the stratosphere is the rocketsonde data obtained at 30 active stations and archived at World Data Center-A (WDC-A), Asheville, North Carolina. The data contain systematic bias due to the time of observation and systematic errors of each particular sonde and technique of data analysis used, in addition to random instrumental errors. Although WDC-A exercises care to minimize obvious data errors, the user usually accepts the mean values as representative, which may not be the case. The rocket launchings are usually conducted at local noon with the exception of the measurements by the Union of Soviet Socialist Republic (USSR), which are conducted at night. The predominance of noon launchings places a bias in the mean values originating from the diurnal tide. This is particularly noticeable in meridional winds (Nastrom et al., 1975). The infrequency of the soundings and the incomplete global coverage create many statistical and analytical problems. This is illustrated by comparison of the monthly mean winds whose variance is equal in magnitude to the mean wind speed. This is true even for the strong zonal winds, which are observed to have significant longitudinal variations in the upper stratosphere from the monthly mean, such as between West Geirnish and Ft. Greely. It is obvious that present wind measurements are inadequate to accurately describe the dynamics of the

stratosphere. The accuracy of the measurements is difficult to determine from the limited number of simultaneous soundings. The problem of systematic errors in technique is illustrated by the results of comparative rocketsonde tests performed jointly by the United States, USSR, France, Japan, and the United Kingdom (Finger et al., 1975).

Comparison of temperature soundings found fair agreement (temperature difference less than $\pm 5^{\circ}\text{C}$) among those of the United States, Japan, and the United Kingdom. A table of temperature adjustments has been recommended for use with French and Russian data, which departed significantly from the other measurements. The wind measurements were in substantial agreement (root-mean-square differences less than 5 meters per second), except for the Russian results above 40 kilometers. These tests, which involved 85 soundings in 29 comparisons, illustrate the difficulty in establishing a uniform reference for a global network. The accuracy of the rocketsonde data is estimated to be ± 0.5 meter per second in velocity and 1 degree in direction for machine-calculated data (CIAP Monograph I, Chapter 9, 1975). Intercomparison measurements and comparison with cloud motion indicate a precision of approximately ± 5 meters per sounding (Bauer, 1976). This error is too large for accurate determination of meridional flow, as pointed out by Danielson in CIAP Monograph I. Confidence in CMRN data will come at the expense of additional observation stations and more frequent soundings. International cooperation must be emphasized to achieve better uniformity in CMRN data.

Realistic increases in the CMRN data rate are probably unlikely, and it is necessary to turn to satellite observations and other techniques to supplement the data. Objective analysis techniques for satellite radiation data and rocketsonde data exist (Gelman and Negatami, 1976), which can automatically prepare synoptic analyses of the 5-, 2-, and 0.4-millibar levels. The lack of vertical resolution of the satellite radiance information plus real space and time variability are the principal causes for the root-mean-square difference of 5 to 14 meters per second in velocities between rocketsonde and satellite data. The vertical height resolution is limited to about 10 weighting functions representing the optimum infrared sounding.

Vertical eddy-diffusion coefficients are important parameters that affect the lifetime of constituents in the stratosphere and their impact on ozone depletion. The current use of 1-D models to provide estimates of ozone depletion requires a realistic globally averaged eddy-diffusion coefficient. Vertical eddy-diffusion coefficients, K_z , are currently determined from measurements of altitude profiles of CH_4 and N_2O . The derivation of

K_z requires an accurate description of sources and sinks and the assumption that other forms of transport are not affecting the altitude profile. This latter assumption is seriously challenged below 20 kilometers by the effects of tropopause folding and cumulus convection in the tropics (Reiter, 1975; CIAP Monograph I). At the time of the NAS study, only a few midlatitude profiles existed, which lead to an overconfidence in estimating the eddy-diffusion coefficients. Numerous N_2O measurements conducted by NOAA at tropical, middle, and high latitudes have been recently analyzed for eddy-diffusion coefficients (Schmeltekopf, 1977). Significant variations exist with latitude. It is clear that location of the measurements is an important consideration. Further measurements are needed to cover expected seasonal variations.

AEROSOL MEASUREMENTS

The possible importance of heterogeneous chemistry on aerosols in the stratosphere is discussed in the position paper by DeMore (1977). The situation with regard to chemical effects is characterized by a general lack of specific rate data for possible surface reactions. Fortunately, upper-limit arguments can be used to rule out known heterogeneous effects as being important for removal of CFM's, HCl, ClO, and Cl. However, DeMore (1977) concludes that possible surface catalytic processes involving hydrolysis of chlorine nitrate to produce HNO_3 presently cannot be excluded as being competitive with gas-phase processes. Thus, aerosols may be important to certain aspects of the ozone depletion problem.

An account of the various techniques used to measure aerosols may be found in the position paper of Rosen (1977). No single method can be used to make a definitive measurement of aerosols in the stratosphere. However, if the shortcomings of each technique are taken into account, there does seem to be a "mainstream" of agreement.

- There is reasonably good agreement or consistency among the various methods of measuring the vertical profile of aerosols. The results obtained from simultaneous observations using a photoelectric counter and a lidar technique compare quite favorably. Details of the experiment and the model needed to make the comparison have been presented by Pinnick et al. (1976). Bigg (1975) has found good agreement between simultaneously measured vertical profiles as ob-

tained by the impactor technique and the photoelectric counter. Although the structure in the profiles may vary in time and space, there is essentially agreement that a layer exists at roughly 20 kilometers with a relative maximum in concentration and mixing ratio. This is to be contrasted with the profiles of condensation nuclei (CN, smaller particles) which show no relative maximum. In addition, there appears to be no consensus in the CN measurements above 20 kilometers.

- One of the most important aspects of the 20-kilometer layer is its variation with time. It is generally more useful to study the mixing ratio at the maximum, because this quantity can only be increased by a source and atmospheric mixing will tend to decrease it. Thus, the variation of the peak mixing ratio with time is very clearly related to the source strength of stratospheric aerosols.

The longest continuous record of a direct mixing-ratio measurement has been presented by Hofmann and Rosen (1977). The effect of a volcanic eruption in October 1974 is clearly evident. Although the aerosol decay was apparent after the volcanic eruption, it is not clear if the layer was in a steady-state (nondecaying) condition before this event. A typical average value of the particle concentration at 20 kilometers for the latitude is about 1 per cubic centimeter for sizes larger than 0.3 micron in diameter.

Although the time variation of smaller particles (CN) in the stratosphere has not been adequately studied, preliminary results indicate that it remains fairly constant (Rosen and Hofmann, 1977), again in contrast to the larger particles.

Because of the enormity of the task, very few efforts have been made to systematically determine the global distribution of stratospheric aerosols. Some recent measurements have been reported by Rosen et al. (1975). These results appear to be fairly consistent with the global distribution of mass loading as reported by Lazrus and Gandrud (1974b), although above 20 kilometers there are very few mass measurements available for comparison.

No systematic measurements have yet been reported concerning the global distribution of CN in the stratosphere.

- A summary of almost all direct measurements of the size distribution in the 20-kilometer layer has been presented by Harris and Rosen (1976). In spite of the many inconsistencies, there appears to be a mainstream of agreement. It is also apparent from the foregoing work that, generally, the impactor data give unrealistically high particle concentrations for radii larger than about 0.3 micron. This effect can most likely be attributed to a fundamental problem in the technique itself: the inability to correctly sample volatile aerosols. When the suspect data are taken into account, the mainstream of agreement becomes even more pronounced. Calculations of the mass loading and lidar backscatter cross sections using absolute size distributions consistent with this mainstream of data give excellent agreement with the corresponding measured values (Pinnick et al., 1976). Thus, there is good reason to believe that current knowledge of the size distribution of stratospheric aerosols is reasonably adequate.
- The major chemical component of the present aerosol in the 20-kilometer layer is generally believed to be H_2SO_4 . However, impactor samples indicate that one or more small insoluble dense nuclei can frequently be associated with each liquid particle. The source of these small nuclei could be terrestrial, extraterrestrial, or both.

Areas of uncertainties in aerosol measurements are as follows:

- It is popular belief that, except for after volcanic eruptions, the 20-kilometer aerosol layer is in a steady-state configuration supported by sulfur-bearing gases diffusing up through the tropopause. The best direct data available do not clearly show the existence of a steady-state layer, and it is possible that the layer would not exist without volcanic injections. Until this question is settled by long-term surveillance employing a technique capable of obtaining good quantitative measurements, modeling of the stratospheric aerosol will be impossible. Without a realistic model, it will be difficult to address the effect of man's activity on this stratospheric constituent.
- Although the real part of the index of refraction can probably be determined accurately enough from the chemical composition, the imaginary part is relatively uncertain because it can depend heavily on the impurities present in the aerosol. The complete index of refraction is needed for optical models that assess the effect of aerosols on climate and relating remote sensing data to useful quantities.

- The vertical profile of CN above 20 kilometers is still very uncertain. There is mounting evidence that an appreciable fraction of these particles in the stratosphere may be of extraterrestrial origin. Measurements of CN to at least 40 kilometers are needed to provide baseline information and asymptotic limits on the size distribution used in optical models.
- Although the overall size distribution derived from the mainstream of measurement does not appear to be incorrect, some thought should be certainly given to developing a definitive method for measuring this parameter because none of the present methods are entirely adequate in themselves. In addition, various types of direct measurements designed to test proposed optical models based on proposed size distributions should also be conducted.

The major areas of uncertainty lie in the distribution of CN above 20 kilometers and the existence or nonexistence of a steady-state 20-kilometer aerosol layer.

RECOMMENDATIONS

MEASUREMENTS

Certainly, the present data base of both reactive and nonreactive stratospheric minor constituents needs to be improved and extended before the confidence in model predictions will be improved substantially. Although significant improvements in the data base have been made in the last few years, the stage is now set for measurement programs that will provide considerably more stringent bounds for model simulations.

A clear distinction should be made between the difference in measurement strategies for: (1) the source terms that are decoupled from the stratospheric photochemical scheme because of the long-time constants for photolysis or oxidation processes, and (2) the radical sink terms that are strongly coupled photochemically. For example, high priority should be given to simultaneous observations of HCl and ClO to establish the free-to-stable chlorine ratio, whereas simultaneous measurements of ClO and CH₃Cl are of minor importance.

The proviso that extensive intercomparisons and cross-calibrations be made underlies any continued measurement program. These must be made to settle existing outstanding discrepancies and to assign more

meaningfully the accuracy of the present data base. In conjunction, sensitivity tests of the data inversion techniques of remote sensing methods should be undertaken.

Although simultaneous measurements are of prime importance, dedicated exploratory measurements to identify new species or to confirm as yet undetected species are recommended.

In addition to abundance measurements, programs should be developed to obtain *in situ* measurements of photodissociation coefficients and/or solar flux. At least relative measurements of direct and indirect flux would aid in the detailed model simulation of specific stratospheric missions.

It is also of particular importance for laboratory measurements to be made, under simulated stratospheric conditions, of spectroscopic parameters necessary for the inversion of long-path absorption/emission data. Facilities are available for these studies, and use of them is encouraged.

HYDROGEN SPECIES

The data base of hydroxyl-profile measurements needs to be extended, and the complete altitude range needs to be covered. Hydroxyl measurements should be carried out with simultaneous measurements of at least O_3 and H_2O . Techniques should be developed for the measurement of H , HO_2 , and H_2O_2 . Ground-based measurements of OH should be inter-compared with simultaneous profile measurements to define the stratospheric contributions. Measurements of seasonal, temporal, and latitudinal variability of hydroxyl total amount and stratospheric concentrations should be made. First, 1-D models require at least hemispheric profile averages of abundance measurements. This necessitates a long-term experimental program to determine latitudinal, seasonal, and diurnal trends.

To obtain reasonable hemispheric averages, it is recommended that several new, well-chosen launch sites, consistent with scientific objectives, be established to supplement present sites. An equatorial station should be given high priority. It is also recommended that experiments be conducted over relatively short periods of time during specific seasons to determine reliable seasonal trends. In this respect, greater priority should be given to these missions in order to better utilize existing launch stations. In the intervening periods and latitudes, ground- or aircraft-based column measurements are required to supplement the profile data and to permit routine monitoring as required to supplement the profile data and to

permit routine monitoring of constituent variation. The chosen launch sites should maintain routine upper-air meteorological and ozone measurements in order to correlate measurements and to identify unusual atmospheric conditions.

On a shorter time scale, and while fulfilling some of the requirements of the long-term studies, more extensive programs designed for critically testing the accuracy of model chemistry by simultaneous diurnal and profile measurements are required. Simultaneous measurements of inter-related components of the HO_x , NO_x , and ClO_x cycles should be given greater priority. With present instrumentation, collaboration of several groups would enable key experiments to be attempted in a relatively short time. To define and organize these missions, the establishment of a panel of active scientists is recommended.

Isolated measurements of OH are of little value because it has been demonstrated that this species is apparently briefly variable, and this requires careful definition of its chemical environment (i.e., H_2O , O_3 , O, and T). It is also of little value to measure ClO and HCl or NO , NO_2 , and HNO_3 without knowledge of the OH density, because the (ClO)-to-(HCl) ratio is directly proportional to (OH), and the $(\text{NO}_2)/(\text{HNO}_3)$ ratio is inversely proportional to (OH).

NITROGEN SPECIES

Although reasonable attempts have been made to measure the ratio of species that are expected to be photochemically controlled, none of the NO_x/NO ratios so determined are really in satisfactory agreement with specific model calculations. Further studies by all *in situ* or all long-path techniques are required, as relative measurements of higher accuracy can be made. In view of the current strong ClO_x - NO_x coupling, simultaneous missions of ClO_x , NO_x , and HO_x instrumentation should be attempted.

Simultaneous diurnal NO_x measurements using several techniques should be undertaken to clarify the longstanding controversy regarding the behavior of NO_2 .

The observations that total NO_2 (and thus presumably NO) essentially disappears north of 50° in winter have yet to be explained quantitatively. Both multidimensional model calculations and winter profile measurements at high latitudes are required.

The role of N_2O_5 in stratospheric chemistry needs further clarification by measurements to determine profiles, especially in winter at northern and southern latitudes. This is important because N_2O_5 acts like a reservoir for inactive odd nitrogen.

A detailed assessment of the influence of the rapid NO_2/NO conversion on long-path measurements at twilight is required.

HALOGEN SPECIES

The ratio of ClO to bound forms of chlorine is critical to the depletion of ozone by CFM. New techniques should be developed to measure ClO in order to support the resonance fluorescence measurements. Simultaneous measurements of ClO, Cl, HCl, O_3 , OH, and CH_4 are required to test current chlorine photochemistry models. Measurements of $ClONO_2$, in conjunction with ClO and HCl, are urgently required. Initial measurements of $ClONO_2$ should be made at dawn because concentrations will be larger.

New measurement techniques, such as resonance fluorescence, should be developed for HCl. The latitudinal and seasonal variations of HCl and ClO should be measured.

Other possible chlorine compounds should be investigated, and attempts should be made to measure them if they are determined to be important to atmospheric measures. Filter-impregnated techniques for measuring chlorine compounds should be developed further. The development of any technique to measure the total chlorine content would be a major advance. Simultaneous measurements of HCl and HF should be made, and attempts to develop techniques for measuring other possible fluorine compounds, such as COF_2 and $COFCl$, should be pursued. A possible technique is the further improvement of high-resolution spectroscopic instrumentation.

Concentration profiles of HBr and inventories should be measured.

The injection of chlorine, fluorine, and sulfur compounds by volcanoes into the stratosphere should be monitored.

CHAPTER 4

ONE-DIMENSIONAL MODELS

INTRODUCTION

The one-dimensional (1-D) model is a particular simplification of the atmospheric radiative/chemical/dynamical system in which chemistry is treated in greater detail than radiation or dynamics. Although the amount of chemistry in a 1-D model varies from model to model depending on the problem being examined, in general, it is as complete as our knowledge of laboratory kinetics permits for the simulation of the atmosphere. Transport is introduced parametrically in the diffusion approximation as the vertical altitude-dependent eddy-diffusion coefficient, K_z . Radiation in the ultraviolet and visible wavelength range is treated in some detail, sometimes including the effects of molecular multiple scattering and surface or cloud albedo. Radiative feedback through changes in infrared heating or cooling and changes in ultraviolet heating have been examined but are not usually included in 1-D chemistry models at this time. A more complete description of these processes is included in Chapter 5.

Because the effect of the chlorofluoromethanes (CFM's) on ozone is primarily through chemical processes, the 1-D chemistry model has become the primary predictive tool for assessing possible changes in the natural ozone content. There are many caveats on the use of 1-D models. These have been discussed in the Climatic Impact Assessment Program (CIAP) Report of Findings, as well as in the National Academy of Sciences (NAS) reports on stratospheric flight and on CFM's. Chapter 5 of this report discusses many of the modifications that may have to be made to 1-D model results to account for the effect of feedbacks through radiation and dynamics not included in the models.

The focus of this chapter will be the current status of predictions by 1-D models. The first three sections discuss some aspects of what might be called model mechanics: the parametric simulation of vertical transport, the effects of diurnally varying reactants, and molecular multiple scattering. This is followed by three sections on the status of understanding of stratospheric measurements in terms of current theory. Next, the question of possible sinks for CFM's is discussed, followed by a discussion of the uncertainties involved in making predictions of stratospheric ozone change.

Special care should be taken in interpreting the subsections on comparison of theory and measurements. In general, the comparison is between the result of a 1-D model and a measurement made at one point in space and time. The interpretation of a 1-D model calculation is still a subject of discussion. In general, it represents a global average at each altitude of the species being calculated. By comparison with data, this global average has been shown to resemble the situation at around 30°N latitude (Johnston et al., 1976). Because most of the measurements of minor constituents have been made at this point, there is reason to expect gross quantitative agreement between the measurements and model results. The degree of agreement expected depends critically on what is being compared. For instance, when concentration ratios of species that are closely linked by fast chemical reactions are compared, agreement should be expected within the uncertainties of laboratory data. Good agreement is more likely when the concentrations of the controlling long-lifetime species are well-known. When these supporting measurements are not made, an uncertainty in the comparison comparable to the expected variability of the particular species must be included. When a reactive species is measured without any supporting measurements, the interpretation must include the effects of the temporal and spatial variations arising from a species' relationship with all of the other atmospheric constituents. Such variations might limit the expected agreement with a 1-D model to within a factor of 2.

PARAMETRIC SIMULATION OF NET VERTICAL TRANSPORT IN 1-D MODELS

Net vertical-transport processes in 1-D models of the stratosphere are usually represented through diffusion approximations. The net vertical-diffusion flux, F_z , of any minor trace species in the stratosphere is assumed to be proportional to the gradient of the mixing ratio of that trace species:

$$F_z = -\rho K_z \frac{\partial}{\partial z} (C_i/\rho) \quad (4-1)$$

where C_i is the concentration of the i th trace species, ρ is the air density, and z is the altitude. The diffusion coefficient, K_z , is usually called the vertical eddy-diffusion coefficient. In both the conceptual and operational sense, the term eddy diffusion in 1-D models is a misnomer. In the past, this use has led to unnecessary confusion in the interpretation of 1-D models. Consequently, in the following discussion, K_z will be referred to as the 1-D vertical-diffusion coefficient.

With this representation for the net vertical flux, the time-dependent 1-D continuity equation for the species concentration becomes

$$\frac{\partial C_i}{\partial t} = \frac{\partial}{\partial z} \left[\rho K_z \frac{\partial}{\partial z} (C_i/\rho) \right] + P_i - L_i \quad (4-2)$$

where P_i and L_i are the photochemical production and loss terms, respectively. When appropriate, a third term, S_i , representing any other anthropogenic sources or sinks of C_i are also added to the right side of equation 4-2. If the concentration of C_i is at steady state, equation 4-2 becomes

$$\frac{\partial}{\partial z} \left[\rho K_z \frac{\partial}{\partial z} (C_i/\rho) \right] + P_i - L_i = 0 \quad (4-3)$$

There is a large degree of uncertainty in the interpretation of equation 4-2 or 4-3. Ideally, with both proper time and space averaging of the appropriate variables, K_z , P_i , and L_i , these equations can at least be considered a global representation. Under this ideal condition, the remaining question would be the yet to be demonstrated suitability or accuracy of the diffusion approximation, equation 4-1. Unfortunately, this ideal condition does not exist. Because of the temporal and spatial variations of tropopause height and the intrinsic differences in the dynamic processes of the troposphere and stratosphere, there is no apparent technique for averaging K_z , P_i , and L_i satisfactorily in the global sense. Furthermore, such averaging would require detailed knowledge of the spatial distribution of the trace species at least qualitatively, if not quantitatively. At the present time, such detailed information is mostly unavailable. Consequently, the currently used values of K_z derived from limited data are somewhat different. As will be discussed below, these differences are real and must be considered as part of the uncertainties in 1-D stratospheric models.

CONCEPTUAL BASIS FOR THE INTRODUCTION OF K_z

Since primary concern is with the minor trace species of the atmosphere, it is reasonable to assume that the dominant motion is not dependent on

the local kinematics of individual trace species. For any particular species, C_1 , if equation 4-2 or 4-3 is applicable and if the loss and production processes are known, then, given the measured vertical profiles of C_1 , equation 4-2 or 4-3 can be inverted to obtain K_z . If all the assumptions noted previously are correct, then K_z so obtained should be independent of particular choices of tracer species. Based on current understanding of this kind of analysis, it seems reasonable to ascribe the observed K_z variations to general incompleteness of data rather than to gross error in the conceptual assumptions noted above.

Two kinds of atmospheric tracers have been used to derive K_z vertical profiles. First, there are the chemically reactive tracers, such as CH_4 and N_2O , that are mostly natural in origin. The other tracers are chemically inert; namely, the radionuclides introduced into the stratosphere by past atmospheric nuclear tests. In addition to these tracers, numerical experiments can also be conducted on existing three-dimensional (3-D) general circulation models (GCM's) with idealized inert tracers. By averaging the 3-D results from these numerical experiments, an effective 1-D vertical-diffusion coefficient can also be derived. The results from each of the three types of tracer analyses will be summarized and compared.

CHEMICAL TRACERS

CH_4 and N_2O are identified as reasonable tracers because of their relatively simple chemical-loss mechanisms. Wofsy and McElroy (1973) first derived a K_z profile from the available CH_4 data. Later, Hunten (1975) used the same chemistry (CH_4 loss rate) with a different smoothing of the CH_4 data to obtain a somewhat different K_z profile. Recently, Dickinson (1976), using both CH_4 and N_2O data and the loss rates as given by Chang (1976), has carefully analyzed the various derived K_z profiles arising from differences in data interpretation. Profile B in figure 18 represents an average of Dickinson's results. Profile A is qualitatively similar to the result of Hunten (1975), but multiplied by a factor of 2. This last modification was necessary because the original Hunten profile did not produce a chemical loss rate of CH_4 that is consistent with that used in its derivation. As can be seen, these two profiles (A (NASA, 1976*) and B (Chang, 1976)) are very similar above 25 kilometers. The differences between 10 and 25 kilometers will be discussed in the next section.

*R. S. Stolarski, private communication to model groups giving parameters for model comparison.

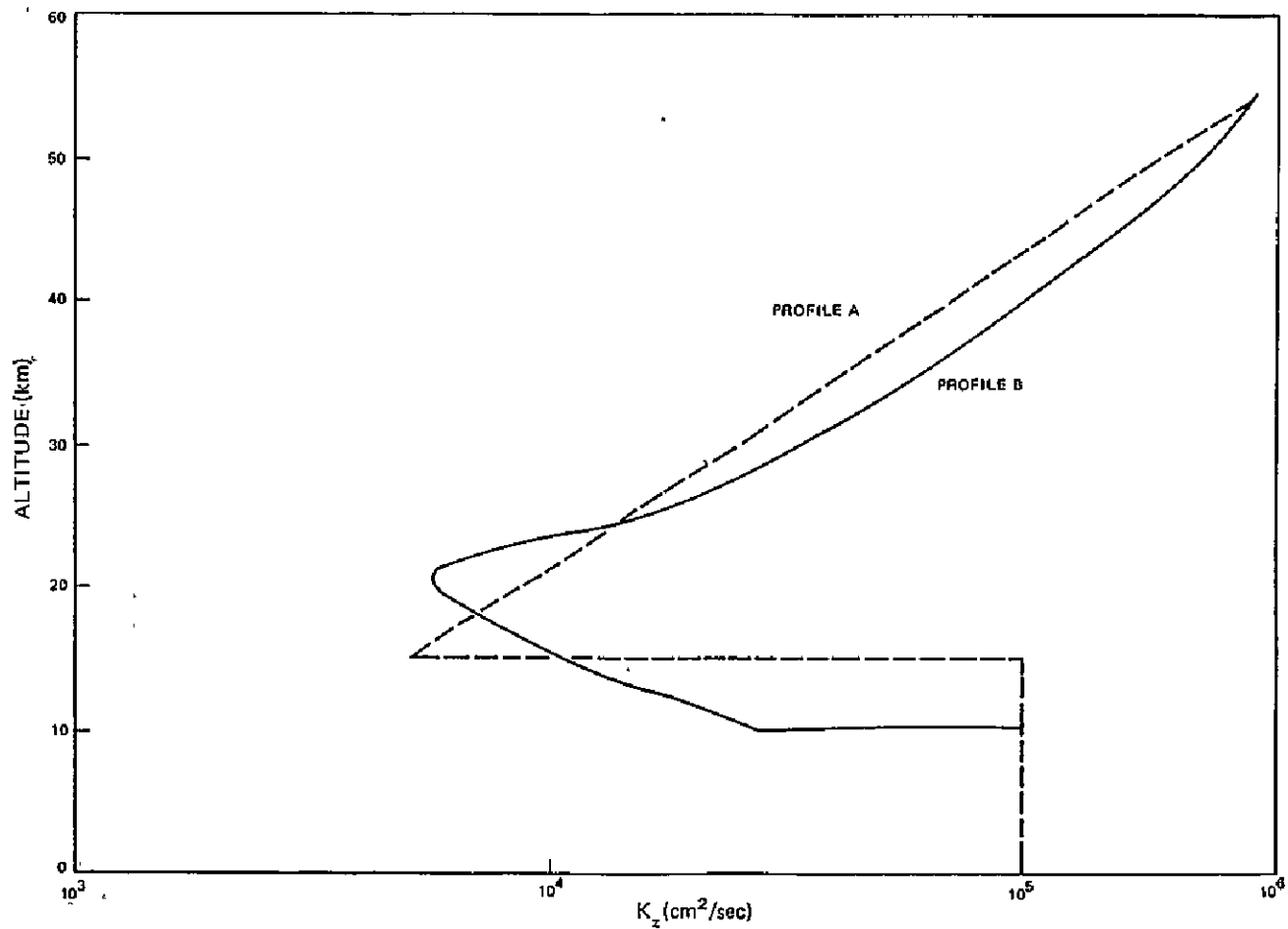


Figure 18. Vertical-diffusion coefficient profiles.

These tracers are useful in that they should be fairly uniform globally and that more than any other tracers they may be assumed to be in steady state. However, their apparently simple chemical loss mechanisms are quite deceptive. The principal loss mechanism for CH_4 is its reaction with OH , whereas for N_2O it is by photodissociation. The concentrations of OH and the photodissociation coefficients $J_{\text{N}_2\text{O}}$ are very model-dependent and contribute significantly to the uncertainties in the derived K_z . Another source of uncertainty is the lack of data above 35 kilometers for both CH_4 and N_2O . There is only one set of rocket data, which, in view of natural variability of all atmospheric trace species, would have to be construed as insufficient. There is also a need for more global data coverage for CH_4 , because most of the existing data in the stratosphere are from one location (Ehhalt, 1972 and 1974). It is unlikely that these uncertainties can be removed in the near future except, perhaps, by the gathering of more high-altitude data.

RADIONUCLIDE TRACERS

Past atmospheric nuclear weapons tests have injected an easily identifiable amount of radionuclides into the stratosphere. These radionuclides are injected either as fine particles (e.g., Sr^{90} , W^{185} , Rh^{102} , Cd^{109} , and Zr^{95}) or as a true gas (C^{14}). Because there are no chemical sources or sinks (except for well-understood radioactive decay) for these tracers, the inversion of equation 4-2 is particularly simple. Unfortunately, this advantage over chemical tracers is almost totally overshadowed by the difficulties caused by the transient (time-dependent) nature of its removal from the stratosphere. Uncertainties in sampling initial distributions and all subsequent distributions in the stratosphere and troposphere raise serious doubts about the conclusiveness of this type of analysis. A detailed discussion of these problems is in Chang (1975). Nevertheless, the available results from the particulate data seem to agree with profile B in the altitude range 10 to 25 kilometers. However, C^{14} data agree better with profile A divided by 2 (Johnston et al., 1976). As a result, there is at least a factor of 2 uncertainty in using these tracers. These results, coupled with the requirements from stratospheric modeling of CH_4 and N_2O , necessitated the present acceptance of both profiles A and B as possible representations in 1-D model. Fortunately, although profiles A and B gave different results for transient behavior, steady-state calculations using these two profiles yield identical predictions of the effect of CFM's on ozone (Chang and Wuebbles, private communication, 1977).

GCM TRACER EXPERIMENTS

Mahlman (1975) conducted two numerical experiments using the transport coefficients from the GCM at Geophysical Fluid Dynamics Laboratory/National Oceanic and Atmospheric Administration (NOAA). One was a midlatitude point-source injection experiment, and the other was a stratified tracer experiment. Using the time history of tracer distributions from these experiments, he was able to derive two profiles of effective 1-D vertical-diffusion coefficients that turn out to be in close agreement with profile B in the altitude range of 10 to 20 kilometers. Between 20 and 25 kilometers, the results from the experiment differ by a factor of 10, but both profiles A and B fall in the middle of his values (more details can be found in his paper). Again, because of the transient nature of Mahlman's (1975) numerical experiments and the lack of comparative analysis from other models, this agreement is not sufficient to demonstrate a preference.

The important point in the assessment of the 1-D vertical-diffusion coefficient, K_z , is the general agreement between the average values of profiles A and B in the range 10 to 20 kilometers. For the SST- NO_x problem, the details of K_z profiles in this altitude range are critical because this is the region of NO_x injection. However, for the CFM- Cl_x problem, the average effective transport rate across this region is the important parameter because CFM's from the ground must pass through this region to higher altitudes to be effective in releasing Cl to catalyze the destruction of ozone. Because the average transport rate across this region is similar in this respect, the effect should also be the same at steady state, as was found by Chang and Wuebbles (private communication, 1977). Consequently, the sensitivity of the ozone distribution to K_z is lower than might at first be expected.

DIURNAL AVERAGING EFFECTS

For an atmosphere with constituents that have chemical or dynamical lifetimes comparable to or less than 24 hours, the natural time-dependent effects must be carefully considered. The direct approach of integrating the diffusion equations with a time step short enough to properly reproduce the essential diurnal effects is too expensive because of the approximately 3 years of model time necessary for achieving true cyclic behavior from a steady-state starting point. Because of this fact and the need to follow the effects of atmospheric perturbations for a century or longer, some form of diurnal averaging is necessary. Diurnal averaging is a procedure that permits the photolysis and gas kinetic rates to be modified so that the long-term behavior of a steady Sun integration is the same as

the true diurnal average of the long-time integration of the fully time-dependent calculation.

A typical example of a nonlinear term contributing to the destruction rate of odd oxygen is

$$k_1 [\text{O}] [\text{ClO}] \quad (\text{cm}^{-3} \text{sec}^{-1})$$

corresponding to the reaction $\text{O} + \text{ClO} \rightarrow \text{Cl} + \text{O}_2$ with the reaction rate constant k_1 . The diurnal integral of this rate is represented by

$$\bar{R} \equiv \int_0^{24 \text{ hr}} k_1 [\text{O}] [\text{ClO}] dt$$

and is frequently approximated by the simple form

$$\bar{R}_A \cong k_1 [\text{O}] [\text{ClO}] T$$

where

$$T = 86,400 \text{ seconds}$$

To evaluate the diurnal effects on ozone reduction due to CFM's in the presence of ClONO_2 , Liu (1977) has run a steady-state program with 24-hour averaged photolysis rates for 30°N equinoctial conditions. The model used a constant 1974 CFM injection rate resulting in a steady-state Cl_x mixing ratio of 5.67 parts per billion (ppb). The reaction rate of ClONO_2 formation was

$$\frac{1.53 \times 10^{-14} \exp(1000/T)}{1.17 \times 10^{-18} \exp(250/T) + M}$$

In steady state, this run gave a column-ozone reduction of 3.5 percent.

When the model is run in the actual diurnal mode, the value of \bar{R} is found to be 60 percent larger than R_A at an altitude of 30 kilometers. Because

of this type of result and the prohibitive cost of direct-time integration for large net model times, care must be taken with the method of diurnal averaging.

Liu's (1977) approach is to make use of the fact that diurnal effects on the long-lived species are small. This permits their densities to be approximated by the solutions of the steady-state model (fixed Sun). For the present calculations, the profiles of H_2O , CH_4 , H_2 , N_2O , CF_2Cl_2 , $CFCl_3$, CO , NO_x , and Cl_x are held fixed at their steady-state values, whereas O_x , HO_x , H_2O_2 , $O(^1D)$, O , O_3 , H , OH , HO_2 , N , NO , NO_2 , HNO_3 , NO_3 , N_2O_5 , Cl , ClO , HCl , and $ClONO_2$ are allowed to vary with time. In addition, for the cases shown in figures 19 through 22, only O_x , HO_x , and H_2O_2 are calculated with diffusive flow.

Let the subscripts denote the steady-state result and d, the diurnal result. Then, after 120 days of integration in the diurnal model, two examples of diurnally averaged rates are:

$$\int_0^{12 \text{ hours}} [O]_d [NO_2]_d dt = 0.74 \int_0^{24 \text{ hours}} [O]_s [NO_2]_s dt$$

and

$$\int_0^{12 \text{ hours}} [O]_d [ClO]_d dt = 1.6 \int_0^{24 \text{ hours}} [O]_s [ClO]_s dt$$

where subscripts d and s denote diurnal and steady-state values, respectively. These results are shown in figures 19 and 20, where the 24-hour averages of $2[O] [NO_2]$ and $2[O] [ClO]$ in the diurnal model are compared to the steady-state model showing that, at 30 kilometers, the Cl_x perturbation due to the introduction of CFM's is enhanced by a factor 1.6 from the ClO diurnal effect alone. The factor is 1 without $ClONO_2$ and increases with increasing formation rate of $ClONO_2$. The foregoing calculation also indicates that the ozone reduction due to the NO_x perturbation is reduced by 25 percent because of the diurnal effects on NO_2 alone. Even though the test cases were not run to a converged cyclic condition, the trend indicates that the final ozone reduction for a true diurnal

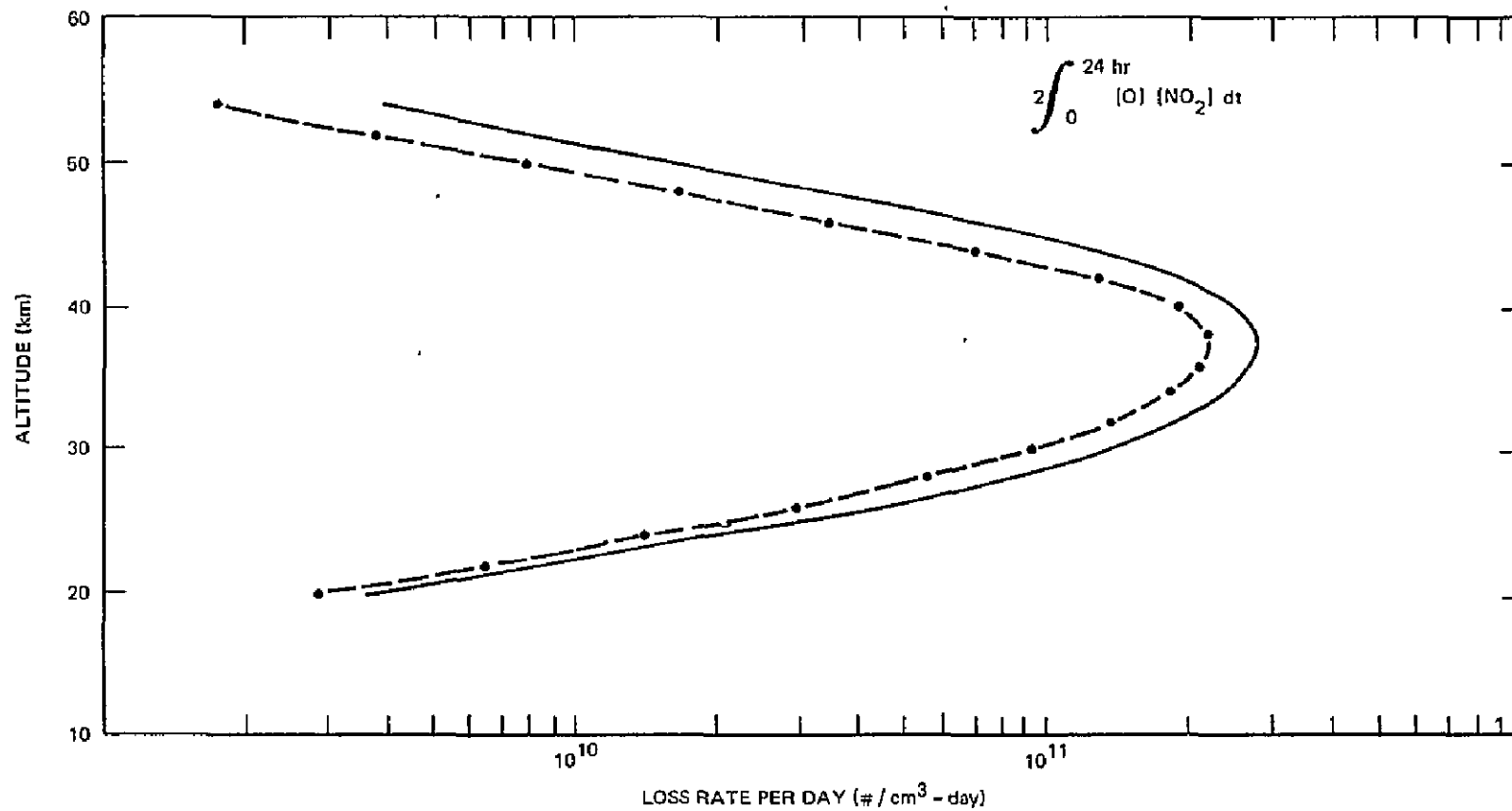


Figure 19. Effect of diurnal averaging on the $O + NO_2$ reaction rate.

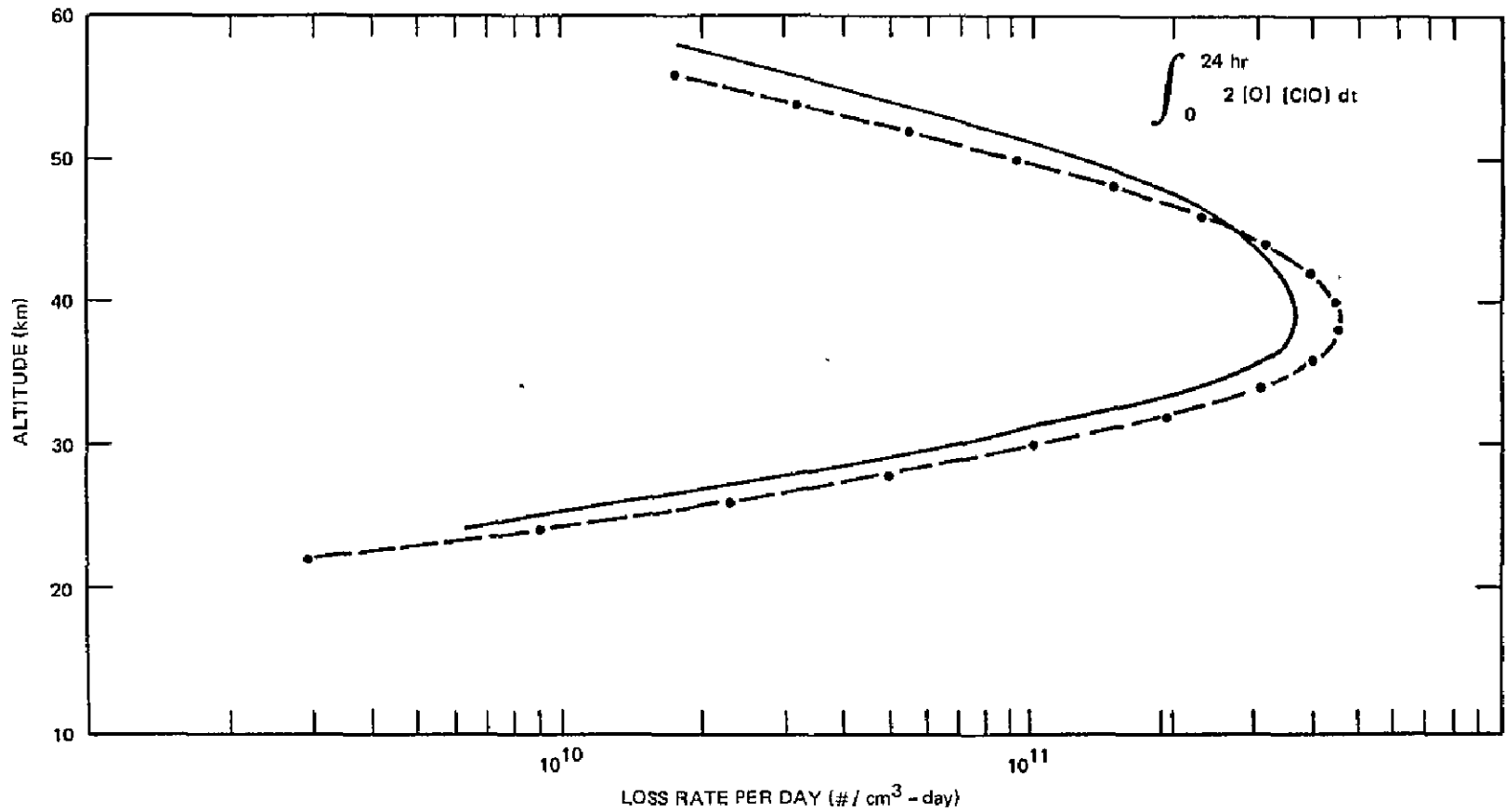


Figure 20. Effect of diurnal averaging on the O + ClO reaction rate.

model is probably about twice the ozone reduction predicted by the steady-state model.

Figure 21 shows the diurnal variations of ClO along with the corresponding steady-state values, which are indicated by arrows. The variations below 40 kilometers are from the conversion of ClO to ClONO₂ at night and the reappearance of ClO in the morning by photodissociation of ClONO₂. Without ClONO₂, ClO behaves as expected and has no diurnal variation below 40 kilometers. Below 50 kilometers, the variation of ClO is due to Cl + O₃ at night and its destruction by ClO + O during the day. The diurnal variations of ClONO₂ and its steady-state values are shown in figure 22. The daytime ClONO₂ density is about 20 percent less than the steady-state values between 20 and 30 km. From the foregoing discussion, it is clear that the problem of diurnal averaging is quite important in models that attempt to calculate the net ozone reduction in the presence of ClONO₂.

MULTIPLE-SCATTERING EFFECTS

The effects of including multiple scattering in the photodissociation-rate calculation are of three types: (1) the effect on photodissociation coefficients, (2) the effect on ambient species concentration profiles, and (3) the effect on model sensitivity to perturbations. The results shown in the following subsections were obtained using the Lawrence Livermore Laboratory 1-D transport-kinetic model (Luthèr and Wuebbles, 1976), which includes ClONO₂. The effect of multiple scattering was incorporated into the photodissociation-rate calculation by applying correction factors obtained from a highly detailed solar-radiation model to the flux, F , based on a pure absorption calculation. A solar zenith angle of 45° was used, and a surface albedo of 0.25 was assumed. The results are qualitatively representative of multiple scattering calculations made using other models.

PHOTODISSOCIATION COEFFICIENTS

Because virtually no radiation reaches the lower troposphere at shorter wavelengths, the effect of multiple scattering is largest for species having strong absorption cross sections at wavelengths greater than 290 nanometers. Computed photodissociation coefficients, including multiple scattering (J_{MS}) and assuming pure absorption (J_{PA}), are compared in table 28 for the same ambient atmosphere.

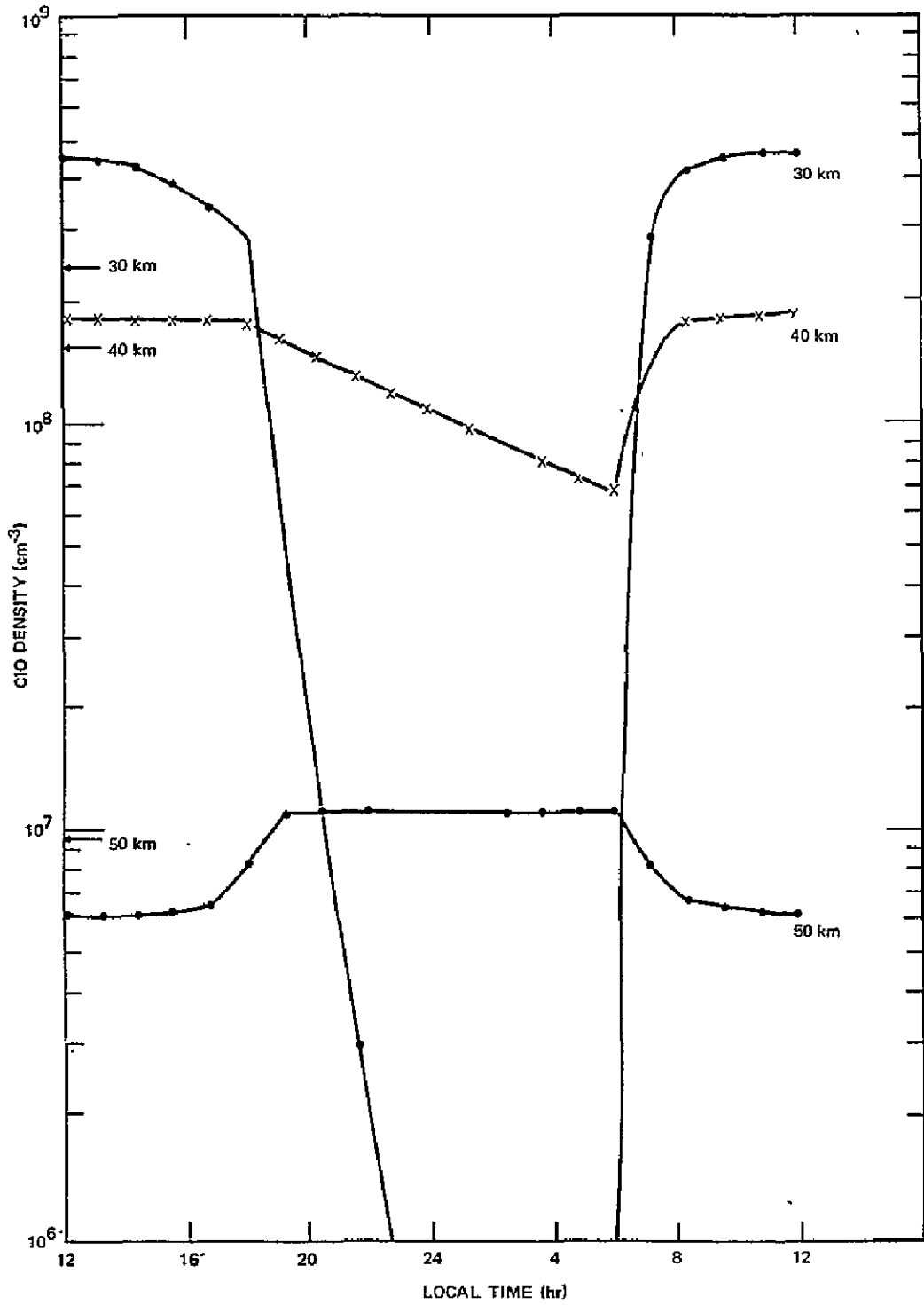


Figure 21. Diurnal variations of ClO along with the corresponding steady-state values.

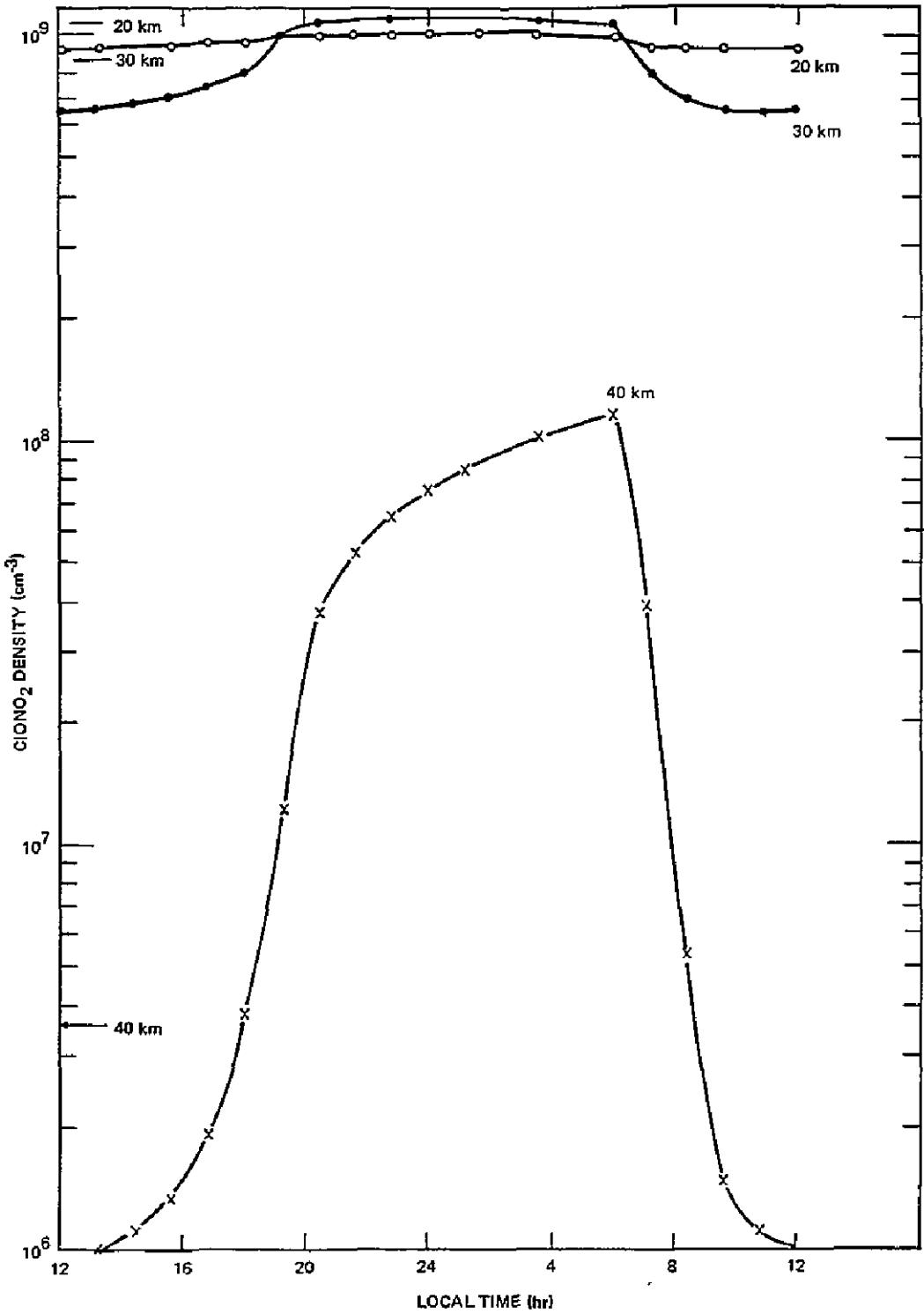


Figure 22. Diurnal variations of ClONO₂ along with the corresponding steady-state values.

Table 28
Comparison of Photodissociation Rates Calculated With and
Without Multiple Scattering ($A_s = 0.25$)

Altitude (kilometers)	J_{PA}	J_{MS}	J_{MS}/J_{PA}
$O_3 + h\nu \rightarrow O(^3P) + O_2$			
10	2.02×10^{-4}	3.01×10^{-4}	1.49
20	2.07×10^{-4}	3.00×10^{-4}	1.45
30	2.41×10^{-4}	3.21×10^{-4}	1.33
40	2.74×10^{-4}	3.49×10^{-4}	1.27
$O_3 + h\nu \rightarrow O(^1D) + O_2$			
10	5.83×10^{-6}	1.08×10^{-5}	1.85
20	7.97×10^{-6}	1.22×10^{-5}	1.53
30	5.78×10^{-5}	6.27×10^{-5}	1.08
40	9.32×10^{-4}	9.14×10^{-4}	0.98
$NO_2 + h\nu \rightarrow NO + O$			
10	4.72×10^{-3}	7.77×10^{-3}	1.65
20	4.74×10^{-3}	7.76×10^{-3}	1.64
30	4.85×10^{-3}	7.68×10^{-3}	1.58
40	4.97×10^{-3}	7.73×10^{-3}	1.56
$HNO_3 + h\nu \rightarrow OH + NO_2$			
10	2.72×10^{-7}	4.82×10^{-7}	1.77
20	3.37×10^{-7}	5.18×10^{-7}	1.54
30	4.98×10^{-6}	5.11×10^{-6}	1.03
40	3.52×10^{-5}	3.52×10^{-5}	1.00
$H_2O_2 + h\nu \rightarrow 2H$			
10	1.90×10^{-6}	3.35×10^{-6}	1.76
20	2.23×10^{-6}	3.46×10^{-6}	1.55
30	6.57×10^{-6}	7.29×10^{-6}	1.11
40	3.51×10^{-5}	3.52×10^{-5}	1.00
$ClO + h\nu \rightarrow Cl + O$			
10	1.72×10^{-5}	3.25×10^{-5}	1.89
20	2.55×10^{-5}	3.82×10^{-5}	1.50
30	1.92×10^{-4}	2.05×10^{-4}	1.07
40	1.64×10^{-3}	1.62×10^{-3}	0.99
$ClONO_2 + h\nu \rightarrow ClO + NO_2$			
10	3.31×10^{-5}	5.57×10^{-5}	1.68
20	3.43×10^{-5}	5.61×10^{-5}	1.64
30	5.22×10^{-5}	7.07×10^{-5}	1.35
40	2.24×10^{-4}	2.38×10^{-4}	1.06

Only those photodissociation reactions significantly affected by multiple scattering are shown in table 28. In an attempt to account for the diurnal variation of photodissociation in the model, the solar flux was halved. The importance of the significant changes in photodissociation-rate coefficients is reflected in the species concentration profiles and in the model sensitivity.

SPECIES CONCENTRATION PROFILES

The effects of multiple scattering on the individual species concentrations making up O_x , HO_x , and NO_x are shown in figures 23, 24, and 25, respectively. The large percentage increase in $O(^1D)$ near 10 kilometers shown in figure 23 occurs when the reference concentration is very small; nevertheless, it is significant in terms of stratospheric chemistry. The increases in $O(^3P)$ and $O(^1D)$ in the 20- to 30-kilometer region are due to increased photolysis of O_3 . Because of differences in reference concentrations, a small percentage decrease in O_3 causes large percentage-increases in the other species. The increase in $O(^3P)$ near 40 kilometers is mainly caused by increased photolysis of NO_2 . The increase in O_3 at this height occurs because the chemical production of O_3 by $O + O_2$ is increased more than the photolysis of O_3 .

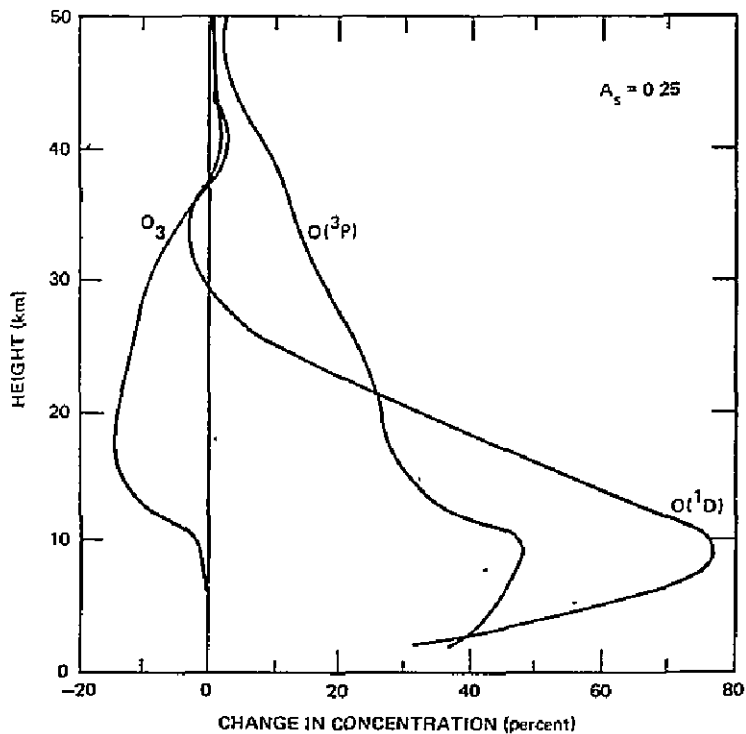


Figure 23. Change in O_x species concentrations attributable to multiple scattering with $A_s = 0.25$.

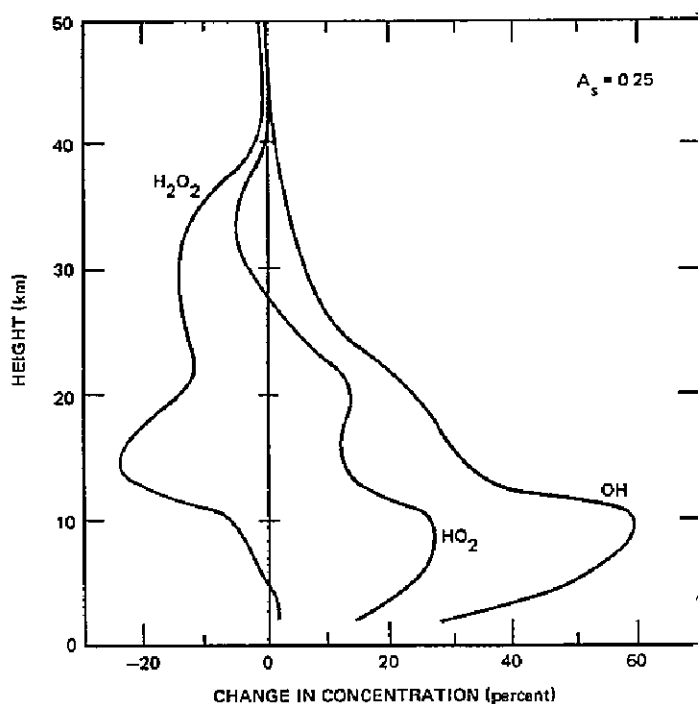


Figure 24. Change in HO_x species concentrations attributable to multiple scattering with $A_s = 0.25$.

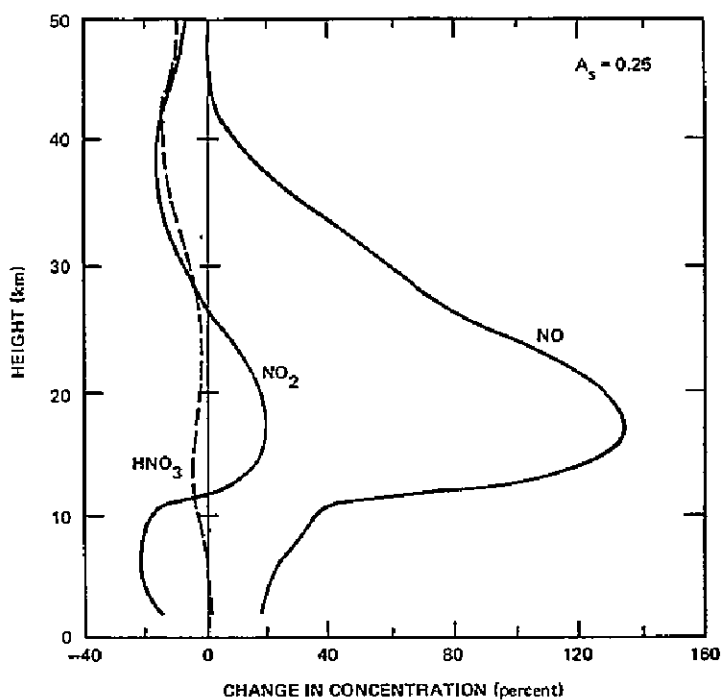
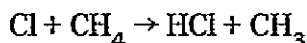
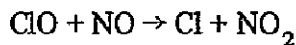
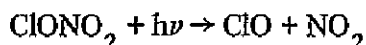


Figure 25. Change in NO_x species concentrations attributable to multiple scattering with $A_s = 0.25$.

As shown in figure 24, the increase in OH results from $\text{HNO}_3 + h\nu \rightarrow \text{OH} + \text{NO}_2$ and $\text{H}_2\text{O}_2 + h\nu \rightarrow 2\text{OH}$. Because the peak concentration in H_2O_2 occurs near 28 kilometers, a small percentage increase in H_2O_2 in this region can cause a large percentage increase in OH. The increase in HO_2 is chemically linked to the increase in OH.

Figure 25 illustrates the very large increase in NO near 20 kilometers due to increased photolysis of NO_2 . The NO_2 concentration increases because of increased photolysis of HNO_3 . There is very little HNO_3 above 30 kilometers, so that $[\text{NO}_2]$ decreases in this region result in $[\text{NO}]$ increases, because it is essentially the only source of NO. As figure 25 indicates, the $[\text{NO}]/[\text{NO}_2]$ ratio is changed significantly in the region between about 10 and 30 kilometers.

As shown in figure 26, the concentration of ClONO_2 is reduced 20 to 40 percent between 20 and 30 kilometers, which is the region of maximum ClONO_2 concentration. Photolysis of ClONO_2 affects several other chlorine-containing species through a complex chain of reactions. Some of the key reactions are:



Because the peak concentration of ClONO_2 occurs near 25 kilometers, photolysis of ClONO_2 acts as a source of ClO in this region. The large increase in NO between 20 and 30 kilometers tends to destroy ClO, leading to a net decrease in ClO in this region and an increase in Cl. The increase in Cl leads to an increase in HCl (figure 27) through the reaction with CH_4 . These results also indicate that inclusion of ClONO_2 has a more significant effect on Cl_x species than the choice of surface albedo.

The significant changes in the species concentration profiles are reflected in the total-column abundances. Ratios of total-column abundances computed with multiple scattering to that with pure absorption are 0.94 (O_3), 0.975 (NO_2), and 1.21 (NO).

Although the foregoing analysis is overly simplified considering the complexity and interaction of the various chemical cycles, the results and discussion are an attempt to summarize the major mechanisms by which multiple scattering changes the species concentrations.

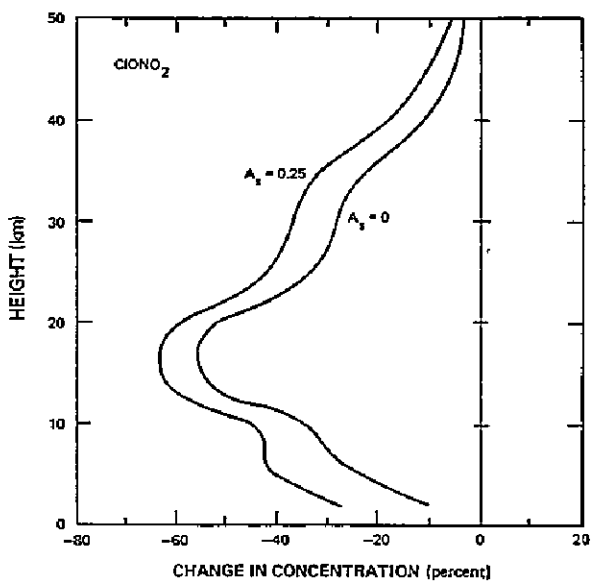


Figure 26. Change in concentration of ClONO_2 attributable to multiple scattering for $A_s = 0$ and 0.25.

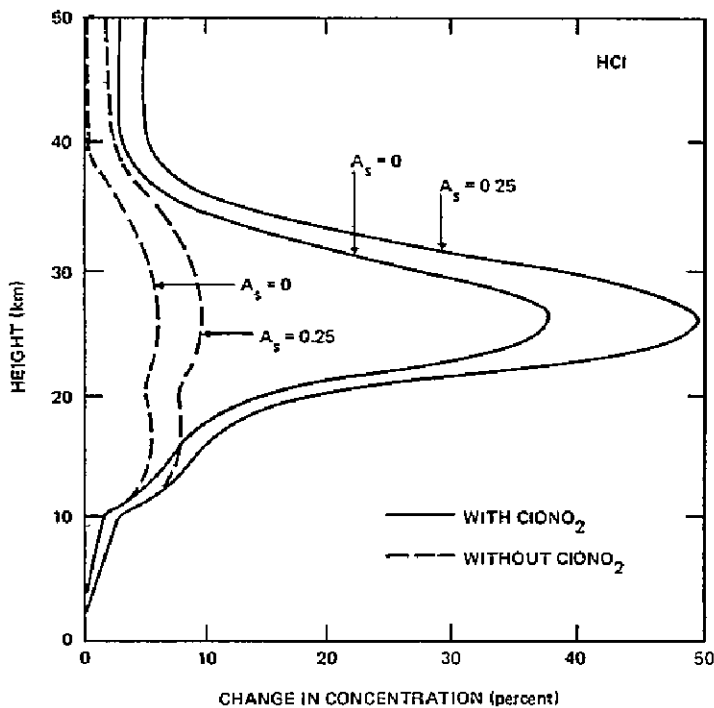


Figure 27. Change in concentration of HCl attributable to multiple scattering.

MODEL SENSITIVITY

Model sensitivity to the release of CFM's at constant production levels was tested for cases with and without ClONO₂. The CFM calculation to steady state assumes that CFCI₃ and CF₂Cl₂ are released at 1973 rates as estimated by McCarthy (1974).

Multiple scattering significantly reduces the sensitivity of the model without ClONO₂. When multiple scattering was included, the ozone reduction decreased to about 0.8 of that computed without multiple scattering. This reduction factor is nearly independent of surface albedo. The model with ClONO₂ is the more realistic model according to the present understanding. Essentially no change occurred in model sensitivity when multiple scattering was included in the model with ClONO₂.

The decrease in sensitivity for the model without ClONO₂ occurs because multiple scattering increases NO₂ photolysis, which increases the NO concentration. Consequently, the importance of the reaction, ClO + NO, is increased relative to ClO + O, thus decreasing the effectiveness of the chlorine catalytic cycle. Multiple scattering causes increased ClONO₂ photolysis and a reduction in the ClONO₂ concentration. Therefore, although the ability of the ClO_x catalytic cycle to destroy O₃ is reduced by multiple scattering, the ameliorating effect of ClONO₂ is also reduced.

SUMMARY

The effect of including multiple scattering in the photodissociation-rate calculation is to significantly alter the photodissociation rates and species concentration profiles. This is particularly true for those processes that are sensitive to wavelengths greater than 290 nanometers. The effect of multiple scattering on the model sensitivity was small for the model including ClONO₂. The small change in sensitivity occurs in spite of the fact that multiple scattering lessens the effectiveness of ClONO₂ in interrupting the O₃-destroying catalytic cycles.

COMPARISON OF THEORY AND MEASUREMENT: HO_x

Among the major subgroups of atmospheric trace constituents that have been identified, the family of hydrogen atom radicals—H, OH, HO₂, and their close relative, H₂O₂—is probably the least understood. For example, only OH has ever been measured in the stratosphere. Although the

infrared emissions of vibrationally excited hydroxyl molecules have been extensively monitored in the past, these data have not led to reliable determinations of H concentrations.

The concentrations of hydrogen gases are strongly affected by the distribution and variability of the hydrogen atom source compounds—water vapor, molecular hydrogen, and methane. These species have been discussed at length in both the CIAP and NAS reports. For example, enough water-vapor measurements have been made to verify its extreme variability in the lower stratosphere, and HO_x concentrations will reflect this variability to a large extent. In discussing hydrogen-oxide measurements, this potential source of uncertainty should be remembered.

Figure 28 summarizes the OH data that have been collected to date. All but one of the OH measurements have been reported in the past 2 years, with many of these experiments using similar resonance fluorescence techniques. Also shown in figure 28 are two theoretical curves representing the results of typical model calculations both with and without the new rate constant for $\text{HO}_2 + \text{NO}$ (i.e., 8×10^{-12} , see reaction 31 in table 1). The theoretical profiles were obtained using a diurnal averaging procedure and indicate average daytime values for OH. When comparing such data with theoretical calculations, one significant point to consider is that the stratospheric and mesospheric OH abundances presented by Anderson (1971 and 1976) were obtained at large zenith angles so as to reduce sunlight interference in the experiments. (Anderson's observations were at 86° in 1971 and 80° in 1976.) OH concentrations will decrease rapidly in twilight. The problem of extrapolating the OH measurements at large zenith angles to average daytime concentrations involves the use of diurnal models such as those previously described in this chapter. The extrapolation factor is probably between 1.5 and 3. However, the determination of this factor is based on some of the less certain chemical-rate constants.

Scaling Anderson's (1971 and 1976) stratospheric OH concentrations upward by a factor of 2 throughout the stratosphere and mesosphere indicates that they are roughly compatible with the lower end of the range of the determination by Burnett (1976) of total integrated vertical daytime OH column abundance (molecules cm^{-2}) (see Chapter 3).

The OH airglow data indicate that mesospheric OH, formed mainly by the reaction $\text{H} + \text{O}_3$, exhibits a large variability, with a time scale of hours to days. Whether or not this is the major source of variability in the Burnett (1976) data is unresolved. Also, it is not known how much of the OH column variability occurs in the stratosphere.

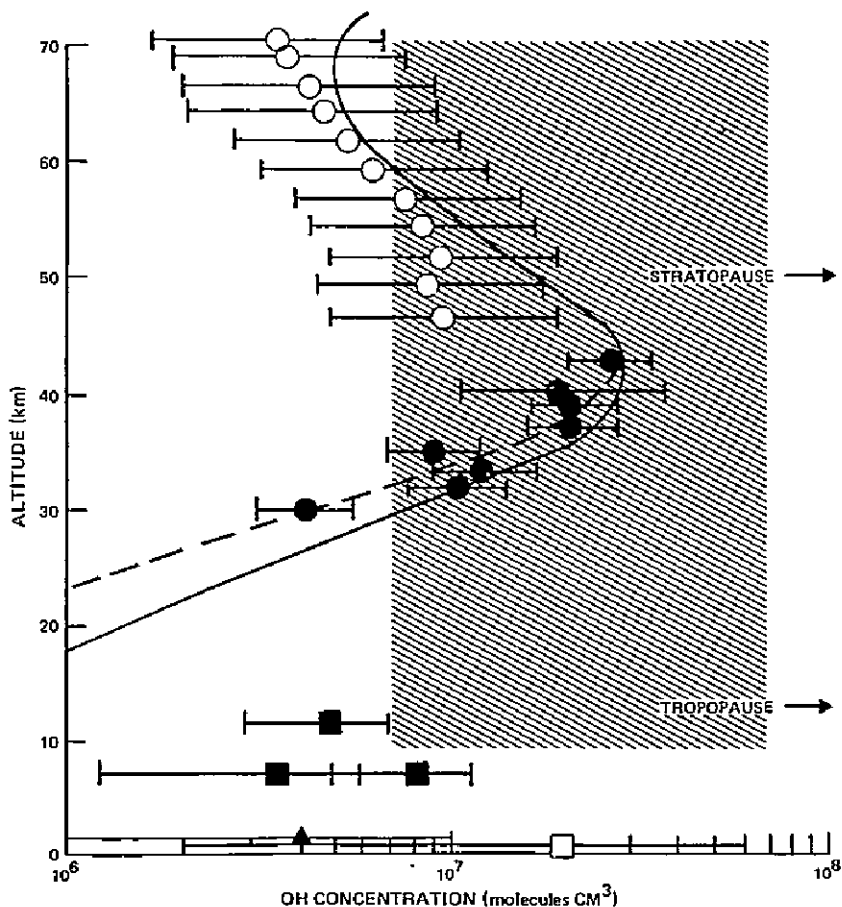


Figure 28. Observed atmospheric hydroxyl radical concentrations. Superimposed are two theoretical curves with (—) and without (- - -) the new rate coefficient of $8 \times 10^{-12} \text{ cm}^3/\text{sec}$ for the reaction of $\text{NO} + \text{HO}_2$ (reaction 31 in table 1). Caution must be exercised in comparing calculated average OH concentrations in daylight with atmospheric observations at large zenith angles.

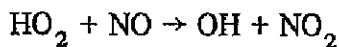
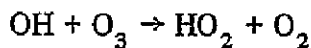
There is a significant gap in the OH data between 10 and 30 kilometers. In these altitude regions, OH partially controls the rate of conversion of HCl into ClO and, thence, into chlorine nitrate.

Early modeling efforts were hampered by the virtually complete lack of knowledge of OH abundances in the stratosphere and the concurrent lack of knowledge of most of its important reaction rates. Anderson's (1971 and 1976) stratospheric OH measurements improved this situation by indicating the expected magnitude of [OH]. The agreement in the shape of the experimental [OH] altitude profile with calculated ones encouraged

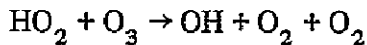
Donahue et al. (1976), among others, to use these measurements in an attempt to narrow the choices for the critical reaction rates $\text{OH} + \text{HO}_2$ and $\text{O} + \text{HO}_2$. The rapidly improving laboratory reaction-rate data for HO_2 is beginning to permit deduction of OH concentration from kinetic data. Reasonable results for the magnitude of $[\text{OH}]$ can be obtained without arbitrary adjustments of the model parameters. It is difficult to assess the validity of such agreement because the present data base is so meager.

The recently measured rate coefficient for $\text{HO}_2 + \text{NO} \rightarrow \text{OH} + \text{NO}_2$ of $8 \times 10^{-12} \text{ cm}^3/\text{sec}$, is a factor of 40 greater than that previously used at stratospheric temperatures. As can be seen from figure 29, the new $\text{HO}_2 + \text{NO}$ rate constant systematically increases the calculated OH concentration at all stratospheric altitudes, but particularly so below 40 kilometers. For example, at 30 kilometers, the OH increase is a factor between 1.5 and 2, depending on the specific model employed.

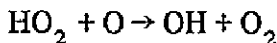
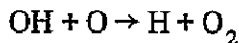
The acceleration of the $\text{HO}_2 + \text{NO}$ reaction and the resultant increase in stratospheric OH abundances leads to changes in the HO_x , NO_x , and Cl_x chemical cycles. In the lower stratosphere, the $\text{OH}:\text{HO}_2$ concentration ratio is now determined largely by the reactions,



with the net rate of ozone catalysis by HO_x being limited by the reaction



In the upper stratosphere and mesosphere, these reactions are superseded by the atomic oxygen processes,



Increased OH leads to more complete conversion of NO_2 into HNO_3 , reducing the stratospheric ratio of NO_2 to HNO_3 . Hydroxyl radicals also generate ozone-active chlorine gases, Cl and ClO, from their stable counterpart, HCl; increased OH thus leads to a more important role for chlorine compounds in ozone-depletion calculations. Both the NO_x and Cl_x interactive effects are discussed further in subsequent sections.

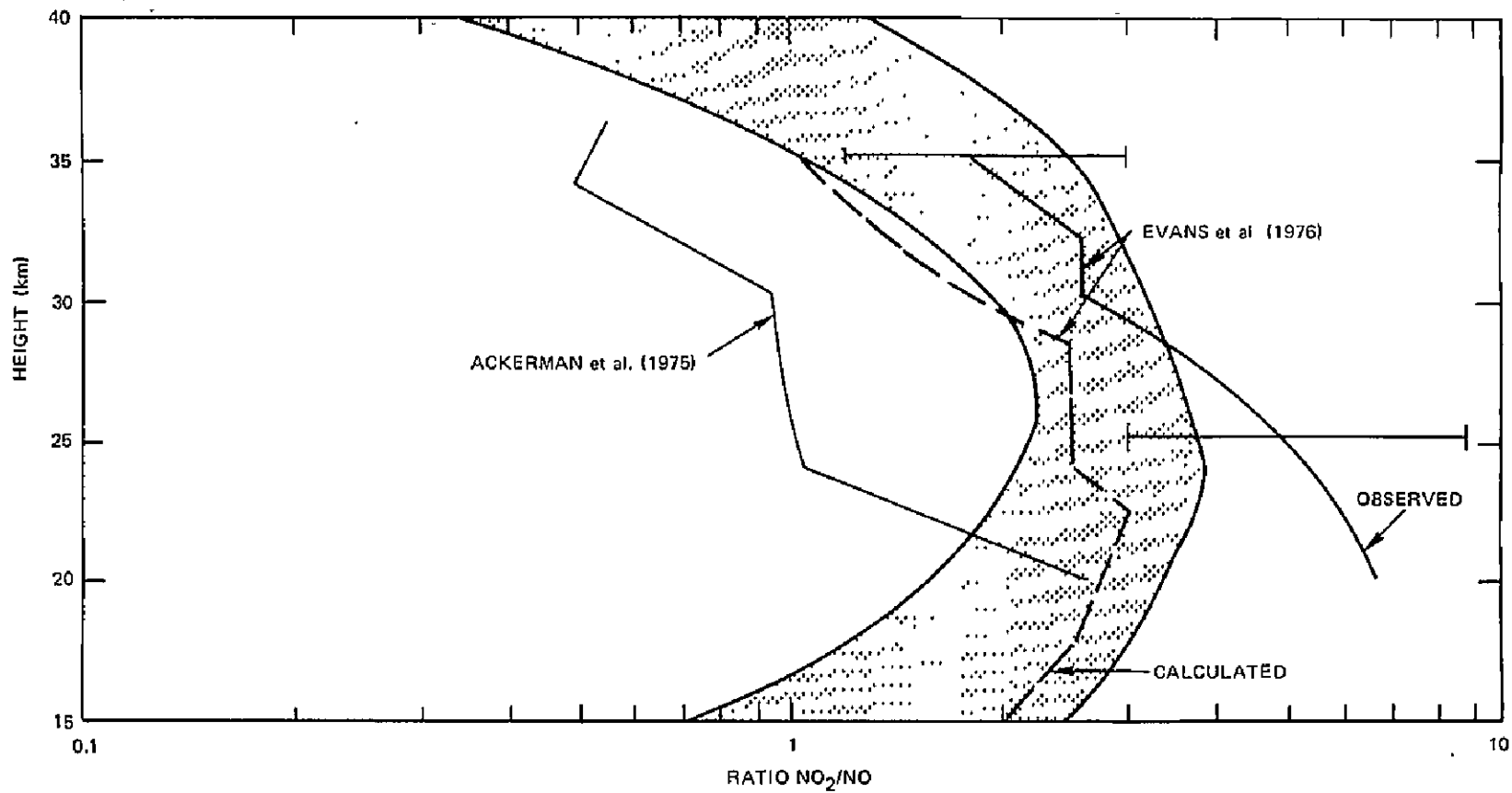


Figure 29. Comparison between observed and calculated $[\text{NO}_2]/[\text{NO}]$ ratio.

The larger $\text{HO}_2 + \text{NO}$ reaction rate results in an increased rate of ozone generation by smog chemistry. When HO_2 is produced during the oxidation of methane and carbon monoxide in air, it can react with NO to give an NO_2 molecule that is rapidly photolyzed into NO and O . The O subsequently reacts with O_2 to form ozone. With the older, smaller $\text{HO}_2 + \text{NO}$ rate constant, HO_2 was much more likely to react with O_3 than NO , destroying ozone in the process. OH concentrations in the troposphere are quite uncertain (see Chapter 3) and are of great significance in determining the efficiency of some of the more reactive halocarbons as sources of stratospheric Cl_x . Tropospheric measurements and improved tropospheric chemical modeling are needed to improve this state of knowledge.

COMPARISON OF THEORY AND MEASUREMENT: NO_x

One-dimensional models have been shown to describe the broad-scale features of the observed distributions of the nitrogen-containing species in the stratosphere; however, a precise quantitative assessment of their reliability and accuracy is not available. One reason for this is the present lack of a sufficient number of accurate observations of the trace species. However, there is also the basic question of how the results of a 1-D model are to be interpreted. The models are intended to simulate average global conditions, but, because the number of observations is limited, it is not presently possible to select the proper specific set of observations for a global average comparison with the model. Furthermore, naturally occurring variations in the nitrogen oxides due to changes in season, latitude, time of day, and stratospheric circulation will be reflected in the observations but are generally treated crudely or not at all in the model.

The usefulness of 1-D models can be judged by their ability to satisfactorily describe the observed ratios of the nitrogen species and also the sum of all the nitrogen species. In this regard, the many observations of $[\text{NO}]$ and $[\text{HNO}_3]$ in the stratosphere below 25 kilometers are of only limited value for testing 1-D models because only one species density was usually measured at a time and because of the great natural variability expected in this region. For example, below 25 kilometers, large day-to-day and seasonal variations are expected in the concentration of ozone, HNO_3 , and total odd nitrogen ($\text{NO} + \text{NO}_2 + 2\text{N}_2\text{O}_5 + \text{HNO}_3 + \text{ClONO}_2$). Accordingly, this subsection will concentrate on experiments in which two or more species were measured simultaneously in regions above 25 kilometers at which photochemical equilibrium is a good assumption for the nitrogen

species. $[\text{NO}_2]$ and $[\text{NO}]$ are in equilibrium with each other during the day with a time scale of approximately 100 seconds. Their ratio is given by

$$\frac{[\text{NO}_2]}{[\text{NO}]} = \frac{[\text{O}_3] \cdot k_{(\text{NO} + \text{O}_3)}}{J_{\text{NO}_2} + [\text{O}] \cdot k_{(\text{NO}_2 + \text{O})}}$$

This ratio provides a good test for 1-D models; however, in addition to the difficulty involved in simultaneous measurements of $[\text{NO}]$, $[\text{NO}_2]$, and $[\text{O}_3]$, the theoretical ratio may be different from the observed one because of errors in the reaction rates or absorption cross section of NO_2 or because radiative scattering is neglected. Furthermore, NO_2 is usually measured at sunset from its solar-absorption spectra so that partial conversion of NO into NO_2 may occur and be reflected in the data.

The most useful measurement of this ratio to date is that of Evans et al. (1976) in which simultaneous measurements of $[\text{NO}]$, $[\text{NO}_2]$, $[\text{HNO}_3]$, and $[\text{O}_3]$ were made from 10 to 35 kilometers on July 22, 1974, at 58°N and the results compared with a diurnal integration of the photochemical equations.

Figure 29 shows that the observed $[\text{NO}_2]/[\text{NO}]$ ratio of Evans et al. (1976) is roughly twice as large as they calculated with a diurnal model using the simultaneously measured ozone profile. They estimate the uncertainty in the observed ratio to be ± 40 percent. A similar error is likely in the calculated ratio because of errors in the observed ozone concentration (± 10 percent), the reaction of NO and O_3 (approximately 25 percent), and in J_{NO_2} . Although the agreement between the theoretical and observed $[\text{NO}_2]/[\text{NO}]$ ratio is reasonable considering the uncertainties involved, this measurement must be interpreted with caution.

As previously mentioned, the observations were made at sunset so that partial conversion of NO into NO_2 may have occurred. Furthermore, while NO is measured *in situ*, NO_2 is measured along a tangent path and therefore may not be indicative of local conditions. In addition, the omission of albedo effects from the diurnal integration can have an important affect on the $[\text{NO}_2]/[\text{NO}]$ ratio.

Also shown in figure 29 is the measured ratio of Ackerman et al. (1975) at approximately 30° latitude. The theoretical $[\text{NO}_2]/[\text{NO}]$ ratio cannot be computed for their data because ozone was not simultaneously measured. Because these are also sunset measurements, the same sources of uncertainty discussed with regard to the data of Evans et al. (1976) must be kept in mind. A range of calculated ratios from several models with self-consistently calculated ozone profiles are also shown in figure 29 even though they should not be directly comparable. These model results are all 24-hour averages.

In conclusion, the attempts to measure the $[\text{NO}_2]/[\text{NO}]$ ratio to date are not yet conclusive tests of the theory, mainly because of the ambiguities associated with sunset measurements. A definitive test will be possible only when *in situ* NO_2 , NO , and O_3 observations at times near midday are compared with diurnal integrations that include the effects of multiple radiative scattering. Actual solar-flux measurements, both direct and diffuse components, between 300 and 400 nanometers would also be quite valuable to compute J_{NO_2} .

It should be pointed out that the $[\text{NO}_2]/[\text{NO}]$ ratio may depend on the Cl_x species if the ClO concentration is as large as that reported by Anderson (1971 and 1976). A small correction also exists for the recently measured fast rate constant for $\text{NO} + \text{HO}_2 \rightarrow \text{NO}_2 + \text{OH}$ of $8 \times 10^{-12} \text{ cm}^3 \text{ molecule}^{-1} \text{ sec}^{-1}$ (see Chapter 1). In this case, the ratio is given by

$$\frac{[\text{NO}_2]}{[\text{NO}]} = \frac{[\text{O}_3] \cdot k_{(\text{NO} + \text{O}_3)} + [\text{ClO}] \cdot k_{(\text{ClO} + \text{NO})} + [\text{HO}_2] \cdot k_{(\text{HO}_2 + \text{NO})}}{J_{\text{NO}_2} + [\text{O}] \cdot k_{(\text{NO}_2 + \text{O})}}$$

If, for example, the ClO concentration is $5 \times 10^8 \text{ cm}^{-3}$ at 30 kilometers, the first two terms in the numerator would be of comparable magnitude, and the $[\text{NO}_2]/[\text{NO}]$ ratio would be approximately 1.8 times its value when Cl_x is not included.

The ratio of $[\text{HNO}_3]$ to $[\text{NO}_2]$ also provides a useful test of 1-D models, although its theoretical value is less certain because it requires knowledge of the OH concentration. This ratio should be observed in regions of

photochemical equilibrium (at low latitudes above 20 kilometers and at middle and high latitudes above 25 kilometers). The ratio is given by

$$\frac{[\text{HNO}_3]}{[\text{NO}_2]} = \frac{k_{(\text{OH} + \text{NO}_2)} \cdot [\text{OH}] \cdot [\text{M}]}{J_{\text{HNO}_3} + k_{(\text{OH} + \text{HNO}_3)} \cdot [\text{OH}]}$$

It is important to note that the equilibrium between $[\text{NO}_2]$ and $[\text{HNO}_3]$ is established over a longer time scale than that between $[\text{NO}]$ and $[\text{NO}_2]$ (approximately 1 day at 25 kilometers versus 100 seconds), but this adjustment time is still shorter than characteristic transport times. The $[\text{HNO}_3]/[\text{NO}_2]$ ratio observed by Evans et al. (1976) during the July 22 flight and their calculated value obtained by diurnal integration for identical conditions are shown in figure 30. Also shown is the range of values obtained in the 1-D models compared at the July update workshop. The ratio calculated by Evans et al. (1976) was in reasonable agreement with the measurements. However, because the OH concentration was calculated rather than measured, this agreement must be considered fortuitous. Since that time, updates of rate coefficients, especially $\text{NO} + \text{HO}_2$, have significantly increased the calculated OH concentration leading to the HNO_3/NO_2 ratios shown by the shaded band in figure 30. Although these are 24-hour averages, the substantial disagreement between the measured and calculated ratios is significantly larger than expected variations during a diurnal cycle.

Observational validation of the $[\text{HNO}_3]/[\text{NO}_2]$ ratio must await OH measurements in the 25- to 35-kilometer region. Nevertheless, simultaneous measurements of only $[\text{HNO}_3]$ and $[\text{NO}_2]$ are of value because they permit an indirect check of OH concentration derived from a model. Here again, $[\text{NO}_2]$ should be measured at times near midday and the effects of multiple radiative scattering included by calculation or direct measurement.

The presence of N_2O_5 has not been established by direct observation although diurnal integrations in 1-D models have shown that it should be an important species in the stratosphere. Recently, King et al. (1976) have attempted to establish an upper limit for the abundance of N_2O_5 , but their results do not rule out the presence of N_2O_5 in substantial amounts.

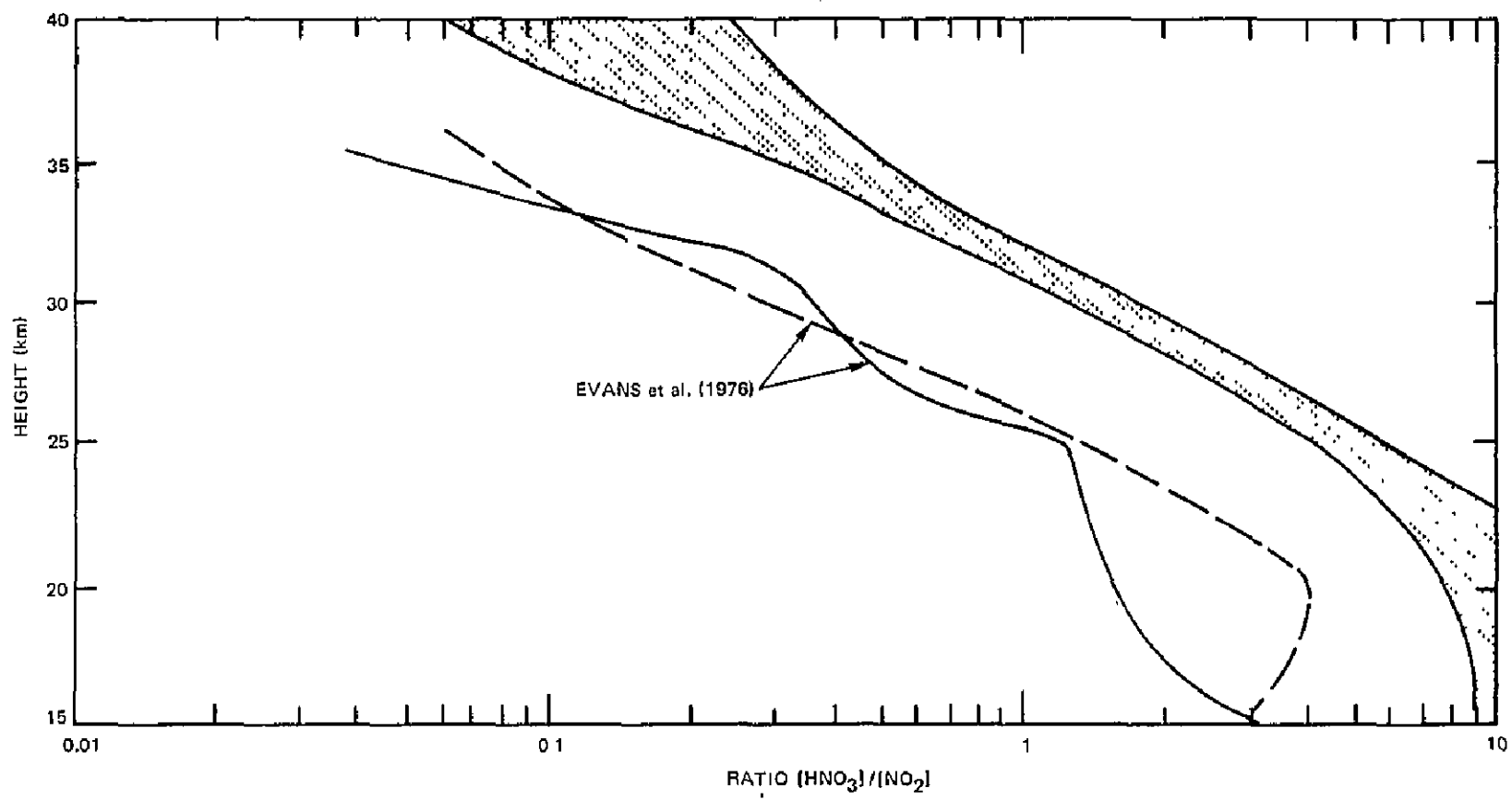


Figure 30. Comparison between observed and calculated $[HNO_3]/[NO_2]$ ratio.

Table 29 lists the ratios $[N_2O_5]/[NO_2]$ and $[N_2O_5]/[HNO_3]$ for times 1 hour after sunrise and 1 hour before sunset. These values were obtained with the model of Kurzeja (1975) except that they are for 30° latitude and include the effects of scattering on photodissociation rates. The ratios of $[N_2O_5]/[HNO_3]$ at sunset are much lower than the sunrise values and are within a factor of 2 of the upper limit ratios of $[N_2O_5]/[HNO_3]$ quoted by King et al. (1976) for sunset conditions.

Table 29
Ratios of N_2O_5 to NO_2 and HNO_3 for Times 1 Hour
After Sunrise (SR) and 1 Hour Before Sunset (SS)

Kilometers	$\frac{[N_2O_5]}{[NO_2]}$ SR	$\frac{[N_2O_5]}{[NO_2]}$ SS	$\frac{[N_2O_5]}{[HNO_3]}$ SR	$\frac{[N_2O_5]}{[HNO_3]}$ SS	N_2O_5 Mixing Ratios (ppbv)	
					Sunrise	Sunset
20	0.33	0.070	0.07	0.02	0.35	0.10
22	0.48	0.088	0.13	0.93	0.65	0.15
26	0.75	0.088	0.4	0.08	1.40	0.28
30	0.78	0.052	0.8	0.1	0.2	0.25
34	0.72	0.014	1.4	0.05	1.4	0.05

The concentration of N_2O_5 can also be inferred from Noxon's (1976) measurements of the diurnal variation of the NO_2 column content. Because NO_2 is converted into N_2O_5 at night, the NO_2 decrease (when divided by 2) should be equal to the production of N_2O_5 . Analysis of Noxon's results indicate an N_2O_5 mixing ratio of approximately 1 part per billion by volume (ppbv), which is consistent with diurnal models (table 29). Thus, N_2O_5 mixing ratios of approximately 1 ppb that are indirectly supported by Noxon's NO_2 observations cannot be ruled out by the upper limits of King et al. (1976). Because N_2O_5 acts as a significant reservoir for NO_x , efforts to determine its concentration should continue.

Although the ratios of the nitrogen oxides are maintained by local photochemical conditions, their sum, which is defined as odd N ($odd\ N = NO + NO_2 + 2N_2O_5 + HNO_3$), is highly transport-dependent. Odd N, produced mainly by the reaction $N_2O + O(^1D) \rightarrow 2NO$ in the stratosphere between 20 and 45 kilometers, is transported downward into the troposphere and upward into the mesosphere. The amount of odd N is an important quantity in the CFM problem for two reasons: (1) large NO_2 concentrations increase the rate of $ClONO_2$ production, and (2) large NO concentrations decrease the ClO to Cl ratio. Both effects work to decrease the calculated ozone-column reduction. Small odd-N concentrations will have the opposite effect.

The odd-N distribution depends on the eddy-diffusion coefficient that governs the rate of N_2O input into the stratosphere and the removal rate of odd N from the stratosphere. It also depends on the photodissociation rate of N_2O , the concentration of $O(^1D)$, and the rate of the reaction $N_2O + O(^1D) \rightarrow 2NO$. The odd-N concentration in the upper stratosphere depends on the dissociation rate of NO. The uncertainty associated with this calculation is illustrated by comparing the models of Crutzen and Isaksen (preprint, 1976) and McConnell and McElroy (1973). The N_2O distributions, odd-N production rates, and odd-N distributions are shown in figures 31, 32, and 33, respectively. As can be seen from these figures, Crutzen and Isaksen's larger odd-N concentrations result from larger N_2O mixing ratios. Their $O(^1D)$ concentrations are also roughly 20 percent larger than those of McConnell and McElroy. The difference between the two N_2O distributions is due to Crutzen and Isaksen's larger eddy-diffusion coefficient below 30 kilometers and to their use of smaller absorption cross sections for N_2O . Although Crutzen and Isaksen's N_2O profile is in better agreement with observations below 35 kilometers, neither profile can presently be ruled out by observations.

In figure 33, the observed odd-N mixing ratios of Evans et al. (1976) and Ackerman et al. (1975) are shown. The Ackerman profile was obtained by adding their measured NO and NO_2 amounts to the calculated HNO_3 mixing ratio of Crutzen and Isaksen (1976). Although neither includes N_2O_5 , this neglect will not seriously affect the results because the measurements were made at sunset when most N_2O_5 has been converted into NO and NO_2 . The observations suggest an odd-N mixing ratio of 1.1 to 1.4×10^{-8} above 30 kilometers, which is consistent with the predictions of most 1-D models. Also shown in figure 33 is a range of results for total odd N above 35 kilometers obtained by eight different models at the July 1977 update workshop.

In the lower stratosphere, comparison between theory and observation is more difficult because of the large natural variability in odd N that accompanies the steep gradient in mixing ratio. Comparison between theory and observation must await a greater number of measurements to establish time and latitudinal averages.

Other sources of odd N have been suggested. Figure 32 shows the source due to cosmic rays as derived by Nicolet (1976) for latitudes greater than 60° and the source due to solar-proton events (Crutzen et al., 1975). The solar-proton event (SPE) of 1972 (the largest described by Crutzen et al.)

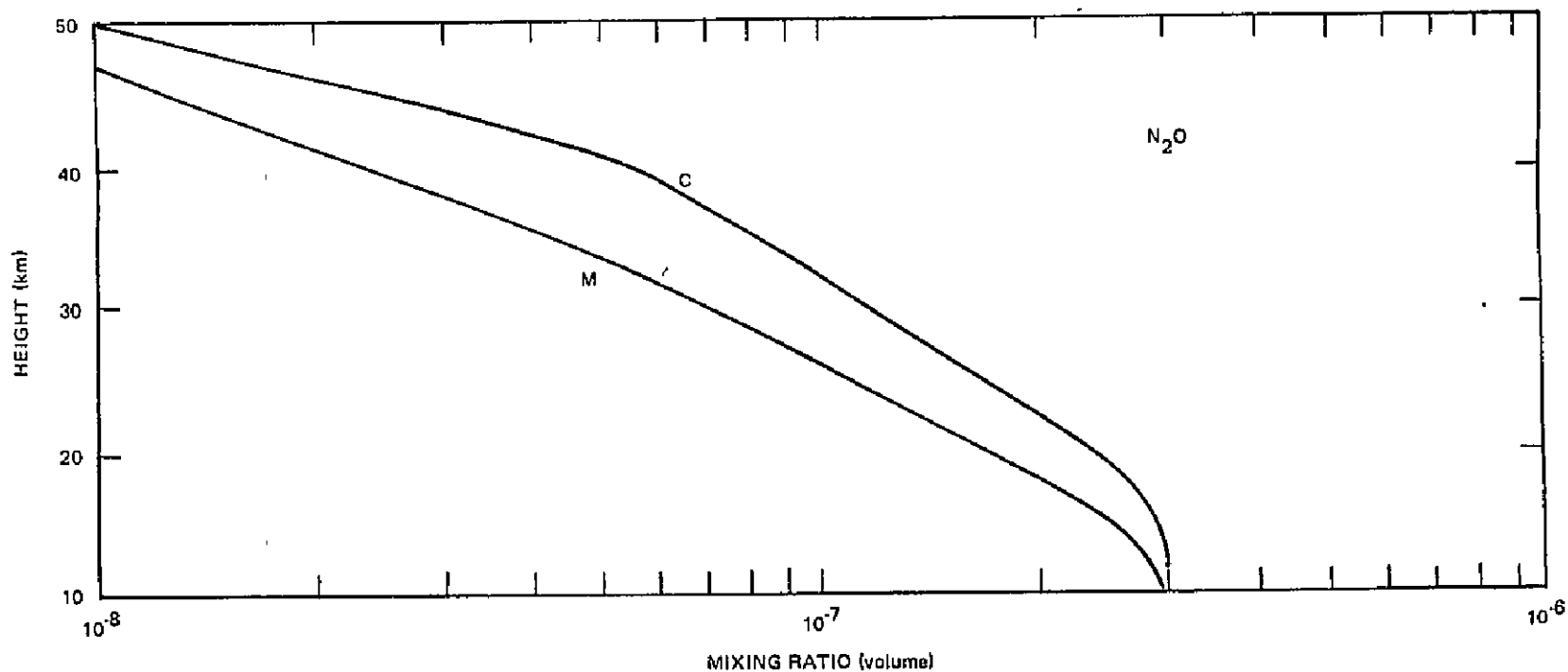


Figure 31. Comparison between N_2O distributions as calculated by McConnell and McElroy (1973) (M) and Crutzen and Isaksen (preprint, 1976) (C).

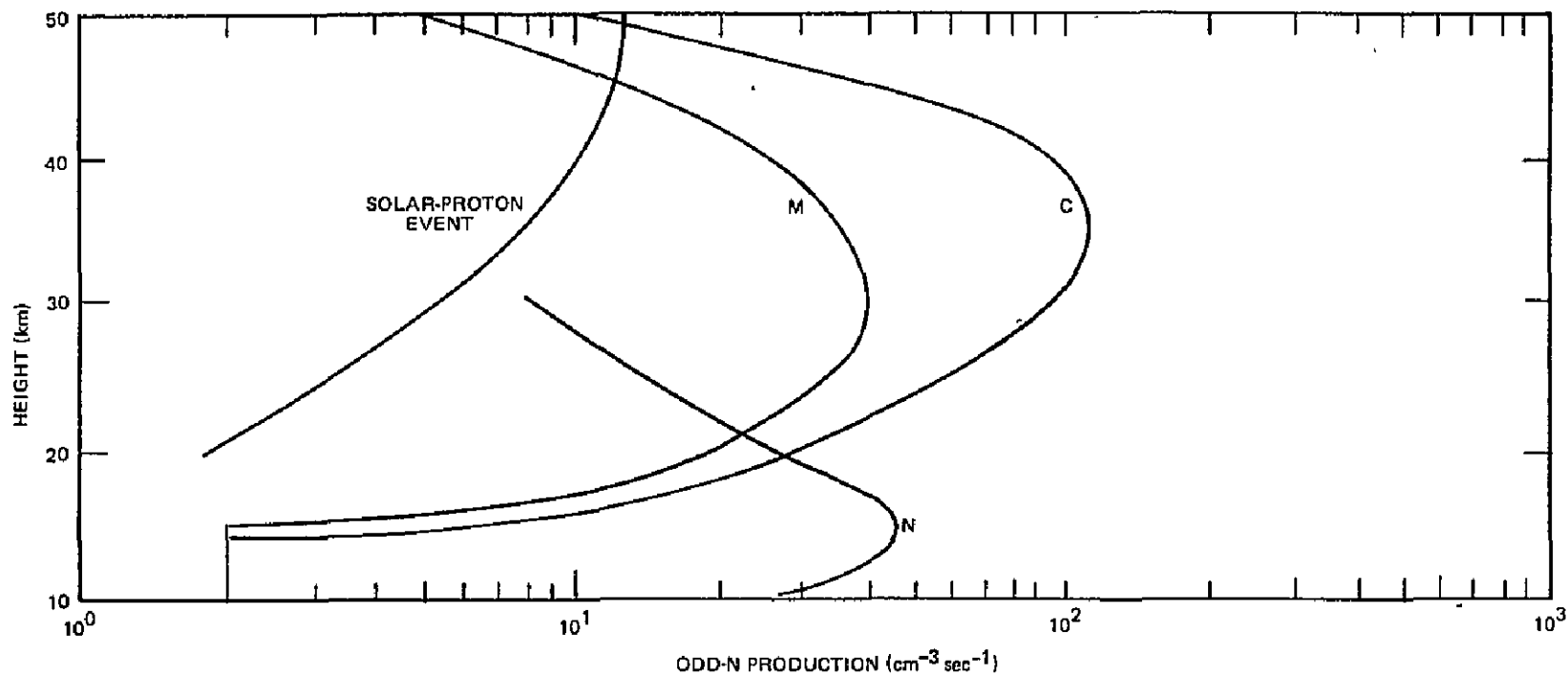


Figure 32. Comparison of odd-N production rates of McConnell and McElroy (1973) (M) and Crutzen and Isaksen (preprint, 1976) (C).

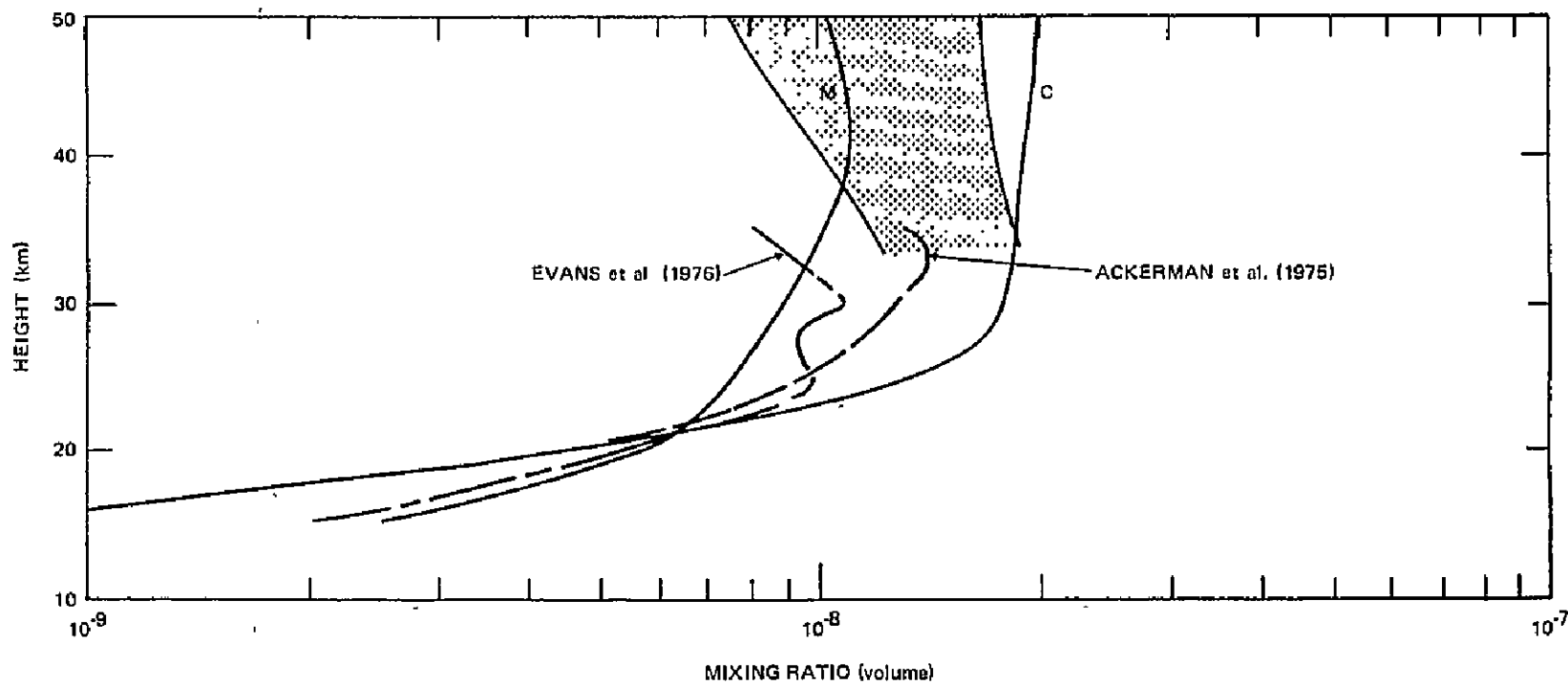


Figure 33. Observed odd-N mixing ratios of Evans et al. (1976) and Ackerman et al. (1975).

has been plotted as a yearly average NO production rate under the assumption that there were no other significant solar-proton events in 1972. The SPE production rates have also been divided by 6 to convert them to a hemispheric average value.

The relatively small NO production from cosmic rays and the low level of input suggests that this source will have very little effect on odd N in the middle and upper stratosphere where ozone destruction is most important. Similarly, NO production from solar-proton events will not have a significant effect on the long-term odd-N budget, but may have an important short-term effect. These two sources of odd N are not included in 1-D models designed for studying the CFM problem, and, considering the small magnitude of these sources compared with production from N_2O , this neglect seems reasonable.

One-dimensional models do not include tropospheric sources for stratospheric odd N. This is based on the assumption that washout and rainout are rapid enough to prevent upward fluxes into the stratosphere and also on the observed increase in the HNO_3 mixing ratio in the lower stratosphere with height that suggests a downward flux of odd N. Tropospheric observations of odd-N species are necessary to confirm this assumption.

Most 1-D models yield maximum odd-N mixing ratios of between 12 and 19 ppbv, which is consistent with the few observations of odd N presently available. However, there is much room for improvement, particularly in predicting the magnitude of the maximum odd-N mixing ratio and in verifying it observationally. More frequent observations of NO, NO_2 , and N_2O above 30 kilometers would be a great aid in establishing the average odd-N mixing ratio and its variability with time.

Modelers should strive for more careful calculation of the dissociation coefficient of NO, which is important for odd-N loss above approximately 35 kilometers. They should be aware that the frequently used J_{NO} values of Cieslik and Nicolet (1973) need correction. (The dissociation rate for their δ (1-0) band should be reduced by a factor of 1/2.2 to make them consistent with the band strengths of Bethke rather than those of Callear and Pilling (see Cieslik and Nicolet, 1973)).

The observed N_2O mixing ratio in the troposphere is used as the lower boundary condition for 1-D models, and additional measurements would help determine which value is most representative in the 0.28- to 0.33-ppmv range currently used by modelers.

This discussion has concentrated on those areas in which 1-D models can be tested with observations so as to minimize ambiguity. In regions in which transport is very important and the 1-D diffusion assumption is most questionable (i.e., the stratosphere below approximately 25 kilometers), not much is to be gained by demanding good *a priori* agreement between the observed and predicted nitrogen-oxide concentrations. Effort is better spent ensuring that 1-D models agree with observations in the region above 25 kilometers in which transport is less important.

Major efforts should be devoted to deciding whether N_2O is the major source of odd N and to establishing the size and variability of odd N in the region above 30 kilometers. This will require more extensive measurements of $[N_2O]$, $[NO]$, and $[NO_2]$ at 30 kilometers and above.

Carefully planned measurement programs of the densities of several species simultaneously, such as that of Evans et al. (1976), should be encouraged. However, significant improvement in deciding the ability of 1-D models to predict the ratios of the NO_2 species cannot be expected until techniques are devised for *in situ* measurement of $[NO_2]$ at times other than sunrise and sunset. Efforts to observe N_2O_5 should continue because diurnal integrations invariably indicate its importance as a reservoir for NO and NO_2 .

COMPARISON OF THEORY AND MEASUREMENT: ClO_x

INTRODUCTION

A useful distinction is that between organic and inorganic molecules containing Cl atoms. As far as is known, the major sources of Cl atoms for the stratosphere are "organic" compounds (e.g., CF_2Cl_2 , $CFCl_3$, CCl_4 , CH_3Cl , and CH_3CCl_3) originating at ground level; one exception is the future Space Shuttle HCl injections. Sources are discussed in the following section. These organic molecules do not affect stratospheric $[O_3]$ directly, but only through their photo-oxidation products, which are inorganic molecules containing Cl atoms (e.g., Cl, ClO, HCl, and $ClONO_2$). The term "odd chlorine" has been coined by aeronomers, in analogy with odd nitrogen, odd oxygen, and odd hydrogen; odd chlorine is equivalent to "inorganic chlorine" in this discussion. The notation "ClX" is widely used to signify odd chlorine, whereas the term " ClO_x " is used to lump together Cl, ClO, and any higher oxides. It should be noted that the ClX grouping can contain any and all Cl-containing molecules that are produced in the

stratosphere from the photo-oxidation of organic chlorine and subsequent reaction, i.e., the concentration, $[CIX]$, of odd chlorine $\equiv [Cl] + [ClO] + [HCl] + [ClONO_2] + [\text{any other inorganic Cl-containing species}]$. Finally, the mixing ratio (by volume) of any species is simply its mole-fraction.

SOURCES OF STRATOSPHERIC ODD CHLORINE

Since Molina and Rowland's first papers (1974 and 1975) on the stratosphere as a sink for the chlorofluoromethanes, CF_2Cl_2 , $CFCI_3$, and CCl_4 , a great deal of thought has been given to other compounds, natural or anthropogenic, that can furnish Cl atoms to the stratosphere. It now seems clear that CH_3Cl (probably natural) furnishes 40,000 to 250,000 metric tons of Cl to the stratosphere per year. This figure is based on Rasmussen's (1976) data, Lovelock's (1976) data, recent measurements by Singh et al. (1976), and from calculations. By comparison, the yearly stratospheric input of Cl atoms due to 1975 usage of CF_2Cl_2 and $CFCI_3$ (with no tropospheric losses) will be about 500,000 metric tons. As a metal cleaner and degreaser, methyl chloroform (CH_3CCl_3), when lost to the atmosphere, probably now represents a 30,000-metric-ton-per-year source (Crutzen and Isaksen, 1976), and its usage is growing. Contributions from manmade C_2Cl_4 , C_2HCl_3 , CH_2Cl_2 , and $CHCl_3$ also may not be neglected, as approximately 0.5 to 3 percent of ground-level emissions can enter the stratosphere bearing Cl atoms. In calculating the flux of each organic Cl form that can enter the stratosphere, the tropospheric decomposition rate is found to be uncertain to some extent. For CF_2Cl_2 , $CFCI_3$, and CCl_4 , the NAS/National Research Council (NRC) report discussed unknown but possible tropospheric removal processes. For the other organic Cl molecules (or chlorocarbons), attack by OH in the troposphere (usually H-abstraction) is an important tropospheric sink. The great uncertainty in tropospheric OH concentrations (easily 1 power of 10 even in models that neglect variations in relative humidity, tropospheric O_3 , and incident ultraviolet) dictates that, when attempting to estimate stratospheric Cl inputs from, for example, CH_3Cl and CH_3CCl_3 , the estimate should be parametrically represented with a range of tropospheric $[OH]$. The possibility of ground-level inorganic sources influencing the stratosphere does not appear to be large, but the tropospheric behavior of HCl on which this dismissal is based has not been firmly established. (See the discussion of HCl tropospheric data in the following section.)

These known sources of stratospheric CIX can be used in atmospheric tracer models to predict CIX concentrations. To date, only 1-D models have been employed toward this end. In these studies, it is assumed that

atmospheric CH_3Cl concentrations are in steady state with CH_3Cl sources and sinks. Time-dependent calculations are required for the CF_2Cl_2 and CFCl_3 inputs because of their history of increasing usage. In such time-dependent calculations, the vertical eddy-mixing coefficient controls the rate of upward mixing from ground level through the tropopause and to the levels above 25 kilometers at which most of the CF_2Cl_2 and CFCl_3 is photolyzed. It is therefore obvious that the stratospheric CIX profile predicted for a given year will vary from model to model, not only in CIX peak concentration but also in profile shape. The range of CIX predictions for late 1976 from several scientific groups is from 1.3 to 2.7 ppbv. Figure 34 shows a calculation for a mid-1976 stratosphere with an eddy coefficient twice as large as that of Hunten (1975). Contributions to the calculated CIX profile from CF_2Cl_2 , CFCl_3 , CCl_4 , and CH_3Cl are noted. In this calculation, the steady-state assumption was applied to CCl_4 , and it was assumed that all four Cl atoms from each CCl_4 are released (i.e., that CCl_2O , etc., are quickly photo-oxidized). The peak mole fraction, 1.9 ppb, is attained by about 35 kilometers. Its value would be higher, between 2.0 and approximately 2.5 ppb, if CH_3CCl_3 and other chlorocarbons were included. It would be lowered if CCl_2O were assumed to be more stable, if a value less than 0.95 ppb were taken for a global average CH_3Cl tropospheric background, and if a slower eddy-mixing rate were assumed.

It should be reemphasized that the CIX concentration, by definition, is the total concentration of inorganic molecules containing Cl. Thus, if and when a stratospheric concentration of ClO or HCl, for example, is measured to be greater than about 2.5 ppb, that measurement cannot have been predicted using 1-D models (based on seasonally averaged tracer data, at best) and the CIX sources just discussed. The highest ClO concentrations in the range Anderson (1971 and 1976) has observed are perhaps three times higher than simple 1-D calculations can yield with known CIX sources. Three obvious possible explanations are: (1) that meteorological variability leads to factors of 3 or more swings in the CIX concentrations above 25 kilometers, (2) that as yet unidentified CIX sources are significant, and (3) that Anderson et al. (1977) have measured Cl from contamination (in their instruments or from, for example, solid-fuel rocket plumes not associated with their program) or have detected nonresonant (with Cl) photons.

Possibility (3) above has been investigated during the design, fabrication, testing, and flight of the Anderson et al. (1977) instruments and seems very unlikely. Indeed, no plausible criticisms currently exist. Possibility

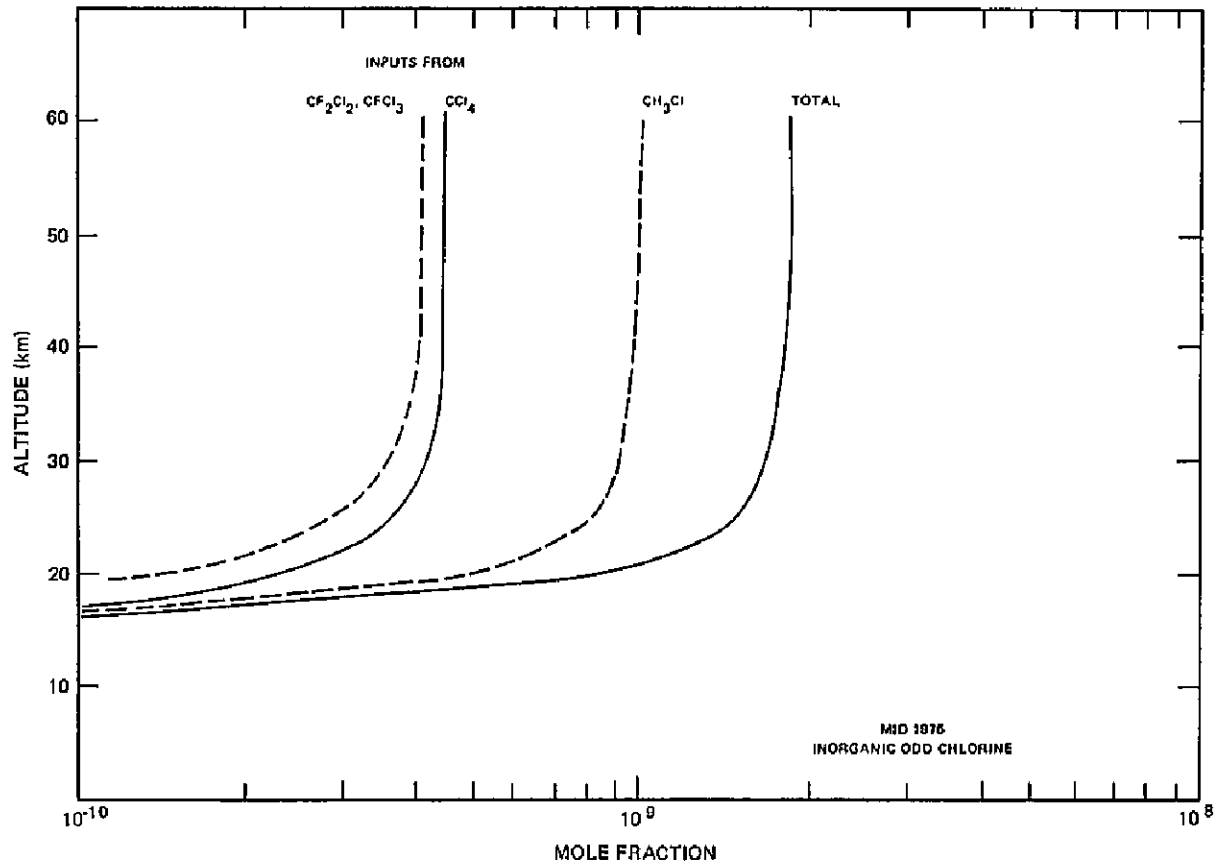


Figure 34. Calculated CIX mode fractions using a mid-1975 stratosphere with a vertical transport coefficient twice as large as Hunten's (1975).

(2) is being explored by many investigators; it will no doubt receive even more attention if, as the ClX data base grows, there appears to be a convergence of ClX concentrations to mean values above, for example, 3.5 ppb. Possibility (1) will require the attention of stratospheric dynamacists for quantitative theoretical assessments, but measurements of the various ClX species at different seasons and latitudes will permit meaningful averaging of the variability. Seasonal, midlatitude averages are probably best for comparison with 1-D model predictions.

MEASUREMENTS AND THEORETICAL PREDICTIONS FOR ClX SPECIES

HCl

Because HCl in the stratosphere should have a photochemical lifetime of hours, its expected variability is less than that for Cl or ClO (photochemical lifetimes of seconds), and, thus, it may be a candidate for comparisons between measured and theoretically predicted concentrations. Figure 35 presents such a comparison. The experimental data are the same as those given in figure 10 with the addition of the recent experimental profile of Eyre and Roscoe (1977), labeled ER in the figure. Several of these profiles indicate a maximum in the HCl concentration between 25 and 35 kilometers with a possible turnover above.

Sample theoretical curves for HCl mixing ratio with altitude, employing the latest rate information for the reaction of HO_2 with NO (see Chapter 1) are shown in figure 35 for two asymptotic values of ClX, 1.6 and 3.2 ppbv. These show a slight flattening of the distribution between 20 and 35 kilometers but no maximum.

The variation between different measurements is comparable to the differences between measurement and observation. Thus, it appears that the budget of stratospheric ClX may be reasonably represented by the view previously outlined. (See figure 34.) On the other hand, it is possible to be very critical of the HCl measurements to date. For example, the filter collections of Lazrus and coworkers actually measure any substance (probably acidic) that yields Cl^- in aqueous solution. Also, Williams et al. (1976) have noted that the HCl absorption at 2925.9 cm^{-1} (the line used in all reports thus far) and its ^{37}Cl counterpart at 2923.7 cm^{-1} appear to be blended, thus implying that the [HCl] deduced from these absorption lines may be higher than is actually present. Further, the R5 H^{37}Cl line at 2995.8 cm^{-1} that should be observed (it lies in a clear interval) has not been seen.

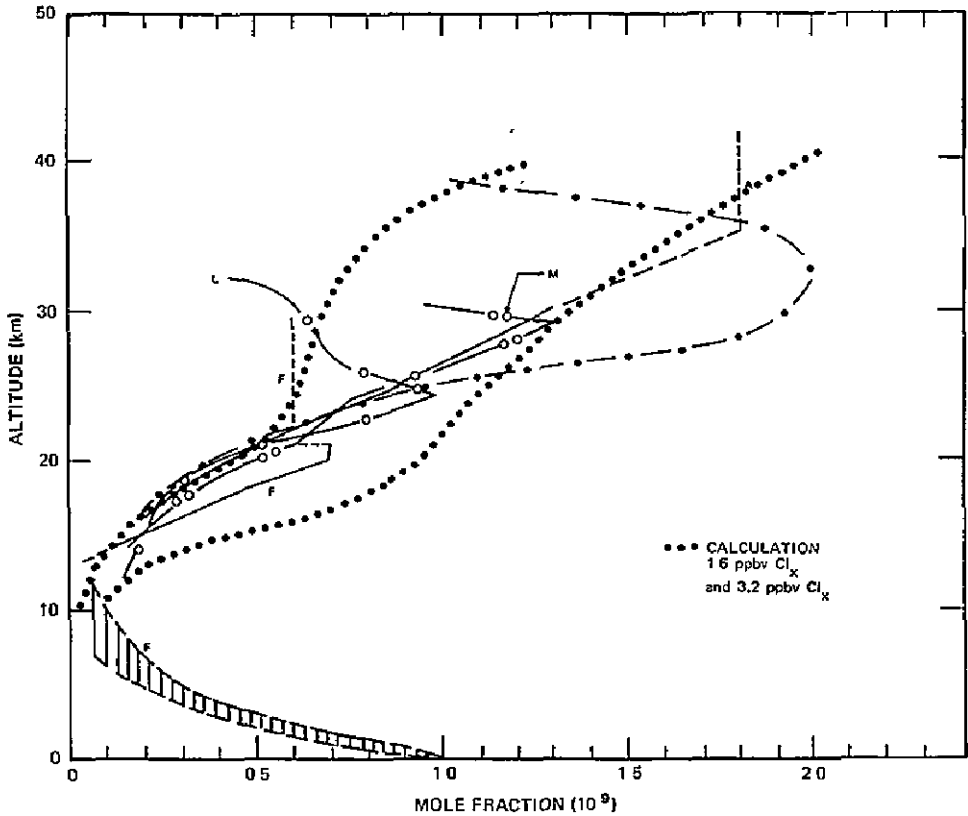


Figure 35. Comparison between measured and prediction HCl concentrations.

Nevertheless, the infrared data do appear to identify stratospheric HCl and, together with the filter paper data, do show that its mole fraction increases with altitude up to about 30 kilometers, consistent with a middle stratospheric source of Cl_X such as the photo-oxidation of CF₂Cl₂, CFCI₃, CH₃Cl, and CCl₄. Measurements to higher altitudes (for example, 40 to 45 kilometers) would be very helpful in deducing the total Cl_X in the stratosphere.

Some mention should also be made of the tropospheric data and predictions for HCl. The view that, in the troposphere, HCl's mole fraction decreases rapidly because of rainout effects is fairly widely accepted now, but the evidence for this view is not as strong as might be desired. The HCl tropospheric scale height deduced by Farmer et al. (1976) ("F" in figure 35) is approximately that predicted from the "H₂O-control" argument that follows, and it leads to the very small HCl mole fractions ($< 10^{-10}$) predicted and measured just above the troposphere. On the other hand,

the feature referred to as the R1 line of the $H^{37}Cl$ fundamental by Farmer et al. (1976) appears as a doublet in the recent spectra of Bradford et al. (1976), neither line of which is positioned properly for HCl (A. Goldman, private communication, 1976). Thus, there is a need for corroborative studies. Similarly, the early analytical procedures of Junge (1957), Duce et al. (1965), and others may have permitted particle-to-gas conversion in the inlet systems of the apparatus, a criticism offered by Stedman et al. (1975) and by Berg and Winchester (1976). In that case, the ground-level HCl mole fraction of 1 to 2 ppb deduced by these workers would be an upper limit. Fortunately, the ground-level concentration of HCl has virtually no effect on stratospheric calculations if rainout is indeed a rapid sink from HCl in the lower troposphere. The actual rainout rates are not well-known, but the available data appear to be consistent with a removal rate fast enough to destroy any coupling between surface HCl and the stratosphere.

The suggestions and evidence just cited have been used to dismiss the influence of ground-level sources of ClX on the stratosphere (e.g., Cicerone et al. (1975); Cicerone (1975); and NAS (1976)). In current models, ClX is removed in the troposphere by assuming a heterogeneous loss term with a rate of approximately $1.7 \times 10^{-6} \text{ sec}^{-1}$ (i.e., a time constant of the order of days). The picture that emerges fits available data on HCl, but, as has been noted, neither the available data nor the theory is compelling. Thus, there will be some continuing uncertainty as to whether ground-level or tropospheric ClX or NO_x sources exert any control over stratospheric ClX and NO_x budgets.

Cl and ClO

The recent measurements by Anderson et al. (1977) by a spectroscopically specific technique (Cl atom resonance fluorescence and chemical conversion of ClO) are the only published or about-to-be-published data. Their results are discussed in Chapter 3 of this report, as is the comparison with noontime ClO and Cl predictions prior to the revised $HO_2 + NO$ reaction rate. As previously mentioned, the ClO data from two flights indicate perhaps 5 ppb ClX in the stratosphere assuming model calculated ratios for $[ClO]/[ClX]$. If there were at least 5 ppb ClX, then variations in $[OH]$ (Burnett, 1976) would cause variations in the $[ClO]/[HCl]$ ratio and the observed $[ClO]$. On the other hand, 5 ppb of ClX cannot be accounted for from known sources, and the agreement between HCl predictions and measurements would be stretched so that the uncertainty limits on the

HCl measurements and theory would no longer overlap. All of the possibilities discussed in the section, "Sources of Stratospheric Odd Chlorine" must be explored, with care taken to calculate diurnal variations in Cl and ClO and to employ proper seasonal and latitudinal groupings. Measured ratios of $[Cl]/[ClO]$ can also be compared with theory, but most of the observations will be dependent on the variability in other species; e.g., $[O]/[O_3]$. Above approximately 35 kilometers, the O/O_3 ratio determines the Cl/ClO ratio.

A comparison of current Cl and ClO measurements with theory is shown in figure 36 for several model calculations. The revised rate constant for $HO_2 + NO$ of $8 \times 10^{-12} \text{ cm}^3 \text{ molecule}^{-1} \text{ sec}^{-1}$ is included. This has the effect of increasing the amount of ClO below 35 kilometers leading to better agreement with the intermediate experimental profile in this region. In all cases, the experimental ClO falls off more rapidly with altitude above 35 kilometers than is theoretically predicted. ClO at 35 kilometers increases by between 12 and 50 percent for a range of models relative to the case with the earlier $HO_2 + NO$ rate constant.

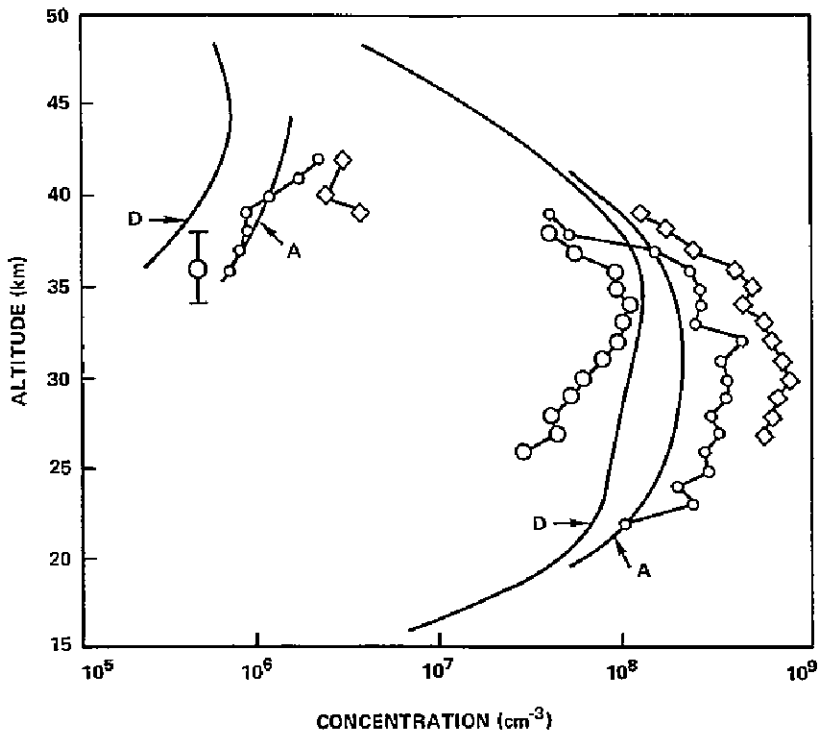
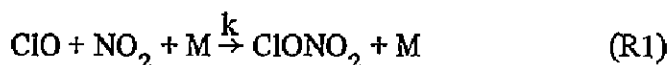


Figure 36. Comparison of calculated and measured ClO and Cl concentrations. Measurements are those of Anderson and coworkers (see figure 12). Calculations are: A - Ames/RDA model with 3.2 ppbv ClX; D - Dupont model with 1.9 ppbv ClX.

ClONO₂

Murcray et al. (1977) have reported upper limits to the ClONO₂ abundance in the stratosphere of 0.8 ppb at 25 kilometers increasing to 2 ppb at 30 kilometers. Further, these numbers were based on absorption coefficients that according to the authors may be a factor of 2 too low. If they are, then the upper limits cited would be reduced proportionally. Comparisons can be made with predictions for September 1975 when there should have been between 1 and 2 ppbv ClX. Doing so leads to calculated concentrations approximately equal to or slightly less than the upper limits of Murcray et al. (1977). If these upper limits are a factor of 2 lower, then the calculations exceed the upper limit at 25 kilometers and approximately equal the upper limit at 30 kilometers.

Theoretical calculations of ClONO₂ concentrations in the stratosphere currently include destruction by sunlight and by reaction with O atoms, with products assumed to be one ClX and one NO_x molecule. Attack by OH appears to be noncompetitive, and heterogeneous decomposition, although seen on some laboratory surfaces, is neglected. Its rate of formation according to reaction

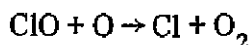
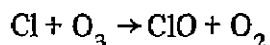


obviously depends on [ClO], [NO₂], and k. Thus, there are possible ClO-poor or NO₂-poor altitudes, times of day, or future ClX-concentration scenarios wherein the rate of formation is limited by the ClO or NO₂ available. Certain of these can spawn nonlinear effects in the calculated effect of ClONO₂ on stratospheric chemistry as, for example, ClX or NO_x is added to the stratosphere.

The lack of laboratory measurements of the pressure dependence of k above 5 torr introduces another uncertainty into ClONO₂ calculations. This is serious because the limited data for atmospheric ClONO₂ and the sensitivity of calculated ClONO₂ levels to the method of calculation already combine to represent a substantial uncertainty in 1-D model calculations of fluorocarbon effects. There is a clear need for higher pressure determinations of k. Another important question is whether reaction R1 can have alternate reaction paths not leading to ClONO₂, a possibility not yet ruled out. Similarly, it remains necessary to determine the products of ClONO₂ photolysis.

Summary of ClX Measurement and Theory

Several things have been learned from the three sets of flight data (Anderson et al., 1977) on stratospheric Cl and ClO. First, the detection and measurement of Cl and ClO, coupled with previous measurements of O(³P) and with laboratory kinetic studies of the reactions



establishes that catalytic removal of O₃ by these reactions is proceeding in the high stratosphere. The measurements to date do not establish the ClO catalytic chain length because of lack of knowledge of total ClX concentrations in the present stratosphere and because of the complications in the middle stratosphere involving ClONO₂.

Also, as mentioned earlier in this chapter and in Chapter 3, two of the flights of Anderson et al. (1977) (July and October 1976) found ClO concentration profiles whose peak values at local noon equaled or exceeded the total ClX concentrations predicted from known sources of ClX. Thus, even 100 percent conversion of HCl to ClO under noontime conditions around 35 kilometers cannot furnish ClO concentrations as high as the midrange of the Anderson et al. measurements. Only the October 1976 flight showed peak ClO mole fractions of about 3 ppb ClX. The possibility must be considered that there is, for example, 5 ppb ClX in the middle-to-upper stratosphere and that the measured variability of [ClO] so far is due to variations of [OH] and [HO₂] (see discussions on HO_x), representing variations in the ratio [ClO]/[HCl] at high altitudes and [ClO]/([HCl] + [ClONO₂]) at lower altitudes. The consequences of this possibility must be examined (i.e., that there is now a ClX mole fraction of about 5 ppbv ClX). It would be necessary to consider immediately the possible origin of 5 ppbv ClX, more than half of which is not accounted for with known sources (see the section on "Sources of Stratospheric Odd Chlorine"). This hypothetical excess of ~3 ppbv ClX could be due to natural sources not yet identified. If so, those sources must be identified to understand all relevant physics and chemistry. It may be possible to predict the ozone perturbations due to CFM usage simply by evaluating the O₃ changes, starting from a stratosphere with 2 to 5 ppbv ClX. However, this would be difficult in the absence of knowledge of the total stratospheric chlorine budget and distribution. If, on the other hand, the hypothetical excess of ~3 ppbv ClX in the 1976 stratosphere is due to anthropogenic

emissions of some Cl-containing molecule, organic or inorganic, then the following questions must be answered: When did these emissions occur? Should they have led to noticeable O_3 perturbations? What molecules and processes are involved in the emissions? When identified and studied, would these additional emissions lead to significant improvements in the understanding of atmospheric chemistry and physics? Whatever the origin of the hypothetical excess ClX, it would also lead to less calculated CH_4 near 40 kilometers than is measured.

Finally, the first measurements of stratospheric Cl and ClO have led to a strengthened realization that measurements of total ClX in the high stratosphere are needed. As noted previously, simultaneous measurements of species that control ratios such as Cl/ClO are also clearly required. More data for ClO and HCl above 35 kilometers are important, as well as an explanation of why both species appear to decrease more rapidly with altitudes above 35 kilometers than is theoretically predicted.

TROPOSPHERIC AND STRATOSPHERIC SINKS FOR CHLOROFLUOROMETHANES

INTRODUCTION

A large body of information on the effects of chlorofluoromethanes, $CFCl_3$ (F-11) and CF_2Cl_2 (F-12), on stratospheric ozone has been assembled and assessed by the Panel on Atmospheric Chemistry, National Academy of Sciences, Washington, D.C. The panel's findings are detailed in the recently released report, *Halocarbons: Effects on Stratospheric Ozone* (NAS, 1976). A variety of tropospheric and stratospheric removal processes for F-11 and F-12 were investigated by the panel. No significant sinks, other than the active removal in the stratosphere originally proposed by Rowland and Molina (1975) and Molina and Rowland (1974) have been identified. (Active removal processes deplete stratospheric ozone; inactive ones do not.) The conclusion of the panel is summarized in table 30. Among the inactive removal processes considered, only dissolution in the oceans has lifetimes (lower limits of 70 years and 200 years for F-11 and F-12, respectively) short enough that its maximum effect would be significant (a 20-percent reduction of predicted ozone destruction). A lower limit of 10^2 years for reactions with neutral molecules in the troposphere was based on the detection limits of the reaction rates with OH radicals in laboratory experiments and is likely to be much too short. Material balance has been made for F-11 and F-12 using estimated atmospheric

Table 30
Removal Times for F-11 and F-12

Process	Removal Time (τ) (years)
Active removal in stratosphere	
Photolysis and O(¹ D) reaction	50;90
Surface processes	
Removal by oceans	> (70,200)
Removal by soil and microbes	> 10 ⁴
Entrapment in polar ice	> 10 ⁵
Tropospheric processes	
Photodissociation	> 5 × 10 ³
Reactions with neutral molecules	>> 100
Direct ionization	> 10 ⁶
Ion-molecule reactions	> 10 ³
Heterogeneous processes	> 6 × 10 ⁴
Lightning	> 10 ⁶
Thermal decomposition	> 10 ⁴
Inactive removal in stratosphere	
Ionic processes	> 10 ⁵
Heterogeneous processes	> 10 ⁸

release and actual atmospheric measurements. The results can be interpreted, with some uncertainty, as consistent with little or no inactive removal for F-11.

Recent laboratory measurements (Ausloos et al., 1977) of the photolysis of F-11 adsorbed on sand indicate the possibility of tropospheric removal when contact is made with sand. Quantitative evaluation is not yet possible.

In the following subsections, some of the removal processes listed in table 30 (taken from the NAS report) and other relevant information not included in the panel report are discussed.

REMOVAL BY OCEANS

The flux from the atmosphere into the oceans for F-11 and F-12 was estimated with a diffusion model formulated by Liss and Slater (1974):

$$F = \frac{D}{Z} \Delta C_1$$

where D is molecular diffusivity, Z is film thickness, and $\Delta C_1 = C_{\text{eq}} - C_w$ is the difference between equilibrium and actual concentration in ocean water. The flux would be maximum when $\Delta C_1 = C_{\text{eq}} = \alpha C_o$ where α is the solubility and C_o is the atmospheric concentration. The removal time is then

$$\tau \geq \frac{N}{\epsilon F_{\text{max}}} = \frac{N}{\epsilon \frac{D}{Z} \alpha C_o}$$

where N is column density and ϵ is fractional surface of oceans on Earth. The panel obtained $\tau \geq 70$ years for F-11 and $\tau \geq 200$ years for F-12. However, Junge (1976) calculated $\tau \geq 208$ years for F-11. The discrepancy resulted from the numerical values used for D , Z , and α . Table 31 compares the two sets of numerical parameters.

Table 31
Oceanic Removal Times for F-11 and F-12^a

D ($10^{-5} \text{ cm}^2 \text{ s}^{-1}$)	Z (10^{-3} cm)	α ($10^{18} \text{ molecules cm}^{-3} \text{ atm}^{-1}$)	τ year	Note
1.2	4	4.4 (F-11), 1.6 (F-12)	≥ 70 (F-11), ≥ 200 (F-12)	b
1.0	7	2.5 (F-11), 1.1 (F-12)	≥ 270 (F-11), ≥ 600 (F-12)	c

^aCalculated for $N = 2 \times 10^{16} \text{ molecules cm}^{-2}$, $C_o = 1 \times 10^{-9} \text{ atm}$, $\epsilon = 2/3$, and at 288 K.

^bNAS (1976).

^cJunge (1976).

Rasmussen et al. (1976) recently reported an average concentration of $0.17 \times 10^{-9} \text{ grams liter}^{-1}$ for F-11 in surface ocean water under an atmospheric mixing ratio of approximately 120 parts per trillion. This concentration is higher than the equilibrium concentration using either Zeininger's solubility measurements (Junge et al., 1976) (by a factor of 2 to 3) or Lovelock's (by a factor of 1.5).

It is clear that more studies and measurements are needed to obtain better estimates of the oceanic removal times for F-11 and F-12.

PHOTODISSOCIATION IN THE TROPOSPHERE

Rebbert and Ausloos (1976) recently reported a photodissociation cross section (or absorption cross section if quantum yield of photodissociation is unity) of $3.7 \pm 0.4 \times 10^{-26} \text{ cm}^2$ at 313 nanometers for CCl_4 at 300 K. Furthermore, the absorption cross section of CCl_4 on the long wavelength edge of the near ultraviolet continuum shows exponential dependence with wavelength. Exponential extrapolation fits Rebbert and Ausloos' cross section at 313 nanometers very well. Because the shape of the absorption bands for CCl_4 , CCl_3F , and CCl_2F_2 are similar, with a red shift from CCl_2F_2 to CCl_3F to CCl_4 , exponential extrapolation is likely to give reasonable estimates of cross sections for CCl_3F and CCl_2F_2 as well. Cross sections of the order of 10^{-25} cm^2 at 280 nanometers and 10^{-28} cm^2 at 313 nanometers for CCl_3F are obtained by extrapolating the cross sections measured by Robbins and Stolarski (1976) and by Chou et al. (in press), corresponding to a removal time of the order of 10^4 years. The cross sections for CCl_2F_2 in the 300-nanometer region are about two orders of magnitude smaller than those of CCl_3F .

REACTION WITH OH RADICALS IN TROPOSPHERE

Reaction R2 is endothermic by about $2 \text{ kcal}\cdot\text{mol}^{-1}$ (Foon and Tait, 1972; and Benson, 1968):

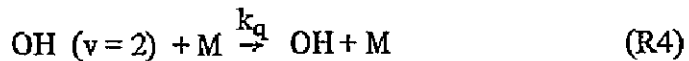


Therefore, the reaction is expected to be too slow at tropospheric temperatures to be a significant removal process (NAS, 1976). However, OH radicals could be formed with vibrational excitation in reaction R3, which is the major tropospheric source of OH radicals. Reaction R3, yielding OH ($v = 2$),



is exothermic by approximately $8 \text{ kcal}\cdot\text{mol}^{-1}$ and could be a fast reaction. Rate constants for OH ($v > 0$) with CCl_3F or CCl_2F_2 have not been reported, but the concentration of OH ($v = 2$) can be estimated by a simple

kinetic scheme. Assume that all OH radicals in the troposphere are formed initially at $v = 2$, followed by deexcitation and eventual removal by chemical reactions,



Important quenchers (M), reactants (R), and relative rates, ($k_q [\text{M}]$ $k_r [\text{R}]$), are listed in table 32. The steady-state concentration of OH($v = 2$) is

$$[\text{OH } (v = 2)] = \frac{k_r [\text{R}]}{k_q [\text{M}]} [\text{OH}]$$

Tropospheric concentrations of $10^6 - 10^7$ molecules cm^{-3} have been measured for OH (Wang et al., 1975; Davis et al., 1976; and Perner et al., 1976). The upper limit for the concentration of OH ($v = 2$) is then

$$[\text{OH } (v = 2)] = \frac{10^{-20}}{10^{-13}} \times 10^7 = 1 \text{ molecule } \text{cm}^{-3}$$

This concentration is too low to contribute significantly to the inactive removal of F-11 and F-12.

REMOVAL BY PYROLYSIS

There is evidence that F-11 in air can be pyrolyzed easily on hot surfaces (Smith et al., unpublished). All processes that use large quantities of air at high temperatures, such as combustion and burning, need to be examined for possible contribution to the inactive removal of F-11 and F-12. The rate of removal for F-11 and F-12 by motor vehicles can be estimated reasonably well. For 1976, 1.1×10^{12} vehicle miles traveled in the United States was projected by the Department of Transportation (Clewell and Koehl, 1974). At an estimated average speed of 40 miles/hour⁻¹, airflow rate into a typical (6-cylinder) engine is approximately 1×10^5 g year^{-1} . Gasoline accounts for approximately 20 percent of the fuel (oil, gas, and coal) consumed in the United States. The worldwide consumption of fuel may be twice that of the United States.

Table 32
Quenching of OH ($v=2$) and Reactions of OH

M	k_q		[M] ^a	k_g [M]
	molecules $\text{cm}^{-3} \text{s}^{-1}$	References		
N ₂ and O ₂	$< 10^{-13}$ ^b	c	1	$< 10^{-13}$
H ₂ O	10^{-11} ^d	e	10^{-2}	10^{-13}
R	k_r		[R] ^a	k_r [R]
	molecules $\text{cm}^3 \text{s}^{-1}$	References		
CH ₄	10^{-14}	f	10^{-6}	10^{-20}
CO	10^{-13}	f	10^{-7}	10^{-20}
O ₃	10^{-13}	f	10^{-8}	10^{-21}

^aMixing ratio.

^bExtrapolated from k_q for OH ($v \geq 4$).

^cStreit and Johnston (1976).

^dMeasured for OH ($v = 1$).

^eSpencer and Glass (in press).

^fAnderson (1976).

Assuming that all other burning processes use approximately the same air/fuel ratio as that of automobile combustion, the total amount of air used in all pyrolytic processes is then $3 \times 10^{16} \text{ } \ell \text{ yr}^{-1}$ globally. The entire atmosphere contains $4.1 \times 10^{21} \text{ } \ell$ air (standard temperature and pressure). If F-11 and F-12 are quantitatively removed in all pyrolytic processes, the removal time would be 1×10^5 year. Finally, allowing a factor of 5 for the fact that pyrolytic processes usually take place in the source region of F-11 and F-12 (Singh, 1976) the removal time is therefore estimated to be approximately 2×10^4 years, which is in good agreement with the panel's estimate.

ION-MOLECULE REACTIONS

Results of laboratory experiments by Campbell (1976) indicate that a sink for F-11 with a lifetime of 70 years (3700 years for F-12) may exist in ion-molecule reactions in the troposphere. The 70-year lifetime was obtained from measured loss rates of F-11 in air by unidentified reactions initiated by γ irradiation and is significantly shorter than the lower limit of 10^3 years estimated by the NAS panel. The scaling factor for the loss rates of F-11 and F-12 from Campbell's (1976) experiments to the actual atmospheric condition depends on the interpretation of removal mechanism for F-11 and F-12 in the experiments. Campbell (1976) concluded that F-11

and F-12 were removed by unspecified terminal ions. However, Fehsenfeld and Albritton (1977) have presented an alternative interpretation that shows that the loss of F-11 could be accounted for by reaction with electrons and leads to a tropospheric lifetime that is roughly 10^4 longer than Campbell's (1976). These two removal mechanisms can be easily tested by further experiments as suggested by Fehsenfeld and Albritton (1977).

ACTIVE REMOVAL IN STRATOSPHERE

Photolysis

Temperature effects on absorption cross sections of CCl_2F_2 and CCl_3F have been determined in the 300- to 210-K temperature range and 200- to 190-nanometer wavelength region (Chou et al., in press; and Bass and Ledford 1976). Stratospheric lifetimes for these molecules are calculated by Chou et al. using the temperature-dependent cross sections and 1-D transport models. The stratospheric lifetime for CCl_2F_2 is 9 to 18 percent longer, depending on the transport model, than that previously calculated using room-temperature cross sections. The corresponding factor for CCl_3F is only 3 to 6 percent. The calculations of Chou et al. also show that reduced cross sections result in an increase in steady-state ClO_x concentration in the middle-upper stratosphere and therefore enhance the ozone removal by the ClO_x catalyzed chain reactions at steady state.

Reactions with $\text{O}(^1\text{D})$ Atoms

Rate constants for reactions of $\text{O}(^1\text{D})$ atoms with F-11 and F-12 have been determined relative to the rate constant of $2.2 \pm 0.2 \times 10^{-10}$ molecules $^{-1}$ cm 3 s $^{-1}$ for reactions of $\text{O}(^1\text{D})$ atom with N_2O (Pitts et al., 1974). Recently, this reference rate constant has been remeasured to be $1.4 \pm 0.1 \times 10^{-10}$ molecules $^{-1}$ cm 3 s $^{-1}$. The rate constants for F-11 and F-12 are therefore correspondingly lower by a factor of 1.6, resulting in longer removal times for $\text{O}(^1\text{D})$ reactions.

CONCLUSION

In summary, no significant inactive removal processes have been suggested for F-12. For F-11, the combined effects of two possible 70-year sinks—solution in the oceans and ion-molecular reactions—could reduce the steady-state concentration of F-11 by 60 percent. However, because F-11

contributes only approximately one-third of total-ozone depletion by CFM's, a 60-percent decrease in its steady-state concentration will result in only approximately 20-percent reduction in predicted ozone depletion.

EFFECT OF TEMPERATURE FEEDBACK MECHANISM

In studies of the natural and perturbed stratosphere, most 1-D-models do not include the effect of temperature coupling (or feedback) mechanisms. For local ozone destruction typical of those resulting from the steady-state CFM injection at the 1975 rate, there will be changes in the stratospheric temperature structure. The subsequent effects of these changes on the stratospheric chemistry and dynamic phenomena need to be examined.

Indications are that temperature coupling for the case of CFM injection at 1975 steady-state rates implies a temperature decrease around 40 kilometers of approximately 10 K. Below 30 kilometers, changes are of the order of 1 degree. Between 35 and 45 kilometers, these temperature changes result in decreased levels of $\Delta O_3/O_3$ due to CFM injection. This is attributable to the negative correlation that exists between O_3 and T in photochemical equilibrium. As a result of the decreased levels of $\Delta O_3/O_3$ between 35 and 45 kilometers, it may be expected that the compensating or "self-healing" effect that occurs at the lower stratospheric levels will be reduced. The balance between the compensating effect at the upper altitude and the reduced "self-healing" effect in the lower stratosphere will determine the net effect on $(\Delta O_3/O_3)$ due to the inclusion of the temperature coupling. Preliminary studies have been conducted in this area; however, resolution of this question will follow with more complete results.

In addition to the impact on the chemical system due to the ΔT arising from CFM injection, there is also the question of the impact on stratospheric dynamics (see Chapter 5 for additional comment). Under the assumptions of a coupled 1-D model, the stratospheric lapse rate between 30 and 40 kilometers is reduced by 40 percent due to temperature changes associated with CFM injection. Such changes in a parameter important to the vertical propagation of planetary waves suggests the possibility of interactions that may significantly impact stratospheric dynamics and, hence, transport mechanisms. Results of a study of the sensitivity of stratospheric dynamics to radiative transfer mechanisms (Ramanathan and Grose, 1977) support this possibility. It is a problem area for future study.

UNCERTAINTIES IN THE PREDICTIONS OF 1-D STRATOSPHERIC MODELS

INTRODUCTION

The NAS panel report (1976) discussed the several sources of uncertainty, both random and systematic, and found that the two principal causes of random error are reaction rates and transport coefficients. They also included in their final predictions of ozone depletion the systematic effects of a possible oceanic sink for CFM's. Their estimate of this uncertainty is still regarded as current. Uncertainties in transport coefficients are discussed in some detail in Chapter 5.

REACTION RATES

Two approaches have been taken to develop reaction-rate uncertainties. Chang et al. (NRC Panel Report, 1976; and NAS Report, 1976) devised a sensitivity study in which individual rates are varied in the Lawrence Livermore Laboratory model to determine the sensitivity, (r), which is defined as follows:

$$r = \frac{\Delta \ln R}{\Delta \ln k}$$

where R is the relative depletion of the ozone column density due to a fixed amount of CIX, and k is the reaction rate constant. The uncertainty, (u_i), due to a particular reaction, (i), is defined as

$$u_i = r_i \ln f_i$$

where f_i is the multiplicative uncertainty of the reaction rate. The total uncertainty, (U), is

$$U = \exp \pm \sqrt{\sum_i u_i^2}$$

The number so obtained has been multiplied by the calculated ozone depletion percentage to give what the NAS report (1976) described as 95-percent confidence limits on the ozone depletion. This method has the obvious weakness that the interdependence of different reactions cannot

be considered. On the other hand, it identifies the specific sources of uncertainty and can serve as a guide to kineticists in choosing where to concentrate their efforts.

The NAS panel report (1976) used this method to calculate an overall reaction-rate uncertainty of a factor of 2.4 on either side of the central value. Their study included uncertainty due to chlorine-nitrate formation and five other chlorine reactions, as well as the reaction, $\text{OH} + \text{HO}_2$. They concentrated on the model sensitivity appropriate to small changes about the central values and did not quote values averaged over some range of variation.

This calculation was repeated on the GSFC model at the time of the January workshop. Sensitivities to all reactions in the model were considered. Significant sensitivities were found to two more reaction rates than the seven originally considered in the NRC report (1976). Thus, the overall uncertainties on either side of the central value were found to be larger.

Table 33 shows the sensitivity results obtained with the current evaluation of reaction rates (Chapter 1) on the improved GSFC model. This model now diffuses odd oxygen, water, molecular hydrogen, and carbon monoxide. The overall uncertainties are smaller, and the asymmetry is more apparent.

A second approach to uncertainty analyses has been taken by Stolarski et al. (1977), who used a Monte Carlo technique to randomly vary all reaction rates independently and simultaneously. The distribution of input reaction rates was assumed to be Gaussian in $\log-k$ space with a width adjusted to the estimated error in the measured reaction rate. The resulting distributions in calculated quantities were usually Gaussian in appearance, and their uncertainty was determined by fitting normal curves to the distributions above and below the central value.

For the current rate set, the Monte Carlo technique gives 95-percent confidence limits of a factor of 1.8 on the high side and 2.86 on the low side about a centerline prediction of 16.5-percent ozone-column depletion (above 15 kilometers) for an addition of 5.7 ppb Cl_x corresponding to steady-state conditions with the 1975 production rates of F-11 and F-12. The high-side uncertainty factor obtained with the sensitivity technique agrees quite well with that obtained by the Monte Carlo approach. On the low side the sensitivity technique gives a somewhat smaller factor of 2.4,

Table 33
Sensitivities and Uncertainties of CFM-Induced Ozone Depletions
Due to Reaction Rates (July Reaction Rate Set)

	GSFC Model					
	0 to -2σ		0 to $+2\sigma$		Central	
	r_1	u_1	r_1	u_1	r_1	u_1
$\text{Cl} + \text{O}_3 \rightarrow \text{ClO} + \text{O}_2$	0.284	0.079	0.235	0.065	0.259	0.071
$\text{ClO} + \text{O} \rightarrow \text{Cl} + \text{O}_2$	0.689	0.317	0.594	0.273	0.643	0.296
$\text{ClO} + \text{NO} \rightarrow \text{Cl} + \text{NO}_2$	-0.191	-0.132	-0.228	-0.157	-0.210	-0.145
$\text{Cl} + \text{H}_2 \rightarrow \text{HCl} + \text{H}$	-0.005	-0.001	-0.005	-0.002	-0.005	-0.001
$\text{Cl} + \text{HO}_2 \rightarrow \text{HCl} + \text{O}_2$	-0.014	-0.019	-0.080	-0.110	-0.037	-0.051
$\text{Cl} + \text{CH}_4 \rightarrow \text{HCl} + \text{CH}_3$	-0.166	-0.137	-0.194	-0.054	-0.194	-0.107
$\text{HCl} + \text{OH} \rightarrow \text{Cl} + \text{H}_2\text{O}$	0.339	0.078	0.277	0.064	0.307	0.071
$\text{ClO} + \text{NO}_2 + \text{M} \rightarrow \text{ClONO}_2 + \text{M}$	-0.252	-0.070	-0.356	-0.246	-0.300	-0.145
$\text{ClONO}_2 + \text{O} \rightarrow \text{ClO} + \text{NO}_3$	0.006	0.004	0.012	0.008	0.009	0.006
$\text{ClONO}_2 + \text{OH} \rightarrow \text{HOCl} + \text{NO}_3$	0.003	0.003	0.009	0.007	0.005	0.005
$\text{O} + \text{O}_2 + \text{M} \rightarrow \text{O}_3 + \text{M}$	-0.272	-0.088	-0.287	-0.092	-0.279	-0.090
$\text{O} + \text{O}_3 \rightarrow \text{O}_2 + \text{O}_2$	-0.071	-0.033	-0.104	-0.048	-0.088	-0.040
$\text{NO} + \text{O}_3 \rightarrow \text{NO}_2 + \text{O}_2$	-0.172	-0.063	-0.163	-0.060	-0.168	-0.062
$\text{OH} + \text{O}_3 \rightarrow \text{HO}_2 + \text{O}_2$	-0.335	-0.231	-0.428	-0.296	-0.381	-0.263
$\text{HO}_2 + \text{O}_3 \rightarrow \text{OH} + \text{O}_2 + \text{O}_2$	0.058	0.080	0.113	0.156	0.086	0.119
$\text{NO}_2 + \text{O} \rightarrow \text{NO} + \text{O}_2$	-0.250	-0.035	-0.265	-0.037	-0.258	-0.036
$\text{OH} + \text{O} \rightarrow \text{H} + \text{O}_2$	-0.001	-0.001	-0.013	-0.009	-0.007	-0.005
$\text{HO}_2 + \text{O} \rightarrow \text{OH} + \text{O}_2$	0.006	0.004	0.020	0.014	0.061	0.042
$\text{HNO}_3 + \text{O} \rightarrow \text{OH} + \text{NO}_3$	-0.007	-0.031	-0.042	-0.029	-0.015	-0.040
$\text{N}_2\text{O} + \text{O}(^1\text{D}) \rightarrow \text{NO} + \text{NO}$	-0.582	-0.268	-0.694	-0.320	-0.631	-0.290
$\text{H}_2\text{O} + \text{O}(^1\text{D}) \rightarrow \text{OH} + \text{OH}$	0.216	0.099	0.204	0.094	0.213	0.098
$\text{H}_2 + \text{O}(^1\text{D}) \rightarrow \text{OH} + \text{H}$	0.007	0.002	0.009	0.002	0.011	0.003
$\text{CH}_4 + \text{O}(^1\text{D}) \rightarrow \text{OH} + \text{CH}_3$	0.027	0.006	0.034	0.008	0.031	0.007
$\text{O}(^1\text{D}) + \text{M} \rightarrow \text{O}(^3\text{P}) + \text{M}$	0.382	0.123	0.372	0.120	0.377	0.121
$\text{N} + \text{NO} \rightarrow \text{N}_2 + \text{O}$	0.040	0.019	0.046	0.021	0.043	0.020
$\text{N} + \text{O}_2 \rightarrow \text{NO} + \text{O}$	-0.037	-0.017	-0.035	-0.016	-0.037	-0.017
$\text{NO} + \text{HO}_2 \rightarrow \text{NO}_2 + \text{OH}$	0.193	0.400	0.218	0.151	0.219	0.303

Table 33 (Continued)

	GSFC Model					
	0 to -2σ		0 to $+2\sigma$		Central	
	r_1	u_1	r_1	u_1	r_1	u_1
$\text{NO}_2 + \text{OH} + \text{M} \rightarrow \text{HNO}_3 + \text{M}$	0.433	0.199	0.394	0.181	0.414	0.191
$\text{OH} + \text{HNO}_3 \rightarrow \text{NO}_3 + \text{H}_2\text{O}$	-0.073	-0.017	-0.095	-0.022	-0.083	-0.019
$\text{OH} + \text{H}_2\text{O}_2 \rightarrow \text{HO}_2 + \text{H}_2\text{O}$	-0.050	-0.035	-0.065	-0.045	-0.058	-0.040
$\text{OH} + \text{HO}_2 \rightarrow \text{O}_2 + \text{H}_2\text{O}$	-0.111	-0.128	-0.277	-0.319	-0.182	-0.210
$\text{OH} + \text{CH}_4 \rightarrow \text{CH}_3 + \text{H}_2\text{O}$	0.015	0.007	0.020	0.009	0.017	0.008
$\text{OH} + \text{CH}_2\text{O} \rightarrow \text{HCO} + \text{H}_2\text{O}$	-0.039	-0.036	-0.033	-0.030	-0.037	-0.034
$\text{HO}_2 + \text{HO}_2 \rightarrow \text{H}_2\text{O}_2 + \text{O}_2$	-0.035	-0.049	-0.077	-0.107	-0.055	-0.076
$\text{CH}_3\text{O}_2 + \text{HO}_2 \rightarrow \text{CH}_3\text{OOH} + \text{O}_2$	0.000	0.000	0.003	0.012	0.001	0.004
	High Side*		Low Side*		Central	
$\sqrt{\Sigma u^2}$	0.625		0.876		0.739	
U	1.87		2.40		2.09	

*The high-side sum is composed of positive values of u_1 from column 0 to $+2\sigma$ and negative values of u_1 from column 0 to -2σ . The reverse is true for the low-side sum.

which may be attributable to the sensitivity study in adequately accounting for the interplay of different reactions as their rates are varied simultaneously.

Caution should be exercised in the application of these numbers. All of them were obtained with the GSFC model, and, although the model has compared quite favorably with other models in recent comparisons, the sensitivity and Monte Carlo studies have not been conducted on other models in their current state. The uncertainty factors should only be applied to the centerline of the model with which they were calculated.

CONCLUSIONS

The NAS report (1976) gave a probable range of 2 to 20 percent for the steady-state column-ozone depletion due to continued CFM release at 1973 rates. This range corresponded to their best estimate of the 95-percent confidence limits for uncertainties about a centerline value of 7 percent. They relied on one model (that of the Lawrence Livermore Laboratories

developed by Chang and coworkers) run with as large a variety of input parameters as computer resources permitted. The approach taken in this report differed in that all of the known active groups in 1-D modeling of the stratosphere were asked to participate. Nine groups participated in a model comparison in which an attempt was made to run a variety of cases of chlorine perturbations on a common set of data. The degree of commonality of the input-data set was greater than that previously achieved in attempts to compare models.

Because of time constraints and differences in model approximations, perfect comparison was not achieved, but the overall results indicated that, given the same problem and input data, the models of the stratosphere will all give essentially the same results. These same modeling groups were then asked to give their best estimate of the steady-state ozone depletion due to continued release of CFM's at their 1975 rates (which are essentially equal to the 1973 rates used by NAS). This is not necessarily meant to be a realistic scenario but is meant to be a diagnostic of model results that provides an easy comparison of ozone-destruction efficiency with past estimates such as the NAS report (1976) or with any future-estimates. The time-dependent scenarios presented in the NAS report are not expected to change significantly, and the comparison of the steady-state values may be used to scale any scenarios desired.

At the time of the January 1977 Workshop at Airlie House, the results of the nine modeling groups for steady-state ozone depletion due to a continuation of the 1975 release rates ranged from 5 to 9 percent when these estimates were made with what they believed were the best values of the rate constants and other input parameters. This 5- to 9-percent range should not be confused with the 2 to 20 percent given by the NAS report (1976). The 5- to 9-percent range represents systematic differences in the models and systematic differences in the inputs chosen by each group as their estimate of the best data. This range does not include all of the uncertainties in rate constants and other input parameters. For instance, if a rate has been measured only once, all groups used the same value, even though our knowledge of the rate should probably be assigned a fairly large uncertainty. Thus, because 5 to 9 percent brackets the centerline value given by the NAS report, the conclusion at the time of the January Workshop was that, although modeling techniques had improved and input data changed, the overall result for column-ozone depletion had come out, by a cancellation of changes, to essentially the same number.

In order to update the model results to account for further changes in rate constants, a second, smaller workshop was held at the Goddard Space

Flight Center in July 1977. The updated rate-constant set is presented and discussed in Chapter 1 of this report. The major change was in the rate for reaction $\text{HO}_2 + \text{NO} \rightarrow \text{OH} + \text{NO}_2$ which is now evaluated to be almost 60 times faster at stratospheric temperatures. This reaction has two direct effects on the efficiency of the chlorine catalytic cycle and, hence, on the CFM ozone depletion. First, it converts HO_2 to OH. The OH is responsible for returning inactive HCl to active Cl. Increasing its rate causes an increase in the ratio of active chlorine to inactive chlorine and, hence, in the catalytic efficiency. Second, the increase in OH increases the conversion of NO_2 (and, thus, NO) to the inactive HNO_3 . This decreases the amount of NO available to shortcircuit the chlorine catalytic cycle via $\text{ClO} + \text{NO} \rightarrow \text{Cl} + \text{NO}_2$; and it decreases the NO_2 available for formation of inactive chlorine nitrate, ClONO_2 . This also leads to an increase in the chlorine catalytic efficiency.

At the July 1977 Workshop, eight of the nine original model groups were represented. They all ran their models again for the case of continued CFM release at 1975 rates, both with the January 1977 evaluation of the $\text{NO} + \text{HO}_2$ rate constant and with the new evaluation. This evaluated rate constant in Chapter 1 is $8 \times 10^{-12} \text{ cm}^3 \text{ molecule}^{-1} \text{ sec}^{-1}$ (i.e., a temperature independent value set equal to Howard and Evenson's (1977) measurement at room temperature). Most of the models were run with a slight temperature dependence assumed. Of the eight models, six use $k = 3 \times 10^{-11} e^{-390/T}$, a value suggested by Howard in his Spring 1977 American Geophysical Union Meeting presentation. One model (LLL) used $4.3 \times 10^{-11} e^{-500/T}$, and two models (Ames/R&D and Ames 2-Dimensional) used the evaluated number, 8×10^{-12} , with no temperature dependence (see Chapter 5).

The maximum difference in these rate expressions at 235 K is less than 40 percent and should be insignificant compared to the factor of 60 change from the previous evaluation, but it is a systematic difference between models (i.e., assuming that the temperature-independent expression yields higher ozone depletions). A few other minor rate differences exist in the comparison. Most of the models were run with the January 1977 rate evaluation with only $\text{NO} + \text{HO}_2$ changed. The Lawrence Livermore Laboratory model was run with $k_{\text{OH}+\text{HO}_2} = 2 \times 10^{-11}$ and with rates for $\text{HO}_2 + \text{O}_3$ closer, but not equal, to the July evaluations. They also used a ClONO_2 formation rate with a pressure-dependence similar to the current (July 1977) evaluation, as did the Ames/R&D models (for the fast $\text{NO} + \text{HO}_2$ only). As is apparent in table 34, these differences appear to be minor compared to the effect of the change in the $\text{NO} + \text{HO}_2$ rate constant.

In addition to the results shown in table 34, the GSFC model was run with the full new rate set exactly as given in Chapter 1, and the resulting depletion was 16.5 percent. An intermediate value for $\text{NO} + \text{HO}_2$ of $\frac{1}{4} \times 3 \times 10^{-11} e^{-390/T}$ was run on the Michigan model, giving an ozone depletion of 8 percent. (Pressure-dependent ClONO_2 formation as shown in Chapter 1 was assumed in this run.) As is apparent from table 34, the agreement between the 1-D temperature uncoupled models has improved since January 1977, even using the same input parameters. The spread is now 5.8 to 8 percent. This decrease in range should be interpreted as a convergence in the tuning of models to nearly identical inputs and assumptions rather than as an increase in the certainty in the answers. When the new $\text{NO} + \text{HO}_2$ rate is used, all of the models (1-D temperature uncoupled) showed an increase in the calculated column-ozone depletion due to continued CFM release at 1975 rates of about a factor of 2 so that the range is from 10.8 to 16.5 percent.

Table 34
Ozone Depletion* (in percent)

Model	Jan. 1977 Rates	Fast $\text{NO} + \text{HO}_2$	Factor Difference
LLL (Lawrence Livermore Laboratories) J. Chang, F. Luther, and W. Duewer	7.5	15.0	2.0
GSFC (NASA/Goddard Space Flight Center) R. Stolarski, D. Butler, and S. Chandra	6.7	13.0	1.9
Dupont P. Jenson, C. Miller, and Filkin	6.0	12.2	2.0
University of Michigan R. Cicerone and S. Liu	5.8	12.0	2.1
Ames/RDA (NASA/Ames Research Center/ R & D Associates) R. Whitten and R. Turco	8.0	16.0	2.0
AER (Atmospheric and Environmental Research, Inc.) N. Sze	5.9	10.8	1.8
NOAA/NCAR (NOAA Aeronomy Lab/ National Center for Atmospheric Research) P. Crutzen and J. McAfee	7.0	12.0	1.7
LaRC Temperature Coupled (NASA/ Langley Research Center) L. Callis and J. Nealy	8.7	12.0	1.4
Ames 2D (NASA/Ames Research Center) R. Whitten and W. Borucki	6.8	16.5	2.4

* Calculated ozone depletion for the January 1977 Workshop rate evaluation and for the update to include the fast rate constant for $\text{NO} + \text{HO}_2$ ($8 \times 10^{-12} \text{ cm}^3 \text{ molecule}^{-1} \text{ sec}^{-1}$ at 300 K). These are steady-state ozone depletions for continued release of CFM's at their 1975 rates (750,000 metric tons/year).

The Langley model included a self-consistent calculation of temperature by a radiative convective model permitting subsequent feedback into temperature-dependent rate constants. This model shows a somewhat larger ozone depletion of 8.7 percent for the January 1977 rate evaluation, but is closer to the midvalue for the change to the fast $\text{NO} + \text{HO}_2$ rate. Unfortunately, this model was not run in the temperature-uncoupled mode, and no other model was available that had been run for both cases in the temperature-coupled mode. Thus, it is difficult to compare the temperature coupled and uncoupled models in any detail to determine if the smaller factor difference in the two cases (1.4) is due to the coupling of temperature. Indications from other models (LLL and GSFC) run for the January 1977 rates are that the column-ozone depletion is the same or larger when temperature is coupled. The Ames 2-D model results are also shown in table 34. They are essentially the same for latitudinally averaged column-ozone depletion as their 1-D results.

All of these results are the response of 1-D models to chlorine perturbations. A key question is: How well does the model response represent the behavior of the atmosphere when it is subjected to such perturbations? One way to obtain such an evaluation is to observe the global change in ozone taking place after a well-characterized perturbation. The only known observation of a catalytic effect of a perturbation on ozone is the comparison of the Nimbus-IV BUV data following the August 1972 solar-proton event with 2-D model calculations by Heath et al. (submitted for publication, 1976). This was a case of NO_x perturbation at high latitude and demonstrated that the observations were consistent with catalytic destruction of O_3 by NO_x .

In general, current evaluations of the relationship between model predictions and the response of the atmosphere rest on the degree of agreement between model calculations and concentrations in the current atmosphere. For this reason, several sections of this report have been devoted to the comparison of theory and field measurement. It was generally accepted by the working group that comparison of the 1-D model results with specific single species measurements should not be expected to be better than a factor of 2 or 3 because of the assumptions inherent in time and spatial averaging and in representing transport in the diffusion approximation.

Emphasis has been placed on the fact that the best comparisons should be those of ratios of constituents whose photochemical exchange times are short compared to transport times. For these, the 1-D model should be expected to give results quite close to experiment. Examples of such measurements would be O/O_3 , $\text{NO}/\text{NO}_2/\text{O}_3$, and Cl/ClO . Results from

such measurements are still sparse. Those that exist are described in Chapter 3 and agree reasonably well with models with either value of the $\text{NO} + \text{HO}_2$ rate constant. The ratio of HNO_3 to NO_2 is a somewhat less certain test of the model photochemistry in that transport time constants are of the same order as chemical time constants. The models should still be in general agreement with measurement over an extended altitude range. In this case, the one measurement of the ratio is in better agreement with 1-D model calculations when the slower rate (January 1977 evaluation) for $\text{NO} + \text{HO}_2$ is used. The same is true of the comparison of calculated ozone profiles with the ozone profile averaged over many measurements. The fast $\text{NO} + \text{HO}_2$ rate yields larger than observed peak ozone concentration, column-ozone content, and tropospheric-ozone concentration. It is not clear at this time whether this is due to an inherent inability of the 1-D diffusion model to simulate the ozone profile in the transport-dominated region to better than about 20 percent, to the fast rate for $\text{NO} + \text{HO}_2$ being incorrect, or to a needed adjustment in other imperfectly known rate constants. Two-dimensional models also predict ozone columns larger than those observed. Thus, although models predict an ozone depletion in the 10.8- to 16.5-percent range using the current best estimates of rate constants, further changes in the predictions cannot be excluded as both the models and the laboratory data are improved.

A further difficulty encountered in comparing 1-D model results to measurements is the upper stratospheric-ozone profile. Above about 30 kilometers, time constants for odd-oxygen destruction become sufficiently short for one to expect a near chemical equilibrium situation, and the model results should be a reasonably accurate representation of the atmosphere in this region. In the 30- to 40-kilometer region, this appears to be so when measurements at midlatitudes are compared to model results. However, near 50 kilometers altitude, the models appear to give consistently lower values than are measured. A further uncertainty is the apparent disagreement between different measurement techniques at this altitude. Until this is resolved, it is not clear exactly how large the actual ozone concentration is at 50 kilometers and above. It is clear that the model results with the current evaluation of rate constants are less than all of the measurements. Some attempts have been made to adjust model inputs in order to lessen this discrepancy. These yield results for ozone depletion generally within the ranges already quoted. The adjustments made are arbitrary, and it is not clear at this time which, if any, are correct.

Any of the model results discussed above may be taken as the best answer for the centerline value of column-ozone depletion depending on an individual's evaluation of the modeling technique and the input parameters

used. Even if a best value is chosen there remains the inherent uncertainty in the prediction due to the propagation of the random uncertainties in the laboratory or field measurements of input parameters through the model calculation. The largest uncertainties seem to be those due to the laboratory reaction rate coefficients. A reassessment of their propagation by a Monte-Carlo technique (see previous section) led to somewhat smaller uncertainties when the current rate evaluation was used. An asymmetry in the probability distribution occurs indicating a saturation effect for large ozone depletions. The 95-percent confidence levels for propagation of random uncertainties (or imprecision) in reaction rates is a factor of 1.8 on the high side and 2.8 on the low side. Systematic errors due to model approximations or missing chemical reactions are not quantitatively evaluable. A goal of a measurements program should be to provide data which minimizes the probability of such systematic errors.

In applying these uncertainties to the centerline values, some caveats must be made which also apply to the centerline values. These estimates are the results of 1-D photochemistry models with all of the transport effects lumped into one diffusion parameter. Latitude dependent effects will be averaged out. More seriously these models do not incorporate feedback effects which operate through the radiation and dynamic fields of the atmosphere to modify any chemical perturbations.

CHAPTER 5

MULTIDIMENSIONAL CFM-O₃ MODELING

INTRODUCTION

The physical structure of the stratosphere is the result of an intricate interplay among a large number of processes that, for simplicity, can be subdivided into categories of radiation, chemistry, and dynamics (RCD). Any physical model of the stratospheric system attempts to incorporate at least parts of these components in a self-consistent fashion. Because it is not possible to model the stratospheric environment in the laboratory, theoretical (mathematical) models must be relied on, subject to observational verification, to simulate stratospheric processes.

The problems of interactive RCD in their complete generality are complicated beyond current ability to model or to understand. The development of a fully generalized model of the atmosphere/ice/ocean RCD system is not anticipated in the foreseeable future. Models are already being developed that are significantly more general and self-consistent than any presently available. However, they will still contain substantial simplifications of the entire system.

It is thus clear that current and anticipated models will differ conceptually from each other only in their degree of simplification and idealization of the real system. However, such models can and do differ drastically in their degree of complexity and degree of interactivity among the RCD components. For example, the computational burden required for today's most complex models may be more than 10^7 times that used in a highly simplified, but meaningful, one-dimensional (1-D) model.

Because a generally applicable model of interactive RCD will not be available in the near future, all models must be defined in terms of the problems of interest and the types of solutions desired. Inevitably, the model chosen is the end product of a series of questions that an investigator must ask and answer in order to proceed in an acceptable manner. Examples of such questions are:

- What type of approach captures the essence of the processes of concern?
- What feedbacks among RCD can be neglected?

Preceding page blank

- Does the model attempt to include processes or feedbacks whose net effects are smaller than uncertainties in the major processes?
- What is the weakest link in the conceptual framework?
- Are the dynamical and radiative simplifications consistent with those made in the chemistry?
- Is there a valid basis for making such decisions?
- Are the model results to be used for diagnosis or prediction?
- If they are to be used for predictive purposes, how can one distinguish between model sensitivity and an inference that the real system will behave similarly?
- For such predictions, how can a confidence interval on the results best be established?
- As the required confidence interval is reduced, at what point does the model become invalid?
- What are the limitations on computer availability?
- Are there pressures for achieving "quick" answers?

The final model chosen is often a very complex end product that reflects these objective and subjective considerations. If an investigator chooses to work on a rather complex problem emphasizing interactions among the various RCD components, he is immediately confronted with the problem of how to work with manageable subsets of the more complex processes that occur separately in the various RCD components. Almost inevitably, the researcher is forced to consider the information learned from noninteractive subset models involving either radiation, chemistry, or dynamics in isolation from the other two. Thus, complicated models of the noninteractive behavior of each of the RCD components are inevitably required for developing manageable subsets for use in interactive calculations.

As an example, complex 1-D chemical models are of utmost importance for enabling researchers to isolate the important chemical processes from the less important and to inspire meaningful approximations and parameterizations. This permits the chemical system to be simplified consistent

with the problem at hand, as well as with the remaining uncertainties in the major components. Analogously, important simplifications have been made in the problems of dynamics and radiative transfer by employing similarly complex, but noninteractive, models.

However, it should be kept in mind that predictions based on simplified noninteractive models (whether one-dimensional or multidimensional) may require modification when the full interaction among radiative, chemical, and dynamical processes is included. In most instances, these interactive processes can be represented properly only in multidimensional models.

Several examples of important feedback among radiative, chemical, and dynamical processes are discussed in the following section. The characteristics of the two-dimensional (2-D) and three-dimensional (3-D) models that have been used in studies of stratospheric ozone are discussed in subsequent sections. The status of these multidimensional atmospheric photochemical models, their current capabilities and limitations, and their possible impact on the chlorofluoromethane O₃ (CFM-O₃) problem in the future are presented in this discussion. Requirements, techniques, and problems of the parameterization of transport in 3-D models are described, the observational needs of multidimensional models are presented, and a summary is provided.

RADIATIVE-DYNAMICAL/PHOTOCHEMICAL FEEDBACK MECHANISMS

BACKGROUND

The National Academy of Sciences (NAS) report, *Halocarbons: Effects on Stratospheric Ozone (1976)*, has identified several sources of uncertainties in the estimates for ozone reduction that may result from release of chlorofluoromethanes (CFM's). One such source is feedback mechanisms, which, if properly included, could modify the calculated effect of CFM's on O₃. The strongly coupled nature of the dynamical, radiative, and photochemical processes in the stratosphere gives rise to several direct and indirect feedback mechanisms. A few of these feedback mechanisms have been included in the state-of-the-art 1-D models, but most have been neglected. Although some of the feedbacks can more readily and properly be incorporated in multidimensional models, such models have not progressed very far in that direction. The net effect is that current models are less interactive than they should be for assessment purposes.

FEEDBACK MECHANISMS

Stratosphere Radiation \rightleftharpoons Stratosphere Chemistry

There are at least two types of feedback in this category. The first concerns the effect of a change in stratospheric temperature, $T(ST)$, on reaction rates, and the second concerns the effect of the increased transparency of the atmosphere in the ultraviolet (UV) that occurs with a decrease in O_3 abundance. The latter coupling gives rise to the "self-healing effect" (NAS report, 1976).

$T(ST) \rightleftharpoons O_3$

The absorption of solar radiation by ozone is the main source of heating within the stratosphere. As a result, O_3 plays a major role in determining the stratospheric thermal structure. The stratospheric temperatures, in turn, influence the O_3 distribution because of the temperature dependence of the rates of the various reactions involved in the production and destruction of ozone. This mutual coupling between $T(ST)$ and O_3 provides a negative feedback in the 1-D models (i.e., the inclusion of this feedback would reduce the model-estimated value of ΔO_3). Here, ΔO_3 refers to the percentage reduction in ozone resulting solely from the addition of CFM's. The effect of this feedback has been considered by Boughner (1975), Ramanathan and Boughner (1975), and Luther (1976). Ramanathan and Boughner (1975) indicate that this feedback reduces the ΔO_3 calculated otherwise by 4 percent, whereas Luther's model indicates a 10-percent reduction in ΔO_3 . Neither of these calculations considers the chlorine-nitrate chemistry. Luther's value of 10 percent, perhaps, provides an upper limit on the magnitude of the negative feedback due to the $T(ST) \rightleftharpoons O_3$ reduction.

Caveats

The 1-D models assume the stratosphere to be in strict radiative equilibrium. Consequently, in the model, at any level in the stratosphere the perturbation in solar heating due to ΔO_3 is balanced locally by an equal perturbation in longwave cooling. In the real-world situation, however, a fraction of the perturbation in solar heating may be compensated by dynamical processes (for example, adiabatic cooling or heating from vertical motion). Hence, the negative feedback mechanism of $T(ST) \rightleftharpoons O_3$, as estimated by 1-D models, needs to be verified by multidimensional models.

Self-Healing Effect

O₃ destruction at the upper levels in the stratosphere is partially compensated by the increase in O₃ at the lower levels due to deeper penetration of solar UV radiation. Again, this effect provides a negative feedback. However, this feedback has been considered in almost all of the 1-D models and, hence, will not be discussed further here.

Stratosphere Chemistry } → T(ST) → { Atmospheric Transports
 ←

In the 1-D models, the transport of chemical species by atmospheric motions is incorporated by the use of an eddy diffusion coefficient, K . The vertical distribution of K is chosen to obtain the best agreement with the observations for the vertical distribution of the species so that, at best, K is appropriate for the present-day stratosphere. However, a global perturbation in O₃ would perturb the vertical, as well as the latitudinal, gradient in $T(ST)$, which, in turn (as will be explained), can perturb the efficiency of the transport processes. This interaction between the gradients in $T(ST)$ and the dynamical transports may give rise to several types of feedback mechanisms: static stability, latitudinal temperature gradient, and radiative response time.

Static Stability Feedback

The reduction in stratospheric O₃ would lead to a reduction in static stability. This conclusion can be inferred from the results of Coakley,* Geophysical Fluid Dynamics Laboratory staff members (1976), and Ramanathan et al. (1976). The perturbation in static stability could affect the mean meridional motions (vertical and latitudinal) and possibly the eddy motions.

Latitudinal Temperature Gradient Feedback

Even for a ΔO_3 that is uniform with respect to latitude, the variations in solar flux and temperature with latitude will affect the latitudinal gradient in solar heating and thermal cooling. The perturbation in radiative heating would affect the latitudinal temperature gradient, which, in turn, would alter the intensity of the zonal winds. Altering the zonal wind intensity would affect the propagation of the planetary scale waves within the

*J. A. Coakley, National Academy of Sciences, private communication, 1976.

stratosphere, since the propagation of these waves may be very strongly dependent on the intensity of zonal winds in the stratosphere (Charney and Drazin, 1961; and Schoeberl and Geller, 1976). Since most of the contribution to large-scale eddy motions in the stratosphere is from planetary scale waves, it is apparent that a perturbation in O_3 may affect the large-scale eddy motions within the stratosphere.

Radiative Response Time Feedback

The radiative response time, h (the time required for a temperature departure from radiative equilibrium to relax to one-half of its initial value or, in an idealized treatment, the inverse of the Newtonian cooling coefficient), is a strong function of temperature, and it is shown in Ramanathan and Grose (1976) that this temperature dependence of h plays a substantial role in determining the mean and eddy motions within the middle and upper stratosphere. When ozone is reduced, the accompanying reduction in $T(ST)$ would reduce h . For example, from figure 8.6 of the NAS report (1976), it is seen that a maximum of 40-percent O_3 reduction occurs at 40 kilometers. (This value includes chlorine-nitrate chemistry.) The 1-D models indicate that a 40-percent reduction would cool the stratosphere at 40 kilometers by about 10 to 15 K (Coakley;* GFDL staff members, 1976; and Ramanathan et al., 1976). From Ramanathan and Grose (1976), a 10- to 15-K reduction in $T(ST)$ at 40 kilometers would reduce h by approximately 30 to 50 percent. Depending on the vertical gradient of the reduction in h , this may either reduce or increase the dissipation of planetary scale waves (i.e., the eddy motions will in general be affected).

To summarize, in view of the mechanisms previously mentioned, it is probable that the O_3 reduction would affect the transport characteristics of the stratosphere. For a 1-D model, the appropriate value of K would be modified. As indicated in the NAS report (1976) and in previous studies, the computed ΔO_3 is sensitive to the value of K . Thus, an initial reduction in O_3 by the CFM's may perturb the value of K , and this perturbation in K may, in turn, affect the O_3 distribution.

In the case of multidimensional models, there is generally some attempt to model this feedback mechanism. For example, in a 2-D model, the meridional transports may vary with the latitudinal temperature gradient. The accuracy with which the feedback mechanism is modeled thus depends on

*J. A. Coakley, National Academy of Sciences, private communication, 1976.

the reliability of the dynamical parameterizations. In a 3-D model, it is realistic to expect increasingly accurate modeling of this feedback mechanism (for example, the fundamental equations of motion automatically incorporate this effect if the radiative heating terms are interactive with O₃ perturbations).

Troposphere Climate \rightleftharpoons Stratosphere Chemistry

The CFM's have direct and indirect effects on the surface and tropospheric temperatures. The direct atmospheric greenhouse effect due to the infrared bands of CFM's in the 8- to 12-micrometer region is estimated in the NAS report (1976) on the basis of 1-D calculations by Ramanathan (1975) to lead to a "steady-state" increase in \bar{T}_s of about 0.5 K for a CFM release held fixed at 1975 rates. The indirect effect concerns the reduction in stratospheric O₃ that may result from addition of CFM's and the subsequent effect of O₃ reduction on the surface and tropospheric temperatures. This indirect effect, through O₃ changes and their subsequent effect on the greenhouse mechanism, is probably smaller than the direct CFM greenhouse effect. These changes in the tropospheric temperatures may subsequently affect the stratospheric chemistry by modifying transport.

Tropopause T-Stratosphere H₂O Feedback

The possibility of this feedback for the ozone reduction problem has been mentioned by Liu et al. (1976). As discussed in the NAS report (1976), this feedback is still in the hypothesis stage and has not been verified by model studies. The concern for this feedback arises from the Mastenbrook (1971) study that indicates that the mixing ratio of H₂O in the stratosphere is approximately equal to the saturation mixing ratio of H₂O at the tropical tropopause temperature. This had led to the suggestion that the H₂O in the stratosphere is determined by the tropopause temperature of the tropics. According to the NAS report (1976), the direct and indirect effects of the CFM's may cause an increase of about 2 to 3 K in the tropopause temperature, which would increase the saturation mixing ratio of H₂O by a factor of 1.4 to 1.7. Liu et al. (1976) conclude that increasing stratospheric H₂O significantly enhances the O₃ reduction caused by a given amount of CFM's. For example, Liu et al.'s (1976) result indicates that doubling the present-day H₂O concentration in the stratosphere nearly doubles the ozone reduction caused by the addition of CFM's. Thus, this coupling provides a positive feedback.

Surface Temperature-Cloud Coupling

As mentioned previously, the direct climatic effects of CFM's is an increase in the global surface temperature, \bar{T}_s . It is conceivable that the increase in \bar{T}_s may alter the global cloud cover (Schneider and Dickinson, 1974). A perturbation in the cloud cover would perturb the solar radiation backscattered by the clouds and, consequently, would affect the photolysis of the trace species. To estimate the magnitude of this feedback, it is necessary first to know the nature of the \bar{T}_s -cloud cover feedback, but, unfortunately, even the sign of this feedback is not known. Cess (1976) estimates from observed cloud climatology that the maximum cloud cover change may be approximately 0.02, from the unperturbed value of 0.4 to 0.5 fractional cloud cover, for a change in \bar{T}_s of 1 K. Although there are presently no model calculations to indicate the effect on O_3 of such a change in cloud cover, available 1-D models could be used for appropriate calculations. It seems unlikely that this effect is large.

Tropospheric Latitudinal Temperature Gradient-Stratospheric Transport Coupling

The 1-D greenhouse calculations indicate only the increase in the globally averaged surface temperature. However, it is known that the response of the surface temperature to perturbations may differ significantly from one latitude to another. For example, the recent 3-D climate model results of Manabe and Wetherald (1975) for the CO_2 -climate problem indicate that the simulated increases in surface temperature and lower tropospheric temperatures are significantly larger (by a factor of 3 to 4) in the polar latitudes than in the equatorial latitudes. A perturbation in the latitudinal temperature gradient would perturb the tropospheric motions, which, in turn, may perturb the stratospheric motions, because mechanical forcing by tropospheric motions is one of the primary energy sources for stratospheric motions. The CFM-climate problem is analogous to the CO_2 -climate problem, and, hence, it appears to be possible that the effect of CFM's on the tropospheric climate can perturb the transport characteristics of the stratosphere.

Caveats

Finally, the results mentioned here for the increase in the surface and tropopause temperatures are based on 1-D radiative-convective model calculations. The limitations on the application of such calculations to the

real world have been discussed in detail in Chapter 6 of the NAS report (1976) and are therefore not repeated here.

CONCLUDING REMARKS

The preceding discussions illustrate the complex coupling and feedback mechanisms among various physical processes and between the troposphere and stratosphere. The mechanisms discussed previously are only some of many that may conceivably occur. It is necessary to have quantitative estimates of the different potential feedback effects to determine which are important and which are negligible. For those discussed previously, it is possible to be semiquantitative in only a few instances.

Quantitative evaluation of feedback mechanisms will generally depend on the development of appropriate fully interactive models. In most cases, this will require use of 3-D models, although, once a feedback mechanism is adequately understood, it might be possible to include it in models of lower dimension by means of appropriate parameterizations. The task of making models fully interactive includes the consideration of all parameterized processes as well as processes that are explicitly modeled. Three-dimensional models are particularly appropriate for investigating feedbacks because they explicitly include many interactions; however, it should be emphasized that many processes are parameterized in present 3-D models. In general, it is essential that careful analysis of the process be made in addition to interactive simulation experiments.

TWO-DIMENSIONAL MODELING

The 2-D model is usually formulated as a phenomenological model similar in general concept to the 1-D model. However, it includes the capability of describing atmospheric latitudinal gradients and seasonal behavior by accounting for the important time-dependent meridional transport in the atmosphere, together with the seasonal and latitudinal variations of the solar zenith angle. Since the models are phenomenological and are not developed completely from first principles, it is essential to develop and substantiate the models by comparison with observations. It should be remembered that, although development from first principles is always desirable, it is only *a priori* necessarily better than a phenomenological model if the development includes a realistic description and calculation of all pertinent physics needed to solve the governing equations. As a result, in either case, extensive testing of the model against actual observations is

needed to verify the results. These tests should encompass at least four general areas: chemical system (reactions and associated rates), atmospheric transport, combined chemistry and transport, and boundary conditions. It should be emphasized that information necessary for a comprehensive testing of a 2-D model is at present limited; therefore, verification of certain aspects and/or regions of the model are also limited. Some of these aspects are pointed out in the following discussion.

Because the purpose of this subsection is to briefly review the current status of 2-D modeling, the history of these models is not included, and only the latest available information on each model has been used. A brief description of some of the pertinent aspects of the models is given, and the general capabilities, limitations, and use of 2-D models in atmospheric problems are then discussed. For a complete description of each model, the reader is referred to the indicated references.

Two-dimensional atmospheric photochemical models have been developed by Brasseur and Bertin (1976), Borucki et al. (1976), COMESA (1975), Crutzen (1975), Harwood and Pyle (1975), Prinn et al. (1975), Turner et al. (1976), Vupputuri (1976a), Whitten et al. (1977), and Widhopf (1975 and 1976). Because Prinn et al. (1975) developed their model as an intermediate model to be used as a source of NO_x distributions for their 3-D model and used measured distributions of ozone rather than calculating the ozone concentrations, there is no further discussion of this model in this section.

TYPES OF MODELS

For purposes of discussion, the current 2-D models can be divided into two classifications. In the strictly photochemical model, the hydrodynamic characteristics of the atmosphere (mean density, temperature, meridional wind field, and eddy-diffusion coefficients) are prescribed and the species conservation equations solved to determine the time-dependent distribution of the atmospheric trace constituents of interest. Atmospheric transport by mean meridional winds and eddies are included in the models. The eddy mixing is developed by using a mixing-length hypothesis developed by Reed and German (1965). Because the transport parameters are obtained directly or indirectly from observations, they are not necessarily unique and must be fully tested to determine their usefulness. Due to uncoupling of the chemistry and transport, these models are designed (as are 1-D models) to investigate small changes in the chemical structure of the atmosphere, which are, in turn, implicitly assumed to have a negligible effect on the transport and temperature distributions.

In the second classification, an atmospheric radiation model is included, and the temperature and mean circulation are calculated as part of the solution. Eddy diffusivities must be prescribed in either approach. The models of Harwood and Pyle (1975), Turner et al. (1976), and Vupputuri (1976b) fall in this second category. Except for Vupputuri's (1976) model, the radiation-coupled models are in too primitive a stage to assess their full capabilities to predict the species distribution in the natural atmosphere throughout the year. This second type of model presents the hope of a more coupled and consistent evaluation of the changes in atmospheric properties that occur as a result of the introduction of pollutants, since the mean circulation and temperature are coupled with the calculation of the species concentration. It should be remembered that the coupling with the transport is not complete since these models are still dependent on a prescription of an important governing parameter (namely, the eddy-diffusion coefficients). A realistic evaluation of the model capabilities must await the completion of more work by the respective workers.

All of the models simulate seasonal changes in the meridional plane (essentially pole to pole, surface to stratopause) except for Vupputuri's (1976b), who considered a steady-state seasonal model (winter, summer) from 10 to 50 kilometers. Thus, interpretation of his results should be made with this inherent limitation in mind.

CHEMICAL MODEL

With regard to the previously outlined tests, all of the 2-D models have, with some variation, essentially relied on the results of 1-D evaluations to ascertain which chemical model to use. Thus, the chemical systems are basically the same, considering the typical O_x, NO_x, and HO_x systems outlined in the Climatic Impact Assessment Program (CIAP, 1975), with the following exceptions. Vupputuri and Widhopf do not consider NO₃ and N₂O₅. Vupputuri (1976b), Brasseur and Bertin, and Whitten et al. have considered ClO_x. COMESA, Crutzen (1975), and Widhopf (1976), include the smog chemistry cycle arising from the oxidation of methane. Presently, only Crutzen (1975) includes the calculation of water vapor; other modelers prescribe this distribution. Basically, the reaction rates used are those recommended by the National Bureau of Standards review; however, there are some important differences. One of the more important of these is the rate at which the reaction $\text{HO}_2 + \text{OH} \rightarrow \text{H}_2\text{O} + \text{O}_2$ proceeds, and others are outlined in the NAS report (1975). The results of each individual model have to be evaluated with these differences in reaction rates and their subsequent effects in mind.

Current differences between measurements of various trace species and 1-D calculations can be more fully evaluated by performing tests using 2-D models since horizontal transport and seasonal variations would be included in the evaluation. These tests are necessary to more fully evaluate the chemical systems used in the atmospheric models and to affirm the choices made using 1-D models. These evaluations depend on the availability of more measurements of the important atmospheric species for adequately determining their seasonal and latitudinal variations. Also, since the models represent average concentrations in either space (zonal) or time (diurnal), numerous measurements are needed in order to make the comparisons of the calculated distributions with data more meaningful. Above all, it should be remembered that the model is as good as the chemistry and transport utilized.

ATMOSPHERIC TRANSPORT PRESCRIPTIONS FOR 2-D MODELS

The eddy-diffusion coefficients used in each model are different, using the turbulent diffusion coefficients of Luther (1973), COMESA, Vupputuri (1976b), improvements of Luther's coefficients (Widhopf, 1976), ones derived by imposing a match between model ozone calculations and observations (Crutzen, 1975; Brasseur and Bertin, 1976; and Whitten et al., 1977) or ones based on observed distributions of O_3 , NO_x , and ^{14}C (Borucki et al.). The mean wind fields used by various modelers include those derived by Louis et al. (1974), Crutzen, (1975), and Widhopf (1976), that obtained from 3-D model calculations (Brasseur and Bertin, 1976), a rather arbitrary prescription (COMESA), mean winds calculated in the model (Vupputuri, 1976b), or mean winds based partially on observations and partially on 3-D model calculations (Borucki et al., 1976).

The simulation of the variation of water vapor in the atmosphere, as well as the dispersion of volcanic debris, has also been used by Crutzen (1975) to develop his transport. Water vapor is very sensitive to the atmospheric exchange between the troposphere and stratosphere and is useful in testing model transport; however, data on water-vapor concentrations in the stratosphere are limited.

Regarding the testing of the atmospheric transport used in models, COMESA and Widhopf have tested their models against the dispersion of radioactive nuclear debris. COMESA finds the downward transport too fast and the poleward transport too small using Luther (1973) eddy diffusivities. These results are in general agreement with those obtained by

Widhopf (1975) using the Luther (1973) coefficients and Louis circulation. Glatt and Widhopf (1976) improved the coefficients of Luther (1973) using as a guide Luther's (1973) unsmoothed (raw) data and the carbon-14 measurements. This approach yielded reasonable agreement of the model calculations with the time-dependent dispersion of carbon-14 throughout the northern latitudes. In addition, good agreement was observed with the dispersion of tungsten-185 in the equatorial regions, and relatively good agreement was obtained with the dispersion of Zr-95 in which particle settling was included to account for this important effect above 20 kilometers.

Fabian and Libby (1973) tested some combinations of mean circulation and eddy-diffusion coefficients and found the best relative agreement with Zr-95 data using the turbulent diffusion coefficients of Luther (1973) and the circulation of Reed and German (1965). In addition, they obtained some estimates of atmospheric residence times.

Tests of model simulation of the dispersion of inert tracers are essentially independent of a knowledge of the photochemistry of the atmosphere and and thus are desirable when applicable. This is especially important for pollution problems, in which not only a knowledge of the chemistry is important, but also a knowledge of the local residence times. In this regard, tests using ozone, N₂O, CH₄, or any other chemical species are dependent on a knowledge of the important chemical sources or sinks for that species and may not be an entirely independent test of the model transport. It should be pointed out, however, that tests using radioactive debris data are subject to the following uncertainties: accuracy of the data, incompleteness of the measurements in space and time, modeling of the rainout/washout sink in the troposphere, and particle settling. These questions make comparisons with inert tracer data somewhat subjective, and care must be taken in the interpretation of the results.

It should also be noted that, due to measurement platform limitations, nuclear debris data are limited to below 25 kilometers and essentially the Northern Hemisphere. This makes model verification in the Southern Hemisphere and above 25 kilometers difficult. The amount of data on the distributions of chemical species used to develop the model transport is also scarce in the Southern Hemisphere and at high altitudes. As a result, these are definite areas in which more information is needed to evaluate/develop atmospheric models.

Only by testing against various specie distributions in the atmosphere (ozone, N_2O , HNO_3 , NO_x , CO, and H_2O) and various inert tracers can a model be adequately verified. This can be done adequately as more measurements of all these constituents become available.

CHEMISTRY AND TRANSPORT

The referenced 2-D models have been used to simulate the distribution of trace species in the natural atmosphere. In one sense, this can be looked upon as another test of the combined model chemistry and transport when compared with data and one which provides information on species concentrations in regions in which measurements have not been made. Each of the models generally shows relatively good agreement with the observations of most atmospheric species. However, these measurements are sparse both in latitude and in time during the year. As with 1-D models, the difficulty in any comparison is that the measurements are made at one place at one specific time of the day, whereas the calculations are diurnal averages and represent "statistically averaged" concentrations. Most of the models are able to reproduce the seasonal and latitudinal variation of the ozone column, some more successfully than others. Those modelers who used ozone as a guide to develop their transport naturally show good agreement with ozone measurements. Detailed information on the calculated monthly variation of the ozone column has not been presented by most of the modelers; however, the distributions shown for particular seasons/months are in reasonable agreement with measurements. Brasseur and Bertin (1976), Crutzen (1975), and Widhopf (1976) have presented these distributions, and their models satisfactorily simulate the monthly variation of the ozone column in the Northern Hemisphere and show adequate agreement in the Southern Hemisphere. COMESA has also presented such comparisons; however, their results do not show good agreement with data.

BOUNDARY CONDITIONS

Boundary conditions used in the models are varied, and, in general, few sensitivity studies have been performed to study the effect of changing them in any given model. More information regarding the flux of various constituents and/or their concentration is needed in order to improve the boundary conditions in any photochemical model. Information is also needed with regard to the latitudinal and seasonal variations at the boundaries. This aspect of the modeling, as well as sensitivity studies of the chemical system (reactions and rates) used in the models, should be given more attention in the future.

APPLICATIONS

Applications of the 2-D models have been used in the analysis of the effect on ozone of NO_x emitted by aircraft and produced by solar-proton events. Various modelers (Crutzen, 1975; Vupputuri, 1976b; and Widhopf et al., 1976) have investigated the effect of NO_x emissions of estimated future fleets of supersonic aircraft during the CIAP. Their globally averaged results were in general agreement with the spectrum of 1-D results; however, they showed a large latitudinal effect as a result of the projected flight corridors. A large seasonal variation was also obtained by Crutzen (1975). More recently, Borucki et al. (1976) have performed similar calculations with their model, obtaining results in general agreement with other 2-D and 3-D model results.

More recently, Hildalgo and Crutzen (1976) and Widhopf et al. (1977) have applied their models to the calculation of the effect of realistic estimates of future supersonic and subsonic fleets. In both studies, it was found that ozone was produced in the troposphere by the subsonic aircraft NO_x emissions, whereas the supersonic aircraft emissions catalytically destroyed ozone. The net difference was a slight (less than 0.6 percent) northern hemispherically averaged increase in ozone with significant latitudinal and seasonal variations. As stated previously, these models include the smog chemistry cycle initiated by methane oxidation by OH.

Crutzen (1975) has also applied his model to the calculation of the effect of the 1972 solar proton event, calculating an ozone reduction in agreement with satellite observations. This is very important since it is the only direct verification of the theory of catalytic ozone destruction by NO_x. It is a good example of a pertinent contribution of a 2-D model because this effect took place in the northern polar region and, hence, could not be adequately treated by a 1-D model.

To date, three 2-D models have been applied to the CFM problem (Vupputuri, 1976; Brasseur and Bertin, 1976; and Whitten et al., 1977). Vupputuri (1976) applied his 2-D steady-state model, including ClO_x and ClONO₂, using constant 1973 injection rates of CF₂Cl₂ and CFCl₃ and ran the solution to a steady state. Unfortunately, this type of model does not have all of the advantages of a time-dependent model, but it does provide some information. Vupputuri (1976) used the reaction rates tabulated in the NAS report (1976) and found a globally averaged decrease of ozone of approximately 8 percent. The maximum reduction was about 10 percent

in the Northern Hemisphere (winter) and decreased to 6 percent in the Southern Hemisphere (summer). The net effect of including ClONO_2 was a factor of 1.4 decrease in the reduction of ozone for the same injection rate.

Brasseur and Bertin (1977) also applied a steady-state version of their model to the CFM problem. These calculations are very preliminary and are to be superseded by a time-dependent calculation in the next few months.

Whitten et al. (1977) have run their time-dependent 2-D model using the CFM release rates of Howard and Hanchett (1975) extrapolated to 1976 and held constant thereafter; the reaction rates are those recommended in this volume, except that the slow rate for reaction 31 ($1.5 \times 10^{-11} \exp(-1100/T) \text{ cm}^3 \text{ sec}^{-1}$) was also used for a comparison run. Chlorine nitrate was included in the model.

The use of the recommended rate coefficient for reaction 31 leads to a globally averaged rise in the predicted ozone-column density of about 15 percent. Widhopf obtained a similar result with his 2-D model. As in the case of 1-D model calculations, predicted OH distributions come into better agreement with Anderson's (1976) measurements when the recommended coefficient for reaction 31 is used.

The predicted 1990 asymptotic chlorine mixing fraction was 1.0 ppbv. The corresponding globally and seasonally averaged ozone reductions were about 1.2 percent (using the slow rate coefficient for reaction 31 and ignoring formation reaction 50 and about 2.9 percent (using the recommended rate coefficient for reactions 31 and 50). Investigation of the relative ozone reduction as a function of altitude showed that it was qualitatively similar above 35 kilometers for both values of rate coefficient 31. However, at lower altitudes, the behavior of the relative ozone reduction was very different. For the low value of rate coefficient 31, an increase in ozone was predicted because of the role of chlorine nitrate. However, when the *recommended* rate coefficient for reaction 31 was used, the predicted ozone below 30 kilometers was found to *decrease* as a result of the nearly fourfold increase in chlorine oxide; only at low latitudes did the predicted ozone experience a slight increase. At midlatitudes, these results are in very good agreement with those obtained with 1-D models.

As discussed previously, the use of a time-dependent 2-D model to investigate the CFM pollution problem would provide information regarding

seasonal and latitudinal variations, interhemispheric mixing, and the importance of variable upward and downward transport. These may be important factors to consider in any comprehensive evaluation of this problem. However, any such calculation using a time-dependent model would require about 10 to 20 hours of CDC-7600 time to simulate the long periods of time involved in calculating some of the scenarios considered by the NAS report (1976). This may be necessary, however, in order to obtain a multidimensional picture of the 1-D results. Various modelers are currently working on ways to reduce the amount of computer time required.

Another point of interest would be the investigation of the indications that there is a 20-percent variation in CFM concentrations between the Northern and Southern Hemispheres and the test of whether multidimensional models can explain/reproduce these measurements.

SUMMARY

Work by various modelers has shown that a 2-D model can be developed that includes a more realistic picture of the atmospheric transport than that of a 1-D model (namely, horizontal transport, latitudinal gradients, and seasonal changes). This can be done with a reasonable expenditure of computer time using a comprehensive chemical model. These phenomena are important because latitudinal gradients are large, and, thus, the upward and downward transport of a constituent need not necessarily be the same or latitudinally uniform as in a 1-D model. This could be important in some pollution studies in which a constituent moves upward at a particular latitude/season and may move downward at another latitude/season at a different rate.

Two-dimensional atmospheric models have been able to adequately simulate the latitudinal/seasonal distributions of many atmospheric trace species, including ozone, NO_y, and HNO₃. They have revealed significant latitudinal and seasonal variations in the distributions of various other atmospheric trace constituents. Inherent in these latitudinal and seasonal variations is the important effect of the corresponding variation of the local solar flux, which can be accounted for in a 2-D model. When applied to NO_x pollution problems, their globally averaged results are in agreement with the range of corresponding 1-D results; however, they also show large latitudinal and seasonal variations about this average. They also provide the ability to study interhemispheric mixing and hemispheric differences and the ability to study atmospheric problems that are basically multidimensional. All of these aspects should be included in any comprehensive

evaluation of the effect of the introduction of a pollutant into the atmosphere. A 2-D model can be used to obtain estimates of these effects, using at least one order of magnitude less computer time than that needed for a 3-D computation.

However, 2-D models are still in a development state in which more data are needed to verify them. They must also be developed further to include scattering effects, more coupling between the dynamics and chemistry, more accurate rainout/washout modeling, better boundary conditions, and more sensitivity studies. The results of these models will enhance current understanding of atmospheric problems.

THREE-DIMENSIONAL MODELING

A 3-D model has the potential to provide the only physically realistic treatment of the transport of trace species in the atmosphere. Calculations (Mahlman, 1975) indicate that there is no correlation between the rate of transport of a trace species and the instantaneous gradient of the species.

These model results are consistent with the implications of observational numerical and theoretical results which show that, under normal conditions, there is a near balance between the horizontal and vertical transport by eddies and the transport by the mean meridional circulation. In fact, even during transient events such as sudden warmings, the net transport is only a small residual difference between opposing large contributions from eddies and the mean meridional circulation. However, the 3-D tracer model of Mahlman (1973) shows that this strong compensation can break down significantly at times, particularly following seasonal circulation transitions. Theory indicates that net transport depends primarily on distributions of thermal and viscous damping and on wave transience, rather than on gradients of mean quantities. However, in 1-D and 2-D models, transport must be parameterized as proportional to some function of the mean concentrations. In 1-D and 2-D models, such a correlation is assumed to exist in the mean.

One-dimensional and two-dimensional models also possess the limitation that transport parameters are assumed to be independent of the distribution of sources and sinks of trace species in the atmosphere and are not permitted to change in response to anticipated dynamical changes. Therefore, these models are limited to treating small local changes. It should be noted in figure 8.6 of the NAS report (1976) that the ozone depletion ratio associated with chlorocarbons is predicted to maximize at an altitude

of approximately 40 kilometers. At this altitude, stratospheric motions are driven at least partially, by the absorption of solar ultraviolet radiation by ozone. Significant changes of the transport rate of trace species due to ozone changes at 40 kilometers should therefore be anticipated even if the total columnar ozone loss should not exceed 10 percent (as previously discussed in this chapter). The temperature structure of the stratosphere could also change, with resulting changes in the rates of the various chemical reactions. A potential change of the transport rate of trace species illustrates the possible limitation of most 1-D and 2-D models of the atmosphere (which are incapable of responding to such a variation of stratospheric climate) and an inherent advantage of most 3-D models.

The ability to simulate atmospheric transport is not the only way in which 3-D models should be capable of providing a more realistic simulation of the atmosphere and of estimating the effects of chlorocarbons. A 3-D model can treat atmospheric inhomogeneity in both space and time. Stratospheric chemistry contains many reactions that introduce into the numerical models terms of the form, $k_{AB} [A] [B]$, where $[A]$ and $[B]$ are species concentrations, and k_{AB} is a reaction rate. This nonlinear term is usually spatially and temporally averaged in the models, and deviations of each species and rate constant from its mean value and correlations are often ignored. The most obvious deficiency in this approach is associated with diurnal variations, because many of the species of stratospheric interest are absent at night. One-dimensional models that incorporate diurnal variations now exist (e.g., Turco and Whitten, 1977), and techniques for incorporating this effect into multidimensional models are being implemented.

On the other hand, spatial correlations should be simulated using multidimensional models. Reactions that have an activation energy exceeding 1000 kilocalories could lead to significant correlations, particularly in view of the substantial (approximately 50 K) temperature variations in stratospheric warmings. Observations of NO and ClO (see chapter 3) suggest variability of more than a factor of 2, and theoretical considerations and NO₂ observations by Noxon (1976) suggest significant latitudinal gradients of some species that are probably associated with conversion to other species such as N₂O₅ and ClONO₂ at high latitudes in winter. Assessments of the effects of latitudinal gradients on these correlations can be made with a 2-D model, but a full assessment of these effects to include local inhomogeneity can be simulated only in a 3-D model.

Furthermore, as pointed out by Martin and Stewart (1976), the variability of atmospheric molecular oxygen concentrations and the strength of the Shumann-Runge bands lead to a mean production rate of odd oxygen which is different from that obtained by calculating the photodissociation rate using a mean profile for molecular oxygen. Similar errors may be introduced in other photodissociation rates that depend on absorption in the Shumann-Runge bands (e.g., H_2O) and by using mean temperatures for strongly temperature-dependent reaction rates (e.g., the destruction of odd oxygen by the $\text{O} + \text{O}_3$ reaction).

Because 3-D models attempt to simulate atmospheric variability, they should provide a more realistic test of the validity of the chlorocarbon/ozone theory from the limited number of observations of chlorine species that will be made during the next 2 years.

Three-dimensional models of the stratosphere have been under development since the time of Hunt and Manabe (1968). Most of these models have been concentrated on representing atmospheric motions, and only recently has much consideration been given to the techniques for including a detailed chemistry. These models consume large amounts of computer time on the fastest available machines (e.g., several seconds to 1 hour per model day), and, thus, the fundamental problem of constructing such a model is in estimating the spatial and temporal scales that must be retained explicitly in order to simulate the stratosphere.

A 3-D model that is sufficiently developed to have the potential for including the minimum required chemistry for the chlorocarbon problem during the next 2 years is that of Cunnold et al. (1975). Large models such as that of Mahlman (private communication, 1977) will probably require 5 years or more to incorporate fully consistent chemistry. The current version of the model of Cunnold et al. (1975) is being revised to provide a more authentic simulation of the atmosphere. At the present time, these models only partially incorporate radiative feedbacks. For example, the model of Cunnold et al. (1975) contains a full treatment of the absorption of solar ultraviolet radiation by ozone, but it parameterizes the absorption of infrared radiation using a Newtonian cooling approximation with a pressure-dependent coefficient. As previously mentioned, substantial changes in this coefficient may occur in response to the accumulation of fluorocarbons. Thus, more realistic treatments of infrared radiation should be incorporated into these models.

It appears that existing 3-D models that include six planetary waves do not provide sufficient horizontal resolution for adequately simulating the

the troposphere/stratosphere exchange process (see Mahlman, 1975). Only one-fourth to one-third of the observed downward transport of ozone of 25 tons per second has been obtained in a model with this resolution. Atmospheric budgets of many chemical species, including chlorocarbons, are controlled by the transport through the tropopause, which, in the mean, occurs in 1 to 2 years. It is therefore important that this vertical transport process be simulated adequately. The amount of parameterized transport required in a 3-D model depends critically on its spatial resolution. (See the following section.) As an initial effort toward achieving most of the transport explicitly, it is planned to increase the horizontal resolution of the Cunnold et al. (1975) model to at least twelve planetary waves. In conjunction with these calculations, it is desirable that more atmospheric observations be made, placing emphasis on the nature of upward transport from the troposphere into the middle stratosphere.

Although it has been shown that the spatial resolution necessary for simulating stratospheric motions is less than that for the troposphere (Washington, 1972), there remains an unresolved question concerning the resolution that is needed in the troposphere in order to simulate adequately the large-scale motions therein that are responsible for the temperature structure of the lower stratosphere. It is assumed that a resolution of twelve planetary waves will also be sufficient for this purpose.

Thus, increased spatial resolution should improve the authenticity of those 3-D models that incorporate a few chemical reactions. In addition, as recently shown by Mahlman (private communication, 1977), increased vertical resolution may be necessary to overcome the common discrepancy that is seen in model results at high latitudes in winter, in which the temperatures at the upper levels of the models are too low by 20 to 50 K. As a result, simulated polar night jets continue to increase in height up to the upper boundary. This feature of the models may be responsible for the achievement of only limited success in the simulation of sudden stratospheric warmings. For example, although substantial temperature oscillations in the stratosphere of a magnitude similar to observations have been obtained within a 2-week period, the calculated zonal structure of the stratosphere has prevented these oscillations from reversing the zonal wind and Equator-to-pole temperature gradient. Proper simulation of these features is important because substantial transports of both heat and trace species occur during both major and minor stratospheric warmings (e.g., Newell et al., 1974; Hartmann, 1977; and Madden, 1975).

It should be possible to incorporate a set of chemical reactions that is consistent with the model resolution into a 3-D model during the next several years. The addition of chemical species to such a model must include a careful assessment of chemical time constants. Species having time constants that are short compared with the model time step (about 1 hour) should be calculated under the assumption of photochemical equilibrium. Each longer time-constant species that is permitted to be transported by the predicted motion field adds approximately 30-percent additional computation time and must therefore be carefully selected. This type of model can be integrated for approximately 3 years, after which dynamical equilibrium of a species such as ozone is attained. However, the ultimate buildup of chlorocarbons in the atmosphere is determined by a balance between input and loss and may take 50 to 100 years to be attained (NAS report, 1976). Thus, calculations that attempt to simulate the continuous accumulation of chlorocarbons in the atmosphere are not possible with a 3-D model; moreover, special techniques that short-circuit the accumulation process must be employed to determine equilibrium distribution of chlorocarbons in such a model.

Although a 3-D model that possesses adequate chemistry for the chlorocarbon/ozone problem would contain some of the dynamical limitations previously outlined and may not predict the global mean-temperature profile, it would provide an assessment of the importance of chemical/dynamical feedbacks and of the inhomogeneity of the atmosphere for this problem. Provided that more detailed dynamical models continue to be developed, even more realistic models of the atmosphere can be expected to be available to answer questions regarding potential climatic changes of the stratosphere during the next decade. Present 3-D models place much more emphasis on dynamics than on radiation and chemistry. Future efforts should aim at a more balanced treatment.

TRANSPORT PARAMETERIZATIONS IN 3-D MODELING OF THE STRATOSPHERE

Chapter 4 discusses the parameterization of transport in 1-D models by the height-dependent eddy-diffusion parameter, K . A previous section in this chapter discusses the use of eddy-diffusion coefficients in 2-D models. It is not generally appreciated, however, that some parameterizations of transport will also probably be needed in 3-D models of the stratosphere. Such parameterizations are required because of the sizable spatial resolution (hundreds of kilometers in the horizontal and several kilometers in the vertical) required for fitting such a problem into even the largest digital

computers, as well as for accomplishing a simulation in a reasonable amount of time. This situation is well-known in the meteorology of the troposphere, in which the spatial resolution is inadequate to explicitly treat atmospheric processes such as clouds, fronts, squall lines, and tornadoes.

In 3-D stratospheric modeling, there are two basic types of transport parameterization problems. The first is the representation of mixing due to motions with space scales less than the minimum scale that can be explicitly resolved by the model. The second type is the parameterization of vertical transport across the tropopause.

SUBGRID-SCALE MIXING

In the numerical solution of any atmospheric transport problem, the distinction between nonturbulent and turbulent transport is arbitrary. It depends on the grid size and time step (i.e., on the averaging volume in four-dimensional space). Transport by all waves whose length is less than two grid distances must be described statistically as turbulent transport.

As the scale of the averaging volume is increased, the statistical description of the turbulent transport is extended to include the effects of larger and larger scale waves. The turbulence then changes by becoming larger in magnitude (large velocity components and displacement) and by becoming more anisotropic and inhomogeneous. Generally speaking, the major contribution to turbulent transport is from the largest scales of motion that cannot be resolved by the grid system (i.e., waves two to three times grid distance). For most general-circulation models with grid distances of more than 300 kilometers, the "turbulence" is still strongly anisotropic, and it can be questioned whether the turbulent transport is adequately described. However, above 15 kilometers, the transport in the stratosphere is increasingly dominated by planetary scale motions that are explicitly resolved in the 3-D models. Thus, except in the lower stratosphere, mixing by quasi-horizontal subgrid scale motion may not be very important.

In addition to the subgrid-scale "waves" that must be treated statistically, there are small-scale turbulent eddies (clear air turbulence) that may also play a role in vertical mixing processes. However, stratospheric turbulence observations (Lilly et al., 1975; and Heck and Panofsky, 1975) indicate that average vertical mixing coefficients for heat in the stratosphere below 20 kilometers are of order $10^2 \text{ cm}^2 \text{ sec}^{-1}$, at least an order of magnitude less than mixing coefficients due to all scales of motions.

If the reasonable assumption is made that mixing coefficients for heat are of the same order of magnitude as mixing coefficients for contaminants, the conclusion is reached that small-scale turbulence is unimportant for vertical transport of trace gases below 20 kilometers. No analogous direct estimates exist above 20 kilometers.

VERTICAL TRANSPORT ACROSS THE TROPOPAUSE

Because many stratospheric trace species have their sources in the troposphere, it is essential to properly represent tropospheric/stratospheric exchange processes. Reiter (1975) has estimated that 70 percent of the total mass of the stratosphere is exchanged with the troposphere each year. Several mechanisms appear to be responsible for the irreversible transport of trace species between the stratosphere and troposphere. The most spectacular types of motion that can produce stratospheric/tropospheric exchange are the intrusions of stratospheric air into the lower troposphere associated with growing extratropical cyclones. These intrusions, which are found in the region of upper-level fronts associated with the tropospheric jet stream, occur in thin laminae. (Typical dimensions are 1 kilometer in the vertical, more than 100 kilometers in the horizontal orthogonal to the wind, and more than 1000 kilometers parallel to the wind). These laminae are then destroyed by vertical mixing on the cumulus scale or by mixing into the surface boundary layer within 1 to 3 days. A large fraction of the stratospheric air is removed by this process in 1 year, but the scales that produce the transport are below or close to the limit of the resolution for a general-circulation model. If this type of transport is underestimated, it could be expected that high-latitude exchange of the stratospheric constituents (such as ozone) would be underestimated and the low-latitude exchange at the confluence of the Ferrel and Hadley cells would be overestimated. Such a pattern of errors does occur with low-resolution general-circulation models. Decreasing averaging volume should decrease the errors and the complexity required in the statistical description, but the burden is then transferred to the computational domain.

A related phenomenon is the transport produced by the mean circulation associated with various jet-stream and longwave systems. A systematic transverse circulation is associated with these jets that produces mean rising motion on the anticyclonic shear side of the jet stream and mean sinking motion on the cyclonic side (Mahlman, 1975). This mechanism is not only capable of returning tropospheric air to the stratosphere, but also appears to be responsible for much of the upward energy flux that excites planetary waves in the stratosphere. Because this process occurs on

large scales, the resulting transport can be explicitly incorporated in 3-D models.

Cumulonimbus convection has often been proposed as a means of transporting trace species from the troposphere to the stratosphere. However, there is some evidence from laboratory convection studies and radioactivity deposition observations (Reiter and Mahlman, 1965) that the collapse of cumulus cells in the stratosphere due to negative buoyancy and the subsequent sinking back into the troposphere may in fact cause entrained stratosphere air to enter the troposphere. So far, there is little evidence to indicate that cumulus convection provides an effective direct source of upward transport across the tropopause. However, convective clouds clearly transport trace species from the lower troposphere to the vicinity of the tropopause.

In the tropical regions, substances that have been brought to the upper troposphere by cumulus convection may be transported upward through the lower stratosphere by the slow mean vertical motion associated with the rising branch of the Hadley cell. This slow rising motion through the cold tropical tropopause has long been accepted as a likely explanation for the observed low concentration of water vapor in the stratosphere (that is, water-vapor mixing ratios in the stratosphere do not exceed the saturation value at the tropical tropopause.) Multidimensional general-circulation models that explicitly compute the tropospheric circulation can explicitly incorporate the large-scale Hadley circulation. However, in models in which the tropopause is used as the lower boundary, the vertical component of the Hadley circulation must be included as a boundary condition. In either case, vertical transports by cumulus clouds can only be included by suitable parameterizations.

OBSERVATIONAL NEEDS OF MULTIDIMENSIONAL MODELS OF THE STRATOSPHERE

The specific concern of this subsection is the observational basis required for ensuring that multidimensional models are producing reasonable information about the overall impact of CFM's. It is important to note at the outset that theoretical modeling and observational studies are, and should be, interactive ventures. Not only are quantitative checks on model outputs required, but also measurement strategies that address important theoretical problems must be designed and completed. The great variability in space and time that exists in the stratosphere in both the meteorological fields (wind, temperature, and pressure) and the ozone distribution

must be understood. It is suspected that most of the ozone variability, at least below 30 kilometers, is due to transport by large-scale motions. Even in the region of local photochemical control, advection of photochemically active minor species such as NO_x and Cl_x will influence the ozone distribution.

Most 3-D models will produce both wind and temperature fields systematically before utilizing these fields in photochemical transport models. Quasi-geostrophic theory can provide such models in the midlatitudes, and balance equations have been used to extend these models to the entire sphere (Cunnold et al., 1975). However, primitive equation models are probably needed for simulating the tropical stratosphere. To compare model dynamics with observations will require temperature measurements with grid resolutions on the order of 1000, 250, and 3 kilometers in the zonal, meridional, and vertical directions, respectively.

Time resolutions on the order of 1 day are also needed. Diagnostic studies utilizing these data will isolate various dynamical and energetic mechanisms, thus increasing the understanding of the stratosphere. When compared to similar studies of multidimensional model output, these studies can help to verify various aspects of the models. Horizontal velocities can be determined from the temperature field and reference-level winds by approximate methods whose accuracy can be matched to that of the temperature observations. Vertical velocities can also be obtained by a number of indirect methods. When combined with global observations of chemical constituents, these velocities can be used to compute transports. Direct wind measurements would provide a valuable check on model output and would verify indirectly determined winds. Horizontal wind components can be measured using the standard meteorological observational network augmented by data utilizing radar, superpressure balloons, and possibly satellite-based Doppler techniques. Such measurements would be most useful in the tropics, but there they would have to be accurate within 2 to 4 msec^{-1} .

In order to establish that transport variability is being reasonably simulated by any given model, global coverage of ozone and of at least one photochemically simple trace constituent with the spatial and temporal resolution previously suggested for temperature will be needed. Remote sensing from satellites is clearly needed for establishing this type of data base. Ozone has been already observed from a number of satellites, albeit with poor vertical resolution below the ozone peak. N_2O and CH_4 are the traditional candidates for a photochemically important tracer. N_2O is preferred primarily because methane can be lost by reaction with species

such as OH, as well as by reaction with O(¹D) and through photolysis, both of which are also sinks for N₂O. The important loss mechanism for N₂O is probably photolysis; if so, this greatly simplifies its transport equation. At present concentrations, the CFM's themselves, particularly CF₂Cl₂ and CFCI₃, may be useful tracers in the stratosphere because they appear to be inert except for photolysis. Furthermore, the distribution of their sources is well-known. Of course, ozone itself should be a good tracer in the lower stratosphere, and its distribution there is the final test of any model.

The Stratospheric and Mesospheric Sounder (SAMS) to be launched in 1978 on Nimbus-G will measure N₂O, as well as other trace constituents, but better vertical resolution will be required. The Limb Infrared Monitor of the Stratosphere (LIMS), also to be flown on Nimbus-G, has better height resolution, but it measures NO₂ and HNO₃ rather than N₂O. The former are important in the scheme for ozone destruction, but their complex photochemistry limits their use as tracers for advective transport.

The data processing task associated with the global coverage described previously is enormous. Ideally, those responsible for data analysis should work in close association with the experimenters. This would permit the data to be reduced in a usable format familiar to the researchers and would alert them to possible problems or limitations inherent in the instrumentation or its operation. The data must not simply be archived. Again, any data analysis should place some emphasis on determining the scales of spatial and temporal variability. It should be noted that significant data analysis has been and is being performed on presently existing data (Angell and Korshover, 1976; Hartmann, 1976; Quiroz, 1975; and Barnett et al., 1975).

The degree to which any model can simulate mass transport of photochemically active trace constituents, including ozone, depends not only on accurately describing advection and/or diffusion processes, but also on quantitatively specifying the sources and sinks of the trace constituents. For this reason, multidimensional models must eventually include both adequate dynamic transport and accurate photochemistry.

One class of observations that is obviously needed for any model attempting to assess the impact of CFM is a series of measurements to validate the photochemistry itself. To do this, it is necessary to measure families of photochemical species such as CFM or NO_x, or representatives of each of the odd nitrogen, chlorine, hydrogen, and oxygen families simultaneously.

In contrast to the global coverage required for describing advective transport (even when parameterized as eddy diffusion), observations designed to test understanding of the photochemistry are local in nature and are best done from balloon, airplane, or space-shuttle platforms.

Microwave measurements from the ground may also help. To minimize meteorological influences on these observations, the minor species are best sampled in the region of local photochemical equilibrium (above 25 to 30 kilometers). Temperature should be measured simultaneously for computing kinetic reaction rates. Photodissociation rates can be accurately specified if the ozone overburden is also measured. However, the solar flux and its variability should be measured more precisely at wavelengths less than approximately 200 nanometers where both CFM and N_2O are photodissociated. Some stratospheric circulation models have bypassed generating the tropospheric circulation, with its vastly varying scales of motion and complex hydrological cycle, by placing their lower boundary in the upper troposphere. These models are advantageous in that they permit highly useful mechanistic studies, but the suppression of a proper troposphere/stratosphere interaction limits their usefulness. If such models are to describe the more general transport in the stratosphere, they will eventually require specification of the variable temperatures and winds along a meteorological reference level in the upper troposphere. The distributions of CFM, N_2O , and H_2O , all of which are precursors of photochemically active minor species, would also have to be specified along such a boundary.

The observations required for describing such a boundary should be part of a program directed toward understanding transport across the tropopause. A great deal more must be known about how the precursors and reservoirs of odd nitrogen, hydrogen, and chlorine enter or leave the lower stratosphere. In particular, the roles of cumulus convection, jet streams, and midlatitude baroclinic systems need more study. (See the previous section on "Vertical Transport Across the Tropopause.") This suggests latitudinal surveys of CFM, N_2O , HNO_3 , and HCl near the tropopause and perhaps correlation of these observations with synoptic-scale meteorological events (e.g., storm systems and temporally varying jet streams). Aircraft and balloons provide suitable instrument platforms.

The standard meteorological observational network and daily analysis can provide some of the necessary information. In particular, it outlines the temporal variability in the upper troposphere of the otherwise low-frequency, vertically propagating planetary waves believed to produce much of the dynamic activity in the upper atmosphere.

Most of the foregoing discussion has addressed models that explicitly generate the large-scale wind field used to study mass transport. Observations of at least two trace constituents are needed for models that parameterize their advective transport as an eddy-diffusion process: one for parameterization and one for independent comparison. Measurements emphasizing the latitudinal and seasonal variations of these tracers and other important photochemically active species are needed in sufficient number that reasonable averages can be computed for comparison with model calculations. Computations for a strongly perturbed stratosphere, however, require understanding of how the coefficients that describe the effective transport in these parameterized models will evolve. Variability with time is not easily included in these models.

In summary, the following measurements are emphasized, in addition to those needed to verify the stratospheric photochemistry itself:

Global coverage of temperature, ozone, and at least two photochemically simple tracers, such as N₂O, with adequate resolution for transport studies (namely, observational spacings of at least 1000, 250, and 3 kilometers in the zonal, meridional, and vertical directions, respectively)

Specification of temperature and wind along at least two meteorological reference levels in the upper troposphere; observations of CFM, NO_y, N₂O, H₂O, HNO₃, and HCl at this reference level and near the tropopause. These observations should be part of a more general program directed toward understanding transport into and out of the lower stratosphere. (See the section on "Vertical Transport Across the Tropopause.")

Several years of coverage are needed for both of these items. Furthermore, analysis should examine spatial and temporal variability. Measurement strategies must include planning and support for this data analysis.

This observational program is an extensive one, but should be undertaken. As a more immediate step toward establishing a useful data base for ongoing modeling efforts, however, it is recommended that one or more International Stratospheric Periods (ISP) be established during which coordinated measurements would be made. The measurement period suitable to averaging is limited by natural variability to 1 to 3 days during winter, 1 week during early fall and late spring, and 2 weeks during summer. The aim of such a measurement program would be to obtain vertical profiles

of temperature and as many constituents as possible for at least one high-latitude, one midlatitude, and one low-latitude station. By also utilizing simultaneous aircraft and satellite observations, it should be possible to obtain an instantaneous global picture of the stratosphere at the time of the ISP.

CONCLUSIONS

ASSESSMENT UNCERTAINTY DUE TO TRANSPORT

One-dimensional models utilizing detailed chemistry with simplified radiation treatments and with all effects of dynamics parameterized by means of a height-dependent eddy diffusion have been used to estimate the CFM effects on ozone in this report, as well as in the NAS Report, *Halocarbons: Effects on Stratosphere Ozone* (1976). The results of these models provide the best available estimate of the CFM effects on ozone that depends on the anticipated CFM-release scenario. These model results also provide the uncertainty of this best estimate. This uncertainty is a result not only of possible errors in the parameterized transport estimates, but also of uncertainties in CFM release rates, stratosphere chemistry, and in the approximation of the real atmosphere by a relatively simple 1-D model. The NAS Report (1976) has quoted the 95-percent uncertainty limits due to the use of a 1-D model for approximating the transport and distribution of chemical species to be given by the best estimate multiplied by a factor of $(1.7)^{\pm 1}$. This uncertainty is for the problem of a continuous CFM-release scenario at constant 1973 levels. The uncertainty with an interrupted release scenario would be less than this. This is due to the nature of the CFM problem in which the CFM's are expected to become uniformly mixed throughout the troposphere before being transported in substantial amounts through the region of minimum transport in the vicinity of the tropopause. This assumes that CFM's are lost from the troposphere mainly by upward transport rather than by *in situ* removal. Because of the expected uniform mixing of CFM's in the troposphere, the uncertainties in vertical transport resulting from the use of a 1-D model are relatively small.

The uncertainties resulting from the use of the 1-D model quoted in the NAS Report (1976) were derived by extensive experimentation with different eddy-diffusion profiles. It is not entirely convincing that such a procedure gives the total uncertainty that results from approximating a 3-D problem by a 1-D model. For instance, the use of a 1-D model assumes the average of a function of several variables to be equal to the

same function of the averaged variables. This approximation, while probably not leading to great errors, should increase the uncertainties from that quoted in the NAS Report (1976). Uncertainty about whether or not transport can be handled correctly in a multiconstituent 1-D model using a single eddy-diffusion profile also leads to a widening of the uncertainty interval. Indeed, the 3-D tracer studies of Mahlman (1975) show that derived 1-D eddy-diffusion coefficients can differ significantly among various tracers. Furthermore, there are a number of feedback effects that, in some cases, are very difficult to quantitatively evaluate and that cannot be treated in a 1-D model. The ultimate feedback effects are the direct and indirect CFM effects on climate that are beyond the scope of this report. The neglect of these feedback effects also leads to a widening of the NAS uncertainty interval that results from using 1-D models to approximate the atmosphere. The extent of the widening of the uncertainty limits implied by the neglect of feedback processes is an open question.

CONTRIBUTIONS OF MULTIDIMENSIONAL MODELS

There is no expectation for the development of a comprehensive multidimensional model incorporating all of the necessary physics and chemistry required for assessment applications. Assessments will always be based on a judicious complement of studies with different models, including 1-D, 2-D, and 3-D models. This procedure permits different physical processes and effects to be treated in adequate detail and provides results that can be incorporated in other models, emphasizing other aspects of the overall problem. It is essential that special care be taken to ensure that all important feedbacks and interactions are included in this process. Although it will probably require at least several years to obtain satisfactory investigation of the comprehensive radiative-dynamical/chemical problems, it is important to emphasize that contributions can be expected in the near term from 2-D and 3-D models, as well as from 1-D models.

Two-dimensional models permit the inclusion of latitudinal and seasonal dependencies of transport, temperature, and the solar flux. Because of the observed variation of O₃ concentration with latitude, the strong change of solar flux and dynamical transports with latitude, and the dependence of reaction rates on temperature, there is reason to expect that realistic 2-D models can provide better assessments or useful information for improving assessments made with 1-D models. The 2-D models must rely on parameterized transport, as is the case with 1-D models; the use of four transport

coefficients instead of the one in a 1-D model means that more observational data are required for parameterization, but eventually a better determination of transport effects on O_3 assessments should result. The 2-D models have a number of limitations arising from the parameterization of effects due to longitudinal variations. Primarily because of such parameterizations, the radiative, dynamical, and chemical 2-D models are not as "fully coupled" as desired.

Three-dimensional models have the advantage of minimizing the parameterization of transport. The scales of motion responsible for most of the transport in the stratosphere can, in fact, be explicitly resolved with feasible grid spacings. This capability will permit a maximum incorporation of feedbacks and interactions that will provide information for upgrading the reliability of 1-D and 2-D models. The 3-D models have already been of some value for diagnostic purposes (for example, for tracer studies, for providing an indication of longitudinal variabilities, and for testing assumptions made in simpler models), and the applications can be expected to increase as the realism of the 3-D models improves. The primary limitations of the 3-D models are related to the extensive computer requirements, which can translate into a great expense if the computations are made for extended simulations and into a requirement for inclusion of a simplified chemistry. As previously emphasized, a proper strategy for investigation must involve a careful complement of 1-D, 2-D, and 3-D studies.

OBSERVATIONAL NEEDS

Observations needed by multidimensional models can be separated into the following categories: (1) those needed for verification of the photochemistry itself, (2) those needed for parameterization of dynamical processes such as eddy transport in 2-D models and subgrid-scale processes in 3-D models, and (3) those needed for determining larger scale winds, whether to derive mean motions for 2-D models or to examine the scales of temporal and spatial variability for comparison with 3-D model output. Each of these categories requires different observational coverage and resolution. Studies for supporting 3-D models require global coverage of temperature and at least two tracers, such as N_2O , with spatial resolutions of 1000, 250, and 3 kilometers in the zonal, meridional, and vertical directions, respectively. Even 2-D models need measurements of the longitudinal variability of tracer concentrations in order to assess the representativeness of a given zonal average, as well as to evaluate the validity of various eddy-transport parameterizations.

Observations required to specify lower boundary conditions for models that do not explicitly include the troposphere should be part of a more general program to study transport across the tropopause and in the lower stratosphere. In particular, more knowledge is needed concerning the roles played by tropical cumulus convection, jet streams, and midlatitude baroclinic systems.

In all cases, data analysis should examine spatial and temporal variability. Furthermore, the difficulty of processing the large quantity of data required by multidimensional models, particularly 3-D models, makes it imperative that measurement strategies include sufficient planning and support for data distribution and analysis.

REFERENCES

- Ackerman, M., 1971, *Mesospheric Models and Related Experiments*, G. Fiocco, ed., D. Reidel, Dordrest, Holland, p. 149.
- Ackerman, M., J. C. Fontanella, D. Frimont, A. Girard, N. Louisnard, and C. Muller, 1975, *Space Science*, **23**, p. 651.
- Ackerman, M., D. Frimont, C. Muller, D. Nevejaus, J. C. Fontanella, A. Girard, and N. Louisnard, 1973, *Nature*, **245**, p. 205.
- Ackerman, M., D. Frimont, A. Girard, M. Gottignies, and C. Muller, 1976, *Geophys. Res. Lett.*, **3**, p. 81.
- Ackerman, M., and C. Muller, 1972, *Nature*, **240**, p. 300.
- Anastasi, C., and I. W. M. Smith, 1976, *J. Chem. Soc., Faraday Trans. II*, **72**, pp. 1459-1468.
- Anderson, G. P., C. A. Barth, F. Cayla, and J. London, 1969, *Am. Geophys. Lett.*, **25**, pp. 341-345.
- Anderson, J. G., 1971, *J. Geophys. Res.*, **76**, p. 7820.
- Anderson, J. G., 1975, *Geophys. Res. Lett.*, **2**, p. 231.
- Anderson, J. G., 1976, *Geophys. Res. Lett.*, **3**, p. 165.
- Anderson, J. G., 1977, Position paper presented at the Chlorofluoromethane Assessment Workshop, Warrenton, Virginia, January 1977.
- Anderson, J. C., and F. Kaufman, 1973, *Chem. Phys. Lett.*, **19**, pp. 483-486.
- Anderson, J. G., J. J. Margitan, and F. Kaufman, 1974, *J. Chem. Phys.*, **60**, pp. 3310-3317.
- Anderson, L. G., 1976, *Rev. Geophys. Space Sci.*, **14**, p. 151.
- Angell, J. K., and J. Korshover, 1976, *Mon. Wea. Rev.*, **104**(1), pp. 63-75.
- Atkinson, R., R. A. Perry, and J. N. Pitts, Jr., 1976, *J. Chem. Phys.*, **65**, pp. 306-310.

- Atkinson, R., and J. N. Pitts, Jr., 1974, *Chem. Phys. Lett.*, **27**, pp. 467-470.
- Atmosphere Environmental Service Department of the Environment,
Ozone Data for the World, in cooperation with the World Meteorological
Organization, Downsview, Canada.
- Attmannspacher, W., and H. V. Dutsch, 1970, *Berichte des Deutsch.
Wetterdienstes*, **16** (120).
- Ausloos, P., R. E. Rebbert, and L. Glasgow, 1977, to be published in the
NBS Journal of Research.
- Balakhnin, V. P., V. I. Egorov, and E. I. Intezarova, 1971, *Kinetics and
Catalysis*, **12**, pp. 258-262.
- Ballash, N. M., and D. A. Armstrong, 1974, *Spectrochim. Acta*, **30A**,
pp. 941-944.
- Bass, A. M., A. L. Ledford, and A. H. Laufer, 1976, *J. Res. NBS*, **80A**,
pp. 143-166.
- Bass, A. M., and A. E. Ledford, Jr., 1976, paper presented at the 12th
Informal Conference on Photochemistry, Gaithersburg, Maryland, June
28-July 1, 1976.
- Barat, J., 1975, *Comptes Rendus*, **280**, series B.
- Barnett, J. J., R. S. Harwood, J. T. Houghton, C. C. Morgan, C. D. Rodgers,
and E. J. Williams, 1975, *Quart. J. Roy. Met. Soc.*, **101**, pp. 423-436.
- Bates, D. R., and P. B. Hayes, 1967, *Planet Space Sci.*, **15**, pp. 189-197.
- Bauer, K. G., 1976, *Mon. Wea. Rev.*, **104**, pp. 922-931.
- Baulch, D. L., D. D. Drysdale, and D. G. Horne, 1973a, *Chemical Kinetics
Data Survey*, V. D. Garvin, ed., NBSIR 73-206, National Bureau of
Standards, Washington, D.C., pp. 49-115.
- Baulch, D. L., D. D. Drysdale, and D. G. Horne, 1973b, "Evaluated Kinetic
Data for High Temperature Reactions," *Homogeneous Gas Phase Reac-
tions of the H₂-N₂-O₂ System*, **2**, Butterworths, London.
- Becker, K. H., W. Groth, and D. Kley, 1969, *Z. Naturforsch.*, **24**, pp. 1280-
1281.

- Becker, K. H., D. Haaks, and T. Tarezyk, 1972, *Z. Naturforsch.*, **27**, p. 1520.
- Bernand, P. P., M. A. A. Clyne, and R. T. Watson, 1973, *J. Chem. Soc., Faraday Trans. I*, **69**, pp. 1356-1374.
- Benson, S. W., 1968, *Thermochemical Kinetics*, John Wiley & Sons, Inc.
- Benson, S. W., F. R. Cruickshank, and R. Shaw, 1969, *Int. J. Chem. Kinet.*, **1**, pp. 29-43.
- Berg, W. W., and J. W. Winchester, 1976, presented at the Non-Urban Troposphere Composition Symposium, Hollywood, Florida, November 1976.
- Bigg, E. K., 1975, *J. Atmos. Sci.*, **32**, pp. 910-917.
- Bigg, E. K., A. Ono, and J. A. Williams, 1974, *Atmos. Environ.*, **8**, pp. 1-13.
- Birks, J. B., J. P. Jesson, L. C. Glasgow, and R. A. Young, 1976, *12th Informal Conference on Photochemistry*, Gaithersburg, Maryland.
- Birks, J. W., B. Shoemaker, T. J. Leck, and D. M. Hinton, 1976, *J. Chem. Phys.*, **65**, pp. 5181-5185.
- Birrer, W. H., 1974, *Pure and Applied Geophysics*, **112** (3), pp. 523-532.
- Bojkov, R. D., 1969, *J. Applied Met.*, **8**, pp. 362-368.
- Borucki, W. J., R. C. Whitten, V. R. Watson, H. T. Woodward, C. A. Riegel, L. A. Capon, and T. Becher, 1976, Paper No. 76-176, *AIAA 14th Aerospace Sciences Meeting*, Washington, D.C., January 1976.
- Boughner, R. E., 1975, paper presented at the 1975 AGU Fall Annual Meeting, San Francisco.
- Boyd, 1976, *J. Atmos. Sci.*, **33**, pp. 2285-2291.
- Bradford, C. M., F. H. Murcray, J. W. Van Allen, J. N. Brooks, D. G. Murcray, and A. Goldman, 1976, *Geophys. Res. Letters*, **3**, p. 387.
- Brasseur, G., 1976, *Etude de l'Environnement*, (25), Institute D'Aeronomie Spatiale de Belgique.

- Brasseur, G., 1977, "Elements Pour Une Etude du Chlore Dans l'Ozone-sphere par la Technique du Modile Mathematique," *Aerospatiale, Note de l'Environnement*.
- Brasseur, G., and M. Bertin, 1976, "Distribution and Circulation of Stratospheric Ozone in the Meridional Plane as Given by a Two-Dimensional Model," *Etude de l'Environnement*, No. 25, Institute D'Aeronomie Spatiale de Belgique.
- Brewer, A. W., 1973, *Pure and Applied Geophys*, 106-108, pp. 919-927.
- Brewer, A. W., C. R. McElroy, and J. B. Kerr, 1974, *Proceedings of the Third Conference on the Climatic Impact Assessment Program*, DOT-TSC-OST-74-15, U.S. Department of Transportation, p. 257.
- Brewer, A. W., and J. R. Milford, 1960, *Proc. Roy. Soc.*, 256 A, pp. 470-495.
- Broadfoot, A. L., 1972, *Astrophys. J.*, 173, p. 681.
- Brown, R. D. H., and I. W. M. Smith, 1975, *Int. J. Chem. Kinet.*, 7, pp. 301-315.
- Brueckner, G. E., and O. K. Moe, 1971, *Space Research XII*, Akademie-Verlag, Berlin, Germany, p. 1595.
- Burkhardt, E. G., C. A. Lambert, and C. K. N. Patel, 1975, *Science*, 188, p. 1111.
- Burnett, C. R., 1976, *Geophys. Res. Lett.*, 3, p. 319.
- Burrows, J. P., G. W. Harris, and B. A. Thrush, 1977, *Nature*, 267, pp. 233-234.
- Butler, D. M., 1976, "Uncertainty of Predictions of Stratospheric Ozone Depletion, a Reaction Rate Sensitivity Study," in preparation, December 1976.
- Cadet, D., 1975, *Quart. J. Roy. Met. Soc.*, 101, pp. 485-493.
- Callis, L. B., V. Ramanathan, R. E. Bonghner, and B. R. Barkstrom, 1975, *Proceedings of the Fourth Conference on the Climatic Impact Assessment Program*, February 4-7, 1975, DOT-TSC-OST-75-38, available

- through the National Technical Information Service, Springfield, Virginia 22161.
- Calvert, J. G., and J. N. Pitts, 1967, *Photochemistry*, John Wiley & Sons, Inc., New York, pp. 230-231.
- Campbell, I. M., B. J. Handy, and R. M. Kirby, 1975, *J. Chem. Soc., Faraday Trans. I*, **71**, pp. 867-874.
- Campbell, M. J., 1976, *Geophys. Res. Lett.*, **3**, pp. 661.
- Castellano, E., and H. J. Schumacher, 1969, *Z. Physik. Chem.*, **65**, pp. 62-85.
- Castellano, E., and H. J. Schumacher, 1975, *Anales Asoc. Quim. Argentina*, **63**, pp. 9-15.
- Cess, R. D., 1976, *J. Atmos. Sci.*, **33**, pp. 1831-1843.
- Chaloner, C. P., J. R. Drummond, J. T. Houghton, R. F. Jarnot, and H. K. Roscoe., 1975, *Nature*, **258**, p. 697.
- Chan, W. H., W. M. Uselman, J. G. Calvert, and J. H. Shaw, 1977, *Chem. Phys. Lett.*, **45**, p. 240.
- Chang, J. S., 1975, In: *Stratosphere Perturbed by Propulsion Effluents*, CIAP Monograph 3, DOT-TSC-75-53, U.S. Department of Transportation.
- Chang, J. S., 1976, In: *Halocarbons: Effects on Stratospheric Ozone*, National Academy of Sciences Report, Washington, D.C., September 1976.
- Chang, J. S., et al., 1976, *Atmospheric Chemistry Committee on Impacts of Stratospheric Change*, preliminary report of panel, National Research Council, September 1976.
- Chang, J. S., and F. Kaufman, 1977, *J. Chem. Phys.*, **66**, p. 4989.
- Chou, C. C., W. S. Smith, H. V. Ruiz, K. Moe, G. Crescentini, M. J. Molina, and F. S. Rowland, 1977, *J. Phys. Chem.*, in press.
- Chou, C. C., W. S. Smith, H. V. Ruiz, K. Moe, G. Crescentini, M. J. Molina, and F. S. Rowland, 1976a, *J. Phys. Chem.*

- Chou, C. C., R. J. Milstein, W. S. Smith, and H. V. Ruiz, 1976b, *J. Phys. Chem.*
- Chou, C. C., G. Crescentini, H. V. Ruiz, W. S. Smith, and F. S. Rowland, 1977, "Stratospheric Photochemistry of CF_2O , CClFO and CCl_2O ," 173rd American Chemical Society National Meeting, New Orleans.
- Christiansen, V. O., J. A. Dahlberg, and H. F. Anderson, 1972, "On the Nonsensitized Photo-Oxidation of 1, 1, 1-Trichloroethane Vapour in Air," *Acta Chem. Scand.*, 26, pp. 3319-3324.
- Christie, A. D., 1973, *Pure and Applied Geophys.*, 106-108, pp. 1000-1009.
- Cicerone, R. J., 1975, *J. Geophys. Res.*, 80, p. 3911.
- Cicerone, R. J., D. H. Stedman, and R. S. Stolarski, 1975, *Geophys. Res. Letters*, 2, p. 219.
- Cieslika, S., and M. Nicolet, 1973, *Planet. Space Sci.*, 21, pp. 925-938.
- Clewell, D. H., and W. J. Koehl, 1974, "Approaches to Automotive Emissions Control," *ACS Symposium Series One*.
- Climatic Impact Assessment Program, Report of Findings, 1974, "Effects of Stratospheric Pollution by Aircraft," DOT-TST-75-50, U.S. Department of Transportation, December 1974.
- Climatic Impact Assessment Program, 1975, "The Natural Stratosphere of 1974," *CIAP Monograph 1*, DOT-TST-75-51.
- Clyne, M. A. A., and I. S. McDermid, 1975, *J. Chem. Soc., Faraday Trans. I*, 71, pp. 2189-2208.
- Clyne, M. A. A., and H. W. Cruse, 1970, *Trans. Faraday Soc.*, 66, pp. 2314-2226.
- Clyne, M. A. A., and P. H. Monkhouse, 1977, *J. Chem. Sec., Faraday Trans. II*, 73, pp. 298-309.
- Clyne, M. A. A., P. B. Monkhouse, and L. W. Townsend, 1976, *Int. J. Chem. Kinet.*, 8, pp. 425-449.

- Clyne, M. A. A., and W. S. Nip, 1976a, *J. Chem. Soc., Faraday Trans. II*, **72**, pp. 838-847.
- Clyne, M. A. A., and W. S. Nip, 1976b, *J. Chem. Soc., Faraday Trans. I*, **72**, pp. 2211-2217.
- Clyne, M. A. A., and R. F. Walker, 1973, *J. Chem. Soc., Faraday Trans. I*, **69**, pp. 1547-1567.
- Clyne, M. A. A., and R. T. Watson, 1974, *J. Chem. Soc., Faraday Trans. I*, **70**, pp. 2250-2259.
- Clyne, M. A. A., and R. T. Watson, 1975, *J. Chem. Soc., Faraday Trans. I*, **71**, pp. 336-350.
- Cox, R. A., and R. G. Derwent, 1975, *J. Photochem.*, **4**, pp. 139-153.
- Cox, R. A., R. G. Derwent, and P. M. Holt, 1976, *J. Chem. Soc., Faraday Trans. I*, **72**, pp. 2031-2043.
- Cox, R. A., and R. G. Derwent, 1976, *J. Photochem.*, **6**, pp. 23-34.
- Cox, and Myers, 1972-1975, COMESA, *The Report of the Committee on Meteorological Effects on Stratospheric Aircraft*.
- Coxon, J. A., W. E. Jones, and D. A. Ramsey, 1976, *12th International Symposium on Free Radicals*, Laguna Beach, California.
- Craig, R. A., 1965, *The Upper Atmosphere: Meteorology and Physics*, Academic Press, New York.
- Crutzen, P. J., and I. Isaksen, 1977, *J. Geophys. Res.*, in press.
- Crutzen, P. C., I. S. A. Isaksen, and G. Reid, 1975, *Science*, **189**, p. 457.
- Crutzen, P. J., 1975, *Proceedings of the Fourth Conference on CIAP*, February 4-7, 1975, DOT-TSC-OST-75-38.
- Cunnold, D., F. Alyea, N. Phillips, and R. Prinn, 1975, *J. Atmos. Sci.*, **32**, pp. 170-194.
- Cunnold, D., F. Alyea, N. Phillips, and R. Prinn, 1976, *J. Atmos. Sci.*, **32**, p. 170.

- Cunnold, D., F. Alyea, and R. Prinn, 1976, *Proceedings of the International Conference*, Dresden, German Democratic Republic, August 7-17, 1976.
- Cunnold, D. M., C. W. Gray, and D. C. Merritt, 1973, *Pure and Applied Geophys.*, 106-108, pp. 1264-1271.
- Cvetanovic, R. J., 1974, *Can. J. Chem.*, 52, pp. 1452-1464.
- Dave, J. V., and C. L. Mateer, 1967, *J. Atmos. Sci.*, 24, pp. 414-427.
- Davidson, J. A., C. M. Sadowski, H. I. Schiff, G. E. Streit, C. J. Howard, D. A. Jennings, and A. L. Schmeltekopf, 1976; *J. Chem. Phys.*, 64, p. 57.
- Davies, M. T. E., 1974, MSc Thesis, University of Toronto, May 1974.
- Davis, D. D., 1976, "Absolute Rate Constants for Elementary Reactions of Atmospheric Importance: Results from the University of Maryland Gas Kinetics Laboratory," Report No. 3, University of Maryland, College Park, Maryland.
- Davis, D. D., W. Heaps, and T. McGee, 1976, *Geophys. Res. Lett.*, 3, p. 331.
- Davis, D. D., G. Machado, B. Conway, Y. Oh, and R. Watson, 1976, *J. Chem. Phys.*, 65, pp. 1268-1274.
- Davis, D. D., J. Prusaczyk, M. Dwyer, and P. Kim, 1974, *J. Phys. Chem.*, 78, pp. 1775-1779.
- DeMore, W. B., 1976, paper presented at the International Conference on the Stratosphere and Related Problems, Logan, Utah, September 1976.
- DeMore, W. B., 1975, *Int. J. Chem. Kinet.*, Symposium No. 1, pp. 273-279.
- DeMore, W. B., and E. Tschuikow-Roux, 1974, *J. Phys. Chem.*, 78, pp. 1447-1451.
- Detwiler, C. R., D. L. Garrett, J. D. Purcell, and R. Tousey, 1961, *Ann. Geophys.*, 17, p. 263.
- Dickinson, R. E., 1976, In: *Halocarbons: Effects on Stratospheric Ozone*, National Academy of Sciences Report, Washington, D.C., September 1976.

- Dobson, G. M. B., 1975, "Observers' Handbook for the Ozone Spectrophotometer" and "Adjustment and Calibration of Ozone Spectrophotometer," *Annals of the International Geophysical Year*, V, Parts II and III, Pergamon Press, New York, pp. 46-114.
- Dobson, G. M. B., 1966, "Forty Years' Research on Atmospheric Ozone at Oxford: A History," Memorandum No. 66.1, University of Oxford.
- Donahue, T. M., R. J. Cicerone, S. C. Liu, and W. L. Chameides, 1976, *Geophys. Res. Letters*, 3, p. 105.
- Donnelly, R. F., and J. H. Pope, 1973, NOAA Technical Report ERL 276-SEL25.
- Drayson, S. R., F. L. Bartman, W. R. Kuhn, and R. Tallamraju, 1972, "Satellite Measurements of Stratospheric Pollutants and Minor Constituents by Solar Occultation," a preliminary report, High Alt. Eng. Lab., Report No. 011023-T, University of Michigan.
- Drummond, J. W., J. M. Rosen, and D. J. Hofman, 1976, paper presented at the International Conference on the Stratosphere and Related Problems, Utah State University, Logan, Utah, September 15-17, 1976.
- Duce, R. A., J. Winchester, and T. Van Nahl, 1965, *J. Geophys. Res.*, 70, p. 1775.
- Duewer, W. H., D. J. Wuebbles, H. W. Ellsaesser, and J. S. Chang, 1976, submitted to *J. Geophys. Res.*, March 1976.
- Dütsch, H. U., 1969, "Atmospheric Ozone and Ultraviolet Radiation," In: *World Survey of Climatology*, D. F. Rex, ed., 4, Elsevier, New York.
- Dütsch, H. U., and C. C. Ling, 1973, *Pure and Applied Geophysics*, 106-108, pp. 1139-1150.
- Dziewulska-Losiowa, A., and C. D. Walshaw, 1975, "The International Comparison of Ozone Spectrophotometers, Belsk, June 24 to July 6, 1974" *Publications of the Institute of Geophysics*, Materialy 2, Prace 89, Polish Academy of Sciences, Panstwowe Wydawnictwo Naukowe, Warszawa.
- Ehhalt, D. H., L. E. Heidt, R. H. Lueb, and A. Roper, 1974, *Proceedings of the Third Conference on the Climatic Impact Assessment Programs*, DOT-TSC-OST-74-15, U.S. Department of Transportation, p. 153.

- Ehhalt, D. H., L. E. Heidt, and E. A. Martell, 1972, *J. Geophys. Res.*, **77**, p. 2193.
- Elliott, D. D., 1971, *Space Res.*, **XI**, pp. 857-861.
- Evans, W. F. J., J. B. Kerr, D. I. Wardle, J. C. McConnell, B. A. Ridley, and H. I. Schiff, 1976a, *Atmosphere*, **14**, p. 189.
- Evans, W. F. J., J. B. Kerr, and B. A. Ridley, 1976b, paper presented at the International Conference on the Stratosphere and Related Problems, Utah State University, Logan, Utah, September 15-17, 1976.
- Evans, W. F. J., C. I. Lin, and C. L. Midwinter, 1976c, *Atmosphere*, **14**, p. 172.
- Eyre, J. R., and H. K. Roscoe, 1977, *Nature*, **266**, p. 243.
- Fabian, P., and W. F. Libby, 1974, *Proceedings of the Third Conference on Climatic Impact Assessment Program*, February 4-7, 1975, DOT-TSC-OST-75-15, pp. 103-116.
- Falconer, P. D., and J. D. Holdeman, 1976, *Geop. Res. Lett.*, **3**, pp. 101-?.
- Farmer, C. B., O. F. Raper, and R. H. Norton, 1976, *Geophys. Res. Lett.*, **3**, p. 13.
- Fehsenfeld, F. C., and D. L. Albritton, 1977, *Geophys. Res. Letters*, **4**, p. 61.
- Ferguson, W. C., L. Slotin, and D. W. G. Style, 1936, *Tran. Faraday Soc.*, **32**, pp. 956-962.
- Fettis, G. C., and J. H. Knox, 1964, "Rate Constants of Halogen Atom Reactions," G. Porter, ed., *Progress in Reaction Kinet.*, **2**, Pergamon Press, New York, pp. 1-38.
- Finger, F., M. Gelman, F. Schmidlin, R. Leviton, B. Kennedy, 1975, *J. Amt. Sci.*, **32**, pp. 1705-1714.
- Fletcher, I. S., and D. Husain, 1976a, *Can. J. Chem.*, **54**, pp. 1765-1770.

- Fletcher, I. S., and D. Husain, 1976b, *J. Phys. Chem.*, **80**, pp. 1837-1840.
- Fontanella, J. C., A. Girard, L. Gramont, and N. Louisnard, 1974, *Proceedings of the Third Conference on the Climatic Impact Assessment Program*, DOT-TSC-OST-74-15, U.S. Department of Transportation, p. 217.
- Fontanella, J. C., A. Girard, L. Gramont, and N. Louisnard, 1975, *Appl. Opt.*, **14**, p. 825.
- Foon, R., and K. B. Tait, 1972, *J. Chem. Soc., Faraday Trans. I*, **68**, p. 104.
- Garvin, D., and R. F. Hampson, 1975, "Rate and Photochemical Data," *The Natural Stratosphere of 1974, CIAP Monograph 1*, pp. 5-195 to 5-262.
- Gelman, M., and R. Nagatami, 1976, *COSPAR*, **XIX**, June 1976.
- General Motors Corporation, Rochester Products, 1964, *Basic Carburetion Manual*, Rochester, New York.
- Gille, J. C., P. Bailey, F. B. House, R. A. Craig, and J. R. Thomas, 1975, *The Nimbus-6 User's Guide*, pp. 141-161.
- Gille, J. C., P. L. Bailey, R. A. Craig, F. B. House, 1976, *Proceedings of the Joint RC/CACGP Symposium on Radiation in the Atmosphere*, Garmisch-Partenkirchen, FRG, August 19-28, 1976, p. 306.
- Gille, J. C., R. A. Craig, and F. B. House, 1968, *Nimbus-F Limb Radiance Inversion Experiment*, proposal to Goddard Space Flight Center.
- Gille, J. C., R. A. Craig, F. B. House, and J. R. Thomas, 1970, *Nimbus-F Limb Radiance Inversion Experiment*, **1**, Technical Report and Proposal, Honeywell Document 6S-D-47.
- Gillespie, H. M., J. Garroway, and R. J. Donavon, 1977, *J. Photochem.*, **7**, pp. 29-40.
- Glanzer, K., and J. Troe, 1975, *Bunsenges. Phys. Chem. Ber.*, **79**, pp. 465-469.
- Glatt, L., and G. F. Widhopf, 1976, presented at American Geophysical Union Spring Annual Meeting, *EOS Translations*, **54** (4), SA63.

- Goldsmith, P. A., A. F. Tuck, J. S. Foot, E. L. Simmons, and R. L. Newson, 1973, *Nature*, 244, pp. 545-551.
- Goodeve, C. F., and S. Katz, 1939, *Proc. Roy. Soc.*, 172A, pp. 432-444.
- Goodeve, C. F., and F. D. Richardson, 1937, *Trans. Faraday Soc.*, 33, pp. 453-457.
- Graham, R. A., 1975, "Photochemistry of NO_3 and the Kinetics of the $\text{N}_2\text{O}_5 - \text{O}_3$ System," PhD Thesis, University of California, Berkeley.
- Graham, R. A., and H. S. Johnston, 1974, *J. Chem. Phys.*, 60, pp. 4628-4629.
- Greiner, N. R., 1968, *J. Phys. Chem.*, 72, pp. 406-410.
- Gushchin, G. P., 1963, *Studies of Atmospheric Ozone*, Hydrometeorological Press, Leningrad.
- Gushchin, G. P., 1970, *Instructions for Conducting and Interpreting Observations of the Total Content of Atmospheric Ozone*, Hydrometeorological Press, Leningrad.
- Gushchin, G. P., 1972, "Comparison of Ozonometric Instruments," *Actinometry, Atmospheric Optics, Ozonometry*, G. P. Gushchin, ed., translated from Russian, *Gidrometeozdat*, Leningrad.
- Gushchin, G. P., 1976, "On the Technique for Measuring the Total Content of Atmospheric Ozone at the World Network of Stations," Joint Symposium on Atmospheric Ozone (IAOC/ICACGP), Dresden, German Democratic Republic, August 9-17, 1976, to be published.
- Hack, W., K. Hoyer mann, and H. G. Wagner, 1974, *Z. Naturforsch.*, 29, pp. 1236-1237.
- Hack, W., K. Hoyer mann, and H. G. Wagner, 1975, *Int. J. Chem. Kinet.*, Symposium No. I, pp. 329-339.
- Hack, W., G. Mex, and H. G. Wagner, 1976, Max-Planck Institut für Stromungsforschung, Report No. 3, February 1976.
- Hamilton, E. J., Jr., 1975, *J. Chem. Phys.*, 63, pp. 3682-3683.

- Hamilton, E. J., Jr., and R. R. Lii, 1976, to be published in *Int. J. Chem. Kin.*
- Hampson, R. F., Jr., ed., 1973, *Phys. Chem. Ref. Data*, 2, pp. 267-312.
- Hampson, R. F., Jr., and D. Garvin, ed., 1975, "Chemical Kinetic and Photochemical Data for Modelling Atmospheric Chemistry," National Bureau of Standards Technical Note 866.
- Harries, J. E., 1976, *Rev. Geophys. and Space Sci.*, 14, pp. 565-575.
- Harries, J. E., J. R. Birch, J. W. Fleming, N. W. B. Stone, D. G. Moss, N. R. W. Swann, and G. F. Neill, 1974, *Proceedings of the Third Conference on the Climatic Impact Assessment Program*, DOT-TSC-OST-74-15, U.S. Department of Transportation, p. 197.
- Harris, F., and J. Rosen, 1976, *Proceedings of the Williamsburg Aerosol Conference*, December 1976.
- Harris, G. W., and R. P. Wayne, 1975, *J. Chem. Soc., Faraday Trans. I*, 71, pp. 610-617.
- Hartmann, D. L., 1976, *J. Atmos. Sci.*, 33, pp. 1789-1802.
- Hartmann, 1977, "Potential Vorticity and Transport in the Stratosphere," submitted to *JAS*.
- Harwood, R. S., and J. A. Pyle, 1975, "A Two-Dimensional Mean Circulation Model for the Atmosphere Below 80 km," *COMESA Report*.
- Hays, P. B., R. G. Roble, and A. N. Shah, 1972, *Science*, 176, p. 793.
- Heath, D. F., 1973, *J. Geophys. Res.*, 78, p. 2779.
- Heath, D., A. J. Drueger, and C. L. Mateer, 1970, "The Backscatter Ultraviolet Spectrometer (BUV) Experiment," *The Nimbus-IV User's Guide*, R. R. Sabatini, ed., NASA/GSFC, Greenbelt, Maryland, pp. 149-171.
- Heath, D. F., A. J. Krueger, and P. J. Crutgen, 1977, "Influence of a Solar Proton Event on Stratosphere Ozone," in press.
- Heath, D. F., C. L. Mateer, and A. J. Krueger, 1973, *Pure and Applied Geophysics*, 106-108, pp. 1238-1253.

- Heath, D. F., and M. L. Thekaekara, 1976, NASA/GSFC TM X71171, July 1976.
- Heck, W., and H. Panofsky, *Small-Scale Mixing in the Lower Stratosphere*, Department of Meteorology, Pennsylvania State University, University Park, Pennsylvania.
- Heck, W., and H. A. Panofsky, 1975, "Stratospheric Mixing Estimates from Heat Flux Measurements," *CIAP Monograph 1*, pp. 6-90 to 6-92.
- Heidner, R. F., III, and D. Husain, 1973, *Int. J. Chem. Kinet.*, **5**, pp. 819-831.
- Heidner, R. F., III, D. Husain, and J. R. Wiesenfeld, 1973, *J. Chem. Soc., Faraday Trans. II*, **69**, pp. 927-938.
- Heroux, L., and R. A. Swirbalus, 1976. *J. Geophys. Res.*, **81**, p. 436.
- Hidalgo, H., and P. J. Crutzen, 1976, Symposium on the Nonurban Troposphere, Miami Beach, Florida, November 10-12, 1976.
- Hill, W. J., and P. N. Sheldon, 1975, *Geophys. Res. Lett.*, **2**, pp. 541-544.
- Hill, W. J., P. Sheldon, and J. J. Tiede, 1977, *Geophys. Res. Lett.*, in press.
- Hilsenrath, E., and T. E. Ashenfelter, 1976, *Balloon Ozone Measurements Utilizing and Optical Absorption Cell and Ejector Air Sampler*, NASA/GSFC TND-8281, Greenbelt, Maryland, July 1976.
- Hilsenrath, E., L. Seiden, and P. Goodman, 1969, *J. Geophys. Res.*, **74**, pp. 6874-6880.
- Hochanadel, C. J., J. A. Ghormley, and P. J. Ogren, 1972, *J. Chem. Phys.*, **56**, pp. 4426-4432.
- Hofmann, D. J., and J. M. Rosen, 1977, *J. Geophys. Res.*, January 1977.
- Hofmann, D. J., J. M. Rosen, T. J. Pepin, and R. G. Pinnick, 1975, *J. Atmos. Sci.*, **32**, pp. 1448-1456.
- Howard, C. J., 1977, NOAA Environmental Laboratories, Boulder, Colorado.

- Howard, C. J., and K. M. Evenson, 1974, *J. Chem. Phys.*, **61**, pp. 1943-1952.
- Howard, C. J., and K. M. Evenson, 1976, *J. Chem. Phys.*, **64**, pp. 197-202.
- Howard, C. J., and K. M. Evenson, 1977, *EOS AGU Trans.*, **58**, p. 464.
- Howard, P. H., and A. Hanchett, 1975, *Science*, **189**, p. 217.
- Huie, R. E., and J. T. Herron, 1974, *Chem. Phys. Lett.*, **27**, pp. 411-414.
- Hudson, R. D., 1971, *Rev. Geophys. Space Phys.*, **9**, pp. 305-406.
- Hudson, R. D., and L. J. Kieffer, 1975, "Absorption Cross Sections of Stratospheric Molecules," *The Natural Stratosphere of 1974, CIAP Monograph 1*, pp. 5-156 to 5-194.
- Hunt, B., 1969, *Mon. Wea. Rev.*, **97**, p. 287.
- Hunt, B., and S. Manabe, 1968, *Mon. Wea. Rev.*, **96**, p. 503.
- Hunten, D. M., 1975, In: *Atmospheres of the Earth and Planets*, B. M. McCormac, ed., D. Reidel, Dordrecht, Netherlands.
- Illies, A. J., and G. A. Takacs, 1976, *J. Photochem.*, **6**, pp. 35-42.
- Jaffe, R., 1976, "The Photodissociation of HOCl," 172nd American Chemical Society National Meeting, San Francisco.
- Jarchia, L. G., 1963, *Rev. Mod. Phys.*, **35**, p. 973.
- Jayanty, R. K. M., R. Simonaitis, and J. Heicklen, 1976, *J. Photochem.*, **5**, pp. 217-224.
- Johnston, H. S., and R. Graham, 1974, *Can. J. Chem.*, **52**, pp. 1415-1423.
- Johnston, H. S., D. Kattenhorn, and G. Whitten, 1975, *J. Geophys. Res.*, **81**, p. 368.
- Johnston, H. S., E. D. Morris, and J. Van den Bogaerde, 1969, *J. Amer. Chem. Soc.*, **91**, pp. 7712-7727.

- Johnston, H. S., and G. S. Selwyn, 1975, *Geophys. Res. Lett.*, **2**, pp. 549-551.
- Johnston, M. S., G. Whitten, and J. Birks, 1973, *J. Geophys. Res.*, **78**, pp. 6107-6135.
- Jones, I. T. N., and R. P. Wayne, 1970, *Proc. Roy. Soc. Lond.*, **A319**, pp. 273-287.
- Junge, C., 1976, *Z. Naturforsch.*, **31a**, p. 482.
- Junge, C. E., 1957, *Tellus*, **9**, p. 528.
- Kajimoto, O., and R. J. Cvetanovic, 1976, *Chem. Phys. Lett.*, **37**, pp. 533-536.
- Kajimoto, O., and R. J. Cvetanovic, 1976, *J. Chem. Phys.*, **64**, pp. 1005-1015.
- Kaselau, K. H., 1974, *Pure and Applied Geophys.*, **112**, pp. 877-885.
- Kaufman, F., 1975, *Atmospheres of Earth and the Planets*, **219**, B. M. McCormac, ed., D. Reidel Publ. Co., Boston, Mass.
- Kerr, J. B., and C. T. McElroy, 1976, *Atmosphere*, **14**, p. 166.
- King, P., I. R. McKinnon, J. G. Mathieson, and I. R. Wilson, 1976, *J. Atmos. Sci.*, **33**, p. 1657.
- King-Hele, D. G., and E. Quinn, 1961, *J. Atmos. Terr. Phys.*, **27**, p. 197.
- Komhyr, W. D., 1961, "Measurements of Atmospheric Ozone, Moosonee, Canada—July 1, 1957 to July 31, 1960," *Canadian Meteorological Memoirs*, No. 6, Meteorological Branch, Department of Transport.
- Komhyr, W. D., E. W. Barrett, G. Slocum, and H. K. Weickman, 1971, *Nature*, **323**, pp. 390-391.
- Komhyr, W. D., R. D. Grass, and R. A. Proulx, 1968, *Oxonesonde Inter-comparison Tests*, ERL 85-APCL 4, ESSA Research Laboratories, Boulder, Colorado.

- Komhyr, W. D., and T. B. Harris, 1971, "Development of an ECC Ozonesonde," *NOAA Technical Report*, ERL 200-APCL 18.
- Krueger, A. J., 1965, *Proceedings of the Ozone Symposium*, Albuquerque, New Mexico, pp. 24-25.
- Krueger, A. J., and W. R. McBride, 1968, "Rocket Ozonesonde (ROCOZ)—Design and Development," Naval Weapons Center, TP 4512, China Lake, California.
- Krueger, A. J., and R. A. Minzner, 1976, *J. Geophys. Res.*, **81**, pp. 4477-4481.
- Kuis, S., R. Simonaitis, and J. Heicklen, 1975, *J. Geophys. Res.*, **80**, pp. 1328-1331.
- Kulcke, W., and H. K. Paetzold, 1957, *Ann. d. Met.*, **8**, p. 47.
- Kurylo, M. J., 1977, *Chem. Phys. Lett.* (in press).
- Kurylo, M. J., and W. Braun, 1976, *Chem. Phys. Lett.*, **37**, pp. 232-235.
- Kurzeja, R. J., 1975, *J. Atmos. Sci.*, **32**, p. 899.
- Langhoff, S. R., L. Jaffe, and J. O. Arnold, 1976, *Can. J. Phys.*
- Lazrus, A. L., and B. W. Gandrud, 1974a, *J. Atmos. Sci.*, **31**, p. 1102.
- Lazrus, A. L., and B. W. Gandrud, 1974b, *J. Geophys. Res.*, **79**, pp. 3424-3431.
- Lazrus, A. L., B. W. Gandrud, and R. N. Woodward, 1976, *J. Geophys. Res.*, p. 81.
- Lazrus, A. L., B. W. Gandrud, R. N. Woodard, and W. A. Sedlacek, 1975, *Geophys. Res. Lett.*, **2**, pp. 439-441.
- Leu, M. T., and W. B. DeMore, 1976, *Chem. Phys. Lett.*, **41**, pp. 121-124.
- Leu, M. T., C. L. Lin, and W. B. DeMore, 1977, *J. Phys. Chem.* in press.
- Lilly, D. K., D. E. Waco, and S. I. Adelfang, 1975, "Stratospheric Mixing Estimated from High-Altitude Turbulence Measurements by Using Energy Budget Techniques," *CIAP Monograph 1*, pp. 6-81 to 6-90.

- Lin, C. L., and W. B. DeMore, 1973/74, *J. Photochem.*, **2**, pp. 161-164.
- Liss, and Slater, 1974, *Nature*, **247**, p. 181.
- Liu, S. C., 1977, Position paper presented at the Chlorofluoromethane Assessment Workshop, Warrenton, Virginia, January 1977.
- Liu, S. C., R. J. Cicerone, T. M. Donahue, and W. L. Chameides, 1977, *Tellus*, in press.
- Liu, S. C., T. M. Donahue, R. J. Cicerone, and H. L. Chameides, 1976, *J. Geophys. Res.*, **81**, pp. 3111-3118.
- Loewenstein, M., and H. Savage, 1975, *Geophys. Res. Lett.*, **2**, p. 448.
- Loewenstein, M., H. F. Savage, and R. C. Whitten, 1975, *J. Atmos. Sci.*, **32**, p. 2185.
- London, J., and H. U. Dutsch, 1976, Joint IAOC/ICACGP Symposium on Atmospheric Ozone (IAMAP/IUCC), August 1976, Dresden, GDR, Proceedings.
- London, J., J. E. Frederick, and G. F. Anderson, 1977, *J. Geophys. Res.*, in press.
- London, J., and J. Kelley, 1974, *Science*, **184**, pp. 987-989.
- Louis, J. F., J. London, and E. Danielson, 1974, "Interaction of Radiation and the Meridional Circulation of the Stratosphere," IAMAP First Special Assembly, Melbourne, Australia, January 1974.
- Lovelock, J., 1976, In: *Halocarbons: Effects on Stratospheric Ozone*, National Academy of Sciences, Washington, D.C., September 1976.
- Luther, F., 1976, *Lawrence Livermore Laboratory Report*, UCRL-77298, preprint.
- Luther, F. M., 1973, "Monthly Values of Eddy Diffusion Coefficients in the Lower Stratosphere," UCRL Report No. 74616; AIAA Paper No. 73-498, presented to the AIAA/AMS International Conference on the Environmental Impact of Aerospace Operations in the High Atmosphere, Denver, Colorado.

- Luther, F. M., and R. J. Gelinas, 1976, *J. Geophys. Res.*, **81**, pp. 1125-1132.
- Luther, F. M., and D. J. Wuebbles, 1977, position paper for NASA Workshop on CFM Assessment, January 10-14, 1977.
- Madden, R., 1975, *Mon. Wea. Rev.*, **103**, pp. 717-729.
- Mahlman, J. D., 1975, *Proceedings of the Second Conference on CIAP*. U.S. Department of Transportation DOT-TSC-OST-73-4, pp. 321-337.
- Mahlman, J. D., 1975, *Proceedings of the Fourth Conference on the Climatic Impact Assessment Program*, DOT-TSC-OST-75-38, U.S. Department of Transportation, p. 132.
- Majer, J. R., and J. P. Simons, 1964, "Photochemical Processes in Halogenated Compounds," J. Pitts, G. Hammond, and W. A. Noyes, ed., *Advances in Photochemistry*, **2**, Interscience, New York, pp. 137-181.
- Manabe, S., and B. Hunt, 1968, *Mon. Wea. Rev.*, **96**, p. 477.
- Manabe, R., and R. T. Wetherald, 1975, *J. Atmos. Sci.*, **32**, pp. 3-15.
- Manning, R., W. Braun, and M. J. Kurylo, 1977, *J. Phys. Chem.*, in press.
- Margitan, J. J., F. Kaufman, and J. G. Anderson, 1975, *Int. J. Chem. Kinet.*, Symposium No. 1, pp. 281-287.
- Martin, B., and C. Stewart, 1976, *J. App. Met.*, **15**, p. 526.
- Martin, D., J. Girnian, and H. S. Johnston, 1974, paper presented at the 167th American Chemical Society National Meeting, Los Angeles, California.
- Martin, H., and R. Gareis, 1956, *Z. Elektrochemie*, **60**, pp. 959-964.
- Mason, C. J., and J. J. Horvath, 1976, *Geophys. Res. Lett.*, **3**, p. 391.
- Mastenbrook, H. J., 1971, *J. Atmos. Sci.*, **28**, pp. 495-501.
- Mateer, C. L., 1965, *J. Atmos. Sci.*, **22**, pp. 370-381.

- Mateer, C. L., D. F. Heath, and A. J. Krueger, 1971, *J. Atmos. Sci.*, **28**, pp. 1307-1311.
- Matthews, W. A., R. E. Basher, and G. J. Frazer, 1974, *Pure and Applied Geophys.*, **112**, pp. 931-938.
- McCarthy, R. E., 1974, *EOS, AGU Trans.*, **56**, p. 1153.
- McConnell, J. C., and M. B. McElroy, 1973, *J. Atmos. Sci.*, **30**, p. 1465.
- Michael, J. V., D. A. Whytock, J. H. Lee, W. A. Payne, and L. J. Stief, 1977, *J. Chem. Phys.*, in press.
- Miranda, H. A., Jr., J. Dulchinos, and H. P. Miranda, 1973, *Atmospheric Balloon Aerosol Particle Counter Measurement*, AFCRL-TR-0700, Epsilon Laboratories, Inc., Bedford, Massachusetts, November 1973.
- Molina, M. J., and F. S. Rowland, 1974, *Nature*, **249**, p. 810.
- Molina, L. T., and M. J. Molina, 1977, *Geophys. Res. Lett.*, **4**, pp. 83-86.
- Molina, L. T., J. E. Spencer, and M. J. Molina, 1977, *Chem. Phys. Lett.*, in press.
- Moortgat, G. K., and P. Warneck, 1975, *Z. Naturforsch.*, **30A**, pp. 835-844.
- Murcray, D. G., D. B. Barker, J. N. Brooks, A. Goldman, and W. J. Williams, 1975, *Geophys. Res. Lett.*, **2**, p. 233.
- Murcray, D. G., A. Goldman, A. Csoekpoeckh, F. H. Murcray, W. J. Williams, and R. N. Stocker, 1973, *J. Geophys. Res.*, **78**, p. 7033.
- Murcray, D. G., A. Goldman, W. J. Williams, F. H. Murcray, F. S. Bonomo, C. M. Bradford, G. R. Cook, P. L. Hanst, and M. J. Molina, 1977, *Geophys. Res. Letters*, **4**, p. 227.
- Murcray, D. G., A. Goldman, W. J. Williams, F. H. Murcray, J. N. Brooks, R. N. Stocker, and D. E. Snider, 1974, *Proceedings of the International Conference on Structure, Composition and General Circulation of the Upper and Lower Atmospheres and Possible Anthropogenic Perturbations*, Melbourne, Australia, January 1974.

- Murcray, D. G., F. H. Murcray, W. J. Williams, T. G. Kyle, and A. Goldman, 1969, *Appl. Opt.*, **8**, p. 2519.
- Nagata, T., T. Tohmatsu, and T. Ogawa, 1971, *Space Res.*, **11**, pp. 849-855.
- Nastrom, G. D., A. D. Belmont, and D. G. Dartt, 1975, *Quart. J. Roy. Met. Soc.*, **101**, pp. 583-596.
- National Academy of Sciences Report, 1975, "Environmental Impact of Stratospheric Flight," Washington, D.C.
- National Academy of Sciences, 1976, *Halocarbons: Effects on Stratospheric Ozone*, Washington, D.C., September 1976.
- National Research Council Panel on Atmospheric Chemistry, 1976, *Halocarbons: Effects on Stratospheric Ozone*, Washington, D.C., September 1976.
- Newell, R., G. Herman, J. Fullmer, W. Tahnk, and M. Tanaka, 1974, *Proceedings of the International Conference on Structure, Composition, and General Circulation of the Upper and Lower Atmospheres and possible Anthropogenic Perturbations*, Melbourne, Australia, January 14-28, 1974.
- Nicholas, J. F., and R. G. W. Norrish, 1968, *Proc. Roy. Soc.*, **A307**, pp. 391-397.
- Nicolet, 1975, *Rev. Geophys. Space Phys.*, **13**, p. 593.
- Niki, H., P. D. Maker, C. M. Savage, and L. P. Breitenbach, 1977, *Chem. Phys. Lett.*, **45**, pp. 564-566.
- Noxon, J. F., 1975, *Science*, **189**, p. 547.
- Noxon, J. F., 1976, paper presented at the International Conference on the Stratosphere and Related Problems, Utah State University, Logan, Utah, September 15-17, 1976.
- Overend, R., G. Paraskevopoulos, and R. J. Cvetanovic, 1975, *Can. J. Chem.*, **53**, pp. 3374-3382.
- Paetzold, H. K., and F. Pischolar, 1961, *Beitr. Phys. Atmos.*, **34**, pp. 53-68.

- Panofsky, H., and W. Heck, 1974, *Proceedings of the Third Conference on CIAP*, DOT-TSC-OST-74-15, U.S. Department of Transportation, p. 102.
- Parker, D., D. H. Ehhalt, H. W. Patz, V. Platt, E. P. Roth, and A. Volo, 1976, *Geophys. Res. Lett.*, **3**, p. 466.
- Patel, C. K. N., E. G. Burkhardt, and C. H. Lambert, 1974, *Science*, **184**, p. 1173.
- Paukert, T. T., and H. S. Johnston, 1972, *J. Chem. Phys.*, **56**, pp. 2824-2838.
- Perner, D., D. H. Ehhalt, H. W. Patz, U. Platt, E. P. Roth, and A. Volz, 1976, *Geophys. Res. Lett.*, **3**, p. 466.
- Philen, D. L., R. T. Watson, and D. D. Davis, 1977, *J. Chem. Phys.*
- Phillips, L. F., and H. I. Schiff, 1962, *J. Chem. Phys.*, **36**, pp. 1509-1517.
- Pinnick, R. G., and D. J. Hofmann, 1973, *Appl. Opt.*, **12**, pp. 2593-2597.
- Pittock, A. B., 1974, *Proceedings of the International Conference on Structure, Composition, and General Circulation of Upper and Lower Atmospheres and Possible Anthropogenic Perturbations*, Melbourne, Australia, IAMAP, **1**, pp. 455-466.
- Pitts, J. N., Jr., H. L. Sandoval, and R. Atkinson, 1974, *Chem. Phys. Lett.*, **29**, pp. 31-34.
- Poulet, G., G. Le Bras, and J. Combourieu, 1974, *J. Chem. Phys., Physicochim. Biol.*, **71**, pp. 101-106.
- Prabhakara, C., B. J. Conrath, R. A. Hanel, and E. J. Williamson, 1970, *J. Atmos. Sci.*, **27**, pp. 689-697.
- Prabhakara, C., E. B. Rodgers, B. J. Conrath, R. A. Hanel, and V. G. Kunde, 1976, to be published in *J. Geophys. Res.*
- Prinn, R., F. Alyea, and D. Cunnold, 1976, *Bull. Amer. Met. Soc.*, **57**, p. 686.
- Prinn, R. F., F. N. Alyea, and D. M. Cunnold, 1975, *J. Geophys. Res.*, **80**, p. 4997.

C-4

- Quiroz, R. S., 1975, *J. Atmos. Sci.*, **32**, pp. 211-224.
- Ramanathan, V., 1975, *Science*, **190**, pp. 50-52.
- Ramanathan, V., and Boughner, 1975, paper presented at the 1975 AGU Fall Annual Meeting, San Francisco.
- Ramanathan, V., L. B. Callis, and R. E. Boughner, 1976, *J. Atmos. Sci.*, **33**, pp. 1092-1112.
- Ramanathan, V., and W. L. Grose, 1977, paper submitted to *Contributions to Atmos. Sci.—Beitrage zur Physik der Atmosphere*.
- Randhawa, J. S., 1966, *Nature*, **213**, pp. 53-54.
- Rasmussen, R. A., D. Pierotti, J. Krasnec, and B. Halter, 1976, submitted to EPA.
- Ravishankara, A. R., G. Smith, R. T. Watson, and D. D. Davis, 1977, Georgia Institute of Technology, Atlanta, Georgia, in preparation.
- Rebbert, R. E., and P. J. Ausloos, 1976, paper presented at the 172nd ACS National Meeting, San Francisco, California, August 29-September 3, 1976.
- Reed, R. J., and K. E. German, 1965, *Mon. Wea. Rev.*, **93**.
- Regener, V. H., 1960, *J. Geophys. Res.*, **65**, pp. 3975-3977.
- Reiter, E., 1975, *Rev. Geophys. Space Phys.*, **13**, p. 459.
- Reiter and Mahlman, 1965, *Heavy Iodine-131 Fallout over the Midwestern United States, May 1962*, Technical Paper No. 70, Department of Atmospheric Science, Colorado State University.
- Ridley, B. A., and J. T. Bruin, 1977, submitted to *Geophys. Res. Lett.*
- Ridley, B. A., J. T. Bruin, H. I. Schiff, and M. C. McConnell, 1976, *Atmosphere*, **14**, p. 180.
- Ridley, B. A., M. McFarland, J. T. Bruin, H. I. Schiff, and J. C. McConnell, 1977, *Can. J. Phys.*, in press.

- Ridley, B. A., H. I. Schiff, A. W. Shaw; L. Bates, L. C. Howlett, H. LeVaux, L. R. Megill, and T. E. Ashenfelter, 1974, *Planet. Space Sci.*, **22**, p. 19.
- Ridley, B. A., H. I. Schiff, A. Shaw, and L. R. Megill, 1975, *J. Geophys. Res.*, **80**, p. 1925.
- Ridley, B. A., and D. J. Wuebbles, 1976, paper presented at the International Conference on the Stratosphere and Related Problems, Logan, Utah, September 1976.
- Robbins, D. E., 1976, *Geophys. Res. Lett.*, **3**, pp. 213-216.
- Robbins, D. E., L. J. Rose, and W. R. Boykin, 1975, *Ultraviolet Photoabsorption Cross Section for CF₂Cl₂, CFCl₃, and CCl₄*, Johnson Space Flight Center Internal Note, JSC-09937.
- Robbins, D. E., and R. S. Stolarski, 1976, *Geophys. Res. Lett.*, **3**, p. 603.
- Rosen, J. M., 1971, *J. Appl. Meteor.*, **10**, pp. 1044-1045.
- Rosen, J. M., 1976, paper presented at the International Conference on the Stratosphere and Related Problems, Logan, Utah, September 1976.
- Rosen, J. M., and D. J. Hofmann, 1977, *J. Appl. Meteor.*, January 1977.
- Rosen, J. M., D. J. Hofmann, and J. Laby, 1975, *J. Atmos. Sci.*, **32**, pp. 1457-1462.
- Rottman, G. J., 1974, AGU Meeting, San Francisco, California, December 1974.
- Rowland, F. S., and M. J. Molina, 1975, *Rev. Geophys. Space Phys.*, **13**, p. 1.
- Rowland, F. S., J. E. Spencer, and M. J. Molina, 1976, *J. Phys. Chem.*, **80**, pp. 2711-2712.
- Rundel, R. D., D. M. Butler, and R. S. Stolarski, 1976, "Monte-Carlo Analysis of Uncertainty Propagation in a Stratospheric Model: I. Development of a Concise Stratospheric Model," in preparation, December 1976.
- Sandorfy, C., 1976, *Atm. Environ.*, **10**, pp. 343-351.

- Schneider, S. H., and R. E. Dickinson, 1974, *Rev. Geophys. Space Physics*, **12**, pp. 447-493.
- Schoeberl, M. R., and M. A. Geller, 1976, *Aeronomy Laboratory Report*, University of Illinois at Urbana, Illinois and Library of Congress, ISSN 0568-0581.
- Sellers, W. D., and D. N. Yarger, 1969, *J. Appl. Meteor.*, **8**, pp. 357-361.
- Sie, H. K. T., R. Simonaitis, and J. Heicklen, 1976, *Int. J. Chem. Kinet.*, **8**, pp. 85-98.
- Simon, P., 1975, *Bull. Acad. Royale de Belgique*, **61**, p. 399.
- Simonaitis, R., S. Braslavsky, J. Heicklen, and M. Nicolet, 1973, *Chem. Phys. Lett.*, **19**, pp. 601-603.
- Simonaitis, R., R. I. Greenberg, and J. Heicklen, 1972, *Int. J. Chem. Kinetics*, **4**, pp. 497-512.
- Simonaitis, R., and J. Heicklen, 1973, *J. Phys. Chem.*, **77**, pp. 1932-1935.
- Simonaitis, R., and J. Heicklen, 1976a, *J. Phys. Chem.*, **80**, p. 1-7.
- Simonaitis, R., and J. Heicklen, 1976b, "Temperature Dependence of the Reactions of HO₂ with NO and NO₂," typescript, Department of Chemistry, Pennsylvania State University, University Park, Pennsylvania, July 1976.
- Simonaitis, R., and J. Heicklen, 1977, Ionospheric Research Laboratory Scientific Report 454, Pennsylvania State University, University Park, Pennsylvania.
- Singh, H. B., 1977, *Geophys. Lett.*, **4**, p. 101.
- Singh, H. B., L. J. Salas, J. Shiegeshi, and L. Cavanagh, 1976, submitted to EPA.
- Singleton, D. L., S. Furuyama, R. J. Cvetanovic, and R. S. Irwin, 1975, *J. Chem. Phys.*, **63**, pp. 1003-1007.
- Sissons, N. V., 1968, *Ozone Measuring Techniques and Their Assessment for W. R. E. Dropsonde Use*, Weapons Research Establishment, Technical Note SAD 196, Salisbury, South Australia.

- Smith, G. P., and D. M. Golden, 1977, Stanford Research Institute (typescript).
- Smith, I. W. M., 1977, to be published in *Chem. Phys. Lett.*
- Smith, I. W. M., and R. Zellner, 1973, *J. Chem. Soc., Faraday Trans. II*, **69**, pp. 1617-1627.
- Smith, I. W. M., and R. Zellner, 1974, *J. Chem. Soc., Faraday Trans. II*, **70**, pp. 1045-1056.
- Smith, I. W. M., and R. Zellner, 1975, *Int. J. Chem. Kinet.*, Symposium No. 1, pp. 341-351.
- Smith, W. S., C. C. Chou, and F. S. Rowland, 1977, "Photolysis of Chlorine Nitrate at 302.5 nm," paper presented at the 173rd American Chemical Society National Meeting, New Orleans.
- Spencer, J. E., and G. P. Glass, 1977, *Int. J. Chem. Kinetics*, in press.
- Stedman, D. H., W. L. Chameides, and R. J. Cicerone, 1975, *Geophys. Res. Letters*, **2**, p. 333.
- Stedman, D. H., R. J. Cicerone, W. L. Chameides, and R. B. Harvey, 1976, *J. Geophys. Res.*, **81**, pp. 2003-2004.
- Stolarski, R. S., D. M. Butler, and R. D. Rundel, 1976, paper presented at the International Conference on the Stratosphere and Related Problems, Logan, Utah, September 1976.
- Stolarski, R. S., D. M. Butler, and R. D. Rundel, 1976, "Monte-Carlo Analysis of Uncertainty Propagation in a Stratospheric Model: II. Uncertainties due to Reaction Rates," in preparation, December 1976.
- Streit, G. E., and H. S. Johnston, 1976, *J. Chem. Phys.*, **64**, p. 95.
- Streit, G. E., C. J. Howard, A. L. Schmeltekopf, J. A. Davidson, and H. I. Schiff, 1976, *J. Chem. Phys.*, **65**, pp. 4761-4764.
- Sze, N. D., 1973, Thesis, Harvard University, Boston, Massachusetts.
- Takacs, G. A., and G. P. Glass, 1973a, *J. Phys. Chem.*, **77**, pp. 1060-1064.

- Takacs, G. A., and G. P. Glass, 1973b, *J. Phys. Chem.*, **77**, pp. 1948-1951.
- Takacs, G. A., and G. P. Glass, 1973c, *J. Phys. Chem.*, **77**, pp. 1182-1186.
- Thekaekara, M. P., 1973, *Solar Energy*, **14**, p. 109.
- Thekaekara, M. P., 1974, *App. Optics*, **13**, p. 518.
- Trainor, D. W., and C. W. von Rosenberg, Jr., 1974, *J. Chem. Phys.*, **61**, pp. 1010-1015.
- Turco, R. P., 1975, *Geophys. Surveys*, **2**, pp. 153-192.
- Turco, R. P., and R. C. Whitten, 1977a, "One-Dimensional Model Calculations of Ozone Reduction by CFM-Generated Stratospheric Chlorine," unpublished work presented at the NASA Ozone Conference, Glenn Dale, Maryland.
- Turco, R. P., and R. C. Whitten, 1977b, *J. Geophys. Res.*, in press.
- Turner, R. E., K. V. Haggard, and T. S. Chen, 1976, paper presented at the 13th Annual Meeting of the Society of Engineering Science, Hampton, Virginia, November 1-3, 1976.
- Vupputuri, R. K. R., 1976a, addendum to paper presented at the International Conference on the Stratosphere and Related Problems, Utah State University, Logan, Utah, September 1976a.
- Vupputuri, R. K. R., 1976b, *Atmosphere*, **14**(3).
- Wang, C. C., L. I. Davis, Jr., C. H. Wu, S. Jaspar, H. Niki, and B. Weinstock, 1975, *Science*, **189**, p. 797.
- Washington, W., 1972, *Proceedings of the Second Conference on CIAP*, U.S. Department of Transportation, November 14-17, 1972.
- Watson, R. T., 1974, "Rate Constants of ClO_x of Atmospheric Interest," Chemical Kinetics Survey No. 8, NBS-AR 74-516.
- Watson, R. T., 1977, *J. Chem. Phys. Ref. Data*.
- Watson, R. T., D. D. Davis, E. S. Machado, B. C. Conaway, and Y. Oh, 1977, paper presented at the 4th CIAP Conference, February 1975, Boston, Manuscript in preparation, Jet Propulsion Laboratory.

- Watson, R., G. Machado, S. Fischer, and D. D. Davis, 1976, *J. Chem. Phys.*, **65**, pp. 2126-2138.
- Westenberg, A. A., and N. de Haas, 1968, *J. Chem. Phys.*, **48**, pp. 4405-4415.
- White, W. H., J. A. Anderson, D. L. Blumenthal, R. B. Husar, N. V. Gillani, J. D. Husar, and W. E. Wilson, Jr., 1976, *Science*, **194**, pp. 187-189.
- Whitten, R. C., W. J. Borucki, C. A. Riegel, and L. A. Capone, 1977, "Two-Dimensional Model Calculations of Ozone Reduction by CFM-Generated Stratospheric Chlorine," unpublished work presented at the NASA Ozone Conference, Glenn Dale, Maryland.
- Whytock, D. A., J. H. Lee, J. V. Michael, W. A. Payne, and L. J. Stief, 1977, *Chem. Soc., Faraday Trans. I*, in press.
- Whytock, D. A., J. H. Lee, J. V. Michael, W. A. Payne, and L. J. Stief, 1977, *J. Chem. Phys.*, **66**, pp. 2690-2695.
- Whytock, D. A., J. V. Michael, and W. A. Payne, 1976, *Chem. Phys. Lett.*, **42**, pp. 466-471.
- Widhopf, G. F., 1975, *Proceedings of the Fourth Conference on CIAP*, February 4-7, DOT-TSC-OST-75-38, 1975.
- Widhopf, G. F., 1976, presented at American Geophysical Union Spring Annual Meeting, April 1976, *EOS Transactions*, **57**(4), SA64.
- Widhopf, G. F., L. Glatt, and R. Kramer, 1977, AIAA paper 77-131, AIAA 15th Aerospace Sciences Meeting, Los Angeles, California, January 1977.
- Williams, W. J., J. J. Kusters, A. Goldman, and D. G. Murcray, 1976, *Geophys. Res. Lett.*, **3**, p. 383.
- Wofsy, S. C., and M. B. McElroy, 1973, *J. Geophys. Res.*, **78**, p. 2619.
- Wong, E. L., and F. E. Belles, 1972, *Chem. Abstr.*, **76**, p. 18326q.
- Young, Y. L., 1976, *J. Quant. Spectrosc. Radia. Trans.*, **16**, pp. 755-761.

- Zafonte, L., P. L. Rieger, and J. R. Holmes, 1975, "Some Aspects of the Atmospheric Chemistry of Nitrous Acid," *Pacific Conference on Chemistry and Spectroscopy*, Asilomar, California.
- Zahniser, M. S., B. M. Berquist, and F. Kaufman, 1977, *Int. J. Chem. Kinet.*, in press.
- Zahniser, M. S., J. S. Chang, and F. Kaufman, 1977a, University of Pittsburgh, typescript.
- Zahniser, M. S., and F. Kaufman, 1977, *J. Chem. Phys.*, **66**, pp. 3673-3681.
- Zahniser, M. S., F. Kaufman, and J. G. Anderson, 1974, *Chem. Phys. Lett.*, **27**, pp. 507-510.
- Zahniser, M. S., F. Kaufman, and J. G. Anderson, 1976, *Chem. Phys. Lett.*, **37**, pp. 226-231.
- Zander, R., 1975, "Presence de HF Dans la Stratosphere Superieur," *C. R.*, **281**, pp. 213-214.
- Zander, R., G. Roland, B. Del Bouille, 1977, to be published in *Geophys. Res. Lett.*
- Zellner, R., and W. Steinert, 1976, *Int. J. Chem. Kinet.*, **8**, pp. 397-409.

APPENDIX
CHLOROFLUOROMETHANE WORKSHOP
ATTENDEES

LABORATORY MEASUREMENTS

W. DeMore -- Chairman
Jet Propulsion Laboratory

L. Stief -- Vice-Chairman
Goddard Space Flight Center

R. Watson -- Halogen Reaction Rates
Jet Propulsion Laboratory

R. Hampson -- NO_x Reaction Rates
National Bureau of Standards

D. Garvin
National Bureau of Standards

J. Margitan -- HO_x Reaction Rates
University of Michigan

M. Molina -- Photolysis Rates and Quantum Yields
University of California, Irvine

D. Golden
Stanford Research Institute

OZONE MEASUREMENTS AND TRENDS

J. London -- Chairman
University of Colorado

C. Reber -- Vice-Chairman
Goddard Space Flight Center

J. Gille -- Ozone Measurements from Satellites
National Center for Atmospheric Research

W. Komhyr — Ground-Based Ozone Measurements
National Oceanic and Atmospheric Administration

A. Krueger — Ozone Profile Measurements
Goddard Space Flight Center/Colorado State University

J. Angell — Ozone Trend Analyses
National Oceanic and Atmospheric Administration

B. Conrath
Goddard Space Flight Center

A. Belmont
Control Data Corporation

J. Campbell
Langley Research Center

MINOR SPECIES AND AEROSOL MEASUREMENTS

R. Megill — Chairman
Utah State University

G. Newton — Vice-Chairman
Goddard Space Flight Center

A. Lazrus — Halocarbons
National Center for Atmospheric Research

A. Schmeltekopf — N_2O , CH_4 , and others
National Oceanic and Atmospheric Administration

J. Anderson — ClO_x Measurements
Michigan University

B. Ridley — NO_x Measurements
York University (Canada)

W. Heaps — HO_x Measurements
Goddard Space Flight Center

W. Moore — O/O₃ Ratio
Utah State University

J. Rosen — Aerosols
University of Wyoming

E. Good — Winds and Dynamics
Air Force Geophysics Laboratory

D. Heath — Solar-Flux Measurements
Goddard Space Flight Center

R. Rundel
Johnson Space Center

W. Evans
Atmospheric Environment Service (Canada)

D. Murcray
University of Denver

ONE-DIMENSIONAL MODEL CALCULATIONS

R. Stolarski — Chairman
Goddard Space Flight Center

J. Herman — Vice-Chairman
Goddard Space Flight Center

J. Chang — Transport Coefficients
Lawrence Livermore Laboratories

F. Luther — Photodissociation Rate Calculations
Lawrence Livermore Laboratories

S. Liu — Diurnal Effects
University of Michigan

V. Ramanathan — Radiative/Convective Feedbacks
National Center for Atmospheric Research

C. Chou — Tropospheric and Stratospheric Sinks
University of California, Irvine

R. Cicerone – Comparison Theory and Experiment for ClO_x
University of Michigan

R. Kurzeja – Comparison Theory and Experiment for NO_x
National Center for Atmospheric Research

R. Turco – Comparison Theory and Experiment for HO_x
R&D Associates

D. Butler – Uncertainty Analyses
Goddard Space Flight Center

L. Callis
Langley Research Center

R. Boughner
Langley Research Center

J. Nealy
Langley Research Center

W. Duewer
Lawrence Livermore Laboratories

J. McConnell
York University (Canada)

P. Jesson
E. I. Du Pont de Nemours

R. Hirsch
E. I. Du Pont de Nemours

C. Miller
E. I. Du Pont de Nemours

L. Glasgow
E. I. Du Pont de Nemours

S. Wofsy
Harvard University

D. Sze
Environmental Research and Technology, Inc.

J. McAfee
National Oceanic and Atmospheric Administration

S. Chandra
Goddard Space Flight Center

MULTIDIMENSIONAL MODEL CALCULATIONS

M. Geller — Chairman
University of Illinois

J. Hansen — Vice-Chairman
GSFC/Goddard Institute for Space Studies

G. Widhopf — Status of 1-D Models
Aerospace Corporation

D. Cunnold — Status of 3-D Models
Massachusetts Institute of Technology

H. Panofsky — Parameterization of Transport Processes
Pennsylvania State University

G. Mahlman — Radiation, Chemistry, and Dynamics
National Oceanic and Atmospheric Administration

R. Zurek — Observational Needs
Jet Propulsion Laboratory

G. Brasseur
Institut d'Aeronomie Spatiale (Belgium)

J. Holton
University of Washington

D. Hartman
National Center for Atmospheric Research

C. Reigel
San Jose State University

R. Whitten
Ames Research Center

GODDARD SPACE FLIGHT CENTER EDITORIAL COMMITTEE

R. Hudson – Chairman

N. Spencer

W. Bandeen

R. Stolarski

J. Herman

C. Reber

G. Newton

L. Stief

J. Hansen

Ex Officio

R. Greenwood, NASA Headquarters

R. Schiffer, NASA Headquarters


National Aeronautics and
Space Administration

Washington, D.C.
20546

Official Business
Penalty for Private Use, \$300

SPECIAL FOURTH CLASS MAIL
BOOK

Postage and Fees Paid
National Aeronautics and
Space Administration
NASA-451



NASA

POSTMASTER

If Undeliverable (Section 158
Postal Manual) Do Not Return

